RETRAN — A Program for One-Dimensional Transient Thermal-Hydraulic Analysis of Complex Fluid Flow Systems

CCM-5
Volume 1: Equations and Numerics
Research Projects 342 and 889

Computer Code Manual, December 1978

Prepared by

ENERGY INCORPORATED
330 Shoup Avenue
Idaho Falls, Idaho 83401

Principal Investigators

K. V. Moore	M. P. Paulsen
E. D. Hughes	J. F. Harrison
J. A. McClure	J. H. McFadden
C. E. Petersen	K. D. Richert
N. S. Yee	C. M. Moser
F. D. Lang	G. C. Gose
W. G. Choe	N. S. Burrell
R. W. Lyczkowski	J. T. Ching

Prepared for

Electric Power Research Institute
3412 Hillview Avenue
Palo Alto, California 94304

EPRI Project Manager
L. J. Agee
Nuclear Power Division

1356 003

LEGAL NOTICE

This report was prepared by Energy Incorporated (EI) as an account of work sponsored by the Electric Power Research Institute, Inc. (EPRI). Neither EPRI, members of EPRI, EI, or any person acting on behalf of either: (a) makes any warranty or representation, express or implied, with respect to the accuracy, completeness, or usefulness of the information contained in this report, or that the use of any information, apparatus, method, or process disclosed in this report may not infringe privately owned rights; or (b) assumes any liabilities with respect to the use of, or for damages resulting from the use of, any information, apparatus, method or process disclosed in this report.

FOREWORD

The RETRAN computer program described in this report is the result of an extensive code development effort sponsored by the Electric Power Research Institute (EPRI) over the last three years. The effort was initiated as RP342 in response to the utility need for a more realistic appraisal of the blowdown phase of the design basis Loss-Of-Coolant Accident (LOCA). During the term of this effort, the project was expanded such that the computer program, then denoted as RELAP/E, would be general enough to analyze both Boiling Water Reactors (BWR's) and Pressurized Water Reactors (PWR's) for either large or small break LOCA's, from the start of the accident through the injection, REFILL and REFLOOD periods. This major redirection of the project was made in response to the increased emphasis on the important REFLOOD period of a LOCA. During this same time period, the Nuclear Safety Analysis Task Force described the pressing need of the utilities to analyze the non-LOCA condition, I, II, and III events for both PWR's and BWR's. In response to this request, EPRI obtained from Energy Incorporated the RETRAN system analysis submodules through Research Project 889. Thus the RETRAN code package stems from the development of two separate code packages, RELAP/E and RETRAN. Both of these codes were based upon RELAP4/003 update 85, as released by the United States Nuclear Regulatory Commission (NRC) as a portion of the Water Reactor Evaluation Model (WREM). RELAP/E was developed to provide a "best estimate" of thermal-hydraulic behavior for light-water reactor systems subjected to postulated LOCA. RETRAN (RELAP4 TRANSIENT) was developed to describe the thermal-hydraulic behavior of light-water reactor systems subjected to anticipated operational transients and normal start-up and shut-down maneuvers. Because both codes were based on the same thermal-hydraulic differential and state equations of RELAP4, and because RELAP/E was constructed for ease of model incorporation with its semimodular and dynamic structure, the operational transient models were added as options to RELAP/E and the code name RETRAN was retained.

One important aspect of this project is the extensive documentation of the entire RETRAN code. The documentation of the RETRAN code package includes four

separate volumes: In Volume I the general equations and numerical separate volumes: In Volume I the general equations and numerical schemes are derived from first principles and all assumptions and limitations used in these derivations are presented; Volume II is directed at the programmer in that it presents the general coding philosophy, code details, the various RETRAN modules, flow charts, selection logic, and subroutine and function subprogram definitions; Volume III is directed to the user in that it presents a summary program description, input data requirements, error messages, and sample problems; Volume IV is directed to the application of the RETRAN code to specific problems with emphasis on the significance, sensitivity, and limitations of input variables, equations, and models. This report (Volume I) serves as both the final project report and the Theory Manual of the four-volume Computer Code Manual.

The RETRAN code has undergone verification and qualification by the EPRI/UTILITY System Analysis Working Group through a prerelease concept. There were 17 utilities participating in the Prerelease Working Group; the purpose was to develop a version of RETRAN which can be used with confidence by the utility industry. Verification and qualification of RETRAN with the prerelease version involved comparing analyses against measured data and calculations. To accomplish these comparisons, a comprehensive test matrix was developed, and the various components of the matrix were completed by the participating utilities, EPRI and EPRI contractors. The results of the prerelease verification are documented in Volume IV described above.

Lance J. Agee, Project Manager
Nuclear Power Division

ABSTRACT

RETRAN represents a new computer code approach for analyzing the thermal-hydraulic response of Nuclear Steam Supply Systems (NSSS) to hypothetical Loss of Coolant Accidents (LOCA) and Operational Transients. In contrast to the "conservative" approach, RETRAN provides "best estimate" solutions to hypothetical LOCAs and Operational Transients. RETRAN is a computer code package developed from the RELAP series of codes, from reference data, and from extensive analytical and experimental work previously conducted relative to the thermal-hydraulic behavior of light-water reactor systems subjected to postulated accidents and operational transient conditions. The RETRAN computer code is constructed in a semimodular and dynamic dimensioned form where additions to the code can be easily carried out as new and improved models are developed. This report (the first of a four-volume computer code manual) presents the derivation of the general equations, the constitutive models and numerical solution schemes that form the bases of the RETRAN computer code. The three companion volumes describe the programming details, the user input and code output, and the verification and qualification performed with RETRAN.

CONTENTS

Section		Page
I	SUMMARY	I-1
II	FLUID DIFFERENTIAL AND STATE EQUATIONS	II-1
	1.0 Local Fluid Equations	II-2
	1.1 Local Continuity Equation	II-5
	1.2 Local Momentum Equations	II-6
	1.3 Local Energy Equation	II-7
	1.4 Fluid State Equations	II-8
	1.5 Summary of the Local Equations	II-9
	2.0 Macroscopic Fluid Equations	II-11
	2.1 General Equations	II-15
	2.2 Macroscopic Mass Balance	II-15
	2.3 Macroscopic Linear Momentum Balance	II-18
	2.4 Macroscopic Energy Balance Equation	II-23
	2.5 Fluid State Equations	II-28
	2.6 Summary of the Macroscopic Balance Equations	II-29
	3.0 RETRAN Overall Balance Equations	II-32
	3.1 Geometry of the Application Procedure	II-32
	3.2 The RETRAN Mass Balance Equations	II-34
	3.3 The RETRAN Momentum Balance Equations	II-35
	3.4 The RETRAN Energy Balance Equation	II-44
	3.5 Fluid State Equations	II-45
	3.6 Summary of the RETRAN Equations	II-46
III	CONSTITUTIVE MODELS	III-1
	1.0 Linear Momentum Equation	III-1
	1.1 Friction Factor and Two-Phase Multipliers	III-2
	1.2 Local Momentum Losses	III-16
	1.3 Phase Separation (Bubble Rise) Model	III-16

Section		Page
	2.0 Energy Equation	III-36
	2.1 Two-Phase Flow and Heat Transfer Regimes	III-36
	2.2 Heat Transfer Coefficient Correlations	III-42
	2.3 Critical Heat Flux Correlations	III-58
	2.4 Junction Enthalpy and Enthalpy Transport	III-63
	2.5 Condensing Heat Transfer	III-69
	3.0 Critical Flow Models	III-79
	3.1 Sonic or "Self" Choking	III-79
	3.2 Henry-Fauske and Extended Henry-Fauske Choking	III-84
	3.3 Moody Choking	III-89
	3.4 Range of Applicability for Critical Flow Correlations	III-91
IV	HEAT CONDUCTION	IV-1
	1.0 Heat Conduction Equations	IV-1
V	POWER GENERATION	V-1
	1.0 Reactor Kinetics Equations	V-1
	1.1 Fission Heat	V-7
	1.2 Fission Product Decay	V-8
	1.3 Decay of Actinides	V-12
	2.0 Metal-Water Reaction	V-15
	3.0 Direct Moderator Heating	V-19
VI	SYSTEM COMPONENT MODELS	VI-1
	1.0 Centrifugal Pumps	VI-1
	1.1 Two-Phase Flow Effects	VI-7
	2.0 Valves	VI-18
	2.1 Check Valves	VI-18
	2.2 Inertial Valves	VI-20
	3.0 Heat Exchangers	VI-22
	3.1 Conduction Based Heat Exchanger Models	VI-22
	3.2 Nonconduction Heat Exchanger Models	VI-23
	4.0 Trip Controls	VI-25
	4.1 Standard Trips	VI-25
	4.2 OR Trips	VI-26
	4.3 Multiple Actions	VI-27

Section		Page
	4.4 Coincidence Trips	VI-27
	4.5 Indirect Trip	VI-27
	4.6 Reset Trips	VI-27
	4.7 Control System Trips	VI-28
VII	OPERATIONAL TRANSIENT MODELS	VII-1
	1.0 Control System Models	VII-2
	1.1 Model Description	VII-3
	2.0 Transport Delay Model	VII-10
	2.1 General Approach and Assumptions	VII-10
	2.2 Detailed Description and Solution Technique	VII-11
	3.0 Pressurizer Model	VII-13
	3.1 General Approach and Assumptions	VII-13
	3.2 Mass and Energy Equations	VII-14
	3.3 Region Interface Models	VII-16
	3.4 Solution Technique	VII-19
	4.0 Auxiliary DNB Model	VII-21
	4.1 Model Description	VII-21
VIII	NUMERICAL SOLUTION METHODS	VIII-1
	1.0 Fluid Flow	VIII-1
	1.1 Numerical Formulation	VIII-1
	1.2 Solution Methods	VIII-36
	2.0 Solution Method for Heat Conduction Equations	VIII-47
	3.0 Solution Method for Reactor Kinetics Equations	VIII-62
	4.0 Steady-State Initialization of the RETRAN Overall Balance Equations	VIII-68
	4.1 Mass Balance Equations	VIII-69
	4.2 Momentum Balance Equations	VIII-74
	4.3 Energy Balance Equations	VIII-78
	4.4 Overall Balance Equations	VIII-96
IX	DISCUSSIONS, LIMITATIONS AND PRECAUTIONS	IX-1
	1.0 Two-Phase Flow and Heat Transfer	IX-2
	2.0 Nuclear Steam Supply System Geometry	IX-5
	3.0 Computer Programs for Hypothetical Accident Analysis	IX-7

Section		Page
4.0	Operational Transients Model	IX-8
4.1	Transport Delay Model	IX-8
4.2	Pressurizer Model	IX-9
4.3	Control Systems	IX-10
X	REFERENCES	X-1

ILLUSTRATIONS

Figure		Page
II.1-1	Control Volume V in the Flow Field	II-3
II.2-1	Finite Volume Hydraulic Loop Elements	II-13
II.2-2	Geometrically Complex Finite Volume Hydraulic Loop Elements	II-14
II.3-1	Geometry for the RETRAN Equations	II-33
II.3-2	Geometry for RETRAN Momentum Equations with a Variable Area	II-37
III.1-1	Bennett Flow Regime Map for Vertical Upflow	III-14
III.1-2	Modified Bennett Flow Regime Map	III-15
III.1-3	Two-Phase Separation Model	III-19
III.1-4	Junction Quality Integration	III-30
III.2-1	Pool Boiling Curve Representation at a Fixed Pressure	III-37
III.2-2	Flow and Heat Transfer Regimes in Rod Array with Vertical Upflow	III-40
III.2-3	Enthalpy Associated with Energy Exchange	III-67
III.2-4	Heat Transfer Coefficient Transient During Blowdown	III-72
III.2-5	Heat Transfer Coefficient Versus Steam Mixture Weight Ratio (Transient State Measurements)	III-74
III.2-6	Maximum Heat Transfer Coefficient Versus Coolant Energy Transfer Speed into Containment Vessel Atmosphere During Blowdown	III-75
III.2-7	"NRC Containment Systems Branch Position" 6-1 Condensing Heat Transfer Regimes	III-78
III.3-1	Henry-Fauske Critical Flow Chart, Two-Phase Region	III-90
III.3-2	Moody Critical Flow Chart	III-92
VI.1-1	Four-Quadrant Pump Characteristic Curves	VI-2
VI.1-2	Homologous Pump Head Curves	VI-3
VI.1-3	Homologous Pump Torque Curves	VI-4

Figure		Page
VI.1-4	Single-Phase Head Curves for 1-1/2 Loop MOD-1 Semiscale Pumps	VI-8
VI.1-5	Two-Phase Homologous Head Curves for 1-1/2 Loop MOD-1 Semiscale Pump	VI-9
VI.1-6	Torque Versus Speed Type 93A Pump Motor (Rated Voltage)	VI-16
VI.2-1	Check Valve Characteristic Curves	VI-19
VIII.1-1	Typical Computational Mesh for Two Junctions in a Volume	VIII-3
VIII.1-2	Junction Terminal and Initial Node assignment	VIII-6
VIII.1-3	Flow Diagram for Explicit Solution	VIII-40
VIII.1-4	Causal Credit Memory Technique	VIII-45
VIII.2-1	Mesh Point Structure	VIII-48
VIII.2-2	Expanded Mesh Point Structure	VIII-49
VIII.4-1	Typical RETRAN Parallel Flow Path Nodalization	VIII-71
VIII.4-2	Combinations of Input Flow Data Satisfying the Minimum Input Requirements	VIII-72
VIII.4-3	Enthalpy Input Requirements for a Typical Y Network	VIII-82
VIII.4-4	Nodalization of an Open Network	VIII-83
VIII.4-5	Separated Volume Energy Balance	VIII-87
VIII.4-6	RETRAN Initial Value Estimation Scheme	VIII-98
VIII.4-7	RETRAN Steady-State Iteration Scheme	VIII-99

TABLES

Table		Page
III.1-1	RETRAN Values of the Modified Baroczy Two-Phase Friction Multiplier at G = 1.0×10^6 lbm/hr-ft^2	III-7
III.1-2	RETRAN Values of the Baroczy Mass Flux Correction Factor at G = 0.25×10^6 lbm/hr-ft^2	III-8
III.1-3	RETRAN Values of the Baroczy Mass Flux Correction Factor at G = 0.50×10^6 lbm/hr-ft^2	III-9
III.1-4	RETRAN Values of the Baroczy Mass Flux Correction Factor at G = 2.0×10^6 lbm/hr-ft^2	III-10
III.1-5	RETRAN Values of the Baroczy Mass Flux Correction Factor at G = 3.0×10^6 lbm/hr-ft^2	III-11
III.1-6	Beattie Two-Phase Friction Multipliers	III-17
III.2-1	Summary of RETRAN Pre-CHF Heat Transfer Coefficients	III-55
III.2-2	High Mass Flux (G > 200,000 lbm/hr-ft^2) Post-CHF Heat Transfer Coefficients	III-56
III.2-3	Low Mass Flux (G $\leq$ 200,000 lbm/hr-ft^2) Post-CHR Heat Transfer Coefficients	III-57
III.2-4	Uchida Heat Transfer Coefficients	III-71
V.1-1	Radioactive Decay Constants	V-10
V.1-2	Comparison of RETRAN and ANS Standard Decay Heat Calculated Results	V-11
VI.1-1	Pump Characteristics	VI-6
VI.1-2	Semiscale Dimensionless Head Ratio Difference (Single-Phase Minus Two-Phase) Data	VI-11
VI.1-3	Heat Multiplier and Void Fraction Data	VI-12
VI.1-4	Pump Curve Input Data	VI-17
VII.1-1	Control System Model Nomenclature	VII-4
VII.1-2	Models for Control Blocks	VII-5
VII.4-1	Auxiliary DNB Modeling	VII-22

NOMENCLATURE

A = area

A = cross-sectional area of the flow channel

$\bar{A}_h$ = heated wall surface area per unit volume (related to D_{he})

A_i = flow area of volume i

$A_j(t)$ = flow area of junction j (possibly time dependent)

$\bar{A}_w$ = wetted wall surface area per unit volume (related to D_{hy})

A^n_{jj}, A^n_{jp} = Elements of Matrix A^n

B_w = wall-fluid friction coefficient ($\rho|v|f_w/8$)

b = parameter in the bubble rise model

C = speed of sound

C_D = drag coefficient for flow over submerged objects

C_g = speed of sound in vapor

C_o = parameter in the bubble rise model

C_p = specific heat at constant pressure

C_{pf} = specific heat evaluated at film temperature

C_{pg} = specific heat of vapor phase

$C_{p\ell}$ = specific heat of liquid phase

1356 014

C_{pgs} = specific heat of saturated vapor phase

$C_{p\ell s}$ = specific heat of saturated liquid phase

C_v = specific heat at constant volume

$(C_d^*)_j^n$ = coefficient

D = diameter of round tube or pipe

D_{he} = heated equivalent diameter

D_{h_i} = hydraulic diameter of flow area A_i

D_{hy} = wetted equivalent diameter = 4x cross sectional area/wetted perimeter

D_r = diameter of rod in a rod array or an annulus

E = total energy per unit volume

E^* = vector

e = total energy per unit mass

e_j = junction total specific energy = $h_j + \frac{1}{2}\left[\frac{W_j}{\rho_j A_{j(t)}}\right]^2 + z_j - z_i$

$\mathcal{J}_j$ = junction momentum flux factor

F_j = coefficient in linearized junction momentum flux and friction

$$= I_j^{-1} - \left(\frac{K_j S_{gn}(W_j^n)}{\rho_j^n \pm A_j(t^n)1^2} + 2\mathcal{J}_j^n \right) W_j^n$$

1356 015

F_{fi} = Fanning friction pressure loss within each half-volume, $V_i/2$,

$$= \frac{f_i \ell_i \bar{W}_i \bar{W}_i}{D_{h_i} \bar{\rho}_i A^2}$$

F_{fj} = junction friction pressure caused by form drag losses and area changes

$$= \left(\frac{K_j S_{gn}(W_j)}{2\rho_j (A_j(t))} \right) W_j^2$$

F_w = friction pressure gradient due to wall

f = Fanning friction factor for mixture = 4x Moody friction factor

G = mass flux

g = gravitational acceleration = 32.174 ft/s^2

$\tilde{g}$ = volumetric body force vector

g_c = conversion factor = 32.174 $(ft\text{-}lb_m)/(lb_f\text{-}s^2)$

g_x = axial component of acceleration due to gravity

H = slip or holdup ratio = v^g/v^ℓ

h = mixture enthalpy per unit mass = $(\alpha_g \rho_g h_g + \alpha_\ell \rho_\ell h_\ell)/\rho$

$h_{a_{eos}}$ = equation of state for enthalpy of phase "a"

h_c = convective heat transfer coefficient

1356 016

h_i = enthalpy of source volume i, i = K,L

h_j = specific fluid enthalpy of junction j

h_{fg} = heat of vaporization = $h_{gs} - h_{\ell s}$

h_{gs} = enthalpy of saturated vapor phase per unit mass

$h_{\ell s}$ = enthalpy of saturated liquid phase per unit mass

h_{in} = enthalpy at channel inlet

h_o = stagnation mixture enthalpy

h_{out} = enthalpy at channel outlet

$h_{j_{FILL}}$ = prescribed fill junction enthalpy

I = geometric inertia

I_j = geometric "inertia" for junction j

$$= \frac{\ell_k}{2A_k} + \frac{\ell_L}{2A_L}$$

KE_i = kinetic energy at volume center i,

$= \bar{W}_i^2/\bar{p}_i$

K_j = junction friction coefficient, dimensionless

k = thermal conductivity

k_g = thermal conductivity of vapor phase

k_ℓ = thermal conductivity of liquid phase

ℓ_i = length of control volume i

L = length

M = mass of fluid

$\dot{M}_{fg}$ = phase change rate per unit flow area

M_{gb} = mass of steam as bubbles below the mixture interface

M_i = total mass in volume i = $\bar{\rho}_i V_i$

ΔM_i^n = increment of total mass in volume i at time level n+1 = $M_i^{n+1} - M_i^n$

M_i^{n+1} = total mass in volume i at time level t^{n+1}

MF_i = momentum flux terms at volume i centers, = $\bar{w}_i^2/(\bar{\rho}_i A_i^2)$

MF_j = junction momentum flux terms = $\mathcal{J}_j w_j^2 \phi_{tp_j}^2$

m = parameter in bubble rise model

$\dot{m}$ = rate of vapor generation per unit volume

$\dot{m}_a$ = rate of formation of phase "a" per unit volume

Nu = Nusselt number

Nu_g = Nusselt number for the vapor phase

Nu_ℓ = Nusselt number for the liquid phase

NJUN = total number of junction nodes

NVOL = total number of volume nodes

$\tilde{n}$ = outward directed unit vector

p = thermodynamic pressure

$\tilde{p}$ = momentum per unit volume

P_{eos} = equation of state for pressure

P_{Kg} = gravity pressure differential from the center of volume K to junction j

$$= -g \int_k^j \rho \, dz$$

P_{Lg} = gravity pressure differential from junction j to the center of volume L

$$= - g \int_j^k \rho \, dz$$

P_o = stagnation pressure

Pr = Prandtl number

Pr_g = Prandtl number for the vapor phase

Pr_ℓ = Prandtl number for the liquid phase

P_{rod} = rod-to-rod pitch

P_{sat} = saturation pressure

P_t = throat pressure

Q_g = volumetric energy supply

Q_i = rate of heat energy transferred into volume i

Q_w = energy exchange between wall and fluid

q_w = heating rate at the wall per unit length

Q_{CHF} = critical heat flux

q_k = components of conductive heat flux

R = radius of round tube or pipe

R_r = radius of rod in rod array or an annulus

Re = Reynolds number

Re^g = Reynolds number for vapor phase

Re^ℓ = Reynolds number for liquid phase

S_f = surface enclosing the fluid in V_f

$S_{gn}(W_j)$= sign of W_j, = $\pm$ 1

1356 020

S_w = fluid surface in contact with the wall

s = entropy of mixture per unit volume = $(\alpha_\ell \rho_{\ell s} s_{\ell s} + \alpha_g \rho_{gs} s_{gs})/\rho$

s_{go} = entropy of vapor at stagnation conditions

s_{gs} = entropy of the saturated vapor per unit mass

$s_{\ell o}$ = entropy of liquid at stagnation conditions

$s_{\ell s}$ = entropy of the saturated liquid per unit mass

s_o = stagnation mixture entropy

T = temperature of the fluid

T_a = temperature of phase "a"

T_b = temperature of bulk coolant

T_f = film temperature

T_s = saturation temperature

T_w = wall temperature

ΔT_{sat} = $T_w - T_s$

T_{CHF} = wall temperature at critical heat flux

t = time

t^n, t^{n+1} = time levels

Δt^n = time step size at time level t^{n+1}

U = internal energy per unit volume

U_g = internal energy of vapor phase

U_ℓ = internal energy of liquid phase

U_i = total internal energy in volume i = $V_i\ u_i$

U_{gs} = internal energy of saturated vapor phase

$U_{\ell s}$ = internal energy of saturated liquid phase

ΔU_i^n = increment in total internal energy for volume i at time level $t^{n+1} = U_i^{n+1} - U_i^n$

u = average specific internal energy = $(\alpha_g \rho_g u_g + \alpha_\ell \rho_\ell u_\ell)/\rho$

u = internal energy per unit mass

u_a = specific internal energy of phase "a"

u_g = internal energy of vapor phase per unit mass

u_ℓ = internal energy of liquid phase per unit mass

u_{as} = specific internal energy of saturated phase "a" per unit mass

u_{gs} = internal energy of saturated vapor per unit mass

$u_{\ell s}$ = internal energy of saturated liquid per unit mass

V = control volume used in the averaging procedure

V_f = volume of fluid in the control volume

V_i = displacement of volume i

V_m = mixture volume

$\tilde{v}^f_s$ = velocity of the surface S_f

v = average velocity = $(\alpha_g \rho_g v^g + \alpha_\ell \rho_\ell v^\ell)/\rho$

$\tilde{v}$ = velocity vector of fluid with components v_i

$\hat{v}$ = intrinsic velocity

V_{bub} = velocity of steam at an interface relative to the interface velocity

v_z = velocity of fluid in the z direction

v^a = velocity of phase "a"

v^{gb} = velocity of gas in the mixture

W = net flow = $A\rho v = W^\ell + W^g$

$\bar{W}_i$ = average mass flow for volume i

W_p = shaft work of pump

W_j^{n+1} = mass flow into or out of volume i from junction j at time level t^{n+1}

$W^n_{j_{FILL}}$ = prescribed fill mass flow, either positive or negative at time level t^n

ΔW_j^n = increment in junction j flow over time step $\Delta t^n = W_j^{n+1} - W_j^n$

x_{tt} = Martinelli - Nelson - Lockhart parameter

x = thermodynamic quality = $\frac{(h-h_{\ell s})}{h_{fg}}$

X_e = equilibrium quality = $\frac{s_o - s_{\ell s}}{s_{gs} - s_{\ell s}}$

x_f = flowing quality = W^g/W

X_{fa} = flowing quality of phase "a" = W^a/W

X_o = stagnation equilibrium quality

Y = a vector of dependent variables

$\tilde{y}$ = position vector with components y_i

Z_{in} = mixture level

z = vertical distance above reference base

z_i = volume center height above reference height z

z_j = junction height above reference height z

$(\frac{\partial P}{\partial M})_i$ = thermodynamic derivative of pressure at constant total mass

$(\frac{\partial P}{\partial U})_i$ = thermodynamic derivative of pressure at constant total internal energy

GREEK LETTERS

α = vapor volume fraction

α_a = volume fraction of phase "a" ($\alpha_\ell = 1-\alpha_g$)

α_{gm} = average volume fraction of phase "a" in the mixture
= $M_{gb}/\rho_g V_m$

ε = porosity of rod array

μ = viscosity

μ_a = viscosity of phase "a"

μ_g = viscosity of vapor phase

μ_ℓ = viscosity of liquid phase

v_a = specific volume of phase "a" = $1/\rho_a$

ρ = density

ρ_a = thermodynamic density of phase "a"

ρ_g = density of the vapor phase

$\bar{\rho}_i$ = fluid density in volume i, = M_i/V_i

ρ_j = fluid density at junction j

ρ_ℓ = density of the liquid phase

ρ_{as} = density of phase "a" at saturation pressure

$\rho_{a_{eos}}$ = equation of state for fluid density phase of "a"

1356 025

ρ_{gb} = partial steam density in a two-phase mixture

ρ_{gs} = density of saturated vapor

$\rho_{\ell s}$ = density of saturated liquid

ϕ = gravity potential

ϕ^2_{tp} = two-phase friction multiplier

$\phi^2_{tP_i}$ = two phase flow friction multiplier for volume i

$\phi^2_{tP_j}$ = two phase flow friction multiplier for junction j

σ = surface tension

σ_{ij} = shear-stress tensor

T = torque

ω = weight fraction = $\alpha_g\rho_g/\rho$

Θ = "implicit-explicit" proportion multiplier

Ψ_f = property of the fluid

Ψ_i = fraction of each stream orginating in the steam dome

SUBSCRIPTS AND SUPERSCRIPTS

a = phase "a"

b = phase "b"

c = continuous phase

1356 026

g	=	vapor phase
i	=	volume index
i	=	momentum cell center
j	=	junction index
k	=	mass and energy cell center
ℓ	=	liquid phase
o	=	stagnation conditions
s	=	saturation
t	=	throat conditions
w	=	wall
z	=	z-direction
ℓo	=	liquid only
CHF	=	critical heat flux conditions
K,L	=	pertaining to volumes K or L
–	=	control volume average
| |	=	absolute value

I. SUMMARY

I. SUMMARY

RETRAN is a computer code package developed from the RELAP series of codes and reference data from extensive analytical and experimental work previously conducted relative to the thermal-hydraulic behavior of light-water reactor systems subjected to postulated accident and operational transient conditions. RETRAN represents a new computer code approach to perform water reactor accident and operational transient analyses. RETRAN includes proven thermal-hydraulic models obtained from current accident and operational transient analysis codes, as well as improved models from current codes and the addition of newly developed models. Thus, RETRAN is a computer code providing "best estimate" solutions to accident and operational transient problems. In contrast, most accident and operational transient analyses codes incorporate models containing various conservative assumptions and provide so called "conservative" solutions. The degree of safety margin included in these "conservative" solutions is not known or well understood, while any desired safety margin is simply added to a "best estimate" solution.

RETRAN includes homogeneous, equilibrium flow equations as found in RELAP4. However, RETRAN is constructed in a semi-modular and dynamic dimensioned form where additions to the code can be easily carried out as new and improved models are developed. The RETRAN code structure also allows a user the flexibility of adding or subtracting from the number of system volumes and junctions used in the input model without having to reconstruct the entire input.

Consistent with the development objectives for RETRAN, computational efficiency, reliability, solution accuracy and "best estimate" models; RETRAN was structured to be semi-modular and dynamic dimensioned and includes:

- improved numerics,
- an iterative steady-state initialization,
- a two-surface heat transfer model,
- modified fills for time dependent P, h entry,
- friction factors,
- two-phase multipliers,
- flow regime maps,

- constant heat transfer coefficient option,
- improved non-conduction heat exchanger model,
- two-phase heat transfer correlations,
- trip logic models,
- control system models,
- transport delay model,
- non-equilibrium pressurizer models,
- auxiliary DNB model

By using the semi-modular and dynamic dimensional structure, future code developments resulting in new models may be tried and proven before the models are inserted into the code. The gradual progression of incorporating these models and improvements will be much easier within the RETRAN code structure than for a code which does not have a semi-modular and dynamic dimensioned structure. The ultimate goal in developing RETRAN was to provide an effective analytical tool that is flexible and user oriented.

The RETRAN code package stems from the development of two separate code packages, RELAP/E and RETRAN. Both of these codes were based upon RELAP4/003 update 85 as released by the United States Nuclear Regulatory Commission, NRC, as a portion of the Water Reactor Evaluation Model, WREM [I-1]. RELAP/E was developed to provide a "best estimate" to the thermal-hydraulic behavior of light-water reactor systems subjected to postulated accident transients such as those resulting from a hypothetical LOCA. RETRAN (RELAP4 TRANSIENT) was developed to describe the thermal-hydraulic behavior of light-water reactor systems subjected to postulated transients such as those resulting from anticipated operational transients (Condition II events), or transients included in Condition III, or Condition IV events as defined in ANSI N18.2 for Pressurized Water Reactor, PWR, systems and, as suggested, in N-212 ANS-22 for Boiling Water Reactor, BWR, systems. After careful consideration and since both codes were based on the same fluid differential and state equations of RELAP4, and since RELAP/E was constructed for ease of model incorporation with its semi-modular and dynamic structure, the operational transient models were added as options to RELAP/E and the code name RETRAN was retained.

The documentation of the RETRAN Code package includes four separate volumes: In Volume I the general equations and numerical schemes are derived from first

principles and all assumptions and limitations used in these derivations are presented; Volume II is directed at the programmer in that it presents the general coding philosophy, code details, the various RETRAN modules, flow charts, selection logic and subroutine and function subprogram definitions; Volume III is directed at the user in that it presents a program summary description, input data requirements, error messages and sample problems; Volume IV is directed at the application of the RETRAN Code to specific problems with emphasis on the significance, sensitivity and limitations of input variables, equations and models.

In general, the representation of a nuclear steam supply system, NSSS, for transient thermal-hydraulic analyses is relatively complex. For a given system the level of geometric detail can vary depending on the intent of the analysis. For example, detailed modeling of the reactor primary coolant system is required for the transient analysis of a hypothetical LOCA. In contrast, if the transient response of the reactor system to a small pertubation in pump performance is desired, the model can be less detailed since the phenomenon being modeled is a very general response of the system. RETRAN can model flow conditions within both the primary and secondary systems of the reactor and can handle a variety of transient responses within the overall system. In addition to having the capability of various degrees of model sophistication, a model can be established where extensive detail is used to represent one particular part of the system or a particular component combined with a very gross general model for the remainder of the system. An example of this would be the detailed model of a hot fuel channel for DNB analysis where the remaining parts of the system such as the steam generator for a PWR, the pump, piping and upper and lower plenums can be modeled with less detail.

RETRAN contains the same fluid differential and state equations as RELAP4 for describing homogeneous equilibrium flow in one dimension, with improvements for moving interphase fronts. The representations used in previous RELAP codes for control volumes and junctions are used in RETRAN also. The equation systems which describe the flow conditions within the channels are obtained from local fluid conservation equations by use of integral-averaging operations. In this manner, the volume and junction representation can be utilized to represent the fluid transient conditions in any parts of the components which comprise the overall reactor system and to any level of detail which the analyst so chooses within the basic constraints of homogeneous equilibrium flow.

The heat conduction representation capabilities of RETRAN have been increased over previous RELAP versions. The main advantage in RETRAN is the capability to more accurately calculate two-sided heat transfer. The two sided heat transfer representation allows different heat transfer regimes to be determined implicitly on both sides of a boundary so that representations of the heat transfer processes occurring in the steam generator for example, are much more accurate than previously possible. The appropriate heat transfer correlation is selected based on local conditions in each of two flow streams, on either side of a heat-conducting solid.

The reactor kinetics capabilities in RETRAN include the commonly used point kinetics model for the LOCA analysis and operational transient analysis.

The system component models utilized in RETRAN include a pump model which describes the interaction between the centrifugal pump and the primary system fluid, valve models which range in capabilities from simple valves to check valves to inertial valves which can all be signaled open or closed subject to user specified conditions. The flexibility of the valves and their configuration is very important in allowing a wide variety of options to the user for modeling plant response. Several representations for heat exchangers can be modeled by the code. The most realistic method is by the utilization of the previously discussed two-sided heat transfer where the fluid volumes on both the primary side and secondary side of the system are used for determining local conditions. Several more simplistic representations of the heat exchangers take the form of the special boundary condition used in conjunction with a heat conduction model. A non-equilibrium pressurizer can be modeled in RETRAN in which the thermodynamic state solution of each pressurizer region is determined from a distinct mass and energy balance on that region. The timing of feedback effects either from the core or a steam generator can be properly modeled with the transport delay model which considers the movement of fluid through a region as a slug. The auxiliary DNB model provides for the analysis of a hot subchannel with the determination of the DNB ratio as a function of channel position. A variety of trip controls, control system models and trip logic models have been included in RETRAN which can specify control functions typical of a reactor system and the sequence in which they are operated.

One of the most significant improvements represented by RETRAN in contrast to previous versions of large transient analysis codes lies in the numerical methods which are used to solve the differential equations.

Improvements in the sparse matrix inversion technique have resulted in a greatly speeded up flow solution. By taking advantage of this speed up, an iterative technique has been developed which couples time step selection to the flow solution accuracy. In this manner, rapidly changing phenomena are sensed and the time step adjusted. If flows are not changing rapidly, very large time steps are used. This technique, called explicit time step selection, reduces the running time and guarantees a flow solution accurate to within a given tolerance supplied by the user.

The causal volume concept allows selective updating of volume properties based on time rates of change of mass and energy. If these parameters change less than a prescribed amount in any volume, these volumes do not require a call to the state property routines. The net result is a decrease in running time. Similar concepts are also used for the temperature solution of heat conductors.

II. FLUID DIFFERENTIAL AND STATE EQUATIONS

Most engineering analyses of fluid flows are conducted with equation systems which describe the average flow and state of the fluid within the flow channel. In general, the flow field characteristics of interest to engineers are usually average or overall quantities. For example, in the case of single phase, single component flows in simple channels, engineers are usually more interested in the average fluid velocity across the channel rather than the detailed distribution of the velocity within the channel. The equation systems which describe the average conditions within the channel are obtained from the local Navier-Stokes equations by use of averaging operations. Application of the averaging procedures will introduce, among other quantities, the shear stresses acting on the fluid by stationary surfaces bounding the flow field. These stresses are usually accounted for by use of empirical correlations for the friction factor. Empirical correlations are also required and used for situations in which the detailed description of some phenomena is either incomplete or unknown. For example, while exact mathematical definitions are available for all quantities which enter into the averaged equations, evaluation of the definitions, in order to obtain a usable engineering model, will usually require introduction of assumptions and approximations.

A wide variety of averaging procedures has been employed in order to obtain equation systems for engineering analyses. In general, various spatial averages, volume or area averages for example, time averages, and combined space-time averages have been used. All of these procedures will not be reviewed in the present report. A brief summary of the available information is given here. A number of books contain derivations of the different kinds of averaged equations. Among the books which contain equation systems applicable to engineering analyses are those of Bird et al.,[II-1] Hewitt and Hall-Taylor,[II-2] Brodkey,[II-3] Govier and Aziz,[II-4] Slattery,[II-5] and Vennard.[II-6] These books contain several different equation systems which are applicable to many single and two-phase flows of interest to engineers. A large number of equation systems has appeared in the engineering literature directed primarily toward obtaining detailed descriptions of the dynamic behavior of two-phase flows.[II-7 through II-30] These equation systems have been obtained by use of a wide variety of methods and procedures. Among the most general derivations are those of Vernier and Delhaye,[II-27] Ishii[II-28, II-30] and Kocamustafaogullari.[II-29] The

two-phase flow models contained in References II-7 through II-29 are more detailed than the model currently employed in RETRAN. However, some of the averaging procedures used in the derivation of these models are the same procedures employed in this report. In particular, the material in References II-31 through II-33 is directly applicable to the present report.

The fluid balance equations of mass, linear momentum, and energy in RETRAN are integral macroscopic balances.[II-1, II-3, II-5] These equations are derived in the following sections. The equations and models which give the "micro" constitutive equations for momentum and energy exchange between the fluid and the flow channel walls, and the "macro" constitutive equations relating to the flow path geometry are also given.

1.0 LOCAL FLUID EQUATIONS

The macroscopic fluid balance equations can be obtained by application of integral techniques to the local instantaneous Navier-Stokes equations. Because some of the mathematical concepts employed in obtaining the macroscopic equations are the same as those used in obtaining the local instantaneous equations, a short derivation of the local equations will be given here. In the course of this derivation, several mathematical procedures will be employed which will be useful in later discussions.

The local equations are obtained by use of a general property balance [II.1-1,II.1-2] applied to an element of volume V which is in the flow field. The surface of the volume is denoted by S. A representation of the flow field and the volume V is shown in Figure II.1-1. The element of volume moves with the local fluid stream velocity $\tilde{v}$. The property per unit volume of the material will be denoted by Ψ. The property per unit volume Ψ may be any scalar, vector, or tensor property of interest. For the derivation of interest here, Ψ will be assigned as the mass, momentum, and energy per unit volume. The flow of the property per unit area and time across the surface of V is denoted by $\tilde{\Psi}$ and the generation of the property per unit volume and time is denoted by $\dot{\Psi}_g$.

The general status of the property Ψ within V can be established as follows. The time rate of change of the property within the volume V is given by

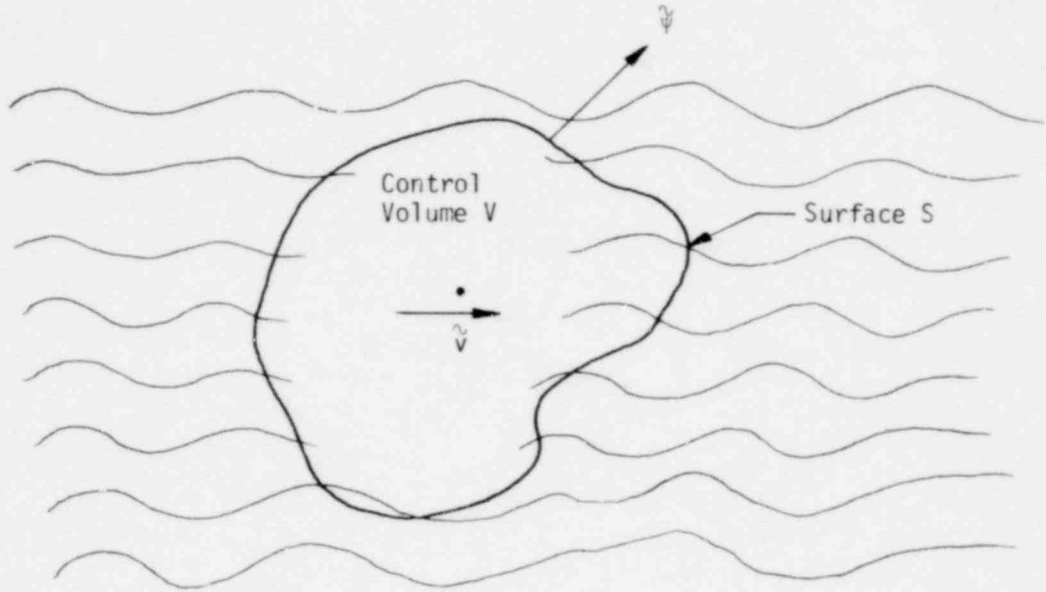

Figure II.1-1 Control Volume V in the Flow Field

$$\frac{d}{dt} \int_V \Psi \, dV \quad . \tag{II.1-1}$$

The net flow of the property across the surface of V is given by the integration of the flux of the property across the surface $\tilde{S}$ as

$$\int_S \tilde{\Psi} \cdot d\tilde{S} \tag{II.1-2}$$

The generation of the property within V is given by

$$\int_V \dot{\Psi}_g \, dV \quad . \tag{II.1-3}$$

The general balance statement for the property can be stated as

$$\begin{bmatrix} \text{the time rate} \\ \text{of change of} \\ \Psi \text{ within V} \end{bmatrix} = -\begin{bmatrix} \text{the net flow of} \\ \Psi \text{ across the} \\ \text{surface of V} \end{bmatrix} + \begin{bmatrix} \text{generation of} \\ \Psi \text{ within V} \end{bmatrix}, \tag{II.1-4}$$

where the negative sign on the right hand side is used because the integral of Equation II.1-2 is negative for net inflow. Substituting Equations II.1-1, II.1-2, and II.1-3 for the respective quantities in Equation II.1-4 gives

$$\frac{d}{dt} \int_V \Psi \, dV = -\int_S \tilde{\Psi} \cdot d\tilde{S} + \int_V \dot{\Psi}_g \, dV \quad . \tag{II.1-5}$$

Equation II.1-5 can be rearranged to a more useful form as follows. The left hand side is expanded by use of the Reynolds transport theorem, or the Leibnitz formula[II.1-1, II.1-2] which gives the time rate of change of an integral as

$$\frac{d}{dt} \int_V \Psi \, dV = \int_V \frac{\partial \Psi}{\partial t} \, dV + \int_S \Psi \tilde{v} \cdot d\tilde{S} \quad , \tag{II.1-6}$$

where the last term on the right hand side accounts for the motion of the surface of V at the velocity $\tilde{v}$. The surface integrals in Equations II.1-5 and II.1-6 are converted to volume integrals by use of Gauss' theorem in the form

$$\int_V \tilde{\nabla}\cdot\tilde{B}\, dV = \int_S \tilde{B}\cdot d\tilde{S} \quad , \qquad \text{(II.1-7)}$$

where the operator $\tilde{\nabla}$ is given by

$$\tilde{\nabla} \equiv \tilde{n}_i \frac{\partial}{\partial x_i} \qquad \text{(II.1-8)}$$

where the $\tilde{n}_i$'s are the unit vectors in the x_i directions.

For application of Equation II.1-7 to II.1-5, $\tilde{B} = \tilde{\Psi}$ and for application to Equation II.1-6, $\tilde{B} = \Psi\tilde{v}$. Substituting Equation II.1-6 into Equation II.1-5 and applying Equation II.1-7 to the surface integrals gives

$$\int_V \frac{\partial\Psi}{\partial t}\, dV + \int_V (\tilde{\nabla}\cdot\Psi\tilde{v})\, dV + \int_V \tilde{\nabla}\cdot\tilde{\Psi}\, dV - \int_V \dot{\Psi}_g\, dV = 0. \qquad \text{(II.1-9)}$$

Since Equation II.1-9 applies to any volume V, the general balance equation for the property Ψ is obtained as

$$\frac{\partial\Psi}{\partial t} + (\tilde{\nabla}\cdot\Psi\tilde{v}) + (\tilde{\nabla}\cdot\tilde{\Psi}) - \dot{\Psi}_g = 0. \qquad \text{(II.1-10)}$$

The local equations are obtained from Equation II.1-10 by substituting the property per unit volume, Ψ, the flux of the property, $\tilde{\Psi}$, and the generation of the property $\dot{\Psi}_g$ into Equation II.1-10. These local equations are developed in the following sections.

1.1 Local Continuity Equation

The conservation of mass, or the continuity equation, is obtained as follows. The property Ψ is the mass per unit volume, or the density ρ. The flux $\tilde{\Psi}$ is zero since the bounding surface S of the volume element V moves with the local velocity $\tilde{v}$. The generation of mass, $\dot{\Psi}_g$, is also zero.

With these definitions, Equation II.1-10 becomes

$$\frac{\partial}{\partial t}\rho + \tilde{\nabla}\cdot\rho\tilde{v} = 0 \quad , \qquad \text{(II.1-11)}$$

or, in terms of the Cartesian summation convention for indices,

$$\frac{\partial}{\partial t}\rho + \frac{\partial}{\partial x_i}\rho v_i = 0 \quad . \qquad \text{(II.1-12)}$$

1.2 Local Momentum Equations

The linear momentum balance, or momentum equation, is obtained as follows. The property Ψ is the momentum per unit volume $\rho\tilde{v}$. The flux of the property $\tilde{\Psi}$ is the surface stress tensor $\bar{\bar{T}}$, which represents the normal and shear stresses acting on the surface S. Momentum can be generated by volumetric body forces such as gravity so that $\dot{\Psi}_g$ is taken as $\rho\tilde{g}$. With these definitions, Equation II.1-10 becomes

$$\frac{\partial}{\partial t}\rho\tilde{v} + (\tilde{\nabla}\cdot\rho(\tilde{\tilde{v}}\tilde{v})) + \tilde{\nabla}\cdot\bar{\bar{T}} - \rho\tilde{g} = 0 \quad . \qquad \text{(II.1-13)}$$

Several operations can be performed with the terms in Equation II.1-13 as follows. The dyadic product $\tilde{\tilde{v}}\tilde{v}$ gives an array of nine components which is a special form of a second-order tensor. This product can be written as

$$\tilde{\tilde{v}}\tilde{v} = v_i v_k \ (i,k = 1, 2, 3), \qquad \text{(II.1-14)}$$

where all possible interactions of the vectors are obtained.

The surface stress tensor, $\bar{\bar{T}}$, is made up of the pressure and the normal and the shear stresses. The details of developing the mathematical form of $\bar{\bar{T}}$ is beyond the scope of the present report. The results for the case of a fluid in which the stress is a linear function of the rate of strain are given by[II.1-1, II.1-3, II.1-4, II.1-5]

$$\bar{\bar{T}} = p\bar{\bar{I}} - \bar{\bar{\sigma}} \ , \qquad \text{(II.1-15)}$$

where

p = pressure
$\bar{\bar{I}}$ = unit tensor
$\bar{\bar{\sigma}}$ = stress tensor.

The components of the stress tensor are given by

$$\sigma_{ij} = -\frac{2}{3}\mu\frac{\partial v_k}{\partial x_k}\delta_{ij} + \mu\left(\frac{\partial v_i}{\partial x_j} + \frac{\partial v_j}{\partial x_i}\right), \qquad \text{(II.1-16a)}$$

where

$$(i,j,k = 1, 2, 3),$$

and

$$\delta_{ij} = \begin{cases} 0, & i \neq j \\ 1, & i = j \end{cases} \qquad \text{(II.1-16b)}$$

and μ is a material property called the viscosity. Substituting Equations II.1-14 through II.1-16 into Equation II.1-13 gives a vector equation for the balance of linear momentum. Each component of the momentum equation can be written as

$$\frac{\partial}{\partial t}\rho v_i + \frac{\partial}{\partial x_j}\rho v_i v_j = -\frac{\partial p}{\partial x_i} + \frac{\partial}{\partial x_j}\sigma_{ij} + \rho g_i \quad , \qquad \text{(II.1-17)}$$

where the shear stresses are given by Equation II.1-16. More detailed development of the momentum equation is given in References II.1-1, II.1-3, II.1-4 and II.1-5.

1.3 Local Energy Equation

Several forms of the energy equation can be written. For the present report, the property Ψ is taken as the sum of the internal energy per unit volume, ρu, and the kinetic energy per unit volume $1/2\ \rho\ \tilde{v}\cdot\tilde{v}$. The flux of the property $\tilde{\Psi}$ is given by the conduction across the surface S and the work done by the surface forces. That is,

$$\tilde{\Psi} = \tilde{q} - \bar{\bar{T}}\cdot\tilde{v} \quad . \tag{II.1-18}$$

The generation of the property is taken as the work due to volumetric forces plus the volumetric supply of energy per unit volume, due to nuclear means for example. That is,

$$\dot{\Psi}_g = \rho\tilde{g}\cdot\tilde{v} + \dot{Q}_g \quad . \tag{II.1-19}$$

Substituting these expressions into Equation II.1-10 gives

$$\frac{\partial}{\partial t}\rho\left(u + \frac{1}{2}\tilde{v}\cdot\tilde{v}\right) + \left(\tilde{\nabla}\cdot\rho\left(u + \frac{1}{2}\tilde{v}\cdot\tilde{v}\right)\tilde{v}\right) = -\left(\tilde{\nabla}\cdot\left(\tilde{q} - \left(\bar{\bar{T}}\cdot\tilde{v}\right)\right)\right) + \rho\tilde{g}\cdot\tilde{v} + \dot{Q}_g \quad . \tag{II.1-20}$$

The constitutive equation for the stresses $\bar{\bar{T}}$ has been given by Equation II.1-16, and the constitutive equation for conduction is given by

$$q_i = -k\frac{\partial T}{\partial x_i} \tag{II.1-21}$$

where k is a material property called the thermal conductivity.

1.4 Fluid State Equations

At this point, the unknown dependent variables can be counted as the density, ρ, three velocity components, v_i (i = 1, 2, 3), the pressure, p, the specific internal energy, u, and the temperature, T, for a total of seven. The number of available equations is counted as one continuity, three momentum, and one energy, for a total of five. Thus, the five differential equations must be supplemented by two additional equations which do not introduce any additional unknowns. These additional equations can be obtained from the fundamental equation of the material [II.1-6] and are usually called the equations of state. These equations of state can be given by

$$\rho = \rho(p,u) \quad , \tag{II.1-22a}$$

and,

$$T = T(p,u) \quad , \qquad \text{(II.1-22b)}$$

where the independent variables are taken to be the pressure and specific internal energy. Other combinations of dependent and independent variables are of course possible. Finally, we note that the material properties μ and k are not constant but instead are functions of the state of the material and that the volumetric energy source $\dot{Q}_g$ must also be specified.

1.5 Summary of the Local Equations

The development of the local equations given above is not meant to be an exhaustive review of the subject. Instead, only a brief outline of the development of the local equations by use of the general property balance has been given. In particular, details of the development of the constitutive equations for the stresses $\bar{\bar{T}}$ and the conduction $\tilde{q}$ have not been given and the many additional forms of the energy equation have not been discussed. The local instantaneous equations are summarized here for convenience. The conservation of mass, or continuity equation, of Equation II.1-12 is given by

$$\frac{\partial}{\partial t} \rho + \frac{\partial}{\partial x_i} \rho v_i = 0 \quad . \qquad \text{(II.1-23)}$$

The balance of linear momentum of Equation II.1-17 is given by

$$\frac{\partial}{\partial t} \rho v_i + \frac{\partial}{\partial x_j} \rho v_i v_j = - \frac{\partial p}{\partial x_i} + \frac{\partial}{\partial x_i} \sigma_{ij} + \rho g_i \quad , \qquad \text{(II.1-24a)}$$

where the shear stresses are given by

$$\sigma_{ij} = - \frac{2}{3} \mu \frac{\partial v_k}{\partial x_k} \delta_{ij} + \mu \left(\frac{\partial v_i}{\partial x_j} + \frac{\partial v_j}{\partial x_i} \right) \quad . \qquad \text{(II.1-24b)}$$

The equation for the sum of the internal and kinetic energy, Equation II.1-20, can be written as

$$\frac{\partial}{\partial t} \rho \left(u + \frac{1}{2} v_i v_i\right) + \frac{\partial}{\partial x_i} \rho \left(u + \frac{1}{2} v_j v_j\right) v_i = \frac{\partial}{\partial x_i}\left(k \frac{\partial T}{\partial x_i}\right) - \frac{\partial}{\partial x_i} p\, v_i$$

$$- \frac{\partial}{\partial x_i} \sigma_{ij} v_j + \rho\, g_i\, v_i + \dot{Q}_g \quad , \qquad \text{(II.1-25)}$$

where the summation convention has been used. The equations of state are

$$\rho = \rho(p,u) \qquad \text{(II.1-26a)}$$

and

$$T = T(p,u). \qquad \text{(II.1-26b)}$$

We assume that the material properties μ and k, as well as the volumetric energy supply $\dot{Q}_g$ are known.

2.0 MACROSCOPIC FLUID EQUATIONS

In general, Equations II.1-23 through II.1-26 provide sufficient information to calculate the distributions of the dependent variables throughout the flow field which the fluid may occupy. Additional information must be supplied for the initial conditions of the fluid and the conditions at the boundaries of the flow field. However, at the present time most engineering analyses, including analyses of hypothetical LOCA's, are conducted with simplified one-dimensional, models of thermal-hydraulic systems. For flows in simple geometries, fairly rigorous averaged models can be obtained along with the necessary constitutive equations. For example, in the case of flow in a straight flow channel with a constant cross sectional area, area averaging of Equations II.1-23 through II.1-26 can be rigorously evaluated. In the process of area averaging, information relating to the detailed distribution of the dependent variables normal to the channel walls is lost and the effects of the distributions are accounted for by the use of empirical constitutive models. It is important to note that for these simple geometries, the flow is essentially one-dimensional.

The case of flow in complex thermal-hydraulic loops is, in many situations of interest, far from one-dimensional. For example, abrupt expansions and contractions and other flow channel geometry changes may occur in the system. Often, the flow may divide from a single stream into multiple streams or converge from multiple streams into a single stream. In the case of NSSS's, although the flow may be essentially one-dimensional during steady-state operation, during hypothetical LOCA's the flow may become very complex. When Equations II.1-23 through II.1-26 are averaged for these complex geometries and flows, a large amount of engineering experience must be employed when the resulting models are applied to analysis of the thermal-hydraulic characteristics of the systems. As noted by Slattery,[II.2-1] the importance of integral, or averaged, models in engineering analysis cannot be overstressed. However, again as noted by Slattery, the simplicity of the models is misleading in that a series of approximations often based on intuitive judgement or related experimental data is an implicit part of the models. Continued comparisons of the predictions of the model with data are necessary in order to

determine both the soundness of the approximations associated with the model and the techniques employed in application of a one-dimensional model to complex, multi-dimensional systems.

In order to obtain the averaged equations, the local instantaneous formulation of Equations II.1-23 through II.1-26 are integrated over a finite volume of the flow system. The equations which are obtained by this procedure express the overall balance of mass, momentum and energy. Usually, four overall balance equations, one each for mass, momentum, energy, and mechanical energy (the Bernoulli equation), are obtained. The latter equation is used in many engineering analyses of steady single-phase flow. Two methods may be used to obtain the overall balances. The first method uses the detailed equations, Equations II.1-23 through II.1-26, which are integrated over the finite volume. In the second method, a general overall balance equation, analogous to Equation II.1-5 is employed along with proper accounting of the property, property fluxes and generation. The first method will yield more detailed accounting of the effects of the local distributions within the finite volume while the second method is more direct since only the overall effects are considered. In general, the model employed in RETRAN and most other engineering models, is a combination of the two approaches in which the former method is employed to obtain information which can be used in the overall equations. For example, the effects of local flow perturbations can be analyzed by use of the former method and the results of the analysis incorporated into the model obtained from application of the latter method. In fact, this process can be extended to the point at which the local instantaneous equations are solved in order to obtain information which can be used in a less detailed model.

Representations of several flow geometries which may be encountered in thermal-hydraulic loops are shown in Figures II.2-1 and II.2-2. The abrupt area change shown in Figure II.2-1a is among the more simple hydraulic loop elements that may be encountered. In addition, for the case of flow from left-to-right, well defined analytical models, which compare well with data, are available. As previously mentioned, the flow in the geometry shown in Figure II.2-1a is essentially one-

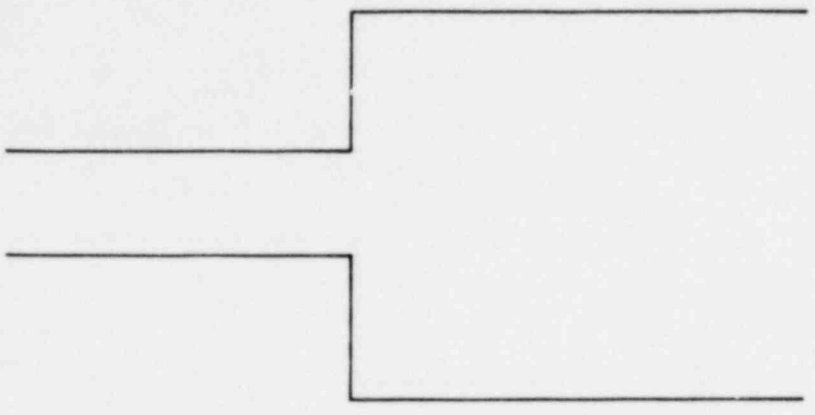

(a) Abrupt Area Change

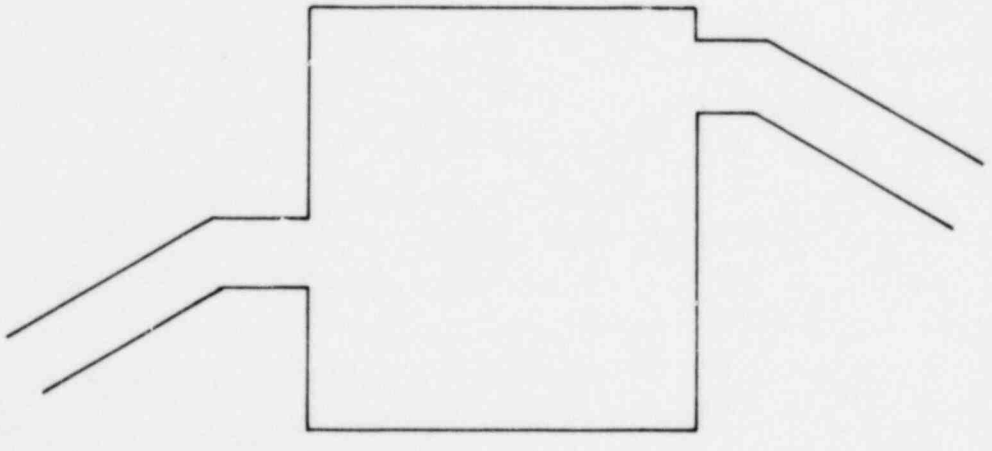

(b) Abrupt Area Changes and Changes in Flow Direction

Figure II.2-1 Finite Volume Hydraulic Loop Elements

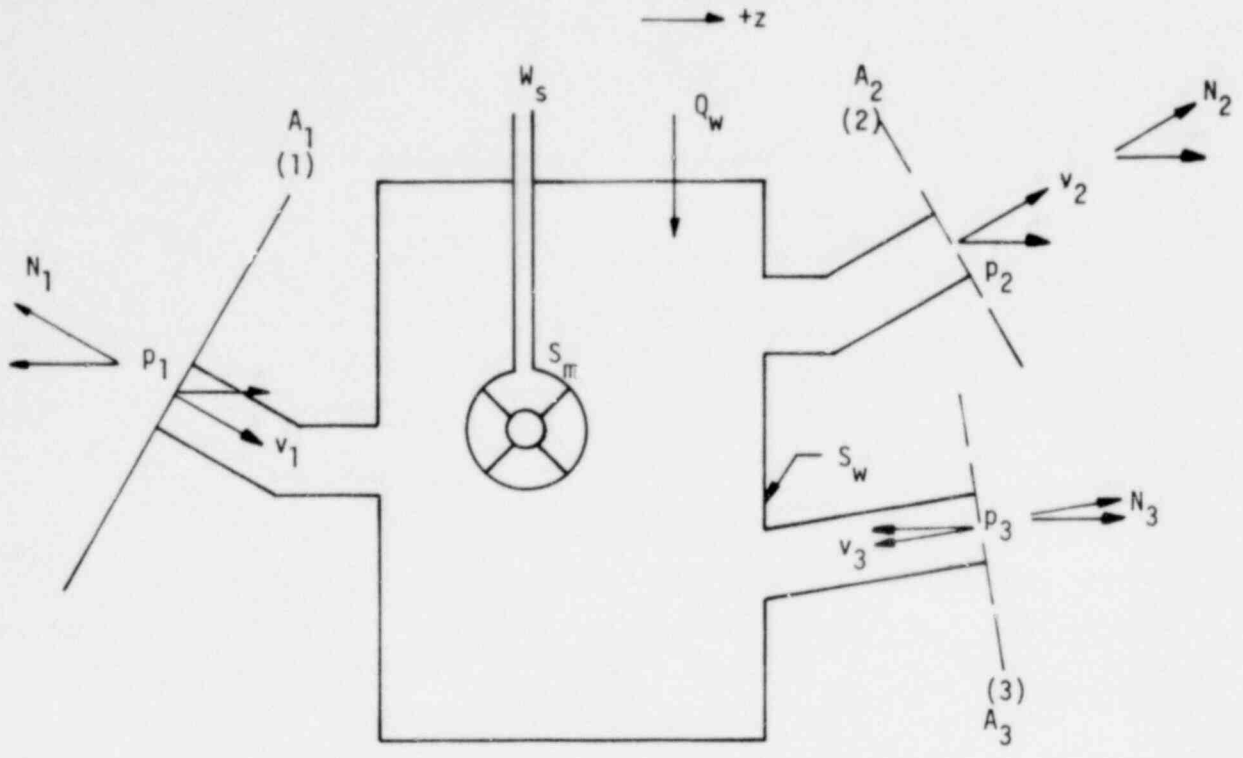

(a) Area and Flow Direction Changes and Possible Flow Divisions and Combining

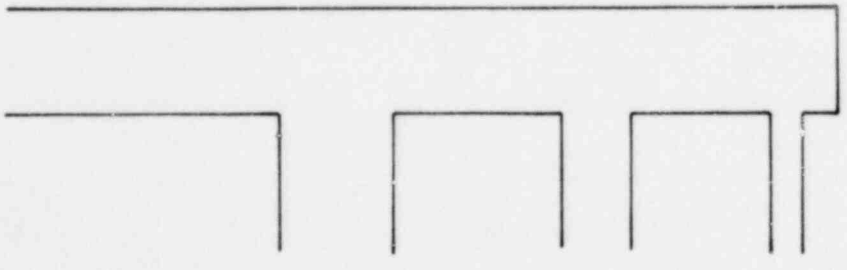

(b) Flow Distribution Manifold

Figure II.2-2 Geometrically Complex Finite Volume Hydraulic Loop Elements

dimensional. The geometries shown in Figures II.2-1b, II.2-2a and II.2-2b are very much more multi-dimensional in nature especially considering the fact that fluid may be flowing into or out of the volumes by a variety of flow paths.

The objective is to obtain an overall description of the thermal-hydraulic characteristics of these complex geometries. This objective will be attained by applying general averaging procedures to the local equations. The results of this operation will be simplified by application of the approximations inherent in the model employed in RETRAN. The finite volume element shown in Figure II.2-2a will be used to illustrate the derivation of the overall balance equations.

2.1 General Equations

The macroscopic balance equations are obtained from the local equations given in the previous sections by use of the generalized Reynolds transport theorem, given by

$$\frac{d}{dt}\int_V \Psi \, dV = \int_V \frac{\partial \Psi}{\partial t} \, dv + \int_S \Psi \, \tilde{v}_s \cdot d\tilde{S} \quad . \qquad \text{(II.2-1)}$$

In Equation II.2-1, V is the control volume, S is the surface of the volume V, and $\tilde{v}_s$ is the velocity of the surface S. The surface S is specified by letting S_w denote the stationary walls of the flow channel, A_j denote the flow surfaces at the entrances and exits of the control volume, and S_m denotes the movable wetted surface which allows transfer of energy between the fluid in the control volume and the surroundings in the form of shaft work. The various aspects of the geometry of the flow channel are shown in Figure II.2-2a. Green's theorem relating volume and surface integrals, Equation II.1-7, will also be employed.

2.2 Macroscopic Mass Balance

The local conservation of mass equation has been given by Equation (II.1-23) as

$$\frac{\partial \rho}{\partial t} + \frac{\partial}{\partial x} \rho v_i = 0 \quad , \qquad \text{(II.2-2)}$$

where ρ is the fluid density and $\tilde{v}$ is the fluid velocity. The property per unit volume for use in Equation II.2-1 is the density, ρ. Substituting the density into Equation II.2-1 gives

$$\frac{d}{dt}\int_V \rho \, dV = \int_V \frac{\partial \rho}{\partial t} \, dV + \int_S \rho \tilde{v}_s \cdot d\tilde{S} \quad . \qquad \text{(II.2-3)}$$

Operating on Equation II.2-2 with $\int_V dV$ gives

$$\int_V \frac{\partial \rho}{\partial t} \, dV + \int_V \frac{\partial}{\partial x_i} \rho v_i \, dV = 0 \quad , \qquad \text{(II.2-4)}$$

and applying Green's theorem, Equation II.1-7, to the second integral gives

$$\int_V \frac{\partial \rho}{\partial t} \, dV + \int_S \rho \tilde{v} \cdot \tilde{n} \, dS = 0 \quad . \qquad \text{(II.2-5)}$$

Substituting Equation II.2-5 into Equation II.2-3 gives

$$\frac{d}{dt} \int_V \rho \, dV = - \int_S \rho \, (\tilde{v} - \tilde{v}_s) \cdot \tilde{n} \, dS \quad . \qquad \text{(II.2-6)}$$

Equation II.2-6 is a general statement of the conservation of mass in the control volume V.

The right-hand side of Equation II.2-6 can be expanded by use of the specifications of the surface S given previously to obtain

$$\frac{d}{dt}\int_V \rho \, dV = - \int_{S_w} \rho(\tilde{v} - \tilde{v}_s) \cdot \tilde{n} \, dS - \int_{\Sigma A_j} \rho(\tilde{v} - \tilde{v}_s) \cdot \tilde{n} \, dS - \int_{S_m} \rho(\tilde{v} - \tilde{v}_s) \cdot \tilde{n} \, dS \quad . \qquad \text{(II.2-7)}$$

Equation II.2-7 is simplified by noting that no mass enters the control volume on the surfaces S_w and S_m and that the surface of the control volume is stationary at the flow area A_j. The latter condition can be approximated in practice by using a control volume which is larger than the moving surface S_m. Substituting this information into Equation II.2-7 gives

$$\frac{d}{dt}\int_V \rho \, dV = - \int_{\Sigma A_j} \rho \tilde{v} \cdot d\tilde{S} \quad . \qquad \text{(II.2-8)}$$

The left-hand side of Equation II.2-8 is the time rate of change of the mass of fluid in the volume V so that Equation II.2-8 can be written

$$\frac{dM}{dt} = - \int_{\Sigma A_j} \rho \tilde{v} \cdot d\tilde{S} = - \int_{\Sigma A_j} \rho \tilde{v} \cdot \tilde{n} \, dS \quad , \qquad \text{(II.2-9)}$$

where

$$M = \int_V \rho \, dV = \bar{\rho} V \qquad \text{(II.2-10)}$$

and $\tilde{n}$ is the outward directed unit normal to the flow areas A_j. Letting α denote the angle between $\tilde{v}$ and $\tilde{n}$, Equation II.2-9 can be written

$$\frac{dM}{dt} = - \int_{\Sigma A_j} (\rho v) \cos\alpha \, dS \quad , \qquad \text{(II.2-11)}$$

where v is the magnitude of the velocity vector $\tilde{v}$.

For the situation shown in Figure II.2-2a with the flow areas at locations (1), (2) and (3) perpendicular to the plane of flow, Equation II.2-11 gives

$$\frac{dM}{dt} = (\rho v A)_1 - (\rho v A)_2 + (\rho v A)_3 \quad , \qquad \text{(II.2-12)}$$

or,

$$\frac{dM}{dt} = \sum_j W_j \, , \qquad \text{(II.2-13)}$$

where

$$W_j = (\rho v A \cos\alpha)_j \qquad \text{(II.2-14)}$$

It is important to note that Equation II.2-11 contains the product (ρv), thus Equation II.2-14 contains the average of this product and not the product of the average values of ρ and v. In almost all engineering analysis models, the assumption used is that the fluid density does not vary appreciably over the areas A_j. The velocity v in Equation II.2-14 is thus an average value over the cross-sectional areas. As mentioned previously above, a wide variety of averaging procedures has been used in obtaining equation systems applicable to engineering analysis of fluid flows.[II.2-1 through II.2-6] The objective of the present report is to document the equation system in RETRAN and thus some of the detailed aspects of averaging procedures are not given. The detailed aspects of the averaging procedures can be found in References II.2-1 and II.2-7 through II.2-10.

2.3 Macroscopic Linear Momentum Balance

The local momentum equations for linearly viscous fluids have been given by Equation II.1-24 as

$$\frac{\partial}{\partial t}\rho v_i + \frac{\partial}{\partial x_j}\rho v_i v_j = -\frac{\partial p}{\partial x_i} + \frac{\partial}{\partial x_j}\sigma_{ij} + \rho g_i, \qquad \text{(II.2-15a)}$$

where

$$\sigma_{ij} = -\frac{2}{3}\mu\frac{\partial v_k}{\partial x_k}\delta_{ij} + \mu\left(\frac{\partial v_i}{\partial x_j} + \frac{\partial v_j}{\partial x_i}\right). \qquad \text{(II.2-15b)}$$

The property per unit volume to be used in the generalized transport equation is $\Psi = \rho\tilde{v}$, so that Equation II.2-1 becomes

$$\frac{d}{dt}\int_V \rho\tilde{v}\, dV = \int_v \frac{\partial}{\partial t}\rho\tilde{v}\, dV + \int_S \rho\tilde{v}(\tilde{v}_s\cdot d\tilde{S}). \qquad \text{(II.2-16)}$$

Operating on Equation II.2-15 with $\int_V dV$ gives

$$\int_V \frac{\partial}{\partial t} \rho v_i \, dV + \int_V \frac{\partial}{\partial x_j} \rho v_i v_j \, dV = - \int_V \frac{\partial p}{\partial x_i} \, dV + \int_V \frac{\partial}{\partial x_j} \sigma_{ij} \, dV + \int_V \rho g_i \, dV \quad . \tag{II.2-17}$$

The first term on the left-hand side of Equation II.2-17 is the quantity required in Equation II.2-16. The other terms in the equation are rearranged as follows. The second term on the left-hand side is rewritten by application of Green's theorem, Equation II.1-7, to obtain

$$\int_V \frac{\partial}{\partial x_i} \rho v_i v_j \, dV = \int_S \rho \tilde{v} (\tilde{v} \cdot d\tilde{S}) \quad . \tag{II.2-18}$$

Applying Green's theorem to the first and second terms on the right-hand side of Equation II.2-17 gives

$$\int_V \frac{\partial p}{\partial x_i} \, dV = \int_S p \bar{\bar{I}} \cdot d\tilde{S} \quad , \tag{II.2-19}$$

and

$$\int_V \frac{\partial}{\partial x_i} \sigma_{ij} \, dV = \int_S \bar{\bar{\sigma}} \cdot d\tilde{S} \quad , \tag{II.2-20}$$

respectively. The last term on the right-hand side of Equation II.2-17 represents the volumetric body force, given by

$$\int_V \rho g_i \, dV = M g_i = \bar{\rho} V g_i \quad . \tag{II.2-21}$$

Substituting Equations II.2-18 through II.2-21 into Equation II.2-17 and then substituting the results into Equation II.2-16 gives

$$\frac{d}{dt} \int_V \rho \tilde{v} \, dV = - \int_S \rho \tilde{v} [(\tilde{v} - \tilde{v}_s) \cdot d\tilde{S}] - \int_S p \bar{\bar{I}} \cdot d\tilde{S}$$

$$+ \int_S \bar{\bar{\sigma}} \cdot d\tilde{S} + \bar{\rho} V \tilde{g} \quad . \tag{II.2-22}$$

The surface integrals on the right-hand side of Equation II.2-22 can be expanded by use of the specifications of the surface $\tilde{S}$ to obtain

$$\frac{d}{dt}\int_V \rho\tilde{v}\, dV = -\int_S \rho\tilde{v}[(\tilde{v} - \tilde{v}_s)\cdot d\tilde{S}] - \int_S p\bar{\bar{I}}''d\tilde{S}$$

$$- \int_{\Sigma A_j} \rho v[(\tilde{v} - \tilde{v}_s)\cdot d\tilde{S}] - \int_{S_w} p\bar{\bar{I}}\cdot d\tilde{S} - \int_{S_m} p\bar{\bar{I}}\cdot d\tilde{S} - \int_{\Sigma A_j} p\bar{\bar{I}}\cdot d\tilde{S} \qquad \text{(II.2-23)}$$

$$+ \int_{S_w} \bar{\bar{\sigma}}\cdot d\tilde{S} + \int_{S_m} \bar{\bar{\sigma}}\cdot d\tilde{S} + \int_{\Sigma A_j} \bar{\bar{\sigma}}\cdot d\tilde{S} + \bar{\rho}V\tilde{g}$$

The first two integrals on the right-hand side of Equation II.2-23 are zero on flow rate of momentum flow into and out of the control volume. Evaluation of the third term gives

$$\int_{\Sigma A_j} \rho\tilde{v}[(\tilde{v} - \tilde{v}_s)\cdot d\tilde{S}] = \sum_{A_j} \rho_j v_j^2 \tilde{A}_j \quad , \qquad \text{(II.2-24)}$$

where $\tilde{A}_j$ denotes a vector the magnitude of which is the flow area A_j. The direction of $\tilde{A}_j$ is parallel to the flow direction and points in the direction of flow.[II.2-2] As shown in Figure II.2-2a, the flow areas are perpendicular to the flow channel walls. The density has been assumed to be constant across the flow areas A_j. The velocity appears in Equation II.2-24 as the area average of the square of the velocity. The assumption that the velocity is uniform over the flow area is usually employed.[II.2-2 through II.2-4] If the detailed velocity distribution is known, the deviation between the average of the velocity squared and the square of the average velocity can be evaluated and thus be accounted for in the momentum equation. The assumption of a uniform velocity distribution is generally acceptable for the case of single phase turbulent flow. Experimental data indicate that velocity distributions in two-phase flows are not as nearly uniform as single-phase flows.[II.2-3] The assumption of uniform velocity distributions is employed in RETRAN.

The fourth through ninth terms in Equation II.2-23 represent various forces acting on the control volume. The fourth and seventh terms represent friction and pressure drag forces due to the stationary walls of the flow channel. The fifth and eighth terms represent friction and pressure drag on the moving surfaces, such as pumps and turbines. The sixth and ninth terms represent the transport

of momentum by pressure and viscous action at the flow areas of the control volume. The contribution of the ninth term is almost always neglected in engineering analyses.

It is important to note that rigorous evaluation of the surface integrals of Equation II.2-23 requires that the detailed pressure and velocity distributions be known within the control volume. In general, these detailed distributions are available for only the simplest of single-phase flows in simple flow channel geometries. For most situations of interest to engineers, experimental data must be available in order to obtain correlations or models for the surface integrals. These data are required for both development and verification of correlations and models.

The abrupt area change shown in Figure II.2-1a is among the more simple flow perturbations. Evaluation of the pressure drag for the case of flow from the left into the expansion requires that the pressure distribution on the stationary surfaces be assumed. Fortunately, the assumption generally employed for this flow results in a model which compares well with data. The flow channel of Figure II.2-2a is extremely complex and a variety of pressure and flow distributions can occur because of the possible distributions of flow into and out of the channel. Evaluation of the integrals of Equation II.2-23 for the case of transient, compressible, two-phase flow in the channel shown in Figure II.2-2a is not possible at the present time. In general, steady-state empirical correlations are employed in analyses of these flows.

As noted above, the fourth and seventh terms on the right-hand side of Equation II.2-23 represent friction and pressure drag forces due to the stationary walls of the flow channel. These terms are modeled as the sum of the shear friction along the walls plus additional contributions to the forces due to local flow perturbations such as expansions, contractions, spacer grids, elbows, and tees and other junctions. For the present time, only a general representation of these drag forces is required. Denoting the wall friction by $\tilde{F}_w$ and the local perturbations by $\tilde{F}_{\ell oc}$, the fourth and seventh terms are written as

$$-\tilde{F}_w - \tilde{F}_{\ell oc} = \int_{S_w} [-p\bar{\bar{I}} + \bar{\bar{\sigma}}]\cdot d\tilde{S} \ . \qquad \text{(II.2-25)}$$

Specific models for $\tilde{F}_w$ and $\tilde{F}_{loc}$ are given in Section III of this report.

The fifth and eighth terms on the right-hand side of Equation II.2-23 represent the contribution to the integral momentum balance due to the moving surfaces. In general, in the case of RETRAN, the moving surfaces are associated with the pumps of the NSSS loops. At steady-state operating conditions, the pumps contribute a pressure increase in the fluid. During hypothetical transients, however, the fluid may begin to influence the behavior of the pumps. Under these conditions, an equation, or model, is required which accounts for the inertia and friction characteristics of the pumps. For the present time, only a general representation of the pump behavior is required. Denoting the pump contribution to the momentum balance by $\Delta\tilde{p}_p$, the fifth and eighth terms on the right-hand side of Equation II.2-23 are written as

$$\Delta\tilde{p}_p = - \int_{S_m} p\bar{\bar{I}}\cdot d\tilde{S} + \int_{S_m} \bar{\bar{\sigma}}\cdot d\tilde{S} \ . \qquad \text{(II.2-26)}$$

The specific form of the pump model available in RETRAN is given in Section VI of this report.

The sixth and ninth terms on the right-hand side of Equation II.2-23 represent the transport of momentum by pressure and viscous action at the flow areas of the control volume. The contribution of the viscous forces is almost always neglected in engineering analyses. Thus, we assume

$$\int_{\Sigma A_j} \bar{\bar{\sigma}}\cdot d\tilde{S} = 0 \ . \qquad \text{(II.2-27)}$$

The sixth integral can be evaluated to obtain

$$\int_{\Sigma A_j} p\bar{\bar{I}}\cdot d\tilde{S} = \sum_{A_j} p\tilde{A}_j \ , \qquad \text{(II.2-28)}$$

where the definition of the vector $\tilde{A}_j$ has been given following Equation II.2-24.

The general macroscopic momentum balance is obtained by substituting Equation II.2-24 through II.2-28 into Equation II.2-23. The resulting equation is

$$\frac{d}{dt}\int_V \rho\tilde{v}\, dV = -\sum_{A_j}\rho_j v_j^2 \tilde{A}_j - \tilde{F}_w - \tilde{F}_{loc} - \Delta\tilde{p}_p - \sum_{A_j}\tilde{p}\tilde{A}_j + \bar{\rho}\tilde{V}\tilde{g} \quad . \qquad \text{(II.2-29)}$$

Equation II.2-29 is a vector equation for the forces acting on the control volume V. The major restriction associated with the derivation of Equation II.2-29 is the assumption of uniform distributions across the flow areas A_j. In addition, the effects of wall friction, local forces, and pump behavior have been assumed to be additive. This assumption can usually be justified by proper application of the equation in practice. Although Equation II.2-29 is quite general, many restrictive assumptions will be employed in order to obtain models and correlations for the second, third and fourth terms on the right-hand side. These models are given in later sections of this report.

Equation II.2-29 is not the equation used in RETRAN. The specific form of the momentum equation in RETRAN is given in Section 3.0 below.

2.4 Macroscopic Energy Balance Equation

The local energy equation has been given by Equation II.1-25. Operating on Equation II.1-25 with $\int_V dV$ gives

$$\int_V \frac{\partial}{\partial t}\rho e\, dV + \int_V \frac{\partial}{\partial x_i}\rho e v_i = \int_V \frac{\partial}{\partial x_i}\, k\,\frac{\partial T}{\partial x_i}\, dV - \int_V \frac{\partial}{\partial x_i} p v_i\, dV \qquad \text{(II.2-30)}$$

$$- \int_V \frac{\partial}{\partial x_i}\sigma_{ij} v_j\, dV + \int_V \rho g_i v_i\, dV + \int_V \dot{Q}_g\, dV \quad ,$$

where

$$e = u + \frac{1}{2} v_j v_j \qquad \text{(II.2-31)}$$

and $\dot{Q}_g$ is the volumetric generation of energy within the fluid and g_i is the i-direction component of the volumetric body force. The property per unit volume for use in the generalized transport theorem, Equation II.2-1 is the energy

$$E = \rho e = \rho(u + \frac{1}{2} v_j v_j) \quad . \qquad \text{(II.2-32)}$$

Substituting Equation II.2-32 into Equation II.2-1 gives

$$\frac{d}{dt}\int_V \rho e \, dV = \int_V \frac{\partial}{\partial t} \rho e \, dV + \int_S \rho e \tilde{v}_s \cdot d\tilde{S} \, . \qquad \text{(II.2-33)}$$

The first term on the left-hand side of Equation II.2-30 is required in Equation II.2-33. The remaining terms in Equation II.2-30 are evaluated as follows.

Applying Green's theorem to the divergence terms in Equation II.2-30 gives the result:

$$\int_V \frac{\partial}{\partial x_i} \rho e \, dV = \int_S \rho e \tilde{v} \cdot d\tilde{S} \, , \qquad \text{(II.2-34a)}$$

for the transport of energy by flow,

$$\int_V \frac{\partial}{\partial x_i}\left(k \frac{\partial T}{\partial x_i}\right) dV = \int_S \tilde{q} \cdot d\tilde{S} \, , \qquad \text{(II.2-34b)}$$

for the conduction contribution,

$$\int_V \frac{\partial}{\partial x_i} p v_i \, dV = \int_S p \tilde{v} \cdot d\tilde{S} \, , \qquad \text{(II.2-34c)}$$

for the pressure-work contribution, and

$$\int_V \frac{\partial}{\partial x_i} \sigma_{ij} v_j \, dV = \int_S (\sigma_{ij} v_j) \cdot d\tilde{S} \, , \qquad \text{(II.2-34d)}$$

for the shear-work contribution. The work due to the volumetric force, the fourth term on the right-hand side of Equation II.2-30, is evaluated as follows. The volumetric body force $\tilde{g}$ can be derived from a scalar potential function of the form

$$\tilde{g} = - \tilde{\nabla} \phi \, . \qquad \text{(II.2-35)}$$

With Equation II.2-35, the fourth term on the right-hand side of Equation II.2-30 can be written as

1356 058

$$\int_V \rho g_i v_i \, dV = - \int_V \rho(\tilde{v}\cdot\tilde{\nabla}\phi) \, dV \ , \qquad \text{(II.2-36a)}$$

or,

$$\int_V \rho(\tilde{v}\cdot\tilde{\nabla}\phi) \, dV = \int_V (\tilde{\nabla}\cdot\rho\phi\tilde{v}) \, dV - \int_V \phi(\tilde{\nabla}\cdot\rho\tilde{v}) \, dV \ . \qquad \text{(II.2-36b)}$$

The first term on the right-hand side of Equation II.2-36b can be transformed to a surface integral by use of Green's theorem. The second term can be rewritten by use of the local continuity equation given by

$$\frac{\partial}{\partial t} \rho + \frac{\partial}{\partial x_i} \rho v_i = 0 \ . \qquad \text{(II.2-37)}$$

Substituting this information into Equation II.2-36b gives

$$- \int_V \rho(\tilde{v}\cdot\tilde{\nabla}\phi) \, dV = - \int_S \rho\phi\tilde{v}\cdot d\tilde{S} - \int_V \phi \frac{\partial\rho}{\partial t} \, dV \ , \qquad \text{(II.2-38a)}$$

or

$$- \int_V \rho(\tilde{v}\cdot\tilde{\nabla}\phi) \, dV = - \int_S \rho\phi\tilde{v}\cdot d\tilde{S} - \frac{d}{dt} \int_V \rho\phi \, dV + \int_S \rho\phi\tilde{v}_s\cdot d\tilde{S} \ , \qquad \text{(II.2-38b)}$$

where Equation II.2-1 has been used and the scalar potential has been assumed to be independent of time. The first and third terms on the right-hand side of Equation II.2-38b can also be combined.

Substituting Equation II.2-34 (a through d) and II.2-38b into Equation II.2-30 and then incorporating the results into Equation II.2-33 gives

$$\frac{d}{dt} \int_V (\rho e + \rho\phi) \, dV = - \int_S \rho e \, (\tilde{v} - \tilde{v}_s)\cdot d\tilde{S} + \int_S \tilde{q}\cdot d\tilde{S} \qquad \text{(II.2-39)}$$

$$- \int_S \tilde{p}v\cdot d\tilde{S} - \int_S (\sigma_{ij}\tilde{v}_j)\cdot d\tilde{S} - \int_S \rho\phi(\tilde{v} - \tilde{v}_s)\cdot d\tilde{S} + Q_g V \ .$$

Equation II.2-39 is the macroscopic energy balance for the control volume. The surface integrals on the right hand side can be expanded by use of the specification of the surface S. Each of the surface integrals will then consist of three contributions: one each for ΣA_j, S_w and S_m. The details of the process of evaluating the integrals are omitted and only the results are given here.

The first integral on the right hand side of Equation II.2-39 is zero on S_w and S_m. On the flow areas A_j it accounts for the energy flowing into and out of the control volume. The results are given by

$$\int_S \rho e(\tilde{v} - \tilde{v}_s)\cdot d\tilde{S} = \sum_{A_j} \rho(u\bar{v} + \frac{1}{2}\overline{v^3})\, A_j \cos\alpha_j \ , \qquad \text{(II.2-40)}$$

where α_j is the angle between $\tilde{v}$ and $\tilde{n}$ at the areas A_j. The second integral represents the energy exchange between the fluid in the control volume and the surroundings. The major contribution is obtained from the solid surfaces bounding the fluid. The contribution by conduction and radiation at the surfaces A_j is generally neglected. However, for some conditions encountered during hypothetical LOCA's, radiation must be accounted for. For our present purposes, only a general representation of the integral is needed and we let

$$Q_w = \int_{S_w+S_m+\Sigma A_j} \tilde{q}\cdot d\tilde{S} \ . \qquad \text{(II.2-41)}$$

The third and fourth integrals represent the pressure-volume and shear, or viscous, work. These integrals are zero on the stationary surfaces S_w. On the moving surfaces S_m, the value of the integrals represents the rate at which work is done by the action of the moving parts. This work will be denoted by $\dot{W}_p$:

$$\dot{W}_p = \int_{S_m} p\tilde{v}\cdot d\tilde{S} + \int_{S_m} (\sigma_{ij}v_j)\cdot d\tilde{S} \ . \qquad \text{(II.2-42)}$$

1356 060

During hypothetical LOCA's, the fluid may transfer work to the pump. On the flow areas A_j, the shear, or viscous, contribution is generally neglected in comparison to the other contributions. The pressure-volume work contribution can be evaluated to give

$$\int_{A_j} p\tilde{\tilde{v}}\cdot d\tilde{\tilde{S}} = \sum_{A_j} p\bar{v}A_j \cos\alpha_j \ . \qquad \text{(II.2-43)}$$

The last surface integral in Equation II.2-39 is zero on S_w and S_m. The integral can be evaluated on the flow areas A_j to obtain

$$\int_S \rho\phi(\tilde{\tilde{v}} - \tilde{\tilde{v}}_s)\cdot d\tilde{\tilde{S}} = \sum_{A_j} \rho\phi\bar{v}A_j \cos\alpha_j \ . \qquad \text{(II.2-44)}$$

Substituting Equation II.2-40 through II.2-44 into Equation II.2-39 gives the macroscopic energy balance equation as

$$\frac{d}{dt}\int_V \rho\ (e + \phi)\ dV = -\sum_{A_j} \rho(u\bar{v} + \tfrac{1}{2}\overline{v^3})\ A_j \cos\alpha_j + Q_w - \dot{W}_p - \sum_{A_j} p\bar{v} \cos\alpha_j$$

$$-\sum_{A_j} \rho\phi\bar{v}A_j \cos\alpha_j + \dot{Q}_g V \qquad \text{(II.2-45a)}$$

or,

$$\frac{d}{dt}\int_V \rho(e + \phi)\ dV = -\sum_{A_j} [\rho u\bar{v} + \tfrac{1}{2}\rho\overline{v^3} + \rho\phi\bar{v} + p\bar{v}]\ A_j \cos\alpha_j$$

$$+ Q_w - \dot{W}_p + \dot{Q}_g V \ , \qquad \text{(II.2-45b)}$$

where

$$e = u + \tfrac{1}{2} v_j v_j \ . \qquad \text{(II.2-45c)}$$

The density, ρ, has been assumed to be constant over the areas A_j. In general, the deviation between $\overline{v^3}$ and $\bar{v}^3$ is neglected in most engineering analyses. In order to complete the energy balance, models are required for Q_w, $\dot{W}_p$, and $\dot{Q}_g$. The models available in RETRAN are given in Section III of this report.

Before closing this section, we note that the macroscopic mechanical energy balance equation can be obtained by the same procedures employed in this section. The local mechanical energy equation is obtained by forming the scalar product of $\tilde{v}$ with the local momentum equation, Equation II.1-24. The macroscopic mechanical energy balance equation is the Bernoulli equation frequently employed in engineering analyses. The Bernoulli equation is generally employed to obtain information relating to the local energy losses caused by flow perturbations such as expansions, contractions, spacer grids, valves, tees, and other junctions. Derivations of the Bernoulli equation have been given by Bird et al.,[II.2-2] Slattery,[II.2-1] and Brodkey.[II.2-4]

2.5 Fluid State Equations

The macroscopic balance equations require the fluid state properties, pressure, p, density, ρ, and temperature, T. This information is obtained from the equations of state for the material. Equations II.1-29 and II.1-30 can be used to obtain state information given by

$$\rho = \rho(p,u) \quad , \tag{II.2-46a}$$

or

$$p = p(\rho,u) \quad , \tag{II.2-46b}$$

and

$$T = T(p,u) \quad . \tag{II.2-46c}$$

For saturated two-phase flow, the state properties are functions of the pressure alone and the thermodynamic quality can be obtained from Equations II.2-46.

Finally, we also note that the fluid transport properties μ and k are also functions of the state of the fluid. General relations for these properties are given by

$$\mu = \mu(\rho,T) \qquad \text{(II.2-47a)}$$

and

$$k = k(\rho,T) \quad . \qquad \text{(II.2-47b)}$$

2.6 Summary of the Macroscopic Balance Equations

A review of the macroscopic balance equations indicates that only a limited amount of information can be obtained from them. The procedure used to obtain the macroscopic equations from the local conditions has averaged out large amounts of detail. Models or correlations are required in order to obtain an accounting of the effects that are represented by the integrals in the general macroscopic equations.

Basically, in order to determine the time rate of change of the properties of the control volume, the state and conditions at all the entrances and exit flow areas A_j as well as the effects of the surfaces bounding the fluid must be specified. In general, the macroscopic balance equations are applied to the case of steady, incompressible flows and then solved for one to three unknown quantities. Application of the macroscopic balance equations to analyses of hypothetical transients in complex thermal-hydraulic loops has resulted in generalization of the usual engineering application procedures associated with these equations. In order to conduct the generalized thermal-hydraulic analyses, many of the results obtained from the steady-state applications are used in the transient form of the equations. In particular, the steady-state equations are generally employed with experimental data in order to determine the wall friction, heat transfer coefficients, local losses, and pump characteristics for example. The correlations and models which result from this process are then used in the general equations for transient analyses. As previously mentioned, in some cases the local equations could be solved for the detailed distributions of the fluid state and flow and the integrals obtained in the macroscopic balances evaluated exactly. In most cases of practical interest, analytical solution of

the local equations is not possible at the present time and numerical solutions would be required.

The macroscopic balance equations require that a large amount of information be supplied in order to obtain a closed equation system. The derivation of the balance equations has introduced the following quantities: (1) geometric details of the flow channel represented by the volume V, the flow areas A_j and the wetted areas S_w and S_m; (2) momentum exchanges and forces due to wall friction, $\tilde{F}_w$, and local flow perturbations $\tilde{F}_{loc}$; (3) momentum exchanges due to moving surfaces, $\Delta\tilde{p}_p$; (4) energy exchanges between the fluid and the flow channel bounding surfaces Q_w; (5) work done on or by the fluid due to moving surfaces, $\dot{W}_p$; and (6) volumetric generation of energy in the fluid, $\dot{Q}_g$. All of these quantities must be specified before the general equation system can be solved. In addition to these specific engineering quantities, implementation of the equation of state of the fluid, in a manner consistent with the variety of processes encountered in hypothetical LOCA's, can present problems of a practical nature. Models and correlations for all of the quantities required for closure of the equation system are given in the following sections of this report.

Most hypothetical LOCA's involve two-phase flow of the NSSS coolant. The two-phase nature of the fluid has not been explicitly introduced into the derivation of the macroscopic balance equations. Thus, the assumption that the two-phase mixture can be treated as a single homogeneous fluid has been implicitly introduced into the derivation of the equations. Basically, the homogeneous fluid assumption implies that the fluid can be characterized by a single velocity and temperature. In the present version of RETRAN, the two-phase nature of the fluid is introduced into the equation system through the models and correlations employed for the constitutive equations required for system closure. That is, the friction, heat transfer, pump characteristics, and the other quantities discussed in the preceding paragraph contain an accounting of the two-phase nature of the coolant. In addition, several models are employed which account for some of the more important clearly non-homogeneous situations which are encountered in hypothetical LOCA's. These models are of a specialized nature and are not intended to be rigorous descriptions of the general behavior of two-phase flow. These models are also given in this report. Discussion of the advantages and disadvantages associated with the use of a homogeneous description of two-phase flows is beyond the scope of the present report. In general, present development efforts

are directed toward obtaining models of the clearly non-homogeneous situations and incorporating the models into the basic homogeneous framework of RETRAN.

A wide variety of methods can be used to solve the general equations developed in preceeding sections. Each of the methods will involve its own assumptions and approximations. The specific form of the equations used in RETRAN is given in the next section. The approximations and assumptions required to obtain the RETRAN equations are clearly indicated. In many cases, the limitations introduced into the equations should be carefully considered when RETRAN is applied to analysis of complex thermal hydraulic systems.

3.0 RETRAN OVERALL BALANCE EQUATIONS

The difficulties associated with analysis of transient thermal-hydraulic phenomena in complex geometries have been discussed in Section 1.0 above. The computer programs employed in these analyses are basically one-dimensional. That is, only one component of the vector equation for balance of linear momentum, Equation II.2-29, is used in the thermal-hydraulic model. In addition, the exact form of the one-dimensional equation is not employed in RETRAN. In order to obtain the momentum equation used in RETRAN, a very basic assumption regarding the geometry of the control volumes and flow paths of the fluid must be made. These assumptions and the method of applying the general equations as used in RETRAN are given in the following sections.

3.1 Geometry of the Application Procedure

The geometric aspects of the RETRAN differential balance equations can be illustrated by reference to Figure II.3-1. Representation of a portion of a straight, constant cross-sectional area flow channel is given in Figure II.3-1. The mass and energy cells, outlined by dashed lines, correspond to the portion of the flow channel to which the macroscopic mass and energy equations are applied. The macroscopic momentum balance equation is applied to the portion of the channel labeled as a "momentum cell". It is important to note that the flow channel walls are parallel to the one direction for which the momentum equation is to be applied. Thus, the vector nature of the momentum equation is lost when the model presently available in RETRAN is used. In effect, the RETRAN momentum equation does not properly account for changes in flow direction of the fluid. In addition, only one "entrance" and one "exit" is associated with each momentum cell.

The center of the mass and energy cells are labeled "k" and "k+1" in Figure II.3-1. The mass and energy cells are generally called "volumes". The center of the momentum cells are labeled "i-1", "i", and "i+1". These locations are generally called the "junctions" or "flow paths". The length of the mass and energy cells is denoted by L_k, the cross-sectional area is denoted by A_k, and the volume is denoted by V_k. The lengths of the various mass and energy cells need not be equal. A flow channel is represented in RETRAN by use of a number of control volumes and the corresponding junctions, or flow paths, between the volumes. In

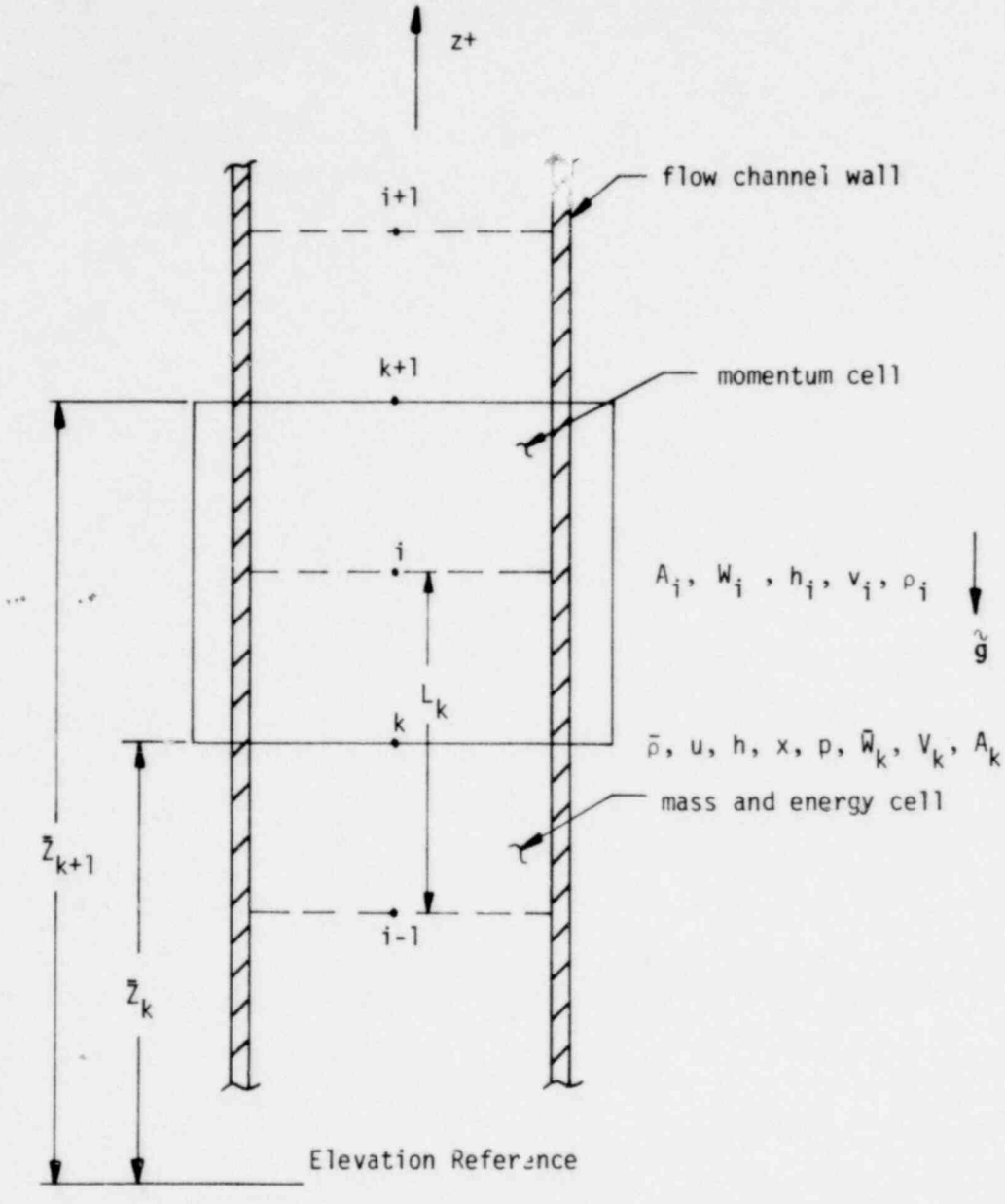

Figure II.3-1 Geometry for the RETRAN Equations

effect, the specification of the flow channel in this manner converts the differential balance equations into a system of differential-difference equations which is then solved by a suitable numerical solution scheme. This representation of a fluid flow channel is sometimes called the "tube-and-tank" method. The differential-difference nature of the equation system will become clear as the RETRAN equations are obtained. For the present time, we will assume that no moving surfaces are present in the flow channel.

3.2 The RETRAN Mass Balance Equations

The macroscopic mass flow equation has been given by Equations II.2-8 and II.2-13 as

$$\frac{d}{dt}\int_V \rho \, dV = \sum_i W_i \ , \qquad \text{(II.3-1)}$$

where the correct sign of the mass flows W_i is determined by the direction of the velocity v_i. Applying Equation II.3-1 to the mass cell "k" of Figure II.3-1 gives

$$\frac{d}{dt}\bar{\rho}V_k = W_{i-1} - W_i \ , \qquad \text{(II.3-2)}$$

for the case of uniform flow in the positive z-direction. The mass flow is given by

$$W = \rho v A \ , \qquad \text{(II.3-3)}$$

and the mass in the cell is given by

$$M_k = \bar{\rho}_k V_k \ . \qquad \text{(II.3-4)}$$

Although the momentum equation in RETRAN is strictly valid for the case of two junctions, a general form of the mass balance equation is used. That is, a control volume may have any number of junctions associated with it. The RETRAN mass equation is given by

$$\frac{dM_k}{dt} = \sum_i W_i \ , \qquad \text{(II.3-5)}$$

where the summation is performed over all junctions "i" associated with volume V_k. Equation II.3-5 is written for each volume V_k in the flow channel again with proper accounting of the sign of W_i.

3.3 The RETRAN Momentum Balance Equations

The macroscopic momentum balance equation has been given by Equation II.2-29. Applying Equation II.2-29 to the momentum cell in Figure II.3-1, again for the case of uniform upflow in the channel gives

$$\frac{d}{dt}\int_{V_i} \rho v \, dV = \bar{\rho}_k v_k^2 A_k - \bar{\rho}_{k+1} v_{k+1}^2 A_{k+1} - F_{w,i} + p_k A_k - p_{k+1} A_{k+1} - \bar{M}_i g_z, \qquad \text{(II.3-6)}$$

where $\bar{M}_i$ is the mass of fluid in volume V_i. As previously noted above, the RETRAN momentum equation does not contain any vector information. All of the areas A_k are assumed to be perpendicular to the z-direction. When RETRAN is applied to analyses of NSSS's, some momentum cells may contain more than two flow areas and these areas may not always be perpendicular to the z-direction. Comparing Equation II.3-6 with Equation II.2-29 will give an indication of the approximations involved in the use of Equation II.3-6. It is especially important to note that the pressure force terms on the right-hand side of Equation II.2-29 are not properly accounted for in the case of multiple junctions on a volume.

The integral on the left hand side of Equation II.3-6 can be evaluated as follows. If we assume that the argument of the integral can be represented by an average value $\rho_i v_i$, Equation II.3-6 can be written

$$\frac{d}{dt}(\rho_i v_i V_i) = \bar{\rho}_k v_k^2 A_k - \bar{\rho}_{k+1} v_{k+1}^2 A_{k+1} - F_{w,i} + p_k A_k - p_{k+1} A_{k+1} - \bar{M}_i g_z \ . \qquad \text{(II.3-7)}$$

The areas A_k are constant in space and time and the volume V_i is given by

$$V_i = A_k\left(\frac{L_k}{2} + \frac{L_{k+1}}{2}\right) . \qquad \text{(II.3-8)}$$

The RETRAN equations are programmed in terms of the mass flows $\bar{W}_k$ and W_i. Equation II.3-7 can be written as

$$\frac{1}{2}(L_k + L_{k+1})\frac{d}{dt}\left(\frac{W_i}{A_k}\right) = \frac{\bar{W}_k^2}{\bar{\rho}_k A_k^2} - \frac{\bar{W}_{k+1}^2}{\bar{\rho}_{k+1} A_k^2} - \frac{1}{A_k} F_{w,i} + p_k - p_{k+1} - \frac{\bar{M}_i}{A_k} g_z \ . \qquad \text{(II.3-9)}$$

Equation II.3-9 is valid only for the case of flow in a channel of constant cross-sectional area. Specific models are required for the wall friction F_{wi} and the mass $\bar{M}_i$ in volume V_i.

Equation II.3-9 is an equation for the mass flow W_i. It is important to note that the mass equation, Equation II.3-5, contains the mass flow W_i on the right-hand side. Thus, the mass flows $\bar{W}_k$ on the right-hand side of Equation II.3-9 are not available from a differential equation and must be obtained as functions of the mass flows W_i which are known. The equations which are used in RETRAN to obtain the $\bar{W}_k$'s are given later in this section.

3.3.1 Incompressible Flow with an Area Change

Equation II.3-9 is not the only momentum equation used in RETRAN. The equations presently in RETRAN can be obtained for the geometry shown in Figure II.3-2. Figure II.3-2 is a representation of a flow channel containing an abrupt area change. The RETRAN momentum equation is obtained by applying Equation II.3-6 to the portions of the flow channel labeled $1/2(L_k)$ and $1/2(L_{k+1})$. For the case of flow into V_i at surface "k" and out of V_i at "k+1", Equation II.3-6 applied to the volume $1/2(V_k)$ gives

$$\frac{d}{dt}\int_{1/2\ V_k} \rho v \ dV = \bar{\rho}_k A_k V_k^2 - \bar{\rho}_i \bar{A}_i (\bar{v}_i)^2 - F_{w,i} + p_k A_k - \bar{p}_i \bar{A}_i - \bar{M}_{1/2\ V_k} g_{z,k'} \qquad \text{(II.3-10)}$$

where the wall friction $F_{w,i}$ and the mass $\bar{M}_{1/2Vk}$ are understood to refer to the distance $1/2(L_k)$ and volume $1/2(V_k)$, respectively. Applying Equation II.3-6 to the volume $1/2(V_{k+1})$ gives

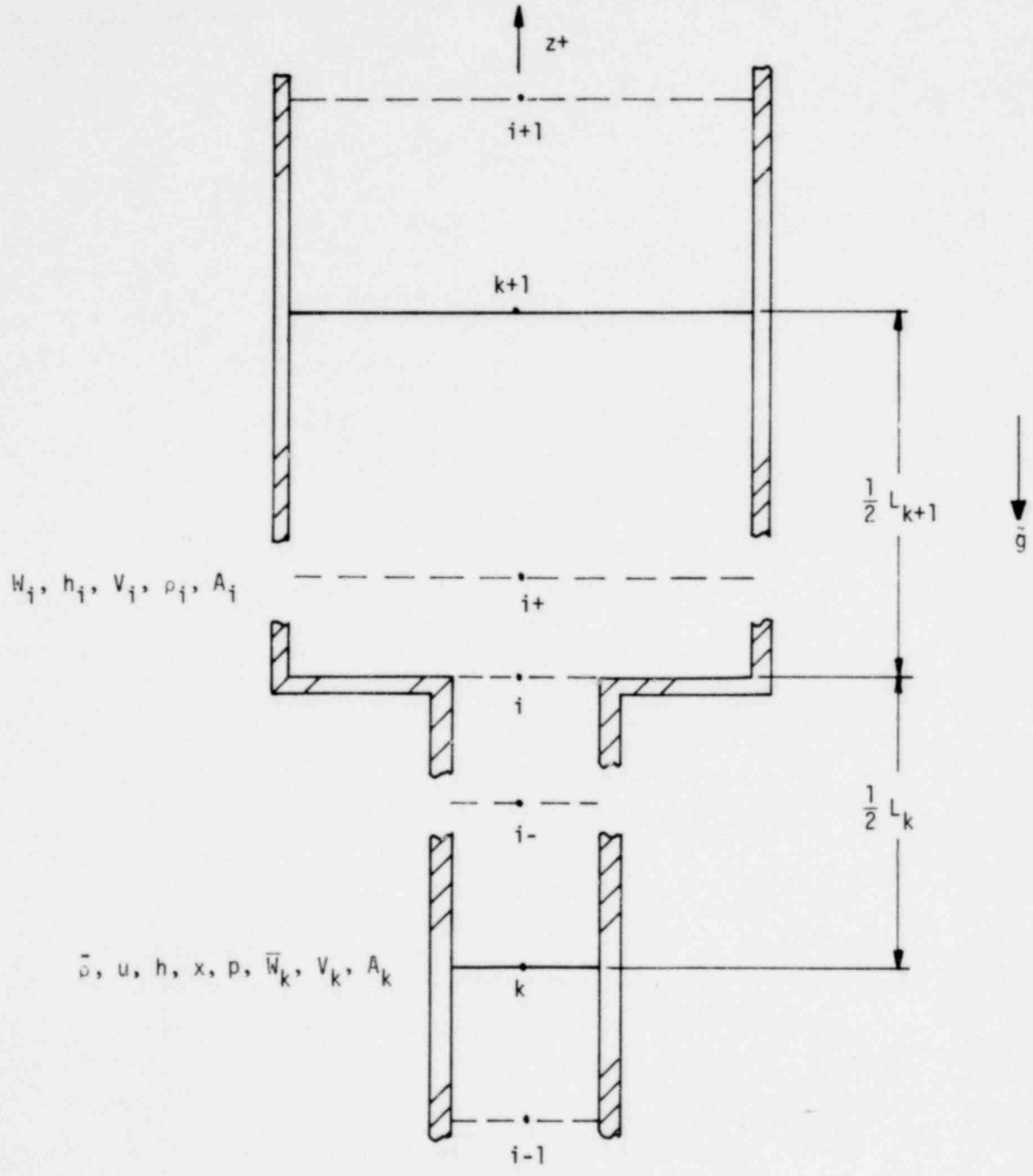

Figure II.3-2 Geometry for RETRAN Momentum Equation with A Variable Area

$$\frac{d}{dt}\int_{1/2\ V_{k+1}} \rho v\ dV = \rho_i^+ A_i^+ (v_i^+)^2 - \bar{\rho}_{k+1} A_{k+1} V_{k+1}^2 - F_{w,i+1} + p_i^+ A_i^+ \qquad \text{(II.3-11)}$$

$$- p_{k+1} A_{k+1} - \bar{M}_{1/2\ V_{k+1}}\ g_{z,k+1}$$

In Equation II.3-10 and II.3-11, the superscripts "-" and "+" refer to positions on either side of the transition portion of the flow channel as shown in Figure II.3-2. The volumes $1/2(V_k)$ and $1/2(V_{k+1})$ are given by

$$\frac{1}{2} V_k = \frac{1}{2} L_k A_k \ , \qquad \text{(II.3-12a)}$$

and

$$\frac{1}{2} V_{k+1} = \frac{1}{2} L_{k+1} A_{k+1} \ . \qquad \text{(II.3-12b)}$$

respectively.

Two models are available in RETRAN that apply to the flow area transition region of the flow channel. Both models are obtained by use of the macroscopic momentum balance of Equation II.3-6 and the macroscopic mechanical energy equation. The latter equation is used because the available information relating to the effects of local flow perturbations such as area changes are usually given in terms of irreversible energy loss coefficients.

Both models incorporate the assumption that the flow in the transition region can be considered to be steady-state flow and that the wall friction forces can be neglected. In addition the model which is described here incorporates the assumption that the fluid is incompressible for purposes of applying the mechanical energy equation. The second model is obtained by partially removing the incompressibility assumption.

Applying the assumption of steady flow to the integral mass balance of Equation II.3-1, and applying the equation to the area transition region gives

$$0 = W_i^- - W_i^+, \qquad \text{(II.3-13a)}$$

or

$$\rho_i^- A_i^- v_i^- = \rho_i^+ A_i^+ v_i^+ = W_i \ . \qquad \text{(II.3-13b)}$$

The incompressible flow assumption gives

$$\rho_i^- = \rho_i^+ \ . \qquad \text{(II.3-13c)}$$

The macroscopic mechanical energy balance for steady incompressible flow[II.3-1] applied to the area transition region gives

$$0 = \frac{1}{2}\rho[(v_i^-)^2 - (v_i^+)^2] + p_i^- - p_i^+ - \frac{1}{2}\rho(v_i^+)^2 e_v \ , \qquad \text{(II.3-14)}$$

where e_v is the irreversible loss coefficient. These coefficients are usually available from tables or experimental data. The irreversible loss coefficients are measures of the amount of turbulence induced into the flow field by the geometric flow perturbations. Thus, the value of e_v for a gradual area expansion is not the same as the value for a gradual area contraction.[II.3-2]

Equations II.3-10, II.3-11, II.3-13, and II.3-14 can be rearranged as follows. In Equation II.3-10, $A_k = A_i^-$, and it can be written

$$\frac{1}{A_k}\frac{d}{dt}\int_{1/2\ V_k} \rho v \ dV = \bar{\rho}_k v_k^2 - \rho_i^-(v_i^-)^2 - \frac{1}{A_k} F_{w,i} + p_k - p_i^- \qquad \text{(II.3-15)}$$

$$- \frac{1}{A_k} m_{1/2\ V_k} g_{z,k} \ .$$

In the same manner, Equation II.3-11 is rewritten as

$$\frac{1}{A_{k+1}}\frac{d}{dt}\int_{1/2\ V_{k+1}} \rho v \ dV = \rho_i^+(v_i^+)^2 - \bar{\rho}_{k+1} v_{k+1}^2 - \frac{1}{A_{k+1}} F_{w,i+1} \qquad \text{(II.3-16)}$$

$$+ p_i^+ - p_{k+1} - \frac{1}{A_{k+1}} \bar{M}_{1/2\ V_{k+1}} g_{z,k+1} \ .$$

Adding Equations II.3-15 and II.3-16 gives

$$\frac{1}{A_k}\frac{d}{dt}\int_{1/2\ V_k}\rho v\ dV + \frac{1}{A_{k+1}}\frac{d}{dt}\int_{1/2\ V_{k+1}}\rho v\ dV = \bar{\rho}_k v_k^2 - \bar{\rho}_{k+1}v_{k+1}^2 + p_k - p_{k+1}$$

$$- \frac{1}{A_k}F_{w,i} - \frac{1}{A_{k+1}}F_{w,i+1} - \frac{1}{A_k}\bar{M}_{1/2\ V_k}\left(g_{z,k}\right) - \frac{1}{A_{k+1}}\bar{M}_{1/2\ V_{k+1}}\left(g_{z,k+1}\right)$$

$$+ \rho_i^+(v_i^+)^2 - \rho_i^-(v_i^-)^2 + p_i^+ - p_i^- \ , \qquad \text{(II.3-17)}$$

where the wall friction $F_{w,i}$ and $F_{w,i+1}$, refer to $1/2(L_k)$ and $1/2(L_{k+1})$, respectively. Equation II.3-17 has not been obtained by a rigorous application of the general momentum balance of Equation II.2-29. Equation II.3-14 is substituted into Equation II.3-17 to obtain

$$\frac{1}{A_k}\frac{d}{dt}\int_{1/2\ V_k}\rho v\ dV + \frac{1}{A_{k+1}}\int_{1/2\ V_{k+1}}\rho v\ dV = \bar{\rho}_k v_k^2 - \bar{\rho}_{k+1}v_{k+1}^2 + p_k - p_{k+1}$$

$$- \frac{1}{A_k}F_{w,i} - \frac{1}{A_{k+1}}F_{w,i+1} - \frac{1}{A_k}\bar{M}_{1/2\ V_k}\left(g_{z,k}\right) - \frac{1}{A_{k+1}}\bar{M}_{1/2\ V_{k+1}}\left(g_{z,k+1}\right)$$

$$- \frac{1}{2}\frac{W_i^2}{\rho_i}\left[\frac{1}{A_{k+1}^2} - \frac{1}{A_k^2}\right] - E_v \ , \qquad \text{(II.3-18)}$$

where Equations II.3-13 have been used. The next to the last term on the right-hand side of Equation II.3-18 employs the conditions at the location "i". The last term on the right-hand side of Equation II.3-18 is given by

$$E_v = \frac{1}{2}\rho_i(v_i^+)^2\ e_v \ , \qquad \text{(II.3-19)}$$

where the coefficient e_v is usually referenced to conditions downstream of the flow perturbation. The irreversible loss term of Equation II.3-19 is used in RETRAN based on the conditions at location "i" and Equation II.3-19 is written as

$$E_v = \frac{1}{2} W_i |W_i| \frac{e_v^*}{\rho_i A_i^2} . \qquad \text{(II.3-20)}$$

The tabulated values of e_v are transformed to e_v^* by use of the steady-state mass balance of Equations II.3-13.

The integrals on the left-hand side of Equation II.3-18 may be evaluated to obtain

$$\frac{1}{A_k} \frac{d}{dt} \int_{V_{k/2}} \rho v \, dV + \frac{1}{A_{k+1}} \frac{d}{dt} \int_{V_{k+1/2}} \rho v \, dV \qquad \text{(II.3-21)}$$

$$= \frac{1}{A_k} \frac{d}{dt} \left[(Mv)_k \right] + \frac{1}{A_{k+1}} \frac{d}{dt} \left[(Mv)_{k+1} \right]$$

where $(Mv)_k$ and $(Mv)_{k+1}$ is the total fluid momentum within each half-volume. An approximate form of Equations II.3-21 is used in RETRAN. The right-hand side of Equation II.3-21 is written as

$$\frac{1}{A_k} \frac{d}{dt} \left[(\rho v A)_k \frac{L_k}{2} \right] + \frac{1}{A_{k+1}} \frac{d}{dt} \left[(\rho v A)_{k+1} \frac{L_{k+1}}{2} \right] = \left(\frac{1}{2} \frac{L_k}{A_k} + \frac{1}{2} \frac{L_{k+1}}{A_{k+1}} \right) \frac{dW_i}{dt} , \qquad \text{(II.3-22)}$$

where the momentum within each half-volume is approximated as the product of an average mass flow times the path length. These half-volume average flows are further approximated as being equal to the flow W_i. These approximations for the temporal derivative of the momentum terms implicitly introduce assumptions associated with mass flow and density distributions. Anomalous results, such as water packing, may arise when these equations are applied to nonhomogeneous systems.

Substituting Equation II.3-20 and II.3-22 into Equation II.3-18 gives

$$\left(\frac{1}{2}\frac{L_k}{A_k}+\frac{1}{2}\frac{L_{k+1}}{A_{k+1}}\right)\frac{dW_i}{dt}=\frac{\bar{W}_k^2}{\bar{\rho}_k A_k^2}-\frac{\bar{W}_{k+1}^2}{\bar{\rho}_{k+1}A_{k+1}^2}+p_k-p_{k+1}-\frac{1}{A_k}F_{w,i}$$

$$\frac{1}{A_k}F_{w,i+1}-\frac{1}{A_k}\bar{M}_{1/2}\,V_k\left(g_{z,k}\right)-\frac{1}{A_{k+1}}\bar{M}_{1/2}\,V_{k+1}\left(g_{z,k+1}\right)$$

$$+\frac{1}{2}\frac{\bar{W}_i}{\rho_i}\left[\frac{1}{A_{k+1}^2}-\frac{1}{A_k^2}\right]-\frac{1}{2}\left|W_i\,W_i\right|\frac{e_i^*}{\rho_i A_i^2}\quad . \qquad \text{(II.3-23)}$$

Several approximations have been used in obtaining Equation II.3-23. For flow in a constant area channel, Equation II.3-23 reduces to the more nearly exact form given by Equation II.3-9. Equation II.3-23 also reduces to the cases of incompressible, steady flow in channels with various flow perturbations. As previously noted, the vector nature of the general momentum equation is not contained in RETRAN and only two flow areas are associated with each momentum cell. Equation II.3-23 can be compared with the more general form given by Equation II.2-29 in order to determine some of the approximations associated with the RETRAN momentum equation.

3.3.2 Compressible Flow with an Area Change

The development of the flow Equation II.3-22 was accomplished with the assumption of incompressible conditions at an area change where the fluid densities on either side were assumed equal in Equation II.3-13c. This assumption neglects the effects of density variations occurring in the narrow regions between i^- and i^+. For most engineering calculations where local velocities are less than 0.3C, this is usually a reasonable approximation.

For isentropic flow with constant sonic speed

$$\left(\frac{\partial P}{\partial \rho_s} \right) = C^2 \ . \qquad \text{(II.3-24)}$$

Hence

$$dp = C^2 d\rho \qquad \text{(II.3-25)}$$

or

$$p_i^+ - p_i^- = C^2 \ (\rho_i^+ - \rho_i^-) \ . \qquad \text{(II.3-26)}$$

Thus, the terms obtained from the combination of Equations II.3-10 and II.3-11 become

$$\rho_i^+ \ v_i^{+2} + p_i^+ - \rho_i^- \ v_i^{-2} - p_i^- = \rho_i^+ \ (v_i^{+2} + C^2) - \rho_i^-(v_i^{-2}+C^2) \qquad \text{(II.3-27)}$$

where for isentropic flow

$$dp + \rho v \ dV = 0 \qquad \text{(II.3-28)}$$

or

$$\frac{d\rho}{\rho} = \frac{dM^2}{2} \ , \qquad \text{(II.3-29a)}$$

hence

$$\frac{\rho_i^+}{\rho_i^-} = e^{-\left[\frac{v_i^{+2} - v_i^{-2}}{2C^2} \right]} \ . \qquad \text{(II.3-29b)}$$

This model neglects the energy loss term but it is reincorporated into the final flow equation.

1356 077

3.4 The RETRAN Energy Balance Equation

The macroscopic energy balance equation has been given by Equation II.2-45b. As in the case of the mass balance, the energy balance is incorporated into RETRAN in a manner which allows two or more flow areas to be associated with each energy cell. Applying Equation II.2-45b to an energy cell V_k gives

$$\frac{d}{dt}\int_{V_k} \rho(e + \phi)\, dV = - \sum_i [\rho uv + \frac{1}{2}\rho v3 + \rho\phi v + pv]_i\, A_i\, \cos\alpha_i Q_{w,k} - W_{p,k} \quad , \tag{II.3-30}$$

where α_i is the angle between the outward directed unit normal to A_i and the velocity v_i. The volumetric generation $\dot{Q}_g$ is not included in the RETRAN equation. The energy e in Equation II.3-30 is

$$e = u + \frac{1}{2} v^2, \tag{II.3-31}$$

where u is the internal energy.

Equation II.3-30 is rearranged as follows for use in RETRAN. The scalar potential ϕ is time independent and the remaining part of the left-hand side can be written

$$\frac{d}{dt}\int_{V_k} (\rho u + \frac{1}{2}\rho v^2)\, dV = \frac{d}{dt}\int_{V_k} \rho u\, dV + \frac{d}{dt}\int_{V_k} \frac{1}{2}\rho v^2\, dV \ . \tag{II.3-32}$$

The first term on the right-hand side of Equation II.3-32 gives

$$\frac{d}{dt}\int_{V_k} \rho u\, dV = \frac{d}{dt} U_k \tag{II.3-33}$$

where U_k is the total internal energy of the fluid in volume V_k. The second term is evaluated by use of an average value of ρv^2 to obtain

$$\frac{d}{dt}\int_{V_k} \frac{1}{2}\rho v^2\, dV = \frac{1}{2}\frac{d}{dt}\frac{\bar{W}_k^2}{\bar{\rho}_k A^2_k} L_k A_k \ . \tag{II.3-34}$$

The right-hand side of Equation II.3-30 is expressed in terms of the junction mass flow W_i and enthalpy h_i

$$h_i = u_i + p_i/\rho_i \quad . \tag{II.3-35}$$

The contribution of the potential energy is measured from the center of mass of the volume V_k. Thus, if a flow junction is at the same elevation as the center of mass of the volume, no potential energy is contributed.

Substituting the above information into Equation II.3-30 gives

$$\frac{dU_k}{dt} = -\frac{1}{2}\frac{L_k}{A_k}\frac{d}{dt}\left(\frac{\bar{W}_k^2}{\bar{\rho}_k}\right) - \sum_i W_i[h_i + \frac{1}{-} v_{i2}^2 + g(Z_i - \bar{Z}_k)] \tag{II.3-36}$$

$$+ Q_{w,k} - \dot{W}_p \ ,$$

where

Z_i = elevation of junction i
$\bar{Z}_k$ = elevation of the center of mass of the volume V_k.

The mass flow W_i is obtained from the momentum equation and, as previously noted, the mass flow $\bar{W}_k$ is not known. In general, Equation II.3-36 gives the time rate of change of the fluid in volume V_k if the conditions at all the flow boundaries are known. Constitutive models are required for the heat addition Q_w and pump work $\dot{W}_p$.

3.5 Fluid State Equations

The macroscopic field balance equations require fluid thermodynamic state information. In general, the mass of fluid in volume V_k is obtained from Equation II.3-5 and the total internal energy from Equation II.3-6. Equations II.2-46 are used to obtain the pressure at the center of the mass and energy cells

$$p_k = p_k\left(\frac{M_k}{V_k} \ , \ \frac{U_k}{M_k}\right) \ , \tag{II.3-37}$$

and the fluid temperature is given by

$$T_k = T_k\left(\frac{M_k}{V_k}\ ,\ \frac{U_k}{M_k}\right) . \qquad \text{(II.3-38)}$$

Additional fluid state information is obtained by use of Equations II.3-37 and II.3-38.

3.6 Summary of the RETRAN Equations

The equations employed in RETRAN are summarized here for convenience. The macroscopic mass balance is given by Equation II.3-5 in the form

$$\frac{DM_k}{dt} = \sum_i W_i \qquad \text{(II.3-39a)}$$

where

$$M_k = \bar{\rho}_k V_k \qquad \text{(II.3-39b)}$$

and

$$W_i = \rho_i v_i A_i \cos \alpha_i \qquad \text{(II.3-39c)}$$

Several forms of the macroscopic momentum balance equation are available in RETRAN. The momentum equations in RETRAN do not contain any vector information and are strictly valid only for the case of two flow areas associated with each momentum cell. Equation II.3-23, which was obtained from steady incompressible flow through a flow perturbation, is given by

$$\left(\frac{1}{2}\frac{L_k}{A_k} + \frac{1}{2}\frac{L_{k+1}}{A_{k+1}}\right)\frac{dW_i}{dt} = \frac{\bar{W}_k^2}{\bar{\rho}_k A_k^2} - \frac{\bar{W}_{k+1}^2}{\bar{\rho}_{k+1} A_{k+1}^2} + p_k - p_{k+1} - \frac{1}{A_k} F_{w,i}$$

$$- \frac{1}{A_{k+1}} F_{w,i+1} - \frac{1}{A_k} \bar{M}_{1/2}\, V_k \left(g_{z,k}\right) - \frac{1}{A_{k+1}} \bar{M}_{1/2}\, V_{k+1}\ g_{z,k+1} \qquad \text{(II.3-40)}$$

$$+ \frac{1}{2}\frac{W_i^2}{\rho_i}\left[\frac{1}{A_{k+1}^2}\right] - \frac{1}{A_k^2} - \frac{1}{2} W_i |W_i| \ \frac{e_v^*}{\rho_i A_i^2} ,$$

where

W_i = mass flow at center of momentum cell V_i

$\bar{W}_k$ = mass flow at center of mass and energy cell

$F_{w,i}$ = friction force in 1/2 (V_k) over length 1/2 (L_k)

$\bar{M}_{i/2V_k}$ = mass of fluid in volume 1/2 (V_k)

e_v^* = irreversible loss coefficient due to flow perturbation

p_k = pressure in volume V_k.

The other terms in Equation II.3-40 are defined in a similar manner for the volume V_{k+1}. Constitutive equations, or models, are required for $\bar{W}_k$, F_w, $\bar{M}$, and e_v^*. If the momentum cell contains moving surfaces, such as associated with pumps, compressors, and turbines, the model must be incorporated into the momentum equation. At the present time, RETRAN contains a model for pumps.

An equation for the total internal energy U_k of the fluid in volume V_k is used in RETRAN. The energy equation is given by Equation II.3-36 as

$$\frac{dU_k}{dt} = -\frac{1}{2}\frac{L_k}{A_k}\frac{d}{dt}\left(\frac{\bar{W}_k^2}{\bar{\rho}_k}\right) - \sum_i W_i\left[h_i + \frac{1}{2}v_i^2 + g(Z_i - \bar{Z}_k)\right] + Q_{w,k} - \dot{W}_p \,. \tag{II.3-41}$$

Constitutive models are required for the enthalpy at the junction h_i, the wall heat transfer $Q_{w,k}$, and the pump work $\dot{W}_p$.

Equations of state for the fluid are used in the form:

$$p_k = p_k\left(\frac{M_k}{V_k}, \frac{U_k}{M_k}\right), \tag{II.3-42a}$$

and

$$T_k = T_k\left(\frac{M_k}{V_k}, \frac{U_k}{M_k}\right). \tag{II.3-42b}$$

1356 081

The macroscopic balance equations require a large amount of information in order to determine the time rate of change of the state of the fluid in the mass, momentum, and energy cells. Basically, all the information at the boundaries of the cells must be specified. Application of the momentum equation to a control volume bounded by the center of the mass and energy cells allows some of the boundary information to be calculated with a differential equation. Other methods of applying the balance equations are of course possible. Equations II.3-39 through II.3-42 form a system of coupled differential-difference equations for the quantities M_k, W_i, U_k, p_k and T_k. All other information required by the equation system must be expressed in terms of these quantities or other equations must be added to the system.

Equations II.3-40 and II.3-41 require the quantities ρ_i, h_i and v_i. The density ρ_i is obtained from an equation of state with the pressure p_i and enthalpy h_i as independent variables. The pressure p_i is determined by application of a steady-state momentum equation from the center of volume V_k to the center of volume V_i. Applying Equation II.3-40 in this manner gives

$$p_i = p_k - F_{w,i} - \frac{1}{A_k} \bar{M}_{1/2} V_k \; g_{z,k} \; , \qquad \text{(II.3-43)}$$

where only the wall friction and gravity heads are used. The enthalpy h_i is determined by use of the enthalpy transport model discussed in a later section of this report. If the enthalpy transport model is not used, the enthalpy h_i is given by

$$h_i = h_k \qquad \text{(II.3-44)}$$

depending upon the direction of flow.

The constitutive models required by the macroscopic balance equations are given in the next section.

III. CONSTITUTIVE MODELS

The derivation of the macroscopic balance equations has introduced several quantities which must be modeled in order that a closed system of equations be obtained. In general, these quantities represent the exchange of momentum and energy between the fluid and the surfaces bounding the fluid. The specific models which are available in RETRAN are given in the following sections.

1.0 LINEAR MOMENTUM EQUATION

The linear momentum balance of Equation II.3-40 requires models for the wall-to-fluid momentum exchange due to wall friction, local flow perturbations, and moving surfaces. A general definition of the forces due to stationary surfaces has been given by Equation II.2-25 as

$$-\tilde{F}_w - \tilde{F}_{\ell oc} = \int_{S_W} [-p\bar{\bar{I}} + \bar{\bar{\sigma}}]\cdot d\tilde{S} \quad . \qquad \text{(III.1-1)}$$

In practice, the surface S_w is divided into a portion to which a friction factor model can be applied plus a portion to which a loss coefficient can be applied. That is, an additive type approach is taken. In many cases, especially when complex flow channels and flow patterns are involved, the use of an additive approach requires that a large amount of engineering experience be used in modeling the flow channel.

Letting $S_{w,f}$ and $S_{w,\ell oc}$ denote the portions of S_w to which the friction and local loss models are to be applied, Equation III.1-1 can be written as

$$-\tilde{F}_w - \tilde{F}_{\ell oc} = \int_{S_{wf}} [-p\bar{\bar{I}} + \bar{\bar{\sigma}}]\cdot d\tilde{S} + \int_{S_{w\ell oc}} [-p\bar{\bar{I}} + \bar{\bar{\sigma}}]\cdot d\tilde{S} \quad . \qquad \text{(III.1-2)}$$

RETRAN contains models for both the wall friction and the local losses due to flow perturbations.

1.1 Friction Factor and Two-Phase Multipliers

A general equation for the wall friction force is obtained by equating the corresponding parts of Equation III.1-2. The wall friction force is given by

$$-\vec{F}_w = \int_{S_{wf}} [-p\bar{\bar{I}} + \bar{\bar{\sigma}}]\cdot d\vec{S} \quad . \tag{III.1-3}$$

Equation II.3-40 requires $\vec{F}_w/A_k$, and Equation III.1-3 is applied to one-half of volume V_k to obtain

$$-\frac{\vec{F}_{w,i}}{A_k} = \frac{1}{A_k}\int_{S_{wf,i}} [-\bar{\bar{p}}\bar{\bar{I}} + \bar{\bar{\sigma}}]\cdot d\vec{S} \quad , \tag{III.1-4}$$

where $S_{wf,i}$ refers to the distance $\frac{1}{2}(L_k)$.

The integral in Equation III.1-4 is evaluated by assuming that the arguments can be represented by an average value to obtain

$$-\frac{F_{w,i}}{A_k} = -\frac{1}{A_k}\, S_{wf,i}\, B_{w,k}\bar{v}_k \quad , \tag{III.1-5}$$

where $B_{w',k}$ is defined by

$$B_{w,k} = \frac{1}{2}\,\bar{\rho}_k|\bar{v}_k|f_{w,k}\,\phi^2_{tp,k} \quad , \tag{III.1-6}$$

with

$f_{w,k}$ = Fanning friction factor for the volume k

$\phi^2_{tp,k}$ = two-phase friction multiplier for the volume k.

The area ratio $S_{wf,i}/A_k$ in Equation III.1-5 can be rewritten to obtain

$$\frac{S_{wf,i}}{A_k} = \frac{S_{wf,i}}{A_k} \frac{\frac{1}{2}(L_k)}{\frac{1}{2}(L_k)} = \left(\frac{\frac{1}{2}(S_{wf,k})}{\frac{1}{2}(V_k)}\right) \frac{L_k}{2} , \qquad \text{(III.1-7)}$$

where the final factor on the right hand side is the wetted surface area per unit fluid volume. The wetted surface area per unit fluid volume is usually given as the equivalent wetted diameter

$$\frac{1/2(S_{w,fk})}{1/2(V_k)} = \bar{A}_{wk} = \frac{4}{D_{hy,k}} . \qquad \text{(III.1-8)}$$

Substituting Equations III.1-6 and III.1-8 into Equation III.1-5 gives the wall friction force as

$$\frac{F_{w,i}}{A_k} = \left(\frac{4}{D_{hy,k}}\right)\left(\frac{L_k}{2}\right) \frac{1}{2} \bar{\rho}_k \bar{v}_k \left|\bar{v}_k\right| f_{w,k} \phi^2_{tp,k} . \qquad \text{(III.1-9)}$$

A similar expression is used for the other half of V_i with the independent variables defined at the center of the volume V_{k+1}. The friction factor $f_{w,k}$ and the two-phase friction multiplier, $\phi^2_{tp,k}$ in Equation III.1-9, are primarily obtained from various representations of experimental data.

The friction factor $f_{w,k}$ is a function of the flow speed, the geometry of the surfaces of the flow channel, and the energy exchange between the fluid and channel walls. A general relationship can be written

$$f_{w,k} = f_{w,k} \text{ (Re, geometric factors, thermal factors, local transport properties, ...).} \qquad \text{(III.1-10)}$$

The expressions used in RETRAN are applicable to flow of single phase fluids in circular flow channels with smooth walls [III.1-1] The wall friction factor for slow speed, or laminar, flow is given by

$$f_{w,k} = \frac{16}{Re_k} , \qquad \text{(III.1-11)}$$

where

$$(f_{w,k} > f_e),$$

and for high speed, or turbulent flow, by

$$\frac{1}{(f_{w,k})^{1/2}} = 0.40 + 4.0 \log_{10} \left[Re_k \, (f_{w,k})^{1/2} \right] \qquad \text{(III.1-12)}$$

The Reynolds number is given by

$$Re_k = \frac{\bar{\rho}_k |\bar{v}_k| D_{hy,k}}{\mu_k} , \qquad \text{(III.1-13)}$$

and a transition friction factor, f_e, is taken to be

$$f_e = .012. \qquad \text{(III.1-14)}$$

The density, $\bar{\rho}_k$, and viscosity, μ_k, are given by

$$\bar{\rho}_k = \frac{1}{\frac{x_k}{\rho_{gs,k}} + \frac{(1 - x_k)}{\rho_{\ell s,k}}} \qquad \text{(III.1-15)}$$

and

$$\mu_k = \begin{cases} \mu_{\ell s} & x<1 \\ \mu_{gs} & x \geq 1 \end{cases} \qquad \text{(III.1-16)}$$

for two-phase flow and the appropriate values are used for the case of single phase vapor and liquid flow. The transition friction factor of Equation III.1-14 provides for a continuous change in the friction factor as a function of the Reynolds number.

With the Reynolds number defined by Equation III.1-13, the wall friction force for two-phase flow can be written as

$$\frac{F_{w,i}}{A_k} = \left(\frac{F_{w,i}}{A_k}\right)_{LO} \phi^2_{tp,k} \qquad \text{(III.1-17)}$$

where $\left(\frac{F_{w,i}}{A_k}\right)_{LO}$ is the wall friction force for single phase liquid flow.

The two-phase friction multiplier, $\phi^2_{tp,k}$, has received an extensive amount of investigation.[III.1-2 through III.1-5] These investigations have been conducted in order to provide information which is necessary to design two-phase fluid flow systems. The two-phase friction multiplier is necessary in order that pumping requirements can be determined for two-phase fluid flow systems. The results of these investigations have shown that the two-phase friction multiplier is a function of the distribution of the phases within the flow channel or the flow regime. An extremely wide variety of physical models and empirical correlations of data have been employed in order to describe the effects of two-phase flow on the pressure gradient. Many of these models and correlations are overall-mixture types of models which cover wide ranges of flow regimes without specific accounting of flow regime effects. In particular, most correlations do not include accounting of the experimentally determined effect of mass flow rate, or mass flux, on the two-phase friction multiplier. Three different two-phase multipliers are available in RETRAN and are discussed in the following sections.

1.1.1 Homogeneous Correlation

One version of the two-phase multiplier included in RETRAN results in a modification to the wall friction force based on a density correction. This multiplier can be used for homogeneous flow, provided a proper correction is made at values of $x \geq 1$, and is given by

$$\phi^2_{tp,k} = 1 + x\left(\frac{\rho_{\ell s}}{\rho_{gs}} - 1\right) . \qquad \text{(III.1-18)}$$

For values of $x \geq 1$, the Fanning friction factor in Equation III.1-13 is based on the flow of a single phase vapor and the two-phase multiplier is equal to unity.

1.1.2 Baroczy Correlation

The correlation of Baroczy [III.1-6, III.1-7] incorporates a mass flux correction factor for the friction multiplier. The Baroczy correlation is made up of two sets of curves as follows. The first set of curves consists of the friction multiplier, $\phi^2_{tp,k}$, at a reference mass flux of 1×10^6 $lb_m/hr\text{-}ft^2$. The multiplier is given as a function of a physical property index

$$\Gamma = \left(\frac{\mu_{\ell s}}{\mu_{gs}}\right)^{0.2} \frac{\rho_{gs}}{\rho_{\ell s}}, \qquad \text{(III.1-19)}$$

with the thermodynamic quality, x, as a parameter. The mass flux correction factor, F_G, is also expressed as a function of Γ with quality as a parameter. The correction factors were obtained for mass flux values of 0.25×10^6, 0.50×10^6, 2.0×10^6, and 3.0×10^6 $lb_m/hr\text{-}ft^2$.

The Baroczy correlation included in RETRAN has been modified in the following manner. The physical property parameter, Γ of Equation III.1-19, has been converted to an equivalent pressure for the saturated steam-saturated liquid water case. The numerical values of the friction multiplier at the reference mass flux $G = 1.0 \times 10^6$ $lb_m/hr\text{-}ft^2$ have been changed from the original values given by Baroczy. The values of ϕ^2_{tp} at $G = 1.0 \times 10^6$ $lb_m/hr\text{-}ft^2$ which are used in RETRAN are given in Table III.1-1. The values of the mass flux correction factor, F_G, for $G = 0.25 \times 10^6$, 0.50×10^6, 2.0×10^6, and 3.0×10^6 $lb_m/hr\text{-}ft^2$ are given in Tables III.1-2 through III.1-5, respectively. Linear extrapolation is used for values of the mass flux less than 0.25×10^6 $lb_m/hr\text{-}ft^2$ and linear interpolation is used for mass flux values between 0.25×10^6 and 3.0×10^6 $lb_m/hr\text{-}ft^2$. For mass fluxes greater than 3×10^6 $lb_m/hr\text{-}ft^2$, the mass flux correction is given by

TABLE III.1-1

RETRAN VALUES OF THE MODIFIED BAROCZY TWO-PHASE FRICTION MULTIPLIER

AT G = 1.0×10^6 $lb_m/hr\text{-}ft^2$

Property Index[a] Γ	Thermodynamic Quality													
	0.001	0.010	0.020	0.050	0.10	0.15	0.20	0.30	0.40	0.50	0.60	0.70	0.90	1.00
0.001	2.11	8.8	15.0	33.5	68	108	150	233	330	500	690	880	1080	1000
0.002	2.09	8.5	14.2	29.5	50	73	96	141	190	276	360	470	580	500
0.003	2.02	8.1	13.2	26.2	41	58	73	105	138	195	255	322	390	333
0.005	1.97	7.1	11.2	22	31	43	53	72	91	125	160	202	243	200
0.007	1.83	5.9	9.1	17.2	25	35	42	56	68	93	116	148	172	143
0.008	1.77	5.5	8.2	15.7	23	32	39	51	62	83	102	130	152	125
0.009	1.69	5.1	7.6	14	21	29.5	35.7	46.5	56	75	93	117	136	111
0.010	1.60	4.7	7.0	12.8	19.2	27.5	33	43	51.5	69	84	106	121	100
0.020	1.24	2.5	3.6	6.6	11	15.8	19	25	29.5	38	44	54	57.5	50
0.03	1.14	1.88	2.55	4.6	7.6	11	13.2	17.8	20.5	27	30	35.5	38	33.3
0.05	1.10	1.50	1.89	3.15	4.6	6.6	8.2	11	13	16.3	18.5	21	22.2	20
0.07	1.08	1.35	1.68	2.55	3.6	4.8	5.8	7.8	9.3	12	13.3	15	15.7	14.3
0.08	1.08	1.31	1.60	2.4	3.25	4.2	5.1	6.8	8.1	10.5	11.8	13	13.6	12.5
0.09	1.07	1.28	1.55	2.25	3.05	3.85	4.5	6.1	7.2	9.4	10.4	11.3	12.0	11.1
0.10	1.07	1.26	1.51	2.12	2.82	3.55	4.2	5.5	6.6	8.5	9.4	10.2	10.8	10.0
0.20	1.04	1.15	1.31	1.61	1.95	2.23	2.55	3.0	3.34	4.2	4.8	5.1	5.25	5.0
0.3	1.02	1.10	1.21	1.40	1.63	1.8	1.92	2.2	2.5	2.9	3.2	3.35	3.42	3.33
0.5	1.02	1.06	1.11	1.20	1.31	1.40	1.45	1.55	1.64	1.82	1.93	2.0	2.02	2.0
0.7	1.01	1.03	1.05	1.10	1.15	1.20	1.22	1.24	1.28	1.34	1.40	1.42	1.43	1.43
0.8	1.01	1.02	1.03	1.06	1.10	1.12	1.13	1.14	1.15	1.20	1.22	1.24	1.25	1.25
0.9	1.00	1.01	1.01	1.02	1.04	1.05	1.06	1.07	1.07	1.08	1.09	1.11	1.11	1.11

[a] Property Index, $\Gamma = \left(\frac{\mu_{\ell s}}{\mu_{gs}}\right)^{0.2} \frac{\rho_{gs}}{\rho_{\ell s}}$

where μ = dynamic viscosity
ρ = density
ℓ = liquid
g = gas
s = saturation

TABLE III.1-2

RETRAN VALUES OF THE BAROCZY MASS FLUX CORRECTION FACTOR

AT G = 0.25×10^6 $lb_m/hr\text{-}ft^2$

Property Index Γ	Thermodynamic Quality								
	0.001	0.010	0.050	0.10	0.20	0.40	0.60	0.80	1.00
0.001	1.40	1.40	1.30	1.493	1.493	1.36	1.255	1.13	1.0
0.002	1.268	1.268	1.15	1.457	1.457	1.306	1.197	1.114	1.0
0.003	1.19	1.19	1.061	1.435	1.435	1.274	1.162	1.106	1.0
0.005	1.168	1.168	1.037	1.41	1.41	1.24	1.140	1.098	1.0
0.007	1.173	1.173	1.082	1.392	1.392	1.253	1.142	1.091	1.0
0.008	1.177	1.178	1.101	1.388	1.388	1.26	1.143	1.09	1.0
0.009	1.179	1.184	1.120	1.382	1.382	1.264	1.144	1.09	1.0
0.010	1.181	1.191	1.135	1.379	1.379	1.268	1.145	1.089	1.0
0.020	1.193	1.236	1.235	1.363	1.363	1.295	1.151	1.087	1.0
0.03	1.201	1.262	1.293	1.371	1.371	1.31	1.153	1.084	1.0
0.05	1.212	1.295	1.369	1.41	1.41	1.33	1.16	1.081	1.0
0.07	1.20	1.283	1.417	1.48	1.48	1.35	1.165	1.08	1.0
0.08	1.19	1.268	1.435	1.516	1.516	1.36	1.17	1.08	1.0
0.09	1.181	1.25	1.452	1.55	1.55	1.37	1.174	1.08	1.0
0.10	1.172	1.238	1.469	1.582	1.582	1.379	1.179	1.079	1.0
0.20	1.120	1.151	1.540	1.77	1.77	1.416	1.189	1.07	1.0
0.3	1 091	1.113	1.40	1.59	1.59	1.309	1.15	1.053	1.0
0.5	1.054	1.067	1.232	1.34	1.34	1.179	1.087	1.031	1.0
0.7	1.03	1.034	1.12	1.178	1.178	1.092	1.045	1.017	1.0
0.8	1.02	1.021	1.077	1.113	1.113	1.059	1.029	1.01	1.0
0.9	1.01	1.011	1.038	1.055	1.055	1.029	1.014	1.005	1.0
1.0	1.0	1.0	1.0	1.0	1.0	1.0	1.0	1.0	1.0

TABLE III.1-3

RETRAN VALUES OF THE BAROCZY MASS FLUX CORRECTION FACTOR

AT G = 0.50 x 10^6 $lb_m/hr\text{-}ft^2$

Property Index Γ	Thermodynamic Quality								
	0.001	0.010	0.050	0.10	0.20	0.40	0.60	0.80	1.00
0.001	1.205	1.288	1.205	1.28	1.27	1.20	1.155	1.088	1.0
0.002	1.17	1.269	1.17	1.276	1.249	1.176	1.13	1.08	1.0
0.003	1.149	1.259	1.149	1.271	1.237	1.161	1.118	1.074	1.0
0.005	1.13	1.245	1.13	1.263	1.23	1.157	1.109	1.07	1.0
0.007	1.127	1.234	1.137	1.258	1.23	1.168	1.11	1.071	1.0
0.008	1.124	1.229	1.14	1.254	1.23	1.171	1.11	1.071	1.0
0.009	1.122	1.224	1.146	1.251	1.231	1.176	1.11	1.071	1.0
0.010	1.12	1.22	1.15	1.25	1.231	1.18	1.11	1.072	1.0
0.020	1.112	1.191	1.175	1.237	1.236	1.202	1.15	1.076	1.0
0.03	1.107	1.176	1.19	1.229	1.239	1.216	1.2	1.079	1.0
0.05	1.100	1.154	1.21	1.22	1.246	1.235	1.27	1.08	1.0
0.07	1.092	1.141	1.23	1.254	1.3	1.245	1.32	1.078	1.0
0.08	1.09	1.134	1.24	1.277	1.337	1.253	1.36	1.075	1.0
0.9	1.088	1.128	1.25	1.297	1.369	1.262	1.4	1.073	1.0
0.10	1.085	1.121	1.259	1.314	1.398	1.27	1.42	1.07	1.0
0.20	1.07	1.085	1.31	1.427	1.56	1.31	1.6	1.059	1.0
0.3	1.06	1.063	1.231	1.33	1.422	1.231	1.2	1.043	1.0
0.5	1.037	1.037	1.133	1.188	1.242	1.133	1.07	1.025	1.0
0.7	1.019	1.019	1.069	1.096	1.123	1.069	1.035	1.012	1.0
0.8	1.01	1.01	1.042	1.06	1.078	1.042	1.021	1.007	1.0
0.9	1.004	1.004	1.021	1.029	1.037	1.021	1.01	1.003	1.0
1.0	1.0	1.0	1.0	1.0	1.0	1.0	1.0	1.0	1.0

TABLE III.1-4

RETRAN VALUES OF THE BAROCZY MASS FLUX CORRECTION FACTOR

AT G = 2.0×10^6 $lb_m/hr\text{-}ft^2$

Property Index Γ	Thermodynamic Quality								
	0.001	0.010	0.050	0.10	0.20	0.40	0.60	0.80	1.00
0.001	0.810	0.700	0.720	0.732	0.740	0.790	0.838	0.920	1.0
0.002	0.835	0.687	0.704	0.728	0.748	0.799	0.848	0.923	1.0
0.003	0.850	0.680	0.697	0.725	0.751	0.804	0.855	0.928	1.0
0.005	0.863	0.690	0.700	0.728	0.755	0.800	0.848	0.919	1.0
0.007	0.870	0.715	0.715	0.738	0.758	0.789	0.830	0.902	1.0
0.008	0.872	0.825	0.720	0.742	0.759	0.782	0.821	0.898	1.0
0.010	0.874	0.741	0.730	0.750	0.760	0.775	0.810	0.888	1.0
0.020	0.885	0.792	0.758	0.773	0.768	0.750	0.770	0.858	1.0
0.03	0.891	0.822	0.773	0.787	0.770	0.731	0.748	0.840	1.0
0.05	0.900	0.860	0.794	0.803	0.775	0.710	0.720	0.816	1.0
0.07	0.913	0.880	0.795	0.795	0.750	0.700	0.700	0.795	1.0
0.08	0.920	0.884	0.792	0.785	0.735	0.685	0.685	0.785	1.0
0.09	0.925	0.889	0.790	0.778	0.722	0.670	0.670	0.778	1.0
0.10	0.929	0.891	0.788	0.770	0.710	0.660	0.660	0.770	1.0
0.20	0.960	0.911	0.770	0.720	0.640	0.585	0.585	0.720	1.0
0.3	0.969	0.933	0.830	0.787	0.728	0.687	0.687	0.787	1.0
0.4	0.975	0.950	0.870	0.840	0.792	0.760	0.760	0.840	1.0
0.6	0.987	0.971	0.928	0.910	0.883	0.868	0.868	0.910	1.0
0.8	0.993	0.989	0.968	0.961	0.948	0.942	0.942	0.961	1.0
0.9	0.997	0.995	0.983	0.980	0.975	0.974	0.974	0.980	1.0
1.0	1.0	1.0	1.0	1.0	1.0	1.0	1.0	1.0	1.0

TABLE III.1-5

RETRAN VALUES OF THE BAROCZY MASS FLUX CORRECTION FACTOR

AT G = 3.0×10^6 $lb_m/hr\text{-}ft^2$

Property Index Γ	Thermodynamic Quality								
	0.001	0.010	0.050	0.10	0.20	0.40	0.60	0.80	1.00
0.001	0.710	0.550	0.570	0.613	0.600	0.680	0.751	0.835	1.0
0.002	0.742	0.520	0.540	0.600	0.610	0.690	0.768	0.835	1.0
0.003	0.762	0.502	0.520	0.590	0.614	0.696	0.776	0.870	1.0
0.005	0.788	0.514	0.523	0.600	0.619	0.686	0.755	0.852	1.0
0.007	0.798	0.554	0.546	0.612	0.620	0.667	0.727	0.830	1.0
0.008	0.801	0.570	0.554	0.620	0.621	0.660	0.715	0.820	1.0
0.009	0.806	0.582	0.562	0.622	0.622	0.650	0.704	0.811	1.0
0.010	0.810	0.595	0.570	0.626	0.623	0.645	0.695	0.803	1.0
0.020	0.832	0.677	0.617	0.654	0.630	0.603	0.635	0.753	1.0
0.03	0.848	0.725	0.644	0.670	0.634	0.580	0.600	0.725	1.0
0.05	0.868	0.787	0.680	0.691	0.640	0.550	0.556	0.690	1.0
0.07	0.887	0.818	0.690	0.690	0.620	0.530	0.530	0.663	1.0
0.08	0.894	0.827	0.690	0.685	0.610	0.520	0.520	0.654	1.0
0.09	0.900	0.833	0.690	0.680	0.600	0.515	0.515	0.648	1.0
0.10	0.906	0.840	0.690	0.675	0.593	0.510	0.510	0.640	1.0
0.20	0.945	0.882	0.690	0.650	0.560	0.475	0.475	0.603	1.0
0.3	0.960	0.913	0.770	0.740	0.670	0.610	0.610	0.702	1.0
0.4	0.970	0.935	0.825	0.800	0.750	0.700	0.700	0.773	1.0
0.5	0.978	0.950	0.868	0.850	0.810	0.775	0.775	0.830	1.0
0.7	0.989	0.973	0.931	0.924	0.900	0.885	0.885	0.910	1.0
0.8	0.992	0.983	0.957	0.952	0.940	0.928	0.928	0.945	1.0
0.9	0.996	0.991	0.979	0.975	0.975	0.968	0.968	0.975	1.0
1.0	1.0	1.0	1.0	1.0	1.0	1.0	1.0	1.0	1.0

$$F_G = \frac{(F_G \text{ at } G = 3 \times 10^6)^{(G/10^6 - 2)}}{(F_G \text{ at } G = 2 \times 10^6)^{(G/10^6 - 3)}} \qquad (G/10^6 > 3) \ . \quad \text{(III.1-20)}$$

One other modification is incorporated into the RETRAN version of the Baroczy correlation. Instead of multiplying the two-phase multiplier for $G = 1 \times 10^6$ $lb_m/hr\text{-}ft^2$ by the mass flux correction, the following equation is used,

$$\phi^2_{tp,k} = 1 + \left[\phi^2_{tp,k}\Big|_{G=1\times10^6} - 1.0\right] F_G \ . \quad \text{(III.1-21)}$$

The original Baroczy model is given by

$$\phi^2_{tp,k}\Big|_G = \phi^2_{tp,k}\Big|_{G=1\times10^6} \ F_G \ . \quad \text{(III.1-22)}$$

Comparing Equation III.1-22 with Equation III.1-21 and examining the basic multipliers given in Table III.1-1 shows the effect of using Equation III.1-22 instead of Equation III.1-21. The modifications which have been incorporated into the RETRAN version of the Baroczy correlation have been developed with experimental data in References III.1-8 through III.1-13.

Substituting Equation III.1-21 into Equation III.1-9 gives the wall-fluid momentum exchange as

$$F_{w,k} = 4\left(\frac{L_k}{2D_{hy,k}}\right)\frac{\bar{\rho}_k \bar{v}_k |\bar{v}_k|}{2} f_{w,k}\left\{1 + \left[\phi^2_{tp,k}\Big|_{G=1\times10^6} - 1\right] F_G\right\}, \quad \text{(III.1-23)}$$

where the two-phase multiplier is given in Table III.1-1 and F_G is obtained as previously discussed.

1.1.3 Beattie Correlations and Bennett Flow Regime Map

While the Baroczy correlation provides a two-phase multiplier which is dependent on the mass flux in the channel, it only indirectly accounts for changes in the friction force which are flow regime dependent. The option of using Beattie's correlations[III.1-14, III.1-15], which are flow regime dependent, has been added to RETRAN. These correlations and a method of determining the volume flow regime are discussed in this section.

1.1.3.1 Bennett Flow Regime Map

The flow regime map of Bennett et al.[III.1-16] is based on visual studies of liquid water-steam flowing upward in a heated vertical tube. The results of the observations were plotted using the coordinates of total mass flux, G, versus the thermodynamic quality, x. Figure III.1-1 represents data obtained at 1000 psia in a 0.5-inch-ID circular conduit. Bennett's map is believed to be more independent of pressure if the thermodynamic quality "x" is converted to the homogeneous volume fraction, α. The relation between quality and α, is given by

$$\alpha = \frac{\frac{x}{\rho_{gs}}}{\frac{(1-x)}{\rho_{\ell s}} + \frac{x}{\rho_{gs}}} \quad . \qquad \text{(III.1-24)}$$

The original flow regime map by Bennett et al. is shown in Figure III.1-1 and the modified flow regime map is shown in Figure III.1-2. In the modified flow regime map, the flow regime boundaries are approximated by straight lines. The map shown in Figure III.1-2 is assumed to apply to both vertical and horizontal flows in RETRAN, although the original map was based on vertical upflow. The flow regime boundary between annular and bubble flows is maintained at $\alpha = 0.24$ for mass fluxes above 3×10^6 lbm/ft^2-hr even though data are not reported beyond this value by Bennett. The upper boundary of annular and wispy annular flow in Figure III.1-1 separates those regions from post CHF conditions. In Figure III.1-2, these two regions are treated as annular flow except when CHF is exceeded, in which case they are treated as post CHF (dispersed) flow.

1356 096

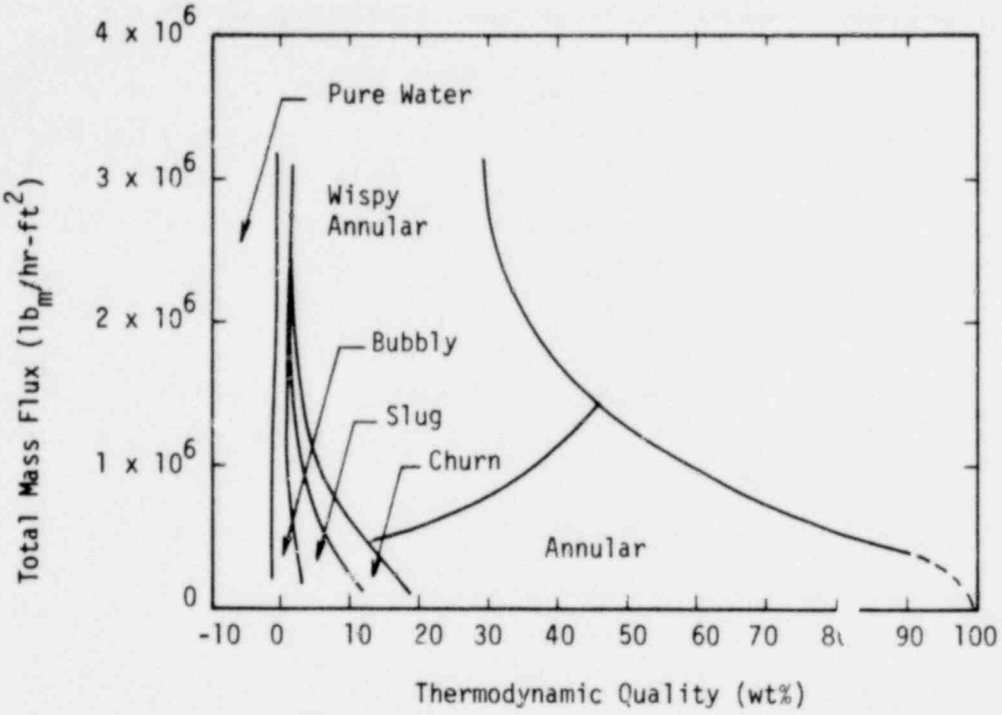

Figure III.1-1 Bennett Flow Regime Map for Vertical Upflow (From Ref. III.1-16.)

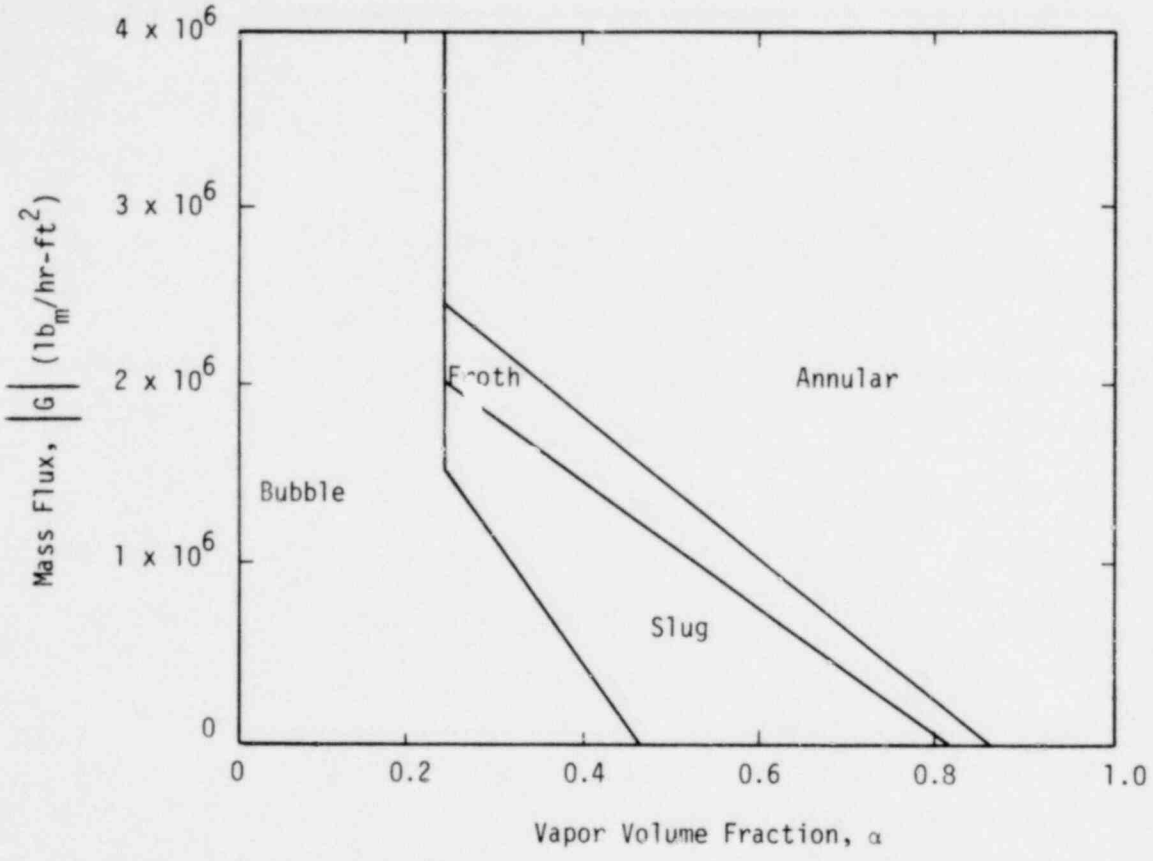

Figure III.1-2 Modified Bennett Flow Regime Map

1.1.3.2 Beattie Two-Phase Multipliers

In an attempt to account for the effect of flow regime on the friction force, Beattie[III.1-14, III.1-15] has developed a set of two-phase multipliers which are flow regime dependent. The Beattie multipliers for two phase flow in pipes have been incorporated in RETRAN to provide a third option for the use of a two-phase multiplier, and are listed in Table III.1-6. In RETRAN, the flow regime for volume "k" is determined from the flow regime map in Figure III.1-2, and the appropriate two-phase multiplier is then computed. The friction loss is then computed from Equation III.1-17.

1.2 Local Momentum Losses

At the present time, local momentum losses are modeled in RETRAN by use of the irreversible loss coefficients associated with the mechanical energy balance. These coefficients, e_v^* of Equation II.3-40, are functions of the geometric details of the flow channel and the flow speed and direction. Tabulations of e_v^* are available in References [III.1-17, III.1-18].

The model used in RETRAN does not contain corrections for two-phase flow effects. [III.1-2, III.1-3, III.1-4]. These coefficients are specified as input values and any value can be used.

1.3 Phase Separation (Bubble Rise) Model

The phase separation or so-called bubble rise model is a combination of a semi-empirical relation for vapor phase, or "bubble" distribution and a differential equation for the mass of vapor at any time in a volume. The model attempts to account for the separation of a flashing two-phase mixture which occurs during the depressurization of vertically oriented vessels. The model was originally developed for RELAP2 which modeled a nuclear reactor system using three control volumes[III.1-19, III.1-20, III.1-21] and was intended to be used only in a single volume. The model was refined and verified by comparison to Semiscale high pressure blowdowns.[III.1-21]

In actuality, the phase separation is a simplified slip model. When slip is incorporated into RETRAN, the phase separation model presented herein must be

TABLE III.1-6

BEATTIE TWO-PHASE FRICTION MULTIPLIERS

Flow regime	Two-Phase Multiplier, $\phi^2_{tp,k}$
Bubble	$\left[1 + x(\rho_{\ell s}/\rho_{gs} - 1)\right]^{0.8}\left[1 + x\left(\frac{(3.5\mu_g + 2\mu_\ell)\,\rho_{\ell s}}{(\mu_g + \mu_\ell)\,\rho_{gs}} - 1\right)\right]^{0.2}$
Froth, slug	$\left[1 + x\,(\rho_{\ell s}/\rho_{gs} - 1)\right]^{0.8}\left[1 + x\,(3.5\rho_{\ell s}/\rho_{gs} - 1)\right]^{0.2}$
Annular	$\left[1 + x\,(\rho_{\ell s}/\rho_{gs} - 1)\right]^{0.8}\left[1 + x\left(\frac{\mu_g \rho_{\ell s}}{\mu_\ell \rho_{gs}} - 1\right)\right]^{0.2}$
Dispersed (Post CHF)	$\left(\frac{\mu_g}{\mu_\ell}\right)^{0.2}\left(\frac{\rho_{gs}}{\rho_{\ell s}}\right)^{0.8}\left[1 + x\left(\frac{\rho_{\ell s}}{\rho_{gs}} - 1\right)\right]^{1.8}$

modified in order to be consistent. Use of the model in a slip modified code is incorrect since all of the water entering a volume is assumed to exist only in the mixture at the bottom of the volume and not in the steam dome.

During a continuous decompression of a large stagnant vertical volume, the partial density of steam bubbles should be the least near the bottom of the volume. This distribution is reasonable since the static pressure will be highest near the bottom plus the fact that the bubbles tend to coalesce as they rise through the mixture. The simplest model approximating this situation is one in which the partial density of bubbles is assumed to increase linearly within the two-phase mixture as shown in Figure III.1-3. Obviously, the model is incapable of describing other bubble concentrations when physical conditions, such as oscillating pressure, lead to more complicated distributions. Other models could be used for the assumed distribution, however.

The assumed linear distribution in the two-phase mixture below the steam dome is

$$\rho_{gb} = m_{gb} \frac{z}{z_m} + b_{gb} \qquad \text{(III.1-25)}$$

where ρ_{gb} is the partial steam density in the two-phase mixture, z is the height above the bottom of the volume, z_m is the height of the mixture interface and m_{gb} and b_{gb} are parameters.

The number of undetermined parameters in Equation III.1-25 is reduced to one by use of the relation for the total mass of the steam.

$$M_{gb} = A \int_0^{z_m} \rho_{gb}\, dz \qquad \text{(III.1-26)}$$

where A is the cross-sectional area and M_{gb} is the mass of the steam, as bubbles, below the mixture interface. Performing the indicated integration and assuming that the control volume area and volume (V_m) are related by

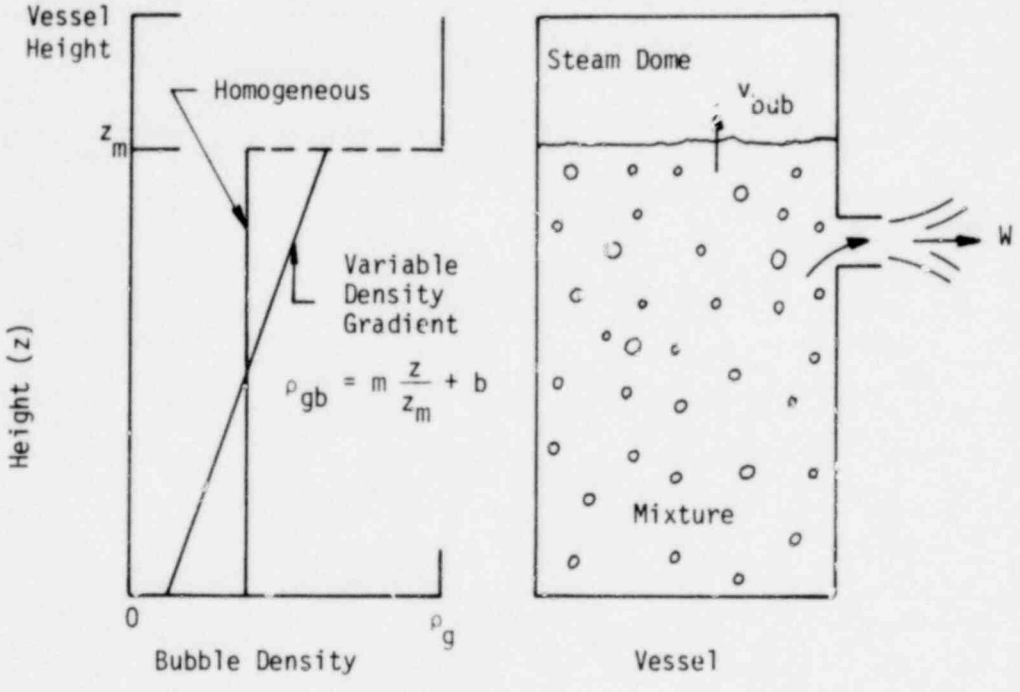

Figure III.1-3 Two-Phase Separation Model

$$Az_m = V_m \qquad \text{(III.1-27)}$$

yields

$$\frac{1}{2} m_{gb} + b_{gb} = \frac{M_{gb}}{V_m} \quad . \qquad \text{(III.1-28)}$$

Clearly, the parameters m_{gb} and b_{gb} are not independent. When $m_{gb}=0$ in Equation III.1-28,

$$b_{gb} = M_{gb}/V_m, \qquad \text{(III.1-29)}$$

which is the uniform average partial density of steam in the two-phase mixture.

When b=0 in Equation III.1-28,

$$m_{gb} = 2\, M_{gb}/V_m. \qquad \text{(III.1-30)}$$

The partial steam density and hence the volume fraction of steam is then zero at z=0. Equation III.1-30 represents the maximum bubble gradient possible. In order to generalize the model, a non-negative parameter, C_o, is defined such that

$$m_{gb} = 2C_o\, M_{gb}/V_m. \qquad \text{(III.1-31)}$$

The parameter b is then obtainable from Equation III.1-28 as

$$b_{gb} = (1 - C_o)\, M_{gb}/V_m. \qquad \text{(III.1-32)}$$

Hence the generalized form of the steam partial density in the mixture is obtained by combining Equations III.1-28, III.1-31, and III.1-32 as

$$\rho_{gb} = \frac{2C_o M_{gb}}{V_m}\left(\frac{z}{z_m}\right) + \frac{(1 - C_o)\, M_{gb}}{V_m} \quad . \qquad \text{(III.1-33)}$$

At the volume bottom, z=0, Equation III.1-33 yields

$$\rho_{gb} = (1 - C_o)\, M_{gb}/V_m \qquad \text{(III.1-34)}$$

In order for ρ_{gb} to be non-negative at z=0, that is,

$$\rho_{gb} \geq 0 \qquad \text{(III.1-35)}$$

C_o must be less than or equal to one. At the steam-mixture interface, $z=z_m$, Equation III.1-33 becomes

$$\rho_{gb} = \frac{(C_o + 1)\, M_{gb}}{V_m} . \qquad \text{(III.1-36)}$$

The partial steam density, ρ_{gb}, of the interface must be less than or equal to the pure steam density, that is,

$$\frac{\rho_{gb}}{\rho_g} \leq 1. \qquad \text{(III.1-37)}$$

Division of Equation III.1-36 by ρ_g and use of Equation III.1-37 results in

$$\frac{M_{gb}}{\rho_g V_m} \leq \frac{1}{C_o + 1} . \qquad \text{(III.1-38)}$$

Since $C_o \leq 1$ in order for ρ_{gb} to be non-negative by Equation III.1-35, Equation III.1-38 becomes

$$\frac{M_{gb}}{\rho_g V_m} \leq \frac{1}{2} . \qquad \text{(III.1-39)}$$

The constraint given by Equation III.1-39 must be used in order for Equation III.1-31 to yield physically meaningful results. The factor $M_{gb}/\rho_g V_m$ is the average volume fraction of steam in the mixture, α_{gm}.

The generalization of the slope parameter, m_{gb}, must be modified for an average volume fraction of steam above 0.5. In order to see how this might be done, rewrite Equation III.1-31 as

$$\frac{m_{gb}}{\rho_g} = 2\, C_o\, \alpha_{gm}. \qquad \text{(III.1-40)}$$

Since Equation III.1-40 can only be used for a $\alpha_{gm} \leq 0.5$, it is reasonable from symmetry arguments to modify this equation for $\alpha_{gm} \geq 0.5$ as

$$\frac{m_{gb}}{\rho_g} = 2\, C_o\, (1 - \alpha_{gm}) = 2\, C_o\, \alpha_{\ell m}, \qquad \text{(III.1-41)}$$

where $\alpha_{\ell m}$ is the average volume fraction of liquid in the mixture. Equation III.1-41 may be rewritten using the definition of α_{gm} as

$$m_{gb} = 2C_o \left(\rho_g - \frac{M_{gb}}{V_m} \right). \qquad \text{(III.1-42)}$$

The b_{gb} parameter then becomes, from Equation III.1-28,

$$b_{gb} = (1 + C_o) \frac{M_{gb}}{V_m} - C_o \rho_g. \qquad \text{(III.1-43)}$$

The expression for the bubble partial density then becomes

$$\rho_{gb} = 2C_o \left(\rho_g - \frac{M_{gb}}{V_m} \right) \left(\frac{z}{z_m} \right) + (1 + C_o) \frac{M_{gb}}{V_m} - C_o \rho_g. \qquad \text{(III.1-44)}$$

At the steam-mixture interface, $z = z_m$, Equation III.1-44 becomes

$$\rho_{gb} = C_o \left(\rho_g - \frac{M_{gb}}{V_m} \right) + \frac{M_{gb}}{V_m}. \qquad \text{(III.1-45)}$$

Since the steam density at the interface must be less than or equal to the pure steam density Equation III.1-37 forces

$$C_o \left(1 - \frac{M_{gb}}{\rho_g V_m}\right) + \frac{M_{gb}}{\rho_g V_m} \leq 1, \qquad \text{(III.1-46)}$$

which simply requires C_o to be less than or equal to one again.

At the bottom of the volume, z=0, Equation III.1-44 becomes

$$\rho_{gb} = (1 + C_o) \frac{M_{gb}}{V_m} - C_o \rho_g. \qquad \text{(III.1-47)}$$

In order for the partial density to be non-negative in Equation III.1-47,

$$(1 + C_o) \frac{M_{gb}}{V_m} - C_o \rho_g \geq 0. \qquad \text{(III.1-48)}$$

Division of Equation III.1-48 by ρ_g and rearranging produces

$$\frac{M_{gb}}{\rho_g V_m} \geq \frac{C_o}{1 + C_o} = \frac{1}{1 + \frac{1}{C_o}}. \qquad \text{(III.1-49)}$$

Since $C_o \leq 1$, Equation III.1-49 becomes

$$\alpha_{gm} = \frac{M_{gb}}{\rho_g V_m} \geq \frac{1}{2}. \qquad \text{(III.1-50)}$$

In summary then, the complete bubble distribution parameters are

$$\left.\begin{aligned} m_{gb} &= 2C_o \frac{M_{gb}}{V_m} \\ b_{gb} &= (1 - C_o) \frac{M_{gm}}{V_m} \end{aligned}\right\} \quad \text{if } 0 \leq \alpha_{gm} \leq \frac{1}{2} \qquad \text{(III.1-51)}$$

$$\left.\begin{aligned} m_{gb} &= 2C_o \left(\rho_g - \frac{M_{gb}}{V_m}\right) \\ b_{gb} &= (1 + C_o)\frac{M_{gb}}{V_m} - C_o\rho_g \end{aligned}\right\} \text{ if } \frac{1}{2} < \alpha_{gm} \leq 1 \qquad \text{(III.1-52)}$$

A development similar to that given above for the partial density of steam in the two-phase mixture can be made for the partial density of liquid in the two-phase mixture. The partial density of the liquid, when summed with the partial density of the steam, yields the partial density of the two-phase mixture. For the purpose of brevity, only the partial mixture density equation is presented as follows without development.

$$\rho_m = m_m \frac{z}{z_m} + b_m \qquad \text{(III.1-53)}$$

where the mixture distribution parameters are given by

$$\left.\begin{aligned} m_m &= 2\ C_o\ (\frac{M_m}{V_m} - \rho_\ell) \\ b_m &= (1-C_o)\frac{M_m}{V_m} + C_o\rho_\ell \end{aligned}\right\} \text{ if } 0 \leq \alpha_{gm} \leq 1/2 \qquad \text{(III.1-54)}$$

$$\left.\begin{aligned} m_m &= 2\ C_o\ (\rho_g - \frac{M_m}{V_m}) \\ b_m &= (1 + C_o)\frac{M_m}{V_m} - C_o\rho_g \end{aligned}\right\} \text{ if } 1/2 < \alpha_{gm} \leq 1 \qquad \text{(III.1-55)}$$

1356 107

The phase separation model is not complete at this point since the total mass of steam in the two-phase mixture, M_{gb}, is not known. In order to obtain this quantity, mass balances need to be performed for the total volume and for the mixture. As already mentioned, the phase separation model is actually a simplified slip model. In order to see the simplifying assumptions, consider the general two-fluid continuity equation [III.1-22]

$$\frac{\partial}{\partial t}(A\alpha_a\rho_a) + \frac{\partial}{\partial z}(A\alpha_a\rho_a v^a) = A\dot{m}_a \qquad \text{(III.1-56)}$$

where $\dot{m}_a$ is the rate of net phase appearance per unit volume, α_a is the volume fraction, ρ_a is the thermodynamic density and v^a is the velocity of phase "a." Equation III.1-56 may be re-written as

$$\frac{\partial}{\partial t}(A\alpha_a\rho_a) + \frac{\partial}{\partial z}(x_a W) = A\dot{m}_a \qquad \text{(III.1-57)}$$

where the flowing quality for a two-phase mixture is defined as

$$x_{fa} = \frac{W_a}{W} = \frac{\alpha_a\rho_\alpha v^\alpha A}{(\alpha_g\rho_g v^g + \alpha_\ell\rho_\ell v^\ell)A} \; . \qquad \text{(III.1-58)}$$

The subscripts and superscripts, ℓ and g, denote the steam and liquid, respectively.

Equation III.1-57 may be converted into an overall balance equation by integrating over the control volume as

$$\int_0^z \frac{\partial}{\partial t}(A\alpha_a\rho_a)\,dz + \int_0^z \frac{\partial}{\partial z}(x_{fa}W)\,dz = \int_0^z A\dot{m}_a\,dz \; . \qquad \text{(III.1-59)}$$

Interchange of the order of integration and differentiation together with the definition of the total mass

$$M_a = \int_o^z A\alpha_a\rho_a \, dz \qquad \text{(III.1-60)}$$

and net rate of production

$$\dot{M}_a = \int_o^z A\dot{m}_a \, dz \qquad \text{(III.1-61)}$$

causes Equation III.1-59 to assume the form

$$\frac{dM_a}{dt} = \sum_{IN} (x_{fa}W)_j - \sum_{OUT} (x_{fa}W)_j + \dot{M}_a \qquad \text{(III.1-62)}$$

where $\sum_{IN}$ or $\sum_{OUT}$ denotes summation over all flow paths or junctions into or out of the volume under consideration. Equation III.1-62 when applied to the control shown in Figure III.1-3 yields the steam mass balance as

$$\frac{dM_g}{dt} = \sum_{IN} (x_{fg}W)_j - \sum_{OUT} (x_{fg}W) + \dot{M}_g \qquad \text{(III.1-63)}$$

Assuming that the steam flows at the same rate as the mixture at the junctions causes the flowing quality to become the thermodynamic quality or simply, the quality, x, as

$$x_{fg} = \frac{\alpha_g\rho_g vA}{(\alpha_g\rho_g v + \alpha_\ell\rho_\ell v)A} = \frac{\alpha_g\rho_g}{\alpha_g\rho_g + \alpha_\ell\rho_\ell} = x \, . \qquad \text{(III.1-64)}$$

Equation III.1-63 then becomes for equal phase velocities,

1356 109

$$\frac{dM_g}{dt} = \sum_{IN} x_j W_j - \sum_{OUT} x_j W_j + \dot{M}_g \quad . \qquad \text{(III.1-65)}$$

The overall balance equation of steam in the mixture is given by

$$\int_o^{z_m(t)} \frac{\partial}{\partial t} (A\rho_{gb})\, dz + \int_o^{z_m(t)} \frac{\partial}{\partial z} (A\rho_{gb} v^{gb})\, dz = \int_o^{z_m(t)} A\dot{m}_{gb} \qquad \text{(III.1-66)}$$

where v^{gb} is the velocity of steam in the mixture. Equation III.1-66 may be integrated over the mixture using the Leibnitz theorem as

$$\frac{\partial}{\partial t}\int_o^{z_m(t)} (A\rho_{gb})\, dz - (A\rho_{gb})\Big|_{z_m} \frac{dz_m}{dt}$$

$$= \sum_{IN} (\phi A\rho_{gb} v^{gb})_j - \sum_{OUT} (\phi A\rho_{gb} v^{gb})_j - (A\rho_{gb} v^{gb})_j\Big|_{z_m} + \int_o^{z_m(t)} A\dot{m}_{gb}\, dz \qquad \text{(III.1-67)}$$

where ϕ_j denotes the fraction of each junction which originates or terminates in the mixture region. If a junction j does not originate or terminate in the mixture region, then ϕ_j=0. If a junction j is partially in the mixture region and partially in the steam dome, ϕ_j is between zero and one depending on the mixture level height with respect to the junction height.

Define the production of steam in the mixture, $\dot{M}_{gb}$ as

$$\dot{M}_{gb} = \int_o^{z_m} A\dot{m}_{gb}\, dz \quad . \qquad \text{(III.1-68)}$$

Assume the steam velocity is equal to the mixture velocity at the junction and use the definition of total mass of steam in the mixture given by Equation III.1-29 in Equation III.1-67 to obtain

$$\frac{dM_{gb}}{dt} = \sum_{IN} \phi_j x_j W_j - \sum_{OUT} \phi_j x_j W_j - (A\rho_{gb})\Big|_{z_m} \left(v^{gb}\Big|_{z_m} - \frac{dz_m}{dt}\right) + \dot{M}_{gb} \quad \text{(III.1-69)}$$

Define

$$v_{bub} \equiv v^{gb}\Big|_{z_m} - \frac{dz_m}{dt} \quad \text{(III.1-70)}$$

to be the velocity of the steam at the steam-mixture interface $z=z_m(t)$ relative to the interface velocity (positive upward). Solving for $\dot{M}_{gb}$ from Equation III.1-66, substituting it into Equation III.1-65 and noting that

$$\dot{M}_g = \dot{M}_{gb} + \dot{M}_{gsd} \quad \text{(III.1-71)}$$

where $\dot{M}_{gsd}$ is the rate of vapor production in the steam dome, then

$$\frac{dM_g}{dt} = \sum_{IN} \Psi_j x_j W_j - \sum_{OUT} \Psi_j x_j W_j + \frac{dM_{gb}}{dt} + Av_{bub}(\rho_{gb})_{z_m} + \dot{M}_{gsd} \quad \text{(III.1-72)}$$

where $\psi_j=1-\phi_j$ is the fraction of each stream originating in the steam dome.

Solving for the rate of bubble formation and dropping the rate of vapor formation in the steam dome, Equation III.1-59 assumes the form

$$\frac{dM_{gb}}{dt} = \frac{dM_g}{dt} - \left[\sum_{IN} \Psi_j x_j W_j - \sum_{OUT} \Psi_j x_j W_j\right] - Av_{bub}(\rho_{gb})_{z_m} \quad \text{(III.1-73)}$$

To complete the development of the phase separation model, equations for the junction quality x_j, and the fraction of steam flowing at a junction and originating in the steam dome ψ_j, must be developed. The junction quality is defined to be

$$x_j = \frac{\int_B^{z_m} \rho_{gb}(z)\, dA + \int_{z_m}^{C} \rho_g\, dA}{\int_B^{z_m} \rho_m(z)\, dA + \int_{z_m}^{C} \rho_g\, dA} \qquad \text{(III.1-74)}$$

assuming that the junction gas and liquid phase velocities are equal. Figure III.1-4 illustrates the integration over the circular junction area, where

$$dA = 2y\,dz \qquad \text{(III.1-75)}$$

since the circular area may be described in Cartesian coordinates as

$$r^2 = y^2 + (z-A)^2 \quad . \qquad \text{(III.1-76)}$$

Equation III.1-76 is rearranged to define y as a function of r and z and is substituted into Equation III.1-75 giving

$$dA = 2(r^2 - A^2 - z^2 + 2Az)^{1/2}\, dz \quad . \qquad \text{(III.1-77)}$$

Combining Equations III.1-25, III.1-53, III.1-74, and III.1-77, the integral equation for the junction quality is obtained

$$x_j = \left[\frac{M_{gb}}{z_m}\int_B^{z_m} z(r^2 - A^2 - z^2 + 2Az)^{1/2}\, dz + b_{gb}\int_B^{z_m} (r^2 - A^2 - z^2 + 2Az)^{1/2}\, dz + \rho_g\int_{z_m}^{C} (r^2 - A^2 - z^2 + 2Az)^{1/2}\, dz\right] \Bigg/ \left[\frac{M_m}{z_m}\int_B^{z_m} z(r^2 - A^2 - z^2 + 2Az)^{1/2}\, dz + b_m\int_B^{z_m} (r^2 - A^2 - z^2 + 2Az)^{1/2}\, dz + \rho_g\int_{z_m}^{C} (r^2 - A^2 - z^2 + 2Az)^{1/2}\, dz\right]. \qquad \text{(III.1-78)}$$

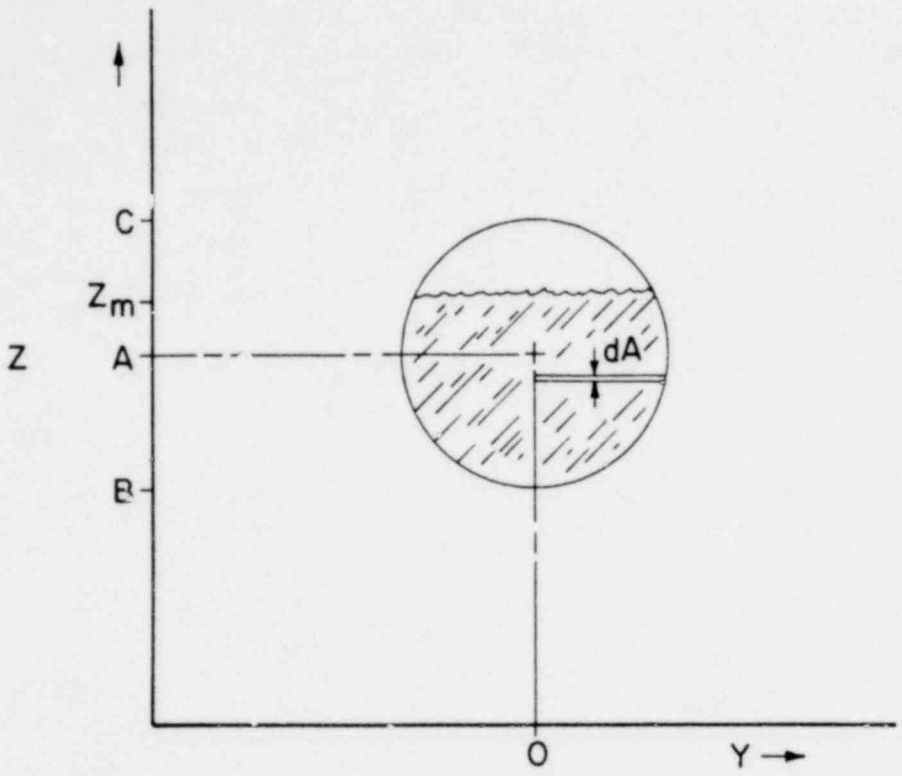

Figure III.1-4 Junction Quality Integration

The integral term representing the area of the junction occupied by the mixture or pure steam, depending on the integration limits, is given by

$$A_{m,s}\Big|_{z_1}^{z_2} = 2\int_{z_1}^{z_2} (r^2 - A^2 - z^2 + 2Az)^{1/2}\, dz \qquad \text{(III.1-79)}$$

and has the solution

$$A_{m,s}\Big|_{z_1}^{z_2} = (z-A)\ r^2 - (z-A)^2\ ^{1/2} + r^2 \sin^{-1}\ \frac{z-A}{r}\Big|_{z_1}^{z_2} . \qquad \text{(III.1-80)}$$

The second integral form represents the integrated mixture or gas bubble mass residing within the junction area in excess of that which would be present if there where no partial density gradients through the mixture. The general form of the integral is given by

$$M_{m,gb}\Big|_{z_1}^{z_2} = 2\int_{z_1}^{z_2} z(r^2 - A^2 - z^2 + 2Az)^{1/2}\, dz\ , \qquad \text{(III.1-81)}$$

and has the solution

$$M_{m,gb}\Big|_{z_1}^{z_2} = -\frac{2}{3}\pi r^2 - (z-A)^2\ ^{3/2} + A(z-A)\ r^2 - (z-A)^2\ ^{1/2} + Ar^2 \sin^{-1}\ \frac{z-A}{r}\Big|_{z_1}^{z_2} . \qquad \text{(III.1-82)}$$

The above equation can be expressed in terms of the area integral given by Equation III.1-80 as follows,

$$M_{m,gb}\Big|_{z_1}^{z_2} = -\frac{2}{3}\pi r^2 - (z-A)^2\ ^{3/2} + A\, A_{m,s}\Big|_{z_1}^{z_2} . \qquad \text{(III.1-83)}$$

Both the mixture and gas bubble mass integrals are evaluated between the limits B and z_m. Substituting these integration limits into Equation III.1-83) yields

$$M_{m,gb} \int_B^{z_m} = A\, A_{m,s} \int_B^{z_m} - \frac{2}{3} \pi r^2 - (z_m - A)^2 \Big)^{3/2} . \qquad \text{(III.1-84)}$$

The area integral for the integration limits B to z_m is given by

$$A_{m,s} \int_B^{z_m} = (z_m - A)\, r^2 - (A_m - A)^2 \Big)^{1/2} + r^2 \sin^{-1} \left(\frac{z_M - A}{r} \right) + \frac{r^2}{2} . \qquad \text{(III.1-85)}$$

The area integral for the junction area residing above the mixture level (integration limits z_m to C) can be recast in terms of the area defined by Equation III.1-85 as follows

$$A_{m,s} \Big|_{z_m}^{C} = \pi r^2 - A_{m,s} \Big|_B^{z_m} . \qquad \text{(III.1-86)}$$

The three integrals given by Equations III.1-84, III.1-85 and III.1-86 are normalized using the full junction area (all terms in numerator and denominator of Equation III.1-78 are effectively divided by the junction area), resulting in the following,

$$\alpha_m = \frac{A_{m,s} \Big|_B^{z_m}}{r^2} = \frac{1}{2} + \frac{1}{\pi} \left[\left(\frac{(z_m - A)}{r} \right) 1 - \left(\frac{z_m - A}{r} \right)^2 \right)^{1/2}$$

$$+ \sin^{-1} \left(\frac{z_m - A}{r} \right) \Bigg] \qquad \text{(III.1-87)}$$

$$\alpha_s = \frac{A_{m,s} \Big|_{z_m}^{C}}{\pi r^2} = (1 - \alpha_m) \qquad \text{(III.1-88)}$$

$$Z^* = \frac{M_{m,gb}\Big|_B^{Z_m}}{\pi r^2} = A\,\alpha_m - \frac{2}{3}\pi r\left[1 - \left(\frac{z_m - A}{r}\right)\right]^{3/2} \qquad \text{(III.1-89)}$$

where

α_m = fraction of the junction area occupied by the two-phase mixture

α_s = fraction of the junction area occupied by pure steam (above mixture level)

Z^* = effective height at which the average mixture and gas bubble partial densities exist.

Combining Equations III.1-78 and III.1-87 through III.1-89 leads to a general equation for the junction quality for flows leaving a separated volume. The equation is

$$x_j = \frac{m_{gb}\ell + \alpha_m b_{gb} + \rho_g(1-\alpha_m)}{m_m\ell + \alpha_m b_m + \rho_g(1-\alpha_m)} \qquad \text{(III.1-90)}$$

where

$\ell = \frac{z^*}{z_m}$ = effective height relative to the mixture height.

The development given above for the junction quality was derived for a vertically oriented junction with the mixture level residing within the bounds defined by the junction radius. Three other combinations are possible which are not directly applicable from the development given for Equation III.1-90. The first case exists when the mixture level resides above the upper bound of a vertically oriented junction and the second case is present when horizontally oriented junctions are exposed to the two-phase mixture. In both cases, the average mixture properties that the junction is exposed to are defined at the junction height, and the fraction of the junction area exposed to the mixture is unity. A third case exists when the mixture level resides below a circular junction, i.e. $z_m \leq z_j - r$, and the junction quality is not dependent upon the mixture

properties. Consequently, for covered vertical junctions, uncovered vertical junctions, and horizontal junctions, the following unique values of α_m and ℓ are used

$$\alpha_m = 1.0 \quad \begin{array}{l}\text{for vertical junctions where } z_m \geq (z_j + r) \\ \text{for horizontal junctions}\end{array}$$

$$\alpha_m = 0.0 \quad \text{for vertical junctions where } z_m \leq (z_j - r)$$

and

$$\ell = \frac{z_j}{z_m} \quad \begin{array}{l}\text{for vertical junctions where } z_m \geq (z_j + r) \\ \text{for horizontal junctions}\end{array}$$

$$\ell = 0.0 \quad \text{for vertical junctions where } z_m \leq (z_j - r).$$

The Ψ_j term appearing in Equation III.1-73 is defined as the fraction of steam flowing at a junction which originates in the steam dome of the donor volume. Ψ_j is therefore given by

$$\Psi_j = \left[\rho_g \int_{z_m}^{C} (r^2-A^2-z^2+2Az)^{1/2}\, dz\right] \left[\frac{M_{gb}}{z_m}\int_{B}^{z_m} z(r^2-A^2-z^2+2Az)^{1/2}\, dz + b_{gb}\int_{B}^{z_m} (r^2-A^2-z^2+2Az)^{1/2}\, dz + \rho_g \int_{z_m}^{C} (r^2-A^2-z^2+2Az)^{1/2}\, dz\right]. \quad \text{(III.1-91)}$$

The equation for Ψ_j given above is similar to the definition of x_j defined by Equation III.1-78. Due to the similarity between the two equations, the development for Ψ_j is not presented in detail. The final generalized equation is given by

$$\Psi_j = \frac{\rho_g(1-\alpha_m)}{m_{gb}\,\ell + \alpha_m b_{gb} + \rho_g(1-\alpha_m)}, \quad \text{(III.1-92)}$$

1356 117

which also applies for vertically oriented junctions with the mixture level residing between the bounds defined by the junction radius. For vertical or horizontal junctions exposed to the two-phase mixture only

$$\Psi_j = 0 \begin{cases} \text{for horizontal junctions where } z_j \leq z_m \\ \text{for vertical junctions where } (z_j + r) \leq z_m. \end{cases} \quad \text{(III.1-93)}$$

If the horizontal or vertical junction is exposed to the steam dome only,

$$\Psi_j = 1 \begin{cases} \text{for horizontal junctions where } z_j > z_m \\ \text{for vertical junctions where } (z_j - r) > z_m. \end{cases} \quad \text{(III.1-94)}$$

With the definition of x_j and Ψ_j completed, the RETRAN phase separation model is fully defined.

2.0 ENERGY EQUATION

The macroscopic energy balance of Equation II.3-41 requires models for the energy transfer Q_w. During hypothetical LOCA's, an extremely wide range of transient, two-phase heat transfer regimes may be encountered in the core of the NSSS, the steam generators, and the pipes of the hydraulic loop. The two-phase heat transfer model in RETRAN has been designed primarily for analysis of forced convection two-phase heat transfer in the core of the NSSS. The heat transfer model, in general, incorporates several approximations which are used when special situations, such as very low flow rates, are encountered. Several recent reviews of the two-phase flow heat transfer literature have been given that can be used as sources of information for updating the RETRAN model.[III.2-1 through III.2-6]

2.1 Two-Phase Flow and Heat Transfer Regimes

The boiling curve is generally employed as a convenient reference for discussion
of the behavior of heated surfaces. A representation of a pool boiling curve at a fixed pressure is shown in Figure III.2-1. A brief discussion of the characteristics of the physical processes associated with two-phase heat transfer and the various paths shown in Figure III.2-1 is given here.

- The characteristics of the boiling curve for pool boiling depend upon the type of energy exchange processes employed to obtain the data. In general, the path ABDEF is obtained by use of temperature controlled surfaces as the surface temperature is increased.

- For the case of a heat flux controlled surface, for both forced convection and pool boiling, the path ABDD'F is obtained as the heat flux is "increased". Point D' represents the new equilibrium state of the surface at the heat flux value q_{CHF}.

- In general, the boiling processes do not follow the same path on "cooldown" as they do on "heatup". For the case of pool boiling, the paths FEDBA and FEE'BA have been obtained.

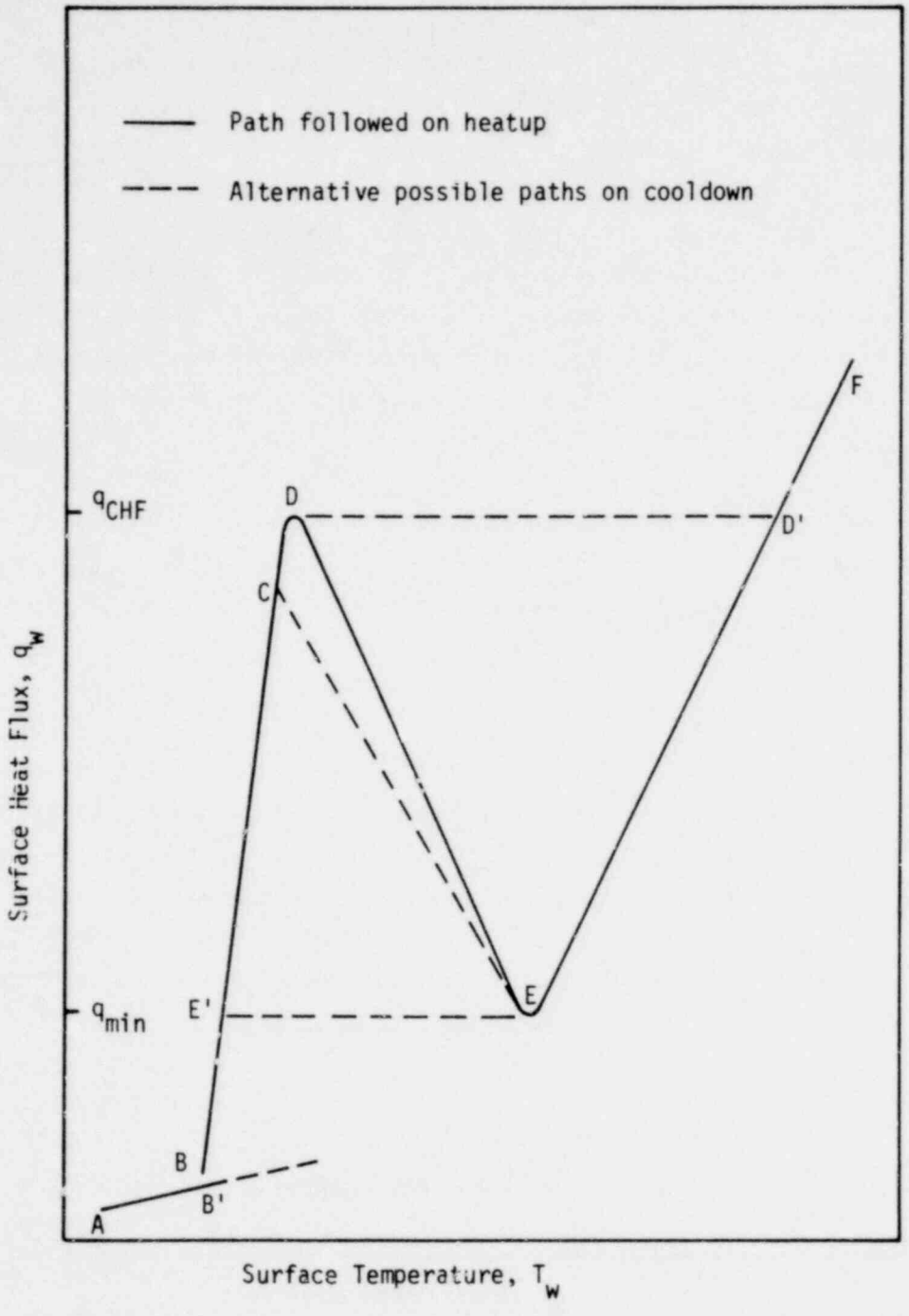

Figure III.2-1 Pool Boiling Curve Representation at a Fixed Pressure

- For the case of forced convection with uniform heat flux in the direction of flow, the path FD'DBA is followed as the heat flux is decreased.[III.2-1, III.2-7] That is, the hysteresis associated with the pool boiling curve is not present.

- At steady operating conditions, a NSSS fuel rod is a heat-flux-controlled surface (neglecting the effects of void feedback) with a non-uniform distribution of heat flux along the rod. Experimental results have shown that the path FD'EE' may be obtained upon reduction of the heat flux for a portion of a nonuniformly heated surface.[III.2-7, III.2-8, III.2-9]

- The transition boiling region, path EC of Figure III.2-1, for forced convection has been obtained by use of a transient technique which produces a quench curve for a portion of the test section.[III.2-7] This curve follows the path FECE' of Figure III.2-1. The heat flux at point C is less than the initial heat flux of point D.

- Some experimental information[III.2-10 through III.2-14] is available which indicates that the minimum heat flux, point E of Figure III.2-1, has different values for steady-state and transient conditions. That is, under transient quench tests, the wall superheat at which the minimum heat flux is attained is higher than the value under steady-state conditions. The condition of the surface of the heated element affects the transient results.[III.2-14]

During hypothetical LOCA's, the fuel rods of NSSS's may behave as heat flux-controlled surfaces for some parts of the transient and as temperature-controlled surfaces for other parts of the transient. In addition, due to the wide range of flow rates encountered during hypothetical incidents, forced convection, pool boiling and free convection types of conditions may occur. For the case of forced convection, the "boiling curve" at a given pressure is in fact a family of curves with the mass flux as a primary parameter and the thermodynamic quality as a secondary parameter for each value of the mass flux.

The two-phase flow and heat transfer regimes which may occur in NSSS cores are shown in Figure III.2-2. A brief description of these regimes is given here and the relationships to Figure III.2-1 are indicated.

- At the inlet of the flow channels shown in Figure III.2-2, forced convection to single phase liquid is occurring. For the case of relatively high flow rates, the heat transfer coefficient for this regime is fairly well known. For low flow rates, when gravity or free convection effects can be important, the correlations employed in this region must include accounting of these effects. The single phase forced convection region corresponds to the path AB of Figure III.2-1.

- The subcooled boiling regimes shown in Figure III.2-2 occur when the flow channel average fluid temperature is less than the saturation temperature. The temperature of the fluid adjacent to the clad surface, however, is at or above the local saturation temperature and thus boiling may begin. The wall superheat required to initiate boiling is in general a function of the micro-structure of the clad surface, the thermo-physical properties of the fluid and the thermodynamic state of the fluid. Most empirical descriptions employed in engineering analyses do not contain accounting of all of these details. In addition, no distinction is made between the partial and fully developed subcooled boiling conditions. That is, fully developed subcooled boiling will be assumed. Empirical correlations will be employed to determine the surface temperature at point B and along the path BCD of Figure III.2-1.

- The nucleate boiling regime occurs as the bulk fluid energy attains the local saturation state. For some flow rates and rod-fluid energy exchange rates, the fluid may not attain the saturation state before the CHF point is reached. This latter condition usually occurs at higher flow rates and heat flux as shown in Figure III.2-2b.

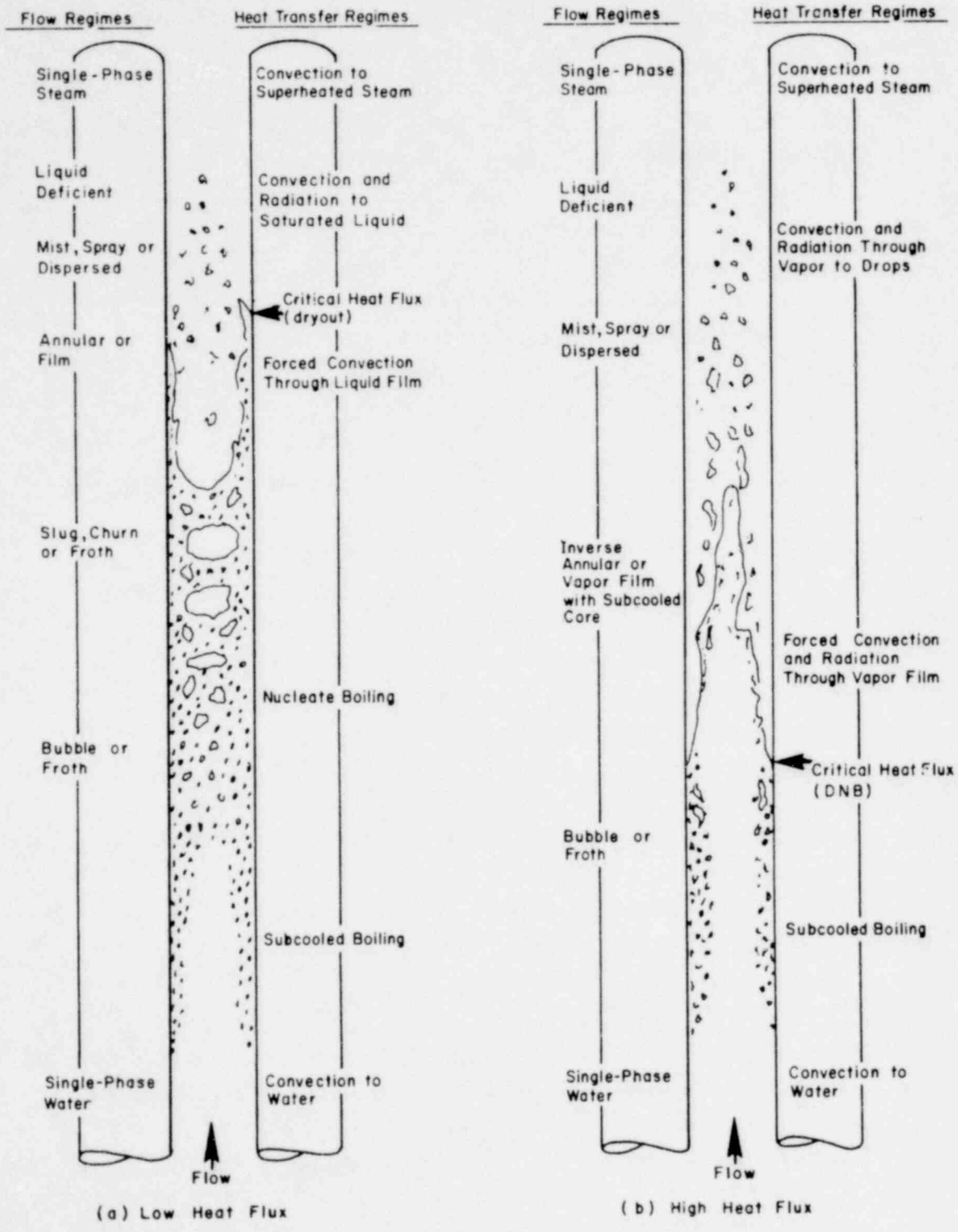

Figure III.2-2 Flow and Heat Transfer Regimes in Rod Array with Vertical Upflow

1356 123

- The forced convection vaporization heat transfer regime is characterized by the presence of a liquid film on the heated surface.

- The critical heat flux, point D of Figure III.2-1, is a complex function of the state and flow rate of the coolant and the geometry of the flow channel. The critical heat flux is usually determined by use of empirical correlations.[III.2-15 through III.2-29]

- The transition boiling (unstable film boiling) regime, paths DE or EC of Figure III.2-1, may occur during some portions of a LOCA because of the very high temperatures at which rewetting of a hot surface may occur. This boiling regime is generally characterized by an unstable vapor film adjacent to the heated surface. The vapor film is broken up by areas of liquid that intermittently wet the surface. As previously noted, this regime is generally associated with temperature controlled surfaces. Experimental results indicate that part of the reflood heat transfer period may be characterized as approximately a constant temperature period. That is, the surface temperature varies slowly with time. In addition, for the case of high rewetting temperatures, the surface temperature may be too high for fully developed surface boiling to occur.

- Downstream of the CHF location, the clad surface is covered with vapor and the energy exchange is primarily characteristic of convection to vapor. This heat transfer regime corresponds to the ED'F region of Figure III.2-1. Although the heat transfer is primarily to vapor, liquid in the form of droplets may also contribute to the energy exchange. Several heat transfer models are available for the liquid dispersed and liquid deficient regimes of Figures III.2-2a and III.2-2b.[III.2-7, III.2-8, III.2-30 through III.2-35] The inverse annular regime of Figure III.2-2b, however, has not been investigated as much as the liquid dispersed and liquid deficient regimes. At sufficiently high clad surface temperatures, radiative energy exchange must be accounted for in the post-CHF regime.

- As energy is transferred to the vapor and droplets, eventually all of the liquid will be evaporated and the vapor will become superheated. Heat transfer to the superheated steam will be described by use of the appropriate single-phase heat transfer coefficient correlation. Under some conditions, vapor may condense and droplets may wet and accumulate on the clad surface. Condensation, rewetting and accumulation may occur on the parts of the clad surface which are lower in temperature than the saturation temperature. Under these conditions, a liquid film may form on the clad and form a rewetting front which falls along the clad under the action of gravity.

Many of these two-phase heat transfer regimes occur during the core-reflood portion of hypothetical LOCA's. The heat transfer coefficients available in RETRAN are given in the next section.

2.2 Heat Transfer Coefficient Correlations

The energy exchange between the fluid and the flow channel walls is given by Equation II.2-41 as

$$Q_w = \int_{S_w+S_m+\Sigma A_j} \tilde{q} \cdot d\tilde{S} \ , \qquad \text{(III.2-1)}$$

where

$$q_i = -k \frac{\partial T}{\partial x_i} . \qquad \text{(III.2-2)}$$

Equation III.2-1 is evaluated by assuming that the argument of the integral can be represented by an average value to obtain

$$Q_w = h_c A_{w,h} (T_w - T_b) \qquad \text{(III.2-3)}$$

where

h_c = heat transfer coefficient (Btu/hr ft^2 °F)

$A_{w,h}$ = heated surface area in the volume V_k (ft^2)

T_w = wall surface temperature (°F)

T_b = average fluid temperature (°F).

In general, Equation III.2-3 accounts for the convective contribution of the energy exchange. If radiative exchange is important, both between solid surfaces and between a surface and the fluid, Equation III.2-3 should be modified to include an accounting of the radiative energy exchange.

The heat transfer coefficient h_c is flow regime dependent. As noted previously, an extremely wide range of thermal-hydraulic conditions are encountered during hypothetical LOCA's. In some cases, the data base required for development of correlations is not yet available and the models in RETRAN must be considered to be preliminary. Many of the heat transfer coefficient correlations for two-phase flow, especially the correlations for critical heat flux, are not dimensionless. The dimensions employed in RETRAN are listed here.

h_c = heat transfer coefficient, Btu/ft^2-hr-°F
k = thermal conductivity, Btu/ft-hr-°F
D_{he} = heated equivalent diameter, ft, in.
D_{hy} = wetted equivalent diameter, ft, in.

Pr = Prandtl Number, $\frac{C_p \mu}{k}$

Re = Reynolds Number, $\frac{GD_e}{\mu}$

G = mass flux, lb_m/ft^2-hr
G' = $G/10^6$
μ = viscosity, lb_m/ft-hr
C_p = specific heat, Btu/lb_m-°F
T_b = bulk coolant temperature, °F

1356 126

T_{sat} = saturation temperature, °F
T_w = wall temperature, °F
ΔT_{sat} = $T_w - T_{sat}$, °F
D = diameter, in.
Q_w = heat flux, Btu/ft^2-hr
p = pressure, psia
x = quality
ρ = density, lb_m/ft^3
$h_{\ell s}$ = saturated liquid enthalpy, Btu/lb_m
h_{fg} = heat of vaporization, Btu/lb_m
h_{in} = inlet enthalpy, Btu/lb_m
L = channel length, in.
D^*_{hy} = $\sqrt{D_r(D_r + D_{he})} - D_r$, where D_r = rod diameter, in.
g = local acceleration due to gravity, ft/sec^2
g_o = gravitational constant, ft-lb_m/lb_f-sec^2
σ = surface tension, lb_f/ft
Q = volumetric flow rate, ft^3/sec
A_{flow} = flow area, ft^2

and subscripts

CHF = critical heat flux conditions
g = vapor
ℓ = liquid
gs = saturated vapor conditions
ℓs = saturated liquid conditions
v = superheated vapor conditions
w = wall.

The heat transfer coefficients for each of the two-phase heat transfer regimes are given in the following sections.

2.2.1 Single-Phase Heat Transfer

As shown in Figure III.2-2, both single-phase liquid and single-phase vapor flow may occur. The heat transfer coefficient is given by the Dittus-Boelter[III.2-36] correlation

$$\frac{h_c D_{he}}{k_\ell} = 0.023 \left(\frac{GD_{he}}{\mu_\ell}\right)^{0.8} \left(\frac{C_p \mu_\ell}{k_\ell}\right)^{0.4} \qquad \text{(III.2-4a)}$$

for the liquid, and

$$\frac{h_c D_{he}}{k_g} = 0.023 \left(\frac{GD_{he}}{\mu_g}\right)^{0.8} \left(\frac{C_p \mu_g}{k_g}\right)^{0.4} \qquad \text{(III.2-4b)}$$

for the vapor. The fluid properties are evaluated at the bulk fluid temperature and no correction is included for large bulk temperature to wall temperature differences. Equations III.2-4 are usually considered to be valid for fully turbulent flow of the fluid when the Reynolds number satisfies

$$\left(\frac{GD_{he}}{\mu}\right) \geq 10{,}000. \qquad \text{(III.2-5)}$$

In RETRAN, Equations III.2-4 are used for all values of the Reynolds number. If the heat transfer coefficient is calculated to be less than 5 Btu/hr-ft^2-°F, it is set to the value of 5 Btu/hr-ft^2-°F. Additional information relating single phase heat transfer coefficients is given in References III.2-35 through III.2-42. The RETRAN model can be determined by use of these references.

2.2.2 Fully Developed Subcooled Boiling

At the present time in RETRAN, the heat transfer mechanisms of bubble nucleation and partial nucleate boiling are not modeled. Instead, Equation III.2-4a is used until the wall temperature is calculated to be greater than or equal to the wall temperature obtained from a fully developed subcooled boiling correlation. Most correlations of fully developed subcooled and saturated boiling can be expressed in the form

$$T_w = T_{sat} + \Psi\, Q_w^n , \qquad \text{(III.2-6)}$$

where Ψ and n may be functions of the micro-structure of the heated surface and the physical properties of the fluid.[III.2-2, III.2-3, III.2-38, III.2-43

through III.2-52] Generally, n takes on values between 0.33 and 0.50 and the dependency of Ψ on the solid-fluid properties has been better defined for the case of pool boiling than for forced convection. The fully developed subcooled boiling correlation of Thom, et al.[III.2-37] is used in RETRAN. The wall temperature is given in terms of the saturation temperature of the fluid by the equation

$$T_w = T_{sat} + 0.072e^{-p/1260} Q_w^{1/2} . \qquad \text{(III.2-7)}$$

This correlation is valid only for water and is based on data in the following ranges of conditions:

Vertical upflow of water

Round tube:	0.5-in. diameter, 60-in. length
Annulus:	0.7-in. ID, 0.9-in. OD, 12-in. length
Pressure:	750 to 2000 psia
Mass flux:	0.77×10^6 to 2.80×10^6 $lb_m/hr\text{-}ft^2$
Heat flux:	to 0.5×10^6 $Btu/ft^2\text{-}hr$.

In the RETRAN heat transfer model, Equation III.2-7 is used for both subcooled and saturated fully developed boiling. In addition, there are no models to check on suppression of nucleation and fully developed surface boiling is assumed to occur until the homogeneous void fraction reaches the value

$$\alpha = 0.80 . \qquad \text{(III.2-8)}$$

Then, between $\alpha = 0.80$ and $\alpha = 0.90$, if the critical heat flux value has not been exceeded, a linear interpolation of the heat flux between the Thom correlation, Equation II.2-7, and the forced convection vaporization correlation is used.

As noted previously, there are no models for the case of low coolant flow rate in the pre-CHF heat transfer coefficient correlations.

2.2.3 Forced Convection Vaporization

The forced convection vaporization heat transfer regime is generally associated with the annular and annular-dispersed flow regimes. Heat is transferred by

conduction and convection to the liquid film adjacent to the heated surface and evaporation of the liquid occurs at the vapor-liquid interface. This pre-CHF heat transfer regime corresponds to the path BD of Figure III.2-1 and the "low" heat flux case of Figure III.2-2. Criteria for suppression of nucleation within the liquid film[III.2-46, III.2-53] are not available in RETRAN.

The forced convection vaporization heat transfer regime is assumed to occur if the vapor void fraction satisfies $\alpha \geq 0.90$.

Most of the heat transfer coefficient correlations for the forced convection vaporization boiling regime are written as modifications of related single phase heat transfer coefficients in the form

$$\frac{h_c}{h_c'} = K_1 \left(\frac{1}{x_{tt}} \right)^n . \qquad \text{(III.2-9)}$$

In Equation III.2-9, h_c' is the reference single phase heat transfer coefficient and x_{tt} is the Martinelli-Lockhart-Nelson parameter for turbulent-turbulent two-phase flow.[III.2-54, III.2-55] Equation III.2-9 has been used by Dengler and Addoms,[III.2-56] Bennett, et al., [III.2-53] Guerrieri and Talty,[III.2-57] and Schrock and Grossman.[III.2-58] Correlations and various modifications of Equation III.2-9 have been given by Collier and Pulling,[III.2-59] Davis and David,[III.2-60] and Chen.[III.2-61]

The reference single-phase heat transfer coefficient, h_c', has been used in two forms. Dengler and Addoms[III.2-56] based the single phase reference coefficient on the total flow (liquid plus vapor) and the transport properties of the liquid as

$$h_c' = 0.023 \left(\frac{\rho_\ell v_\ell D_{he}}{\mu_\ell} \right)^{0.8} \left(\frac{C_{p\ell} \mu_\ell}{k_\ell} \right)^{0.4} \frac{k_\ell}{D_{he}} , \qquad \text{(III.2-10a)}$$

where

$$\rho_\ell v_\ell = \rho_m v \qquad \text{(III.2-10b)}$$

and ρ_m and v are the mixture density and velocity, respectively. Guerrieri and Talty[III.2-57] and Schrock and Grossman[III.2-58] evaluate h_c' for the superficial liquid mass flux and the liquid transport properties as

$$h_c' = 0.023\left(\frac{\rho_\ell v_\ell D_{he}}{\mu_\ell}\right)^{0.8}\left(\frac{C_{p\ell}\mu_\ell}{k_\ell}\right)^{0.4}\frac{k_\ell}{D_{he}}, \qquad \text{(III.2-11a)}$$

where

$$\rho_\ell v_\ell = \rho_m v\ (1-x). \qquad \text{(III.2-11b)}$$

Equation III.2-11b corresponds to using the unevaporated liquid as the reference Reynolds number. In general, Equation III.2-11 with Equation III.2-9 have given better comparisons with data than Equations III.2-10.

The Schrock and Grossman correlation in RETRAN is given by

$$\frac{h_c D_{he}}{k_\ell} = 0.023\left(\frac{\rho_m v(1-x)\,D_{he}}{\mu_\ell}\right)^{0.8}\left(\frac{C_{p\ell}\mu_\ell}{k_\ell}\right)^{0.4}\left[(2.50)\left(\frac{1}{x_{tt}}\right)^{0.75}\right], \qquad \text{(III.2-12)}$$

where the term in square brackets corresponds to Equation III.2-9 with K_1=2.50 and n=0.75. The Martinelli-Lockhart-Nelson parameter for turbulent-turbulent flow is

$$\frac{1}{x_{tt}} = \left(\frac{x}{1-x}\right)^{0.9}\left(\frac{\rho_{\ell s}}{\rho_{gs}}\right)^{0.50}\left(\frac{\mu_g}{\mu_\ell}\right)^{0.1}. \qquad \text{(III.2-13)}$$

The constants K_1=2.50 and n = 0.75 were determined by use of data which covered the ranges of conditions:

Water in round tubes

Diameter:	0.1162 to 0.4317 in.
Length:	15 to 40 in.
Pressure:	42 to 505 psia
Mass flux:	0.175×10^6 to 3.28×10^6 lb_m/ft^2-hr
Heat flux:	0.06×10^6 to 1.45×10^6 Btu/ft^2-hr
Exit quality:	0.05 to 0.57.

For pre-CHF heat transfer, Equation III.2-12 is used for all values of the mass flux, $G = \rho_m v$, and the fluid properties are evaluated at the average coolant temperature (saturation).

2.2.4 Forced Convection Transition Boiling

The forced convection transition boiling heat transfer correlation is used when the mass flux satisfies $G > 200{,}000$ $lb_m/hr\text{-}ft^2$. The model is a straight line (see Figure III.2-1) given by,

$$Q_w = Q_{CHF} - h_c (T_w - T_{w,CHF}). \qquad \text{(III.2-14)}$$

The heat transfer coefficient, h_c, is taken from the report by McDonough, Milich, and King[III.2-62] and is a function of only the pressure, p. Three values of h_c were given by McDonough, et al., as listed here.

p (psia)	h_c (Btu/hr-ft^2-°F
2000	979.2
1200	1180.8
800	1501.2

The heat transfer coefficient is based on data which cover the following ranges of conditions:

Vertical upflow of water in round tubes

Diameter:	0.152 in.
Length:	12.5 in.
Mass flux:	0.2×10^6 to 1.4×10^6 lb_m/ft^2-hr

Wall Temperature: $T_w < 1030°F$

Pressure: 800, 1200, and 2000 psia.

The correlation is incorporated into RETRAN by use of the following two equations. For pressure greater than 1200 psia, the heat transfer coefficient is given by

$$h_c = h_c|_{1200} - \left(h_c|_{1200} - h_c|_{2000}\right)\left(\frac{p - 1200}{800}\right) , \qquad \text{(III.2-15a)}$$

and for $p \leq 1200$ psia, h_c is given by

$$h_c = h_c|_{1200} + \left(h_c|_{800} - h_c|_{1200}\right)\left(\frac{1200 - p}{400}\right) . \qquad \text{(III.2-15b)}$$

The wall temperature at the critical heat flux condition is determined by the Thom correlation, Equation III.2-7, evaluated with the critical heat flux Q_{CHF}. If the wall heat flux, Q_w, is calculated to be greater than Q_{CHF}, Q_w is set equal to Q_{CHF}. If Q_w is calculated to be less than 0.01 Btu/hr-ft^2, Q_w is set equal to 0.01 Btu/hr-ft^2.

2.2.5 Pool Transition and Stable Film Boiling

The pool transition and stable film boiling models are used if the mass flux satisfies $G \leq 200{,}000$ lb$_m$/hr ft^2. These heat transfer regimes correspond to the regions DEF and FEC of Figure III.2-1. In general, the post-CHF heat transfer model for low flow rates is highly empirical and mostly untested.

The heat transfer coefficient for pool stable film boiling is obtained from the Berenson[III.2-63] correlation given by

$$h_c = 0.425 \left[\frac{k_g^2 \rho_g (\rho_{\ell s} - \rho_{gs}) g h_{fg}}{\mu_g (T_w - T_{sat}) \frac{\lambda_c}{2}}\right]^{1/2} , \qquad \text{(III.2-16)}$$

where λ_c is the critical disturbance wave length, Laplace's criteria, given by

$$\frac{\lambda_c}{2\pi} = \left[\frac{g_o \sigma}{g(\rho_{\ell s} - \rho_{gs})}\right]^{1/2} . \qquad \text{(III.2-17)}$$

The disturbance wave length of Equation III.2-17 is taken as the representative geometric dimension for use in the Berenson stable film boiling correlation. Additional discussion of characteristic dimensions for stable film boiling has been given by Collier.[III.2-7] Collier[III.2-7] also gives a comparison of the Berenson correlation with other pool stable film boiling correlations. The constant multiplier, 0.425, in the Berenson correlation was determined for the case of stable film boiling from a horizontal flat plate facing upwards.

In the RETRAN program, Equation III.2-16 is evaluated with the saturation state properties of the vapor. The heat flux can then be written in the form

$$Q_w = F(p)(T_w - T_{sat})^{3/4}, \qquad \text{(III.2-18)}$$

where F(p) is given by

p	F(p) (Btu/ft^2-hr-°F$^{0.75}$)
15	128
100	236
500	412
1000	510
1500	615
2000	705.

Linear interpolation is used to obtain values of F(p) for values of the pressure between the tabulated values.

The pool transition boiling heat flux is obtained by interpolating between the maximum, or critical heat flux and the minimum heat flux. These conditions correspond to points D and E of Figure III.2-1. Pool transition boiling is assumed to occur when Q_w in Equation III.2-1 is less than 20,000 Btu/hr-ft^2. Experimental data for pool boiling of water at atmospheric pressure indicate that minimum heat fluxes ranging from 10,000 to 30,000 Btu/hr-ft^2 can be expected. [III.2-2, III.2-64] Correlations are available which predict the minimum heat flux.[III.2-2, III.2-65, III.2-66] The temperature difference, T_w-T_{sat}, for the maximum heat flux, is taken as 20°F. The temperature difference, T_w-T_{sat}, corresponding to the minimum heat flux, is obtained from Equation III.2-18 with Q_w = 20,000 Btu/hr-ft^2. The wall heat flux in the transition regime is given by

$$Q_w = 20{,}000 \left(\frac{\Delta T_{min}}{T_w - T_{sat}} \right)^{\left[\frac{1.504}{\ell n(\Delta T_{min}/20)} \right]} \qquad \text{(III.2-19)}$$

where Equation III.2-18 gives

$$\Delta T_{min} = \frac{20{,}000}{F(p)}^{4/3} . \qquad \text{(III.2-20)}$$

However, if $(T_w - T_{sat})$ is determined to be less than 20°F, Q_w is set to a maximum value of 90,000 Btu/hr-ft^2. The value Q_w = 90,000 Btu/hr-ft^2 was set by the observation that forced convection CHF data at low flows and high qualities contain values in the range of 90,000 Btu/hr-ft^2.[III.2-19, III.2-67]

As previously noted, the pool transition boiling model is highly empirical and mostly untested.

2.2.6 Forced Convection Stable Film Boiling

The forced convection stable film boiling model is used if the mass flux satisfies G>200,000 lb$_m$/hr-ft^2. Stable film boiling corresponds to the post-CHF region EF of Figure III.2-1. There are several models available in the literature for the high quality, liquid-deficient regime of Figure III.2-2.[III.2-2, III.2-3, III.2-7, III.2-8, III.2-30 through III.2-35] As in the case of the forced convection vaporization correlations, many of these models are based on modifications of the Dittus-Boelter type of correlation for single-phase flow. Less information is available regarding heat transfer in the inverse annular flow regime. The heat transfer model in RETRAN does not differentiate between the two regimes. In addition, the model employed in RETRAN does not account for superheating of the vapor but instead uses the fluid saturation temperature to calculate the wall heat flux. The RETRAN program contains both the Groeneveld [III.2-35] and the Dougall-Rohsenow[III.2-68] correlations.

Groeneveld[III.2-35] has derived a heat transfer coefficient correlation based on an extensive set of experimental data. Two correlations are available in RETRAN. The general form of the Groeneveld correlation is given by

$$\frac{h_c D_{he}}{k_g} = a\left[\frac{GD_{he}}{\mu_g}\left(x + \frac{\rho_{gs}}{\rho_{\ell s}}(1 - x)\right)\right]^b \left[\frac{C_{pg}\mu_g}{k_g}\right]_w^c Y^d, \qquad \text{(III.2-21)}$$

where

$$Y = 1.0 - 0.1\,(1 - x)^{0.4}\left(\frac{\rho_{\ell s}}{\rho_{gs}} - 1\right)^{0.4}, \qquad \text{(III.2-22a)}$$

or

$$Y = 0.10, \qquad \text{(III.2-22b)}$$

whichever is larger.

The Groeneveld correlations are identified in RETRAN by the equation numbers in Reference [III.2-35]. The values of the coefficients a, b, c, and d of Equation III.2-21 are given by

	a	b	c	d
Equation 5.9	3.27×10^{-3}	0.901	1.32	-1.5
Equation 5.7	0.052	0.688	1.26	-1.06

Groeneveld Equation 5.9 was based on data from vertical and horizontal flow in round tubes and vertical flow in annuli. Groeneveld Equation 5.7 is based on the annuli data alone.

The constants were obtained by use of experimental data which covered the following ranges of conditions:

Vertical and horizontal flow of water in round tubes and annuli

Diameter:	0.06 to 1.00 in.
Pressure:	500 to 3100 psia
Mass flux:	0.2×10^6 to 3.0×10^6 $lb_m/hr\text{-}ft^2$

1356 136

Quality:	10 to 90%
Heat flux:	35,000 to 700,000 Btu/ft^2-hr
Vapor Nusselt Number:	95 to 1770
Vapor Prandtl Number:	0.88 to 2.21
Y factor:	0.610 to 0.976
Two-Phase Reynolds Number:	6.6×10^4 to 1.3×10^6

The thermal conductivity in the vapor Nusselt number, $h_c D_{he}/k_g$, is evaluated at the saturation temperature. The two-phase Reynolds number, $Re_g(x+(1-x)\ \rho_{gs}/\rho_{\ell s})$, is evaluated at the saturation temperature. The Prandtl number is evaluated at the wall temperature T_w.

The Dougall-Rohsenow correlation is based on liquid film flow at low pressure. The correlation, a straight forward modification of the Dittus-Boelter type of correlation, is given by

$$\frac{h_c D_{he}}{k_g} = 0.023 \left[\frac{G D_{he}}{\mu_g} \left(x + (1 - x) \frac{\rho_{gs}}{\rho_{\ell s}} \right) \right]^{0.8} \left(\frac{C_{pg} \mu_g}{k_g} \right)^{0.4} , \quad \text{(III.2-23)}$$

where the vapor properties are evaluated at the saturation temperature. The correlation is based on data which cover the following ranges of conditions.

Vertical upflow of Freon-113 in round tubes

Diameter:	0.408 and 0.108 in.
Length:	15 in.
Pressure:	2 to 9 psig
Mass Flux:	3.32×10^5 to 8.18×10^5 lb$_m$/ft^2-hr
Heat flux:	14,400 to 41,800 Btu/ft^2-hr
Quality:	up to 50%.

2.2.7 Range of Application for Heat Transfer Correlations

The range of application for heat transfer correlations used in RETRAN is summarized in Tables III.2-1, III.2-2 and III.2-3.

1356 137

TABLE III.2-1

SUMMARY OF RETRAN PRE-CHF HEAT TRANSFER COEFFICIENTS

	Range of Application
Single phase liquid	Thermodynamic quality equal 0.0. Dittus-Boelter, Equation III.2-4 used.
Fully developed surface boiling	Surface temperature from Dittus-Boelter greater than surface temperature from Thom correlation, Equation III.2-7.
Transition from surface boiling to forced convection vaporization	Homogeneous void fraction greater than 0.80 but less than 0.90.
Forced convection vaporization	Homogeneous void fraction greater than 0.90. Schrock-Grossmann correlation, Equation III.2-11.

These correlations are used for all values of the mass flux. If h_c is calculated less than 5 Btu/hr-ft^2, it is set to 5 Btu/hr-ft^2°F.

TABLE III.2-2

HIGH MASS FLUX (G > 200,000 $lb_m/hr\text{-}ft^2$) POST-CHF HEAT TRANSFER COEFFICIENTS

	Range of Application
Forced convection transition boiling	McDonough, Milich, and King heat transfer coefficient values and interpolation equation is used. $\bar{T}_w$ at CHF given by Thom correlation.
Forced convection stable film boiling	Groeneveld correlations, Equations III.2-21 are used if p > 500 psia. Dougall-Rohsenow, Equation III.2-23 if p < 500, or Dougall-Rohsenow may be used exclusively.
Single phase vapor	Thermodynamic quality equal 1.0. Dittus-Boelter correlation is used.

TABLE III.2-3

LOW MASS FLUX ($G \leq 200{,}000$ $lb_m/hr\text{-}ft^2$) POST-CHF HEAT TRANSFER COEFFICIENTS

	Range of Application
Pool transition boiling	Minimum Q_w taken as 20,000 Btu/hr/ft^2. Maximum Q_w taken as 90,000 Btu/hr-ft^2. $(T_w-T_{sat}) = 20^oF$ at maximum Q_w. (T_w-T_{sat}) at minimum Q_w obtained from Berenson correlation. Equation III.2-18 is used.
Pool stable film boiling	Berenson correlation, Equation III.2-16 is used. See test for more detail. These models are highly empirical and basically untested.
Special cases and interpolations	

2.3 Critical Heat Flux Correlations

The base correlations used to determine the critical heat flux depend on the pressure and mass flux. A wide range of pressure is covered by use of three correlations and an interpolation scheme. The model used for the case of very low mass flow rates is highly empirical and basically untested.

The Babcock and Wilcox Company B&W-2 correlation[III.2-23, III.2-24] is used if the pressure is greater than 1500 psia. The critical heat flux is given by

$$Q_{CHF} = \frac{1.15509 - 0.40703(D_{he})}{(12.71)(3.054G')^{A}} \left[(0.3702 \times 10^{8})(0.59137G')^{B} - 0.15208 \times h_{fg}G\right], \quad \text{(III.2-24)}$$

where

$$A = 0.71186 + (2.0729 \times 10^{-4})\,(p-2000)\ , \quad \text{(III.2-25)}$$

and

$$B = 0.834 + (6.8479 \times 10^{-4})\,(p-2000)\ . \quad \text{(III.2-26)}$$

The correlation is based on data which covers the following ranges of conditions:

Vertical upflow of water in rod bundles	
Heated equivalent diameter of subchannels:	0.20 to 0.50 in.
Heated length:	72 in.
Pressure:	2000 to 2400 psia
Mass flux:	0.75×10^{6} to 4.0×10^{6} $lb_m/hr\text{-}ft^2$
Thermodynamic quality:	-0.03 to 0.20
Uniform axial flux distribution.	

The coefficients A and B of Equations III.2-25 and III.2-26 are evaluated for all values of the pressure, p. In RETRAN, the thermodynamic quality is never less than zero.

The Barnett correlation[III.2-25, III.2-69] is used in the range 1300 > p > 1000 psia. The correlation is based on a data base which covers wide ranges of mass flow, inlet subcooling and geometry but is limited to a pressure of 1000 psia. Barnett used critical heat flux data from annuli as the bases for obtaining a correlation. The annuli data covered the ranges of conditions given by:

Vertical upflow of water	
Diameter of inner rod:	0.375 to 3.798 in.
Diameter of shroud:	0.551 to 4.006 in.
Heated length:	24.0 to 108.0 in.
Mass flux ($G \times 10^{-6}$):	0.140 to 6.20 $lb_m/hr\text{-}ft^2$
Inlet subcooling:	0 to 412 Btu/lb_m
Inlet pressure:	1000 psia
Uniform axial heat flux.	

Although the data cover extensive ranges of conditions, Barnett[III.2-25] indicates that the coverage is neither complete nor systematic.

The annuli data were used to obtain the correlation

$$Q_{CHF} = \frac{A + B\,\Delta h_{in}}{C + L} \times 10^6 , \qquad \text{(III.2-27a)}$$

where

$$A = 67.45\, D_{he}^{0.68}\, (G')^{0.192}\, [1.0 - 0.744\, e^{(-6.512\, D_{hy}\, G')}] \qquad \text{(III.2-27b)}$$

$$B = 0.2587\, D_{he}^{1.261}\, (G')^{0.817} \qquad \text{(III.2-27c)}$$

$$C = 185.0\, D_{hy}^{1.415}\, (G')^{0.212} \qquad \text{(III.2-27d)}$$

and

$$\Delta h_{in} = h_{\ell s} - h_{\ell}. \qquad \text{(III.2-27e)}$$

Equation III.2-27e was evaluated at the inlet of the annuli test sections. For flow in annuli, the heated and wetted equivalent diameters are given by

$$D_{hy} = (D_s - D_I) \qquad \text{(III.2-28)}$$

and

$$D_{he} = (D_s^2 - D_I^2)/D_I \qquad \text{(III.2-29)}$$

where D_s is the diameter of the shroud and D_I is the diameter of the inner rod.

Barnett found that equivalent diameters could be defined which would allow application of the correlation of Equation III.2-27 to prediction of critical heat flux in rod arrays. The equivalent diameter of the inner rod is taken to be

$$D_I = D_r \text{ (the fuel rod diameter)} , \qquad \text{(III.2-30a)}$$

and the equivalent shroud diameter is given by

$$D_s = \sqrt{D_r(D_r + D_{he}^*)} . \qquad \text{(III.2-30b)}$$

In Equation III.2-30b, D_{he}^* is a radial-heat-flux-weighted value of the equivalent heated diameter.[III.2-25, III.2-69] Substituting Equations III.2-30 into Equations III.2-27 gives

$$D_{hy} = \sqrt{D_r(D_r + D_{he}^*)} - D_r , \qquad \text{(III.2-31a)}$$

and

$$D_{he} = D_{he}^* . \qquad \text{(III.2-31b)}$$

Equations III.2-31, which define the annulus equivalent of the rod bundle, are used in the annuli CHF correlation of Equations III.2-27. The heated equivalent diameter D_{he}^* is input into RETRAN.

The Barnett CHF correlation of Equation III.2-27 is not a local conditions correlation.[III.2-25, III.2-69] The coefficient B of Equation III.2-27c differs slightly from the local conditions value which is given by

$$B = 0.25\ D_{he}\ (G'). \qquad \text{(III.2-32)}$$

Barnett±III.2-25] found that the CHF data were better correlated if the local conditions hypothesis was not used and thus obtained the value of B as given by Equation III.2-27c. The lack of a local conditions form of the correlation introduces a degree of uncertainty when the correlation is applied to transient analyses because of the difficulty of uniquely identifying the quantities Δh_{in} and L. At the present time, if Δh_{in} is determined to be less than zero, it is set to zero. The length, L, is an input quantity for RETRAN.

For pressure p < 725 psia, the Modified Barnett±III.2-18] correlation is used. The critical heat flux is given by

$$Q_{CHF} = \frac{A + B\ \Delta h_{in}}{C + L}\ 10^6\ , \qquad \text{(III.2-33a)}$$

where

$$A = 73.71\ D_{he}^{0.052}\ (G')^{0.663}$$

$$\pm 1.0 - 0.315\ e^{(-11.34\ D_{hy}\ G')}\ 1\ 888.6/h_{fg} \qquad \text{(III.2-33b)}$$

$$B = 0.104\ D_{he}^{1.445}\ (G')^{0.691} \qquad \text{(III.2-33c)}$$

$$C = 45.55\ D_{hy}^{0.0817}\ (G')^{0.5866} \qquad \text{(III.2-33d)}$$

$$\Delta h_{in} = h_{\ell s} - h_{\ell}. \qquad \text{(III.2-33e)}$$

The equivalent diameters D_{hy} and D_{he} are given by Equations III.2-31. The correlation is based on experimental data which cover the following ranges of conditions:

Vertical upflow of water in rod bundles

Rod diameter:	0.395 to 0.543 in.
Length:	32.9 to 174.8 in.
Pressure:	50 to 725 psia

Mass flux: 0.03×10^6 to 1.7×10^6 lb_m/ft^2-hr

Inlet subcooling: 6 to 373 Btu/lb_m.

The data do not systematically cover the ranges of conditions. In particular, the very low pressure and mass flux regions are not covered well. The pressure correction contained in Equation III.2-33b is at best a first approximation. Barnett[III.2-69] and Bowring[III.2-26] have given other correlations which contain an accounting of pressure effects.

The three correlations given above are supplemented by an interpolation scheme. The general application procedure can be summarized as listed here:

$p > 1500$	B&W-2
$1500 \geq p \geq 1300$	Interpolation between B&W-2 and Barnett
$1300 > p > 1000$	Barnett
$1000 \geq p \geq 725$	Interpolation between Barnett and Modified Barnett
$725 > p$	Modified Barnett.

For a given pressure between 725 and 1000 lb/in^2 or between 1300 and 1500 lb/in^2, the two relevant correlations are evaluated at that pressure and its corresponding h_{fg}. The two flux values are then weighted to give

$$Q_{CHF} = \frac{(p_R - p)\, Q_{CHF_L} + (p - p_L)\, Q_{CHF_R}}{p_R - p_L}, \qquad \text{(III.2-34)}$$

where p = pressure, and L and R represent the low and high ends of the interpolation range, respectively. A minimum critical heat flux value of 90,000 Btu/ft^2-hr is set if the predicted value falls below this number.

In addition to the CHF correlations previously described, two other options are available in RETRAN. There is a General Electric Company[II.2-70] correlation which is dependent only on quality, and is given by

$$Q_{CHF} = \begin{cases} 10^6\ (0.8\text{-}x) & \text{for } G \geq 0.5 \times 10^6 \text{ lbm/ft}^2\text{-hr} \\ 10^6\ (0.84\text{-}x) & \text{for } G < 0.5 \times 10^6 \text{ lbm/ft}^2\text{-hr.} \end{cases} \quad \text{(III.2-35)}$$

This correlation should be applied for mass fluxes less than 0.75×10^6 lbm/ft^2-hr.

The final CHF correlation in RETRAN was developed at the Savannah River Laboratory [II.2-71] for application with aluminum heaters. This correlation, which is dependent on the fluid velocity and amount of subcooling, is given by

$$Q_{CHF} = 188{,}000\ (1.0 + 0.0515\ v)\ (1.0 + 0.069\ (T_{sat} - T_b)). \quad \text{(III.2-36)}$$

For a mass flux, G, less than 200,000 lb$_m$/ft^2-hr, the critical heat flux is interpolated between 90,000 Btu/ft^2-hr and the value given by the chosen correlation, where the former corresponds to G=0 lb$_m$/ft^2-hr and the latter to G=200,000 lb$_m$/ft^2-hr.

2.4 Junction Enthalpy

The integral energy balance equation includes a term involving the enthalpy at the flow path, or junction, between two volumes. In general, h_{ik} is the enthalpy of the fluid at junction i, leaving donor volume k. Since the local enthalpy is known only at the center of the volume, an expression is needed to compute the enthalpy at a junction.

The junction enthalpy can be expressed as

$$h_{ik} = \bar{h}_k + \frac{1}{2}\left(\frac{\bar{W}_k}{\bar{\rho}_k A_k}\right)^2 + Z_k - \frac{1}{2}\left(\frac{W_i}{\rho_i A_k}\right)^2 - Z_i + \Delta h_{S,Q_{ik}} \quad \text{(III.2-37)}$$

where

$\bar{h}_k$ = average enthalpy of volume k
$\bar{W}_k$ = average mass flow rate in volume k

$\bar{\rho}_k$ = average fluid density for volume k

A_k = flow area of volume k

Z_k = elevation at the geometric center of volume k

W_i = mass flow rate at junction i

ρ_i = density of the fluid flowing out of volume k thru junction i

Z_i = elevation at the center of junction i

$\Delta h_{S,Q_{ik}}$ = change in thermodynamic enthalpy between the center of volume k and junction i, due to phase separation or energy exchange between the fluid in volume k and an external source or sink.

The $\Delta h_{S,Qik}$ term in Equation III.2-37 is a generalization of the enthalpy change due to separation or energy exchange, and may be more exactly treated as Δh_{Sik} or Δh_{Qik} for separation and energy exchange, respectively. Both separation and enthalpy transport treatment may be required for a given junction. However, the separation treatment is used when the mixture level is below the volume height. Conversely, the enthalpy transport treatment is used only when a volume is mixture full, i.e. when the mixture level is equal to the volume height.

The changes in junction enthalpy, Δh_{Qik} and Δh_{Sik}, are changes relative to the volume averaged enthalpy. The junction enthalpy is evaluated immediately upstream of the actual junction flow area, A_i, which connects volume k to another volume. In addition, the junction enthalpy is determined by the fluid properties of the source of flow, W_{ik}. For example, if W_{ik} is the flow out of volume k, then h_{ik} is determined by the properties of volume k. The enthalpy changes given by the terms Δh_Q and Δh_S are discussed below.

2.4.1 Enthalpy Associated with Phase Separation

The enthalpy at the junction of two or more volumes can be different from the volume averaged enthalpy if the void fraction or quality is varying over the length of the volume. In RETRAN the void fraction profile within the volume is determined from a correlation in which the void fraction within the two-phase mixture is assumed to be linear with elevation.[III.2-72, III.2-73, III.2-74] This correlation, also known as the bubble rise model, is a semi-empirical fit to data from a number of high pressure blowdown experiments. For a complete discussion of the bubble rise model and equations, see Section III.1.3.

In computing the contribution to the junction enthalpy due to phase separation, the junction can be modeled as a point vertical height for vertical flow or as a circular area (equal to the junction area) distributed vertically for horizontal flow. The user also has the option to "smooth" the enthalpy due to phase separation if the mixture level is near the junction. In this case, the mass extracted from the volume during the time step is assumed to originate in the region between the mixture level and the junction elevation. If the steam volume is not large enough to supply this mass, the remainder is extracted from the surface of the mixture. When enthalpy "smoothing" is not desired, the enthalpy at the junction is defined by the phase which is then present at the junction, ranging from pure liquid, to the mixture, to pure steam.

If the quality computed at the junction is x_j (see Equation III.1-90), the enthalpy change resulting from phase separation is

$$\Delta h_{S_{ik}} = h_g (x_i - \bar{x}_k) + h_f (\bar{x}_k - x_i) + \frac{1}{2}\left(\frac{W_i}{\rho_i A_k}\right)^2 - \frac{1}{2}\left(\frac{\bar{W}_k}{\bar{\rho}_k A_k}\right)^2 + Z_i - Z_k \qquad \text{(III.2-38)}$$

where

h_g = enthalpy of the saturated gas
h_f = enthalpy of the saturated liquid
$\bar{x}_k$ = average quality of volume k.

The junction enthalpy is obtained by subsituting Equation III.2-38 into Equation III.2-37, yielding

$$h_{ik} = \bar{h}_k + h_g (x_i - \bar{x}_k) + h_f (\bar{x}_k - x_i) . \qquad \text{(III.2-39)}$$

1356 148

2.4.2 Enthalpy Associated with Energy Exchange

If energy is exchanged between the fluid within volume k and the surfaces enclosing the volume, the enthalpy at junction i of volume k may have a different value than the volume averaged enthalpy, $\bar{h}_k$. The change in enthalpy at the junction will depend on the rate of energy exchange with the surrounding surfaces and the flow rate of the fluid.

To evaluate the contribution to the junction enthalpy associated with energy exchange, consider the volume shown in Figure III.2-3. The flow through the volume is from left to right, with volume averaged quantities of $\bar{W}_k$ (flow rate) and $\bar{h}_k$ (enthalpy). To compute the junction enthalpy, h_{ik}, the energy equation is solved for the right half-volume. Neglecting changes in kinetic and potential energy, the energy equation for this half-volume is

$$\frac{dU}{dt} = \bar{W}_k \bar{h}_k - W_{ik} h_{ik} + Q. \qquad \text{(III.2-40)}$$

The continuity equation for this half-volume is

$$\frac{dM}{dt} = \bar{W}_k - W_{ik}. \qquad \text{(III.2-41)}$$

If we assume the time rate of change of pressure within this half-volume is constant, the time rate of change of energy ($U = uM$) can be written as

$$\frac{dU}{dt} = h \frac{dM}{dt} + M \frac{dh}{dt}. \qquad \text{(III.2-42)}$$

Solving Equations III.2-40 and III.2-41 for $\frac{dU}{dt}$ gives

$$h(\bar{W}_k - W_{ik}) + M \frac{dh}{dt} = \bar{W}_k \bar{h}_k - W_{ik} h_{ik} + Q \quad . \qquad \text{(III.2-43)}$$

Four additional assumptions are required to solve Equation III.2-43 for the junction enthalpy. These assumptions are:

(1) The enthalpy changes linearly in the half-volume,

$$h = \frac{\bar{h}_k + h_{ik}}{2} \qquad \text{(III.2-44)}$$

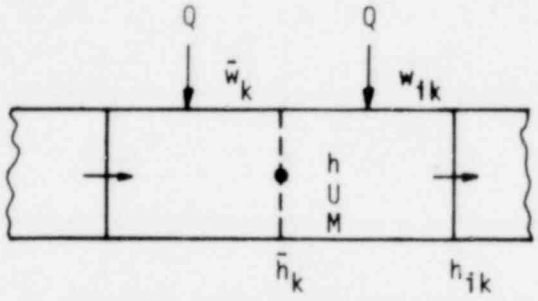

Figure III.2-3 Enthalpy Associated with Energy Exchange

1756 150

(2) The time rate of change of the junction enthalpy and the volume averaged enthalpy is the same,

$$\frac{d\bar{h}_k}{dt} = \frac{dh_{ik}}{dt} \qquad \text{(III.2-45)}$$

(3) The mass of fluid in the half-volume is equal to half the fluid mass of the total volume,

$$M = \frac{M_k}{2} \qquad \text{(III.2-46)}$$

(4) The energy added to the half-volume is equal to half the energy added to the total volume,

$$Q = \frac{Q_{w,k}}{2} \quad . \qquad \text{(III.2-47)}$$

Substitution of Equations III.2-44 to III.2-47 into Equation III.2-43 gives

$$\frac{dh_{ik}}{dt} + \frac{(\bar{W}_k + W_{ik})}{M_k} h_{ik} = -\frac{(\bar{W}_k + W_{ik})}{M_k} \bar{h}_k + \frac{Q_{w,k}}{M_k} \qquad \text{(III.2-48)}$$

which has as a solution,

$$h_{ik} = h_{ik}(0)\, e^{-\Delta t/\tau} + (\bar{h}_k + \frac{Q_{w,k}}{M_k} \tau)(1 - e^{-\Delta t/\tau}) \qquad \text{(III.2-49)}$$

where

$h_{ik}(0)$ = junction enthalpy at start of time step

Δt = size of time step

and

$$\tau = \frac{M_k}{\bar{W}_k + W_{ik}} \quad .$$

1356 151

The change in the junction enthalpy due to energy exchange is given by

$$\Delta h_{Q_{ik}} = (h_{ik}(0) - \bar{h}_k)e^{-\Delta t/\tau} + \frac{Q_{w,k}}{M_k}\ \tau(1 - e^{-\Delta t/\tau}). \qquad \text{(III.2-50)}$$

The junction enthalpy for the enthalpy transport treatment is now obtained by combining Equations III.2-37 and III.2-50 as follows.

$$h_{ik} = \bar{h}_k + \frac{1}{2}\left(\frac{\bar{W}_k}{\bar{\rho}_k A_k}\right)^2 + Z_k - \frac{1}{2}\left(\frac{W_i}{\rho_i A_i}\right)^2 + Z_i$$

$$+ (h_{ik}(0) - \bar{h}_k)\ e^{-\Delta t/\tau} + \frac{\tau\ Q_{w,k}}{M_k}\ (1 - e^{-\Delta t/\tau}). \qquad \text{(III.2-51)}$$

2.5 Condensing Heat Transfer

Heat transfer correlations for condensing steam, which are applicable to large, complicated structures such as nuclear containments, presently have a scarce data base. Several conditions affect the rate of condensing heat transfer:

(1) Local steam, air and impurity concentrations
(2) Surface conditions
(3) Geometry of each heat conductor
(4) Turbulence

Containment buildings are large in comparison to most experiments reported in the literature by an order of magnitude or more, with the exception of a few experiments in containment-sized buildings. The size of the building, with multiple and sometimes complicated paths for convection, can cause great disparity between local conditions due to transport time and history of condensing during transport to the local area. Thus the local steam, air and impurity concentrations will tend to vary in space and time. The local surface conditions will affect the mode of condensation: dropwise, filmwise or a combination of the two. No experimental work can be found in the literature on tall vertical walls. Heat transfer will be enhanced in the lower parts of tall walls if the condensate forms riverlets rather than uniform sheets. Local velocities as well as film thickness or droplet diameter affect the amount of turbulence and once in the turbulent regime, increased turbulence enhances

condensation. In a containment analysis performed using RETRAN, all of these effects must be integrated over the whole volume; hence, the need to rely on large-scale experiments using realistic blowdowns. In that case one must guard against blanket use of the resulting data.

Two correlations commonly used for condensing steam heat transfer in containments are given by Uchida and Tagami[III.2-75, III.2-76, III.2-77]. These correlations are discussed individually and in combination as used for minimum containment pressure calculations for PWR ECCS performance evaluations[III.2-78] in the following sections.

2.5.1 Uchida Heat Transfer Coefficient

The Uchida correlation for condensing steam in the presence of noncondensibles is based on the short note contained at the end of his paper dealing mainly with core sprays[III.2-75]. Experiments were performed with mixtures of steam and various kinds of noncondensible gases. The data show that the type of noncondensible is unimportant, but the mass ratio of noncondensible to steam is very important. The experiments were carried out on relatively small (5.5 inches wide by 11.8 inches high) vertical surfaces. No discussion is given in terms of velocities, turbulence, surface conditions, material type or thickness. The Uchida correlation was converted to British units and put into RETRAN in tabular form, as listed in Table III.2-4.

2.5.2 Tagami Heat Transfer Coefficient

The data presented by Tagami and associates are presented in two papers[III.2-76, III.2-77]. Data are presented for both steady-state and transient behavior in the second paper and for only transient behavior in the first. The band of the Tagami data covers heights of cylinders from 300 mm to 900 mm (11.8 inches to 35.4 inches) and Tagami claims that the heat transfer coefficient varies with the fourth root of the condensing surface heights, but the scatter in the data makes it difficult to evaluate this conclusion. In addition, the Tagami data do not cover the higher steam-to-air ratios as do the Uchida data.

In the first paper, Tagami presents data for two blowdowns, as shown in Figure III.2-4. One has a relatively high flow rate and ends in 10 seconds and

TABLE III.2-4

UCHIDA HEAT TRANSFER COEFFICIENTS

Mass Ratio (lb air/lb steam)	Heat Transfer Coefficient (Btu/hr-ft^2-°F)	Mass Ratio (lb air/lb steam)	Heat Transfer Coefficient (Btu/hr-ft^2-°F)
50*	2	3	29
20*	8	2.3	37
18*	9	1.8	46
14	10	1.3	63
10	14	0.8	98
7	17	0.5	140
5	21	0.1	280
4	24	0.0*	500

*Beyond limits of reported data, added to give table reasonable bounds.

1356 154

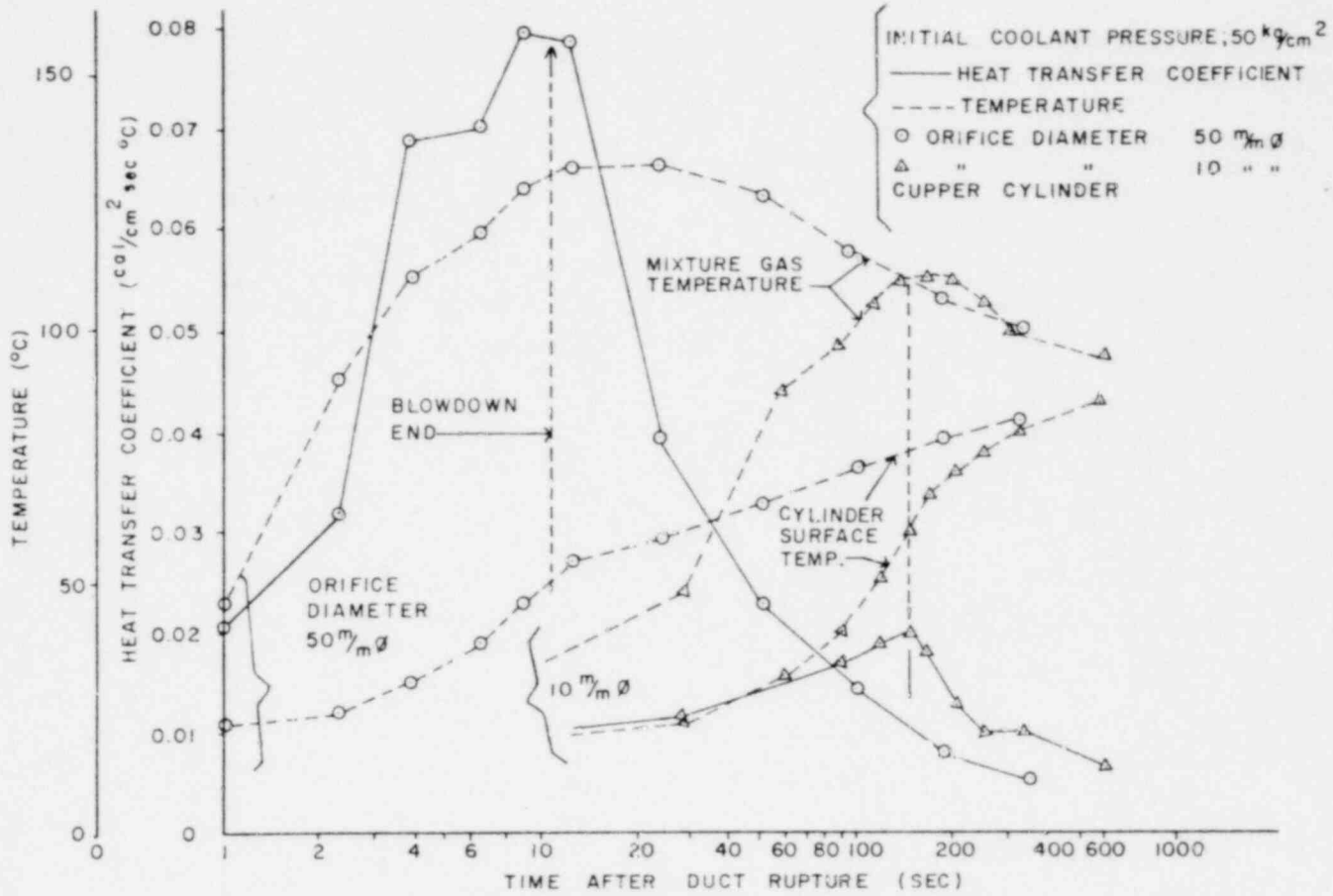

Figure III.2-4 Heat Transfer Coefficient Transient During Blowdown

the other has a relatively low flow rate and lasts about 150 seconds. The computed time-dependent heat transfer coefficients for these tests are shown in Figure III.2-5, which conclusively shows that during the blowdown and for some time afterwards, the heat transfer coefficient is much higher than the steady-state heat transfer coefficient. A correlation was developed from these tests based on the total coolant energy per containment vessel volume up to the time that peak pressure was attained, as shown by the formula

$$h_{MAX} = a \left(\frac{Q}{Vt_p} \right)^b \qquad \text{(III.2-52)}$$

where

h_{MAX} = the maximum heat transfer coefficient during blowdown,
Q = total energy in blowdown mass,
V = free containment volume,
t_p = time interval from beginning of blowdown until peak pressure is reached, and

a,b = empirical constants.

Tagami shows a line through the middle of his data in Figure III.2-6, but does not list his evaluations of a and b.

Slaughterbeck[III.2-79] expresses the correlation as

$$h_{MAX} = 72.5 \left(\frac{Q}{Vt_p} \right)^{0.62} \qquad \text{(III.2-53)}$$

for British units, and references the Westinghouse expression, which is

$$h_{MAX} = 75.0 \left(\frac{Q}{Vt_p} \right)^{0.60} \qquad \text{(III.2-54)}$$

1356 156

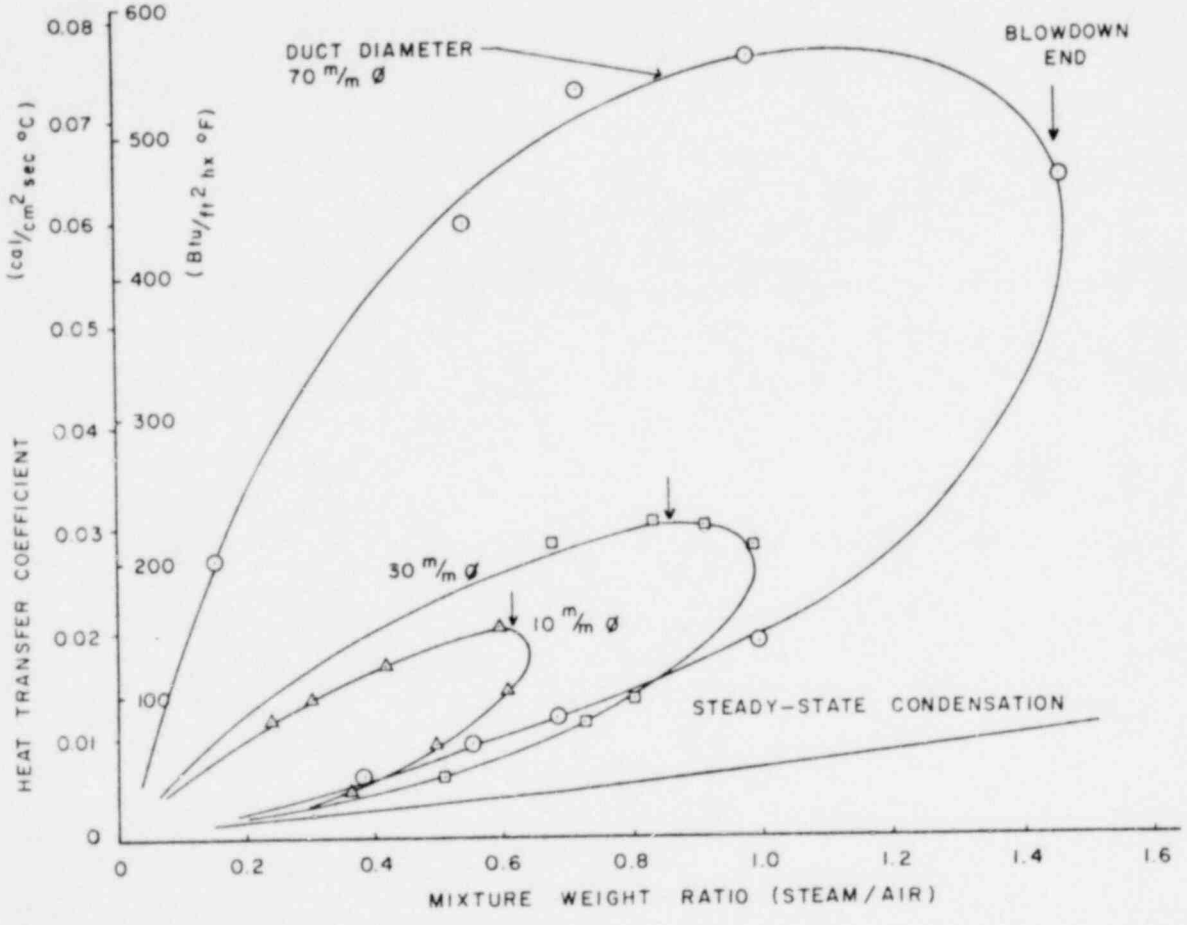

Figure III.2-5 Heat Transfer Coefficient vs. Steam Mixture Weight Ratio (Transient State Measurements)

1356 157

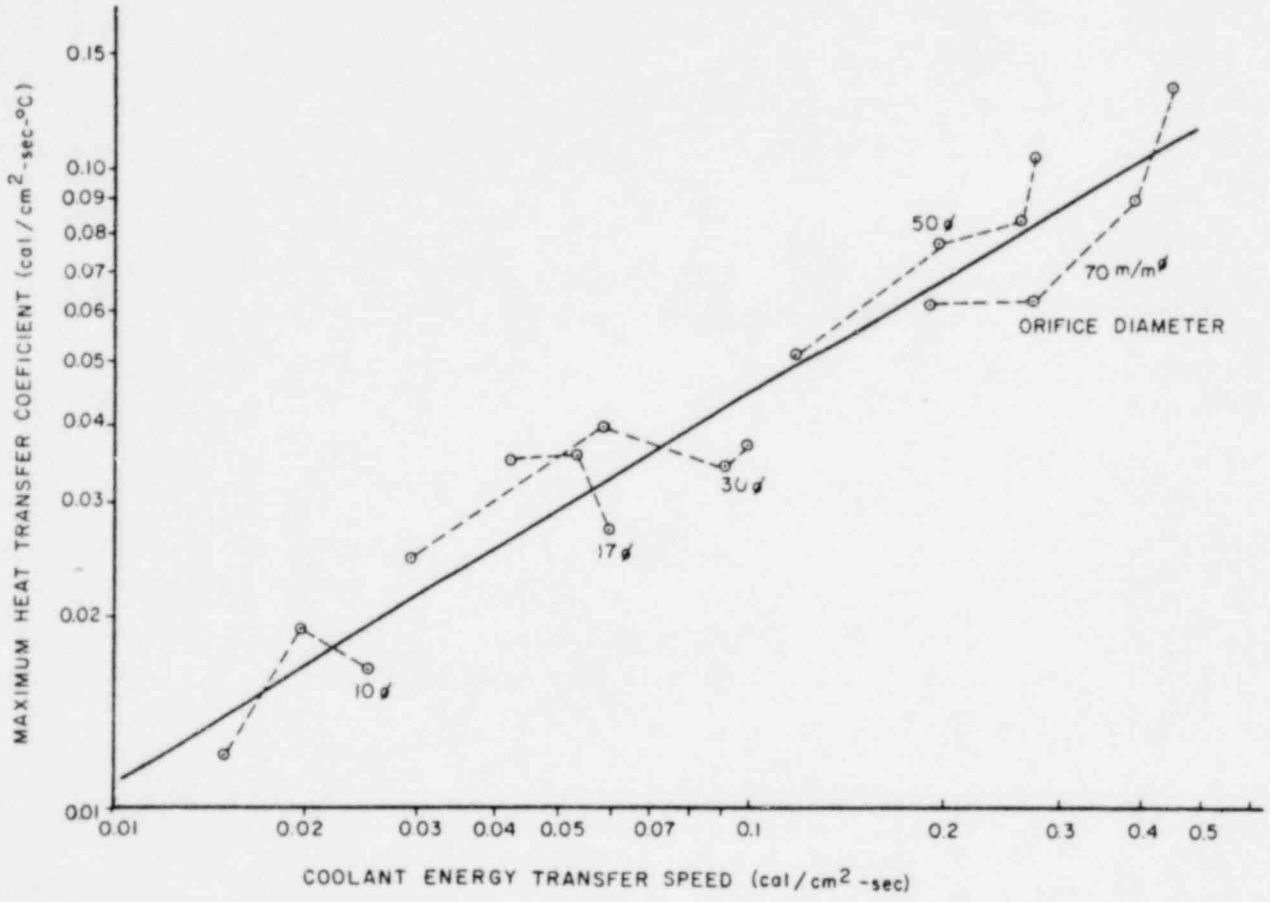

Figure III.2-6 Maximum Heat Transfer Coefficient vs. Coolant Energy Transfer Speed into Containment Vessel Atmosphere During Blowdown

It appears that the variations in a and b are merely independent determinations from the graph by the different people performing the calculations. Any one of the two sets of empirical constants will fit the data well.

2.5.3 CSB 6-1 Heat Transfer Coefficient

The heat transfer coefficient used to attain minimum containment pressure calculations for PWR ECCS performance evaluations is documented in Reference III.2-78. In effect, the heat transfer coefficient model is a combination of the Uchida and Tagami correlations discussed above, with conservatisms added to ensure high heat transfer to exposed heat sinks during the blowdown and post blowdown phases of a transient.

Prior to the blowdown characterized by high turbulence in the containment volume, a constant heat transfer coefficient is used. The constant value is given by

$$h_{INT} = 8.0 \text{ Btu/hr-ft}^2\text{-}^\circ\text{F} \qquad \text{(III.2-55)}$$

During the blowdown phase, a linear increase in the condensing heat transfer coefficient is assumed, from h_{INT} to a peak value of four times greater than the maximum calculated condensing heat transfer coefficient at the end of blowdown, using the Tagami correlation as given by Equation III.2-53. The condensing steam heat transfer coefficient for the time frame bounded by pre-blowdown and end of blowdown is given by

$$h_B = h_{INT} + \left[\frac{4h_{MAX} - h_{INT}}{t_p}\right]\Delta t_B \text{ (Btu/hr-ft}^2\text{-}^\circ\text{F)} \qquad \text{(III.2-56)}$$

where

Δt_B = elapsed time since blowdown initiation (sec) $(0 \leq \Delta t_B \leq t_2 - t_1)$.

The long term post-blowdown phase of the accident is characterized by low turbulence in the containment atmosphere. Consequently, it is assumed that the condensing heat transfer coefficients are 1.2 times greater than those predicted by Uchida's data shown in Table III.2-4. During the transition phase of the

transient, between the end of blowdown and the long-term post-blowdown phase, a reasonably conservative exponential transition in the condensing heat transfer coefficient is assumed. The transition and post-blowdown heat transfer coefficient is given by

$$h_{PB} = 1.2\ h_U + [h_{MAX}(t_p) - 1.2\ h_U]\ e^{-0.025\ \Delta t_{PB}} \quad (Btu/hr\text{-}ft^2\text{-}^oF) \qquad (III.2\text{-}57)$$

where

Δt_{PB} = elapsed time since end of blowdown (sec) $\quad (0 \leq \Delta t_{PB} \leq t - t_2)$.

The various regions modeled by the CSB 6-1 condensing heat transfer coefficient are illustrated by Figure III.2-7.

1356 140

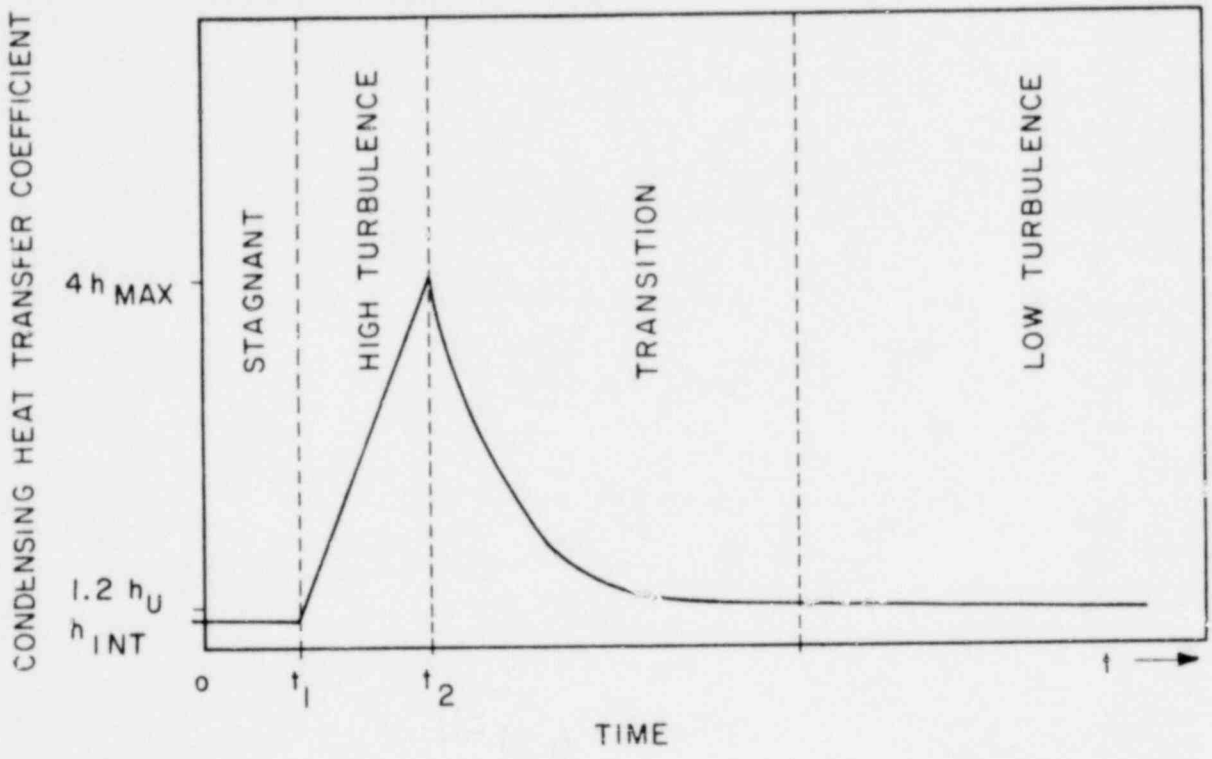

Figure III.2-7 NRC Containment Systems Branch Position 6-1 Condensing Heat Transfer Regimes

1356 161

3.0 CRITICAL FLOW MODELS

RETRAN has several critical flow options available to the user:

(1) Sonic or "self choking"
(2) Extended Henry-Fauske
(3) Henry-Fauske
(4) Moody
(5) None of the above.

The first two options may be used to check for "subcooled choking," that is, the possibility of critical flow when a volume is on the average subcooled or saturated single phase fluid but flashing is expected to exist somewhere between the volume center and a junction. Flow is computed at junction nodes. However, pressure and energy are computed at volume nodes. Thus, not all the quantities needed to check for critical flow are available at the same point since critical flow calculations require knowledge of the thermodynamic state of the fluid which is only known at volume centers and may be considerably different than at the junction. Thus, the general criterion for choking is

$$W_j \geq C_j A_j(t)\, G_{CRIT}\,(p_i, h_i) = W_{CRIT}, \qquad \text{(III.3-1)}$$

where G_{CRIT} is the critical mass flux in $lb/(s\text{-}ft^2)$ evaluated at the pressure, p_i, and enthalpy, h_i, the "source" or "from" volume. The source volume enthalpy is modified to account for kinetic energy changes and heating or cooling from the volume center to the junction using the boiling model and separation effects. A gravity head correction is applied to the volume pressure. When flow is from volume K to volume L, the properties of volume K are used to calculate W_{CRIT}. If W_j changes sign, W_{CRIT} would be calculated using volume L properties. The user supplied discharge coefficient, C_j, and the time dependent junction flow area, A_j, are used to calculate W_{CRIT}.

3.1 Sonic or "Self" Choking

The sonic choking option uses the computation of the homogeneous equilibrium model (HEM) speed of sound defined by

1356 162

$$C_{HEM} = \sqrt{\left(\frac{\partial p}{\partial \rho}\right)_s} \quad , \qquad \text{(III.3-2)}$$

where s is the specific entropy of the mixture. Values of C_{HEM} are computed in the steam tables.

The assumptions needed to arrive at Equation III.3-2 are

(1) The phases move at equal velocity.

(2) The phases exist at equal temperature.

Thus, the phases are in a state of perfect mechanical and thermal equilibrium. The mass transfer rates between phases can only be due to pressure changes and wall heat transfer. The rate is such that the phase temperatures remain at the saturation temperature corresponding to the local pressure. Some authors[III.3-1] invoke the assumption that the fluid is isentropic, that is, no wall heat transfer or friction. Reference [III.3-2] shows by the Method of Characteristics that this is not necessary. It is important that the wall heat flux be given by non-differential expressions, however. Since local conditions determine the HEM sound speed, any variation in fluid entropy will affect this quantity.

W_{CRIT} is then computed at a junction from

$$W_{CRIT}^{SONIC} = A_j(t) C_{HEM} \rho_j \quad . \qquad \text{(III.3-3)}$$

The calculation of C_{HEM} in the two-phase region is performed by evaluating

$$\left(\frac{\partial p}{\partial \rho}\right)_s = \frac{T\left(\frac{dp}{dT}\right)^2}{C_v \rho^2} \quad . \qquad \text{(III.3-4)}$$

dp/dT is a fundamental two-phase quantity which can be computed from the classical Clausius-Clapyron equation as:

$$\frac{dp}{dT} = \frac{1}{T}\left(\frac{h_g - h_\ell}{v_g - v_\ell}\right) \text{, psi/°R} \quad . \qquad \text{(III.3-5)}$$

1356 163

where v_a are the phase specific volumes in ft^3/lb_m and T is the temperature. C_v is the mixture heat capacity at constant volume defined by

$$C_v = x\left[C_{pg} - 2T\frac{dp}{dT}\left(\frac{\partial v_g}{\partial T}\right)_p - T\left(\frac{dp}{dT}\right)^2\left(\frac{\partial v_g}{\partial P}\right)_T\right] + (1-x)\left[C_{p\ell} - 2T\frac{dp}{dT}\left(\frac{\partial v_\ell}{\partial T}\right)_p - T\left(\frac{dp}{dT}\right)^2\left(\frac{\partial v_g}{\partial T}\right)_T\right]. \quad \text{(III.3-6)}$$

C_{pa} are the heat capacities of each phase at constant pressure and the quality x is:

$$x = (h-h_{\ell s})/h_{fg}\ . \quad \text{(III.3-7)}$$

In terms of the quantities,

$$\beta_g = \rho_g\left(\frac{\partial v_g}{\partial T}\right)_p \quad \text{(III.3-8)}$$

$$\beta_\ell = \rho_\ell\left(\frac{\partial v_\ell}{\partial T}\right)_p \quad \text{(III.3-9)}$$

$$K_g = -\rho_g\left(\frac{\partial v_g}{\partial p}\right)_T \quad \text{(III.3-10)}$$

$$K_\ell = -\rho_\ell\left(\frac{\partial v_\ell}{\partial p}\right)_T\ , \quad \text{(III.3-11)}$$

Equation III.3-6 becomes

$$C_v = x\left[C_{pg} - 2T\left(\frac{dp}{dT}\right)v_g\,\beta_g + T\left(\frac{dp}{dT}\right)^2 v_g\,K_g\right] + (1-x)\left[C_{p\ell} - 2T\left(\frac{dp}{dT}\right)v_\ell\,\beta_\ell + T\left(\frac{dp}{dT}\right)^2 v_\ell\,K_\ell\right]. \quad \text{(III.3-12)}$$

All of the thermodynamic quantities are returned by subroutine STATE.

In the limit as x becomes 0 or 1, the square of the HEM speed of sound becomes

$$\left(\frac{\partial p}{\partial \rho}\right)_s\Bigg|_{x=1} = \frac{1}{\rho_g(K_g - \beta_g/\frac{dp}{dT})} \qquad \text{(III.3-13)}$$

and

$$\left(\frac{\partial p}{\partial \rho}\right)_s\Bigg|_{x=0} = \frac{1}{\rho_\ell(K_\ell - \beta_\ell/\frac{d\mu}{dT})} \quad . \qquad \text{(III.3-14)}$$

These expressions contrast with the single phase speeds of sound given by

$$\left(\frac{\partial p}{\partial \rho_g}\right)_{S_g} = \frac{1}{\rho_g K_g - \beta_g^2/C_{pg}} \qquad \text{(III.3-15)}$$

and

$$\left(\frac{\partial p}{\partial \rho_\ell}\right)_{S_\ell} = \frac{1}{\rho_\ell K_\ell - \beta_\ell^2/C_{p\ell}} \quad . \qquad \text{(III.3-16)}$$

The discontinuity between the values in sound speeds given by Equations III.3-13 and III.3-14 vs. Equations III.3-15 and III.3-16 can be considerable, especially near x=0. Such discontinuities may cause stability problems.

In order to check for sonic of "self" choking, an explicit predictive flow calculation is performed as

$$\hat{W}_j^{n+1} = W_j^n + \Delta t^n \left[p_K^n - p_L^n + p_{gK}^n - p_{gL}^n + MF_K^n - MF_L^n - B(W_j^n)^2 \right] \Big/ I_j \qquad \text{(III.3-17)}$$

1356 165

where

$$B = -\mathfrak{F}_j^n + \frac{K_j S_{gn}(W_j^n)}{2\rho_j^n[A_j(t)]^2} \qquad \text{(III.3-18)}$$

and where p_i^n, F_{gi}^n, MF_i^n (i=K,L) are the thermodynamic, gravity and momentum flux pressure terms at the previous time step as defined in the NOMENCLATURE Section.

If

$$\hat{W}_j^{n+1} \geq \left(W_{CRIT}^{SONIC}\right)^n \quad , \qquad \text{(III.3-19)}$$

then W_j^{n+1} is set equal to W_j^n in order to readjust the friction parameter B as

$$B = \left[(p_K^n - p_L^n) + (P_{gK}^n - P_{gL}^n) + (MF_K^n - MF_L^n)\right] \Big/ \left(W_{CRIT}^{SONIC}\right)^2 . \qquad \text{(III.3-20)}$$

The value of B obtained by this operation ensures that the subsequent computation of ΔW_j^n will be approximately zero. Any deviation from zero is probably caused by the difference in numerics between the calculation of $\hat{W}_j^{n+1}$ and the calculation of $\Delta W^n = W^{n+1} - W^n$ as explained in Section VIII. If Equation III.3-19 is not satisfied, the flow at the next time step will become "dechoked" if it was choked.

Since Equation III.3-17 is explicit, if $\hat{W}_j^{n+1}$ is greater than W_{CRIT}^{SONIC}, the value of $\hat{W}_j^{n+1}$ has associated with it an unstable error term which may be appreciable if $\hat{W}_j^{n+1}$ is much greater than W_{CRIT}^{SONIC}.

It should be mentioned that just because the HEM sound speed is used, this does not mean that this is the HEM choking model. The HEM choking model is based on stagnation conditions and not local conditions. For this reason, C_{HEM}^2 is evaluated using the local fluid conditions known at volume centers.

1356 166

3.2 Henry-Fauske and Extended Henry-Fauske Choking

The Henry-Fauske choking option is based on the theory developed by Henry[III.3-3] and published by Henry and Fauske.[III.3-4] First the steady-state equation of vapor and liquid continuity and total momentum are written as:

$$W^{\ell} = \alpha_{\ell}\rho_{\ell}v^{\ell}A = \text{constant} \qquad \text{(III.3-21)}$$

$$W^{g} = \alpha_{g}\rho_{g}v^{g}A = \text{constant} \qquad \text{(III.3-22)}$$

and

$$\frac{d}{dz}\left(W^{\ell}v^{\ell} + W^{g}v^{g}\right) + A\frac{\partial p}{\partial z} = 0 \quad , \qquad \text{(III.3-23)}$$

where friction and mass transfer have been assumed to be negligible. Equation III.3-23 may be rewritten as

$$\frac{d}{dz}\left[W^{\ell}v^{\ell} + W^{g}v^{g})W/W\right] + A\frac{\partial p}{\partial z} = 0 \qquad \text{(III.3-24)}$$

where W is the total flow rate. Defining the flowing qualities

$$x_f = \frac{W^g}{W} \qquad \text{(III.3-25a)}$$

and

$$1 - x_f = \frac{W^{\ell}}{W} \quad , \qquad \text{(III.3-25b)}$$

expanding Equation III.3-24 and using Equations III.3-21 and III.3-22 results in

$$W\frac{\partial}{\partial z}\left[(1 - x_f)v^{\ell} + x_f\, v^{g}\right] + A\frac{\partial p}{\partial z} = 0 \quad . \qquad \text{(III.3-26)}$$

Rearranging Equation III.3-26 results in

$$G = \frac{-dp/dz}{d\left[(1 - x_f)\, v^{\ell} + x_f\, v^{g}\right]/dz} \qquad \text{(III.3-27)}$$

where G is the mass flux given by

$$G = W/A \ . \qquad \text{(III.3-28)}$$

Henry[III.3-3] assumes that G attains a maximum when

$$\left(\frac{\partial G}{\partial p}\right)_t = 0 \qquad \text{(III.3-29)}$$

where subscript t refers to the local (throat) conditions.

Application of Equation III.3-29 to Equation III.3-27 results in

$$G^2_{CRIT} = -\left\{\frac{d}{dP}\left[\left(\frac{x_f H + (1 - x_f)}{H}\right)\ [(1 - x_f)\ Hv_\ell + x_f v_g]\right]\right\}^{-1}_t \qquad \text{(III.3-30)}$$

where the slip ratio H is defined as

$$H = \frac{v_g}{v_\ell} \ . \qquad \text{(III.3-31)}$$

Equation III.3-30 may be further expanded as

$$G^2_{CRIT} = -\Bigg\{H\Big[[1 + x_f(H - 1)]x_f \left.\frac{dv_g}{dg}\right|_t + \Big[v_g\Big(1 + 2x_f(H - 1)\Big) \qquad \text{(III.3-32)}$$

$$+ Hv_\ell\left(2(x_f - 1) + H(1 - 2x_f)\right)\left(\frac{dx_f}{dp}\right)_t + h[1 + x_f(H - 2)$$

$$- x_f^2(H - 1)]\left(\frac{dv_\ell}{dp}\right)_t + x_f(1 - x_f)\ Hv_\ell - \frac{v_g}{H}\left(\frac{dH}{dp}\right)_t\Bigg\}^{-1}_t \ .$$

1356 168

Henry and Fauske now make some assumptions:

1) H = 1 which implies that

$$\left.\frac{dH}{dp}\right|_t = 0 \qquad \text{(III.3-33)}$$

2)

$$\left.\frac{dv_\ell}{dp}\right|_t = 0 \qquad \text{(III.3-34)}$$

which implies v_ℓ is constant and equal to $v_{\ell o}$, the liquid specific volume at the inlet to the test section.

3) Although mass transfer was neglected in order to arrive at Equations III.3-21 and III.3-22, $\frac{dx_f}{dp}$ is not assumed to be zero. It is assumed to be correlated by

$$\left.\frac{\partial x_f}{\partial p}\right|_{t_{k=1}} = N \left.\frac{\partial x_e}{\partial p}\right|_t \qquad \text{(III.3-35)}$$

were x_e is some equilibrium quality. N is assumed to be given by

$$N = x_e/0.14 \qquad x_e \leq 0.14 \qquad \text{(III.3-36a)}$$

$$N = 1.0 \qquad x_e \geq 0.14 \qquad \text{(III.3-36b)}$$

4) The equilibrium quality x_e is equated to x_o, the equilibrium quality at the entrance to the test section.

5) The steam expands adiabatically and therefore

$$pv_g^n = \text{constant} \qquad \text{(III.3-37)}$$

where n is the thermal equilibrium polytropic exponent as derived by Tangren et al.[III.3-5].

6) $1 - x_o \simeq 1.$ (III.3-38)

Assumptions (1-6) above reduce Equation III.3-32 to

$$G^2_{CRIT} = \left[\frac{x_o v_g}{np} + (v_g - v_{\ell o}) N \left. \frac{\partial x_e}{\partial p} \right|_t \right]^{-1}_t \quad \text{(III.3-39)}$$

The model chosen for the equilibrium quality, x_e, is

$$x_e = \frac{s_o - s_{\ell s}}{s_{gs} - s_{\ell s}} \quad \text{(III.3-40)}$$

where s_{as} are the phase entropies at the local (throat) equilibrium conditions and s_o is the test section inlet mixture entropy.

Equation III.3-35 then can be correlated by

$$\left. \frac{dx_f}{dp} \right|_{t_{H=1}} = -\left[\frac{(1 - x_o) \frac{ds_\ell}{dp} + x_o \frac{ds_g}{dp}}{s_{go} - s_{\ell o}} \right]_{t_{H=1}} = N \left. \frac{dx_e}{dp} \right|_t \quad \text{(III.3-41)}$$

where s_{go} and $s_{\ell o}$ are the test section inlet phase entropies. Using

$$\left[\frac{1}{s_{go} - s_{\ell s}} \right] \left. \frac{ds_\ell}{dp} \right|_t = N \left[\frac{1}{s_{gs} - s_{\ell s}} \frac{ds_{\ell s}}{dp} \right]_t \quad \text{(III.3-42)}$$

and the relations

$$T_g ds_g = dh_g - v_g \, dp \quad \text{(III.3-43)}$$

and

$$\left.\frac{ds_g}{dp}\right|_t = -\frac{C_{pg}}{p_t}\left(\frac{1}{n} - \frac{1}{\gamma}\right) \quad , \qquad \text{(III.3-44)}$$

where γ is the isentropic coefficient, the final form of G^2_{CRIT} becomes

$$G^2_{CRIT} = \left[\frac{x_o v_g}{np} + (v_g - v_{\ell o})\left\{\left[\frac{(1 - x_o)N}{s_{gs} - s_{\ell s}}\right]\frac{ds_{\ell s}}{dp}\right.\right. \qquad \text{(III.3-45)}$$

$$\left.\left. - \frac{x_o C_{pg}(1/n - 1/\gamma)}{p(s_{go} - s_{\ell o})}\right\}\right]^{-1}_t .$$

Henry and Fauske then relate the throat conditions to the stagnation conditions via the mixture momentum equation

$$\frac{d}{dz}\left(\frac{v^2}{2}\right) + [(1 - x_o)\, v_{\ell o} + x_o\, v_g]\frac{dp}{dz} = 0 \quad . \qquad \text{(III.3-46)}$$

Equation III.3-41 is integrated between the stagnation and total (throat) conditions to give

$$(1 - x_o)\, v_{\ell o}\,(P_o - p_t) + \frac{x_o \gamma}{\gamma - 1}\,[P_o v_{go} - p_t v_{gt}] \qquad \text{(III.3-47)}$$

$$= \frac{[(1 - x_o)v_{\ell o} + x_o v_{gt}]^2}{2}\; G^2_{CRIT}$$

where P_o is the stagnation pressure.

Equations III.3-45 and III.3-47 constitute the basic equations programmed and used to generate the choking tables in RETRAN. For given x_o and P_o, Equations

III.3-45 and III.3-47 must be solved iteratively to yield G_{CRIT}. A plot of the Henry-Fauske Tables is shown in Figure III.3-1 for the two-phase region. The check for choking is performed using Equation III.3-1 to calculate W_{CRIT}^{HENRY}, that is,

$$W_{CRIT}^{HENRY} = C_j A_j(t) G_{CRIT}^{HENRY} (h_i, p_i). \qquad \text{(III.3-48)}$$

If the explicit predicted flow given by Equation III.3-17 is greater than or equal to W_{CRIT}^{HENRY}, the friction coefficient is then readjusted in order to make $\Delta W_j^n = 0$.

3.3 Moody Choking

The Moody choking option is based on the theory developed by Moody.[III.3-6] The assumptions of the Moody critical flow model are the same as those of the HEM except that the two phases are permitted to travel at different velocities. By combining the total energy equation and the continuity equation for two-phase flow, the mass flow rate can be expressed as:

$$G = H \left\{ \frac{2(h_o - h_{\ell s} - x_e h_{fg})}{[H(1-x_e)v_\ell + x_e v_g]^2 [(H^2-1)x_e + 1]} \right\}^{1/2} . \qquad \text{(III.3-49)}$$

The critical flow rate is given by applying the criteria for a maximum:

$$(\partial g/\partial H)_p = 0 \qquad \text{(III.3-50)}$$

$$(\partial g/\partial p)_H = 0 . \qquad \text{(III.3-51)}$$

Application of Equation III.3-50 to Equation III.3-49 leads to

$$H = (v_g/v_f)^{1/3} . \qquad \text{(III.3-52)}$$

The maximum flow rate is found numerically by incorporating Equation III.3-52 into Equation III.3-49 and searching for the pressure which minimizes the resulting expression for given stagnation enthalpy, h_o, and pressure, P_o. This procedure was done for RETRAN and the results incorporated as a table. Figure

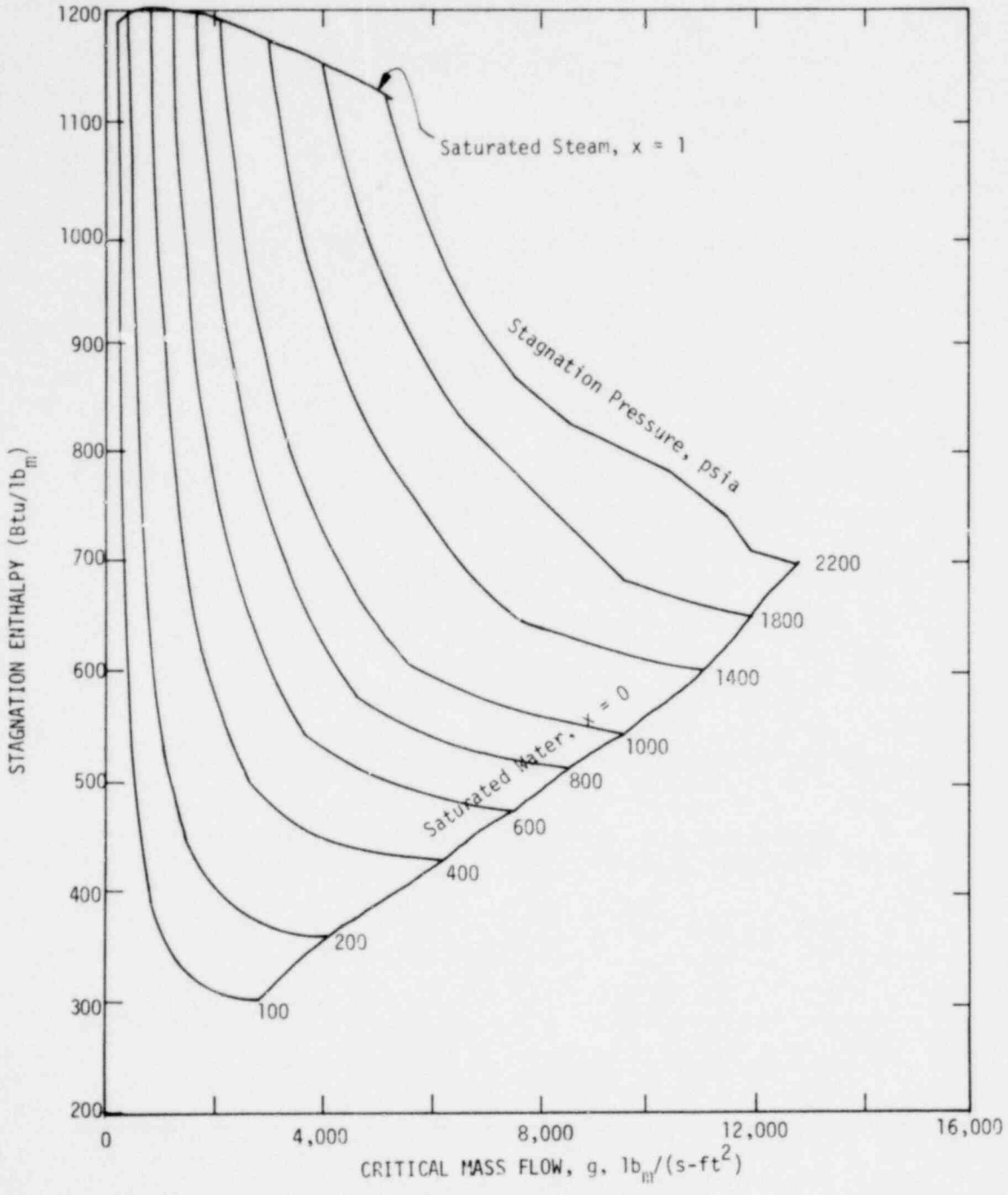

Figure III.3-1 Henry-Fauske Critical Flow Chart, Two-Phase Region

1356 173

III.3-2 is a plot of that table. The logic and check for choking is the same as for the Henry-Fauske and sonic critical flow model.

3.4 Range of Applicability for Critical Flow Correlations

The following section presents the range of applicability for sonic, Henry-Fauske and Moody choking.

3.4.1 Sonic

The sonic choking option is not a correlation in the sense that it was derived from data. It is a non-empirical expression. The major restriction to application is that it must be assumed that the phases are in complete thermal and mechanical equilibrium; that is, the phases move at the same velocity and exist at the same temperature. The expression for the critical sonic mass flux is

$$G_{CRIT}^{SONIC} = \frac{(h_g - h_\ell)}{(v_g - v_\ell)\sqrt{C_v}} \qquad \text{(III.3-53)}$$

3.4.2 Henry-Fauske

The Henry-Fauske model of critical flow is a semi-empirical modification of the sonic choking model. The value is given implicitly by the two equations

$$G_{CRIT}^2 = \left[\frac{x_o v_g}{nP} + (v_g - v_{\ell o})\left\{\frac{(1 - x_o)N}{s_{gs} - s_{\ell s}}\frac{ds_{\ell s}}{dp} - \frac{x_o C_{pg}(1/n - 1/\gamma)}{p(s_{go} - s_{\ell o})}\right\}\right]_t^{-1} \qquad \text{(III.3-54)}$$

and

$$(1 - x_o)\ v_{\ell o}\ (P_o - p_t) + \frac{x_o \gamma}{\gamma - 1}\left[P_o\ v_{go} - p_t\ v_{gt}\right] \qquad \text{(III.3-55)}$$

$$= \frac{\left[(1 - x_o)\ v_{\ell o} + x_o\ v_{gt}\right]^2}{2}\ G_{CRIT}^2$$

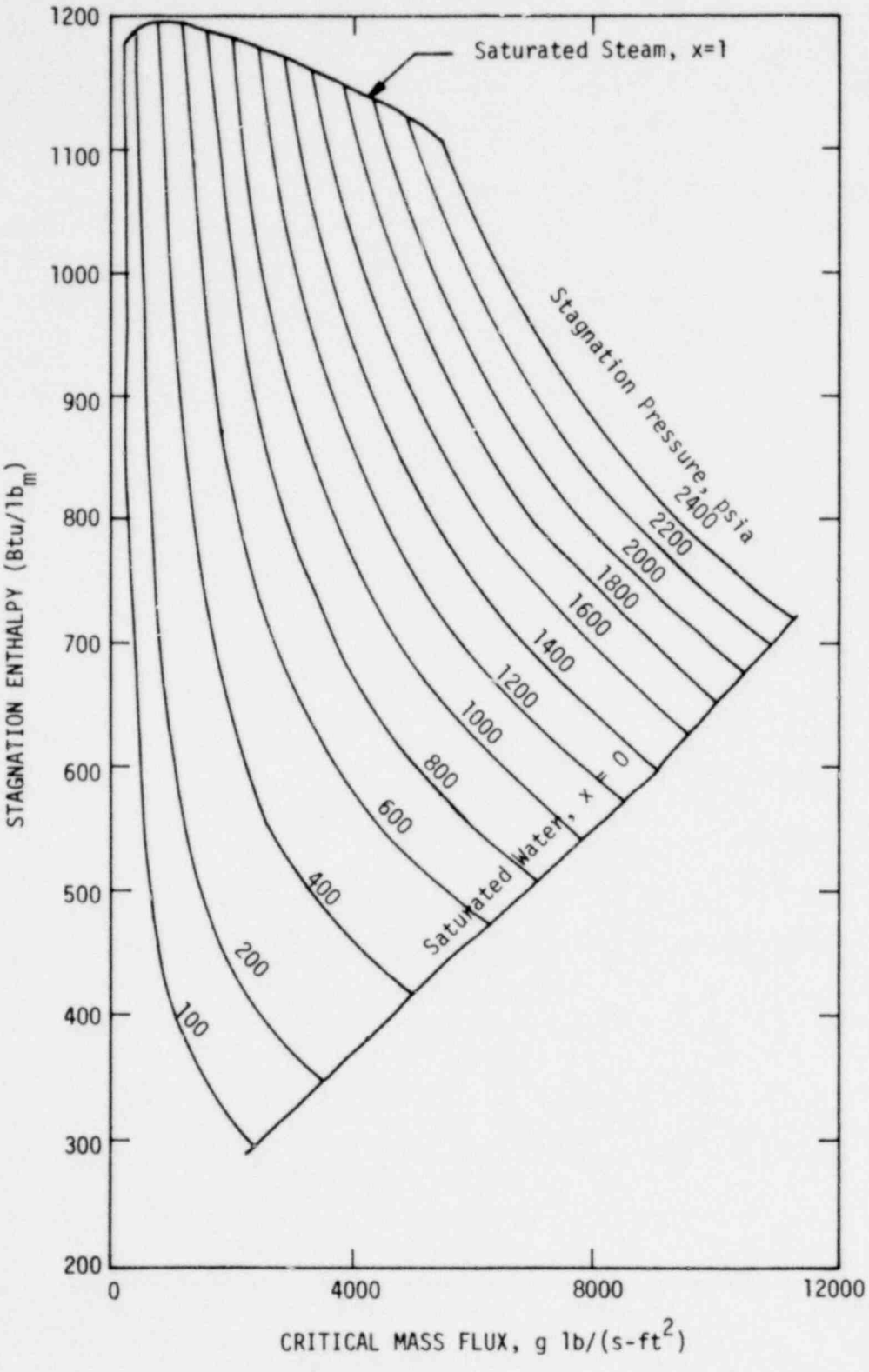

Figure III.3-2 Moody Critical Flow Chart

1356 175

where

$$N = x_\ell / 0.14 \qquad x_e < 0.14$$

$$N = 1.0 \qquad x_e > 0.14$$

The Henry-Fauske model[III.3-3] compared well with two-phase steam-water critical flow data over the range:

Pressure: 17.6 - 882 psia

Quality: 10^{-3} - 1.0

and with saturated and subcooled water over the range:

Saturated Water: Pressure: 50-200 psia

Subcooled Water: Pressure: 50-200 psia
Temperature: 250-350°F .

3.4.3 Moody

The Moody model is the only option which allows for relative motion between phases. The sonic and Henry-Fauske models require that the slip ratio, H, equals one. The Moody model can be considered as an extension of the sonic model to allow for slip between the phases and is not empirical.

The model consists of the expressions

$$G = H \left\{ \frac{2(h_o - h_{\ell s} - x_e h_{fg})}{[H(1 - x_e)v_\ell + x_e v_g]^2 [H^2 - 1) x_e + 1]} \right\}^{1/2}, \qquad \text{(III.3-56)}$$

1356 176

where the slip ratio, H, is obtained from

$$H = (v_g/v_\ell)^{1/3}. \qquad \text{(III.3-57)}$$

The maximum flow rate is found numerically by searching for the pressure which maximizes Equation III.3-56 for given stagnation enthalpy, h_o, and pressure, p_o.

Moody[III.3-6] compared his results favorably with steam-water data over the range

Quality: 0.01 - 1.0

Pressure: 14.7 - 400 psia.

IV. HEAT CONDUCTION

Problems in engineering and physics often require the transport of energy through solids. For many such cases, heat energy is transported via the thermal conduction process. The solution to such problems for homogeneous, isotopic materials and regular geometry is well known.[IV-1,IV-2] As the problems become more complex, so also do the solutions and when temperature dependent properties are considered, analytical solutions do not exist and numerical techniques must be used. The equations for heat flow are developed for the general case and approximations or restrictions introduced as necessary.

1.0 HEAT CONDUCTION EQUATIONS

Consider a solid body where the temperature, at a point (x,y,z) at an instant in time, is specified by some continuous function T(x,y,z,t). If various parts of the body have different temperatures, i.e., T(x,y,z,t) is not a constant, heat will flow from the hotter regions to cooler regions. Near some point m(x,y,z) within the body, assume there exists a surface S consisting of small elements of area ΔS. Then it is assumed in the theory of heat flow that the amount of heat ΔQ passing through the element of surface ΔS in the time Δt is proportional to $\Delta S \Delta t$ and the normal derivative of temperature $\partial T/\partial \tilde{n}$, where $\tilde{n}$ is normal to the element of surface ΔS and in the direction of decreasing temperature. The proportionality factor is the thermal conductivity k(x,y,z). Thus, for isotropic materials (where k does not depend upon $\tilde{n}$)

$$\Delta Q(x,y,z,t) = -k(x,y,z)\ \Delta t\ \Delta S\ \frac{\partial T(x,y,z,t)}{\partial \tilde{n}} \quad . \qquad \text{(IV.1-1)}$$

Fourier's law is a statement of Equation IV.1-1 for the amount of heat passing through unit area of the surface in unit time.

$$q(x,y,z,t) = -k(x,y,z)\ \frac{\partial T(x,y,z,t)}{\partial n} \quad . \qquad \text{(IV.1-2)}$$

The heat flow equation is derived by considering the variation of the quantity of heat in an arbitrary volume V bounded by a smooth closed surface S during a time interval Δt. The time rate of change of the heat content within the volume

is equal to the difference in amount produced within the volume and the amount flowing through the bounding surface. The resulting equation is given by

$$\rho C_p \frac{\partial T}{\partial t} = \vec{\nabla} \cdot (k \vec{\nabla} T) + Q \qquad \text{(IV.1-3)}$$

where

C_p = specific heat of the material or amount of heat required to change a unit mass by one degree in temperature

ρ = material density

k = thermal conductivity

Q = heat source density or amount of heat absorbed or released per unit volume per unit time.

T = temperature

t = time

The quantities C_p, ρ, and k may be a function of the temperature T as well as the space variables.

Acceptable boundary conditions for Equation IV.1-3 include the function T specified on the bounding surface, the normal derivative of T, specified on the bounding surface, or a combination of both.

For heat flow problems in RETRAN, Equation IV.1-3 is used in its one-dimensional form given by

$$\rho C_p \frac{\partial T(x,t)}{\partial t} = \frac{\partial}{\partial x} \left[k(x,T) \frac{\partial T(x,t)}{\partial x} \right] + Q(x,t). \qquad \text{(IV.1-4)}$$

The boundary conditions are a combination of surface temperature and heat flux specified at the surface. In almost all cases the surface is either insulated, an axis of symmetry, or a heat transfer surface to a fluid. Initial conditions for the time dependent problems are obtained by solving the steady-state form of Equation IV.1-4.

V. POWER GENERATION

The primary energy source in the RETRAN code is from fissions in reactor fuel. A secondary energy source is the metal-water reaction between the fuel element cladding and steam if cladding temperatures exceed the reaction threshold.

Fission power in the program is calculated during the course of a problem within the approximations of the point kinetics model for the neutronic or prompt component. The reactivity for each time step may include control rod motions and feedback effects from moderator and fuel. The fission power component arising from decay of fission products may be tracked separately. Following shutdown of the neutronic component of fission power, the decay power follows the ANS standard decay curve.[V-1]

1.0 REACTOR KINETICS EQUATIONS

The neutron kinetics model, commonly known as point kinetics or space independent reactor kinetics, is founded in and derives its justification from time dependent transport theory. The governing equations are

$$\frac{1}{v(u)} \frac{\partial \phi(\bar{r},u,\bar{\Omega},t)}{\partial t} = S(\bar{r},u,\bar{\Omega},t)$$

$$+ \int_{u'} du' \int_{\bar{\Omega}'} d\bar{\Omega}' \, \Sigma_s (\bar{r},u',t) \frac{h_s}{2} (u,\mu_o|u',\bar{\Omega}')\phi(\bar{r},u',\bar{\Omega}',t) \qquad (V.1\text{-}1)$$

$$+ \int_{u'} du' \int_{\bar{\Omega}'} d\bar{\Omega}' \, \frac{h_p(u)}{4\pi} \, (u')(1 - \beta) \, \Sigma_f (\bar{r},u',t)\phi(\bar{r},u',\bar{\Omega},t)$$

$$+ \Sigma_i \lambda_i \frac{h_i(u)}{4\pi} C_i(\bar{r},t) - \Sigma_t (\bar{r},u,t)\phi(\bar{r},u,\bar{\Omega},t) - \bar{\Omega}\cdot\bar{\nabla}\phi(\bar{r},u,\bar{\Omega},t)$$

and

$$\frac{\partial C_i(\bar{r},t)}{\partial t} = \int_{u'} du' \int_{\bar{\Omega}'} d\bar{\Omega}' \, \Sigma_f(\bar{r},u',t)\,(u')\beta_i \phi(\bar{r},u',\bar{\Omega}t) - \lambda_i C_i(\bar{r},t) \qquad \text{(V.1-2)}$$

where

$\bar{r}$ = spatial coordinate

u = lethargy coordinate

$\bar{\Omega}$ = angular coordinate

$\hat{\Omega}$ = unit vector in direction Ω

t = time

$\phi(\bar{r},u,\bar{\Omega},t)$ = neutron flux

$v(u)$ = neutron velocity

$S(\bar{r},u,\bar{\Omega},t)$ = explicit source

$\Sigma_s(\bar{r},u,t)$ = macroscopic scattering cross section

$h_s d\mu_o du$ = probability that a neutron with coordinates $u',\bar{\Omega}'$ will scatter into the ring of width $d\mu_o$ centered about $\bar{\Omega}'$ and at angle μ_o with lethargy du about u.

$h_p(u)$ = prompt fission spectrum

$\nu(u)$ = neutrons per fission

β = $\Sigma_i \beta_i$ fraction of fission neutrons produced as delayed neutrons

$\Sigma_f(\bar{r},u,t)$ = macroscopic fission cross section

λ_i = decay constant of i-th delayed neutron precursor

$h_i(u)$ = $\delta(u-u_i)$ delayed neutron spectrum

$C_i(\bar{r},t)$ = precursor concentration of i-th delayed neutron group

$\Sigma_t(\bar{r},u,t)$ = total macroscopic cross section

β_i = fraction of neutrons from fission produced by i-th precursor.

The transport equation is reduced to the point reactor kinetics equations following Henry[V.1-1] by the use of perturbation weighting functions. The particular weighting function chosen is the adjoint function of the critical system corresponding to the one of interest. In a critical system the value of the precursor concentration is given by

$$\lambda_i C_{ic}(\bar{r}) = \int_{u'} du' \int_{\bar{\Omega}'} d\bar{\Omega}' \, \Sigma_{fc}(\bar{r},u') \nu_c(u') \beta_i \phi_c(\bar{r},u',\bar{\Omega}') \qquad (V.1\text{-}3)$$

where the subscript c denotes critical values of the variables. The time independent source free adjoint equation is given by

$$\int_{u'} du' \int_{\bar{\Omega}'} d\bar{\Omega}' \, \Sigma_{sc}(\bar{r},u) \frac{h_{sc}}{2}(u',\mu_o|u,\bar{\Omega}) \phi_c^*(\bar{r},u',\bar{\Omega}')$$

$$+ \int_{u'} du' \int_{\bar{\Omega}'} d\bar{\Omega}' \frac{h_t(u')}{4} \nu_c(u) \Sigma_{fc}(\bar{r},u) \phi_c^*(\bar{r},u',\bar{\Omega}') \qquad (V.1\text{-}4)$$

$$- \Sigma_{tc}(\bar{r},u)\phi_c^*(\bar{r},u,\bar{\Omega}) + \bar{\Omega}\cdot\bar{\nabla}\phi_c^*(\bar{r},u,\bar{\Omega}) = 0$$

where the total fission spectrum is

$$h_t(u) = (1-\beta)\, h_p(u) + \Sigma_i \beta_i h_i(u)$$

A key assumption in the derivation is that the neutron flux may be written as separable functions: one describing the gross time behavior of the system and the second representing the time dependent shape of the flux. Thus, let

$$\phi(\bar{r},u,\bar{\Omega},t) = \Phi(\bar{r},u,\bar{\Omega},t)\ T(t) \qquad \text{(V.1-5)}$$

where

T(t) represents the gross time behavior,

and

$\Phi(\bar{r},u,\bar{\Omega},t)$ is a time dependent shape function.

The spatial, energy, and angular dependence is eliminated by integration over these variables. Thus, multiply Equation V.1-1 by $\phi_c^*(\bar{r},u,\bar{\Omega})$ and Equation V.1-4 by $\Phi(\bar{r},u,\bar{\Omega},t)T(t)$ and integrate over all $(\bar{r},u,\bar{\Omega})$. The resulting equations are subtracted.

Finally, multiply Equation V.1-3 by $\phi_c^*(\bar{r},u,\bar{\Omega})\ \frac{h_i(u)}{4}$ and integrate over all $(\bar{r},u,\bar{\Omega})$. The following quantities are used to obtain the point kinetic equations.

$$F(t) = \int du \int d\bar{\Omega} \int d^3r \int du' \int d\bar{\Omega}'\ \frac{h_t(u)}{4\pi}\ \Sigma_f(\bar{r},u',t)\nu(u')\phi_c^*(\bar{r},u,\bar{\Omega})\phi(\bar{r},u',\bar{\Omega},t) \qquad \text{(V.1-6)}$$

Prompt Neutron Generation time, $\Lambda(t)$

$$\Lambda(t) = \frac{1}{F(t)} \int du \int d\bar{\Omega} \int d^3r\ \frac{\phi_c^*(\bar{r},u,\bar{\Omega})}{v(u)}\ \Phi(\bar{r},u,\bar{\Omega},t) \qquad \text{(V.1-7)}$$

Effective Delayed Neutron Fraction in Group i, $\bar{\beta}_i(t)$

$$\bar{\beta}_i(t) = \frac{1}{F(t)} \int du \int d\bar{\Omega} \int d^3r \int du' \int d\bar{\Omega}' \quad (u')\beta_i \frac{h_i(u)}{4\pi} \Sigma_f(\bar{r},u',t)\phi_c^*(\bar{r},u,\Omega)\Phi(\bar{r},u',\bar{\Omega}',t) \tag{V.1-8}$$

Effective Source Strength, Q(t)

$$Q(t) = \frac{1}{\Lambda(t)F(t)} \int du \int d\bar{\Omega} \int d^3r \; \phi_c^*(\bar{r},u,\bar{\Omega})S(\bar{r},u,\bar{\Omega},t) \tag{V.1-9}$$

Total Effective Delayed Neutron Fraction, $\bar{\beta}(t)$

$$\bar{\beta}(t) = \Sigma_i \overline{\beta_i(t)} = \frac{1}{F(t)} \int du \int d\bar{\Omega} \int d^3r \int du' \int d\bar{\Omega}' \; \{h_t(u) - (1 - \beta)h_p(u)\}^*$$

$$(u')\Sigma_f(\bar{r},u',t)\phi_c^*(\bar{r},u,\bar{\Omega})\Phi(\bar{r},u,\bar{\Omega},t) \tag{V.1-10}$$

Average Delayed Neutron Precursor Density, $\overline{C_i(t)}$

$$\overline{C_i(t)} = \frac{1}{\Lambda(t)F(t)} \int du \int d\bar{\Omega} \int d^3r \; C_i(\bar{r},t)\phi_c^*(\bar{r},u,\bar{\Omega}) \frac{h_i(u)}{4\pi} \tag{V.1-11}$$

Reactivity, $\bar{\rho}(t)$

$$\bar{\rho}(t) = \frac{1}{F(t)} \int du \int d\bar{\Omega} \int d^3r \; [-\phi_c^*(\bar{r},u,\bar{\Omega})\hat{\Omega}\cdot\nabla\Phi(\bar{r},u,\bar{\Omega},t)$$

$$- \phi(\bar{r},u,\bar{\Omega},t)\hat{\Omega}\cdot\nabla\phi_c^*(\bar{r},u,\bar{\Omega}) - \phi_c^*(\bar{r},u,\bar{\Omega})\Phi\{\bar{r},u,\bar{\Omega},t)\{\Sigma_t(\bar{r},u,t) - \Sigma_{tc}(\bar{r},u)\}$$

$$+ \int du' \int d\bar{\Omega}' \phi_c^*(\bar{r},u,\bar{\Omega})\Phi(\bar{r},u',\bar{\Omega}',t)\{\Sigma_s(\bar{r},u',t) \frac{h_s}{2\pi}(u,\mu_o\, u',\bar{\Omega}')$$

$$- \Sigma_{sc}(\bar{r},u') \frac{h_s}{2}(u,\mu_o\, u',\bar{\Omega}') + \frac{h_t(u)}{4\pi}(\nu(u')\Sigma_f(\bar{r},u',t) - \nu_c(u')\Sigma_{fc}(\bar{r},u'))\}] \tag{V.1-12}$$

Using the definitions in Equations V.1-6 through V.1-12 and carrying out the operations described above, the point kinetics equations are given as

$$\Lambda(t)F(t)\frac{dT(t)}{dt} + T(t)\frac{d}{dt}[\Lambda(t)F(t)] + Q(t)\Lambda(t)F(t)$$

$$+ \rho(t)T(t)F(t) - \beta(t)T(t)F(t) + \Sigma_i\lambda_i C_i(t)\Lambda(t)F(t) \qquad \text{(V.1-13a)}$$

and

$$\Lambda(t)F(t)\frac{dC_i(t)}{dt} = \beta_i(t)T(t)F(t) - \lambda_i C_i(t)\Lambda(t)F(t), \qquad \text{(V.1-13b)}$$

where the bars have been dropped from the averaged quantities. Dividing Equation V.1-13 by $\Lambda(t)\,F(t)$, one obtains

$$\frac{dT(t)}{dt} = \left[\frac{\rho(t) - \beta(t)}{\Lambda(t)} - \frac{1}{\Lambda(t)G(t)}\frac{d}{dt}\{\Lambda(t)F(t)\}\right] T(t) + \Sigma_i\lambda_i C_i(t) + Q(t)$$

and

$$\frac{dC_i(t)}{dt} = \frac{\beta_i(t)}{\Lambda(t)}T(t) - \lambda_i C_i(t) \quad . \qquad \text{(V.1-14)}$$

Additional assumptions applied to Equation V.1-14 are that flux shape, prompt neutron generation time, delayed neutron fraction, and fission cross section are constant in time. Thus, Λ, F, and β_i are constants. Defining the new variables

$$\ell^* = \frac{\Lambda}{\beta}$$

$R(t) = \frac{\rho(t)}{\beta}$ reactivity in dollars

$n(t) = T(t)$ normalized reactor flux or power level

$S(t) = Q(t)$ explicit neutron source

1356 187

produces the usual space independent reactor kinetics equations given by

$$\frac{dn(t)}{dt} = \frac{R(t) - 1}{\ell^*} n(t) + \Sigma_i \lambda_i C_i(t) + S(t)$$

$$\frac{dC_i(t)}{dt} = \frac{\beta_i n(t)}{\beta \ell^*} - \lambda_i C_i(t) \ . \qquad \text{(V.1-15)}$$

1.1 Fission Heat

Power generation from fission sources may be spatially distributed within the point kinetics approximation. The distribution of the power and also any reactivity feedback effects are fixed during initialization with each node following the same time behavior. The power level is controlled by the reactivity term, R(t), in Equation V.1-15 and scaled by the initial power level.

Contributions to the system reactivity include explicit functions of time which simulate control mechanisms, and feedback reactivity effects from fuel and moderator changes. Spatially dependent reactivity coefficients may be specified for feedback effects. At any time the system reactivity is given by

$$R(t) = R_o + [R(t) - R(0)]_{exp} + \Sigma_i R_i(t) - \Sigma_i R_i(0) \qquad \text{(V.1-16)}$$

where

R_o = initial reactivity (must be zero for steady state)

R_{exp} = explicit reactivity function

R_i = feedback reactivity from i-th spatial node.

Both the explicit reactivity and feedback terms are normalized such that their initial values are zero. Feedback effects considered in RETRAN include moderator density, fuel temperature, and water temperature. The form of the equation for the i-th spatial node is

$$R_i(y) = W_\rho^i R_\rho \left[\frac{\rho^i(t)}{\rho^i(0)} \right] + W_{FT}^i R_{FT}(T_F^i(t) + \alpha_{FT}^i T_F^i(t) + \alpha_{WT}^i T_W^i(t) \quad \text{(V.1-17)}$$

where

W_ρ^i = weighting factor for moderator density reactivity

R_ρ = water density reactivity function

ρ^i = water density in i-th node

W_{FT}^i = weighting factor for fuel temperature reactivity

$R_{FT}(T_F^i)$ = fuel temperature reactivity function

T_F^i = average fuel temperature in i-th node

α_{FT}^i = fuel temperature coefficient of reactivity in i-th node

α_{WT}^i = moderator temperature coefficient of reactivity in i-th node

T_w^i = average water temperature in i-th node.

The reactivity functions and temperature coefficients in Equation V.1-17 are alternate methods of describing the feedback phenomena. Normally only one of the methods is used at a given node.

1.2 Fission Product Decay

Power generation continues in a reactor core after the fission source ceases because of fission product decay. The rate at which this heat source decays varies depending on the operating history of the core. The decay rate becomes slower with increasing exposure due to the buildup of the longer lived fission products. The model for the fission product decay heat in RETRAN is similar in concept to the delayed neutron model. The decay heat source represents the

beta and gamma transitions from excited nuclei formed either as fission products or from (principally) captive reactions. Attempting to account for most decay chains exactly would be impractical if not impossible because of a lack of precise data. It has been found emperically that, within measurement precision, the decay heat source can be fitted to a polynomial of eleven exponentials. The energy release data for infinite operating time have been used in the data fitting. These data have been tabulated as an ANS standard[V.1-2] and are given in Table V.1-1. The data in the table are normalized to unit power level and fitted by a polynomial of eleven exponentials of the form

$$\Gamma_d = \sum_{j=1}^{11} E_j \, e^{-\lambda_j t} \qquad (V.1\text{-}18)$$

where

Γ_d = normalized fission product decay energy

E_j = amplitude of j-th term

λ_j = decay constant of j-th term

t = elapsed time since shutdown.

Equation V.1-18 is constrained by requiring that $\Gamma_d(0) = 0.07$. Functional values from Equation V.1-18 and their percentage error relative to the ANS standard values are given in Table V.1-2.

Although the fission product decay chains are scattered over many nuclides, the form of Equation V.1-18 is the same as assuming eleven decay heat groups which behave as the delayed neutron groups. By defining a "concentration" for each decay heat group and interpreting the E_j's in Equation V.1-18 as yield fractions, the decay heat precursor concentrations can be represented by

$$\frac{d\gamma_j(t)}{dt} + \lambda_j \gamma_j(t) = E_j \, n(t) \qquad (V.1\text{-}19)$$

TABLE V.1-1

RADIOACTIVE DECAY CONSTANTS

Group	E_j	$\lambda_j (sec^{-1})$
1	0.00299	1.772
2	0.00825	0.5774
3	0.01550	6.743×10^{-2}
4	0.01935	6.214×10^{-3}
5	0.01165	4.739×10^{-4}
6	0.00645	4.810×10^{-5}
7	0.00231	5.344×10^{-6}
8	0.00164	5.726×10^{-7}
9	0.00085	1.036×10^{-7}
10	0.00043	2.959×10^{-8}
11	0.00057	7.585×10^{-10}

TABLE V.1-2

COMPARISON OF RETRAN AND ANS STANDARD DECAY HEAT CALCULATED RESULTS

Time (sec)	PETRAN	ANS STD	% Error
0.0000E+00	0.069900	---	0.0000
1.0000E-01	0.068900	0.067500	2.0741
1.0000E+00	0.062800	0.062500	0.4800
2.0000E+00	0.059200	0.059000	0.3390
4.0000E+00	0.055400	0.055200	0.3623
6.0000E+00	0.053100	0.053300	-0.3752
8.0000E+00	0.051400	0.051200	0.3906
1.0000E+01	0.049900	0.050000	-0.2000
2.0000E+01	0.044900	0.045000	-0.2222
4.0000E+01	0.039800	0.039600	0.5051
6.0000E+01	0.037200	0.036500	1.9178
8.0000E+01	0.035300	0.034600	2.0231
1.0000E+02	0.033700	0.033100	1.8127
2.0000E+02	0.028400	0.027500	3.2727
4.0000E+02	0.023400	0.023500	-0.4255
6.0000E+02	0.021300	0.021100	0.9479
8.0000E+02	0.020100	0.019600	2.5510
1.0000E+03	0.019200	0.018500	3.7838
2.0000E+03	0.016100	0.015700	2.5478
4.0000E+03	0.012800	0.012800	0.0000
6.0000E+03	0.011200	0.011200	0.0000
8.0000E+03	0.010300	0.010500	-1.9048
1.0000E+04	0.009760	0.009650	1.1399
2.0000E+04	0.008010	0.007950	0.7547
4.0000E+04	0.006260	0.006250	0.1600
6.0000E+04	0.005460	0.005660	-3.5336
8.0000E+04	0.005050	0.005050	0.0000
1.0000E+05	0.004790	0.004750	0.8421
2.0000E+05	0.004090	0.004000	2.2500
4.0000E+05	0.003390	0.003390	0.0000
6.0000E+05	0.003050	0.003100	-1.6129
8.0000E+05	0.002840	0.002820	0.7092
1.0000E+06	0.002690	0.002670	0.7491
2.0000E+06	0.002190	0.002150	1.8605
4.0000E+06	0.001680	0.001660	1.2048
6.0000E+06	0.001440	0.001430	0.6993
8.0000E+06	0.001290	0.001300	-0.7692
1.0000E+07	0.001190	0.001170	1.7094
2.0000E+07	0.000906	0.000890	1.7978
4.0000E+07	0.000698	0.000680	2.6471
6.0000E+07	0.000619	0.000620	-0.1613
8.0000E+07	0.000577	0.000570	1.2281
1.0000E+08	0.000551	0.000550	0.1818
2.0000E+08	0.000491	0.000485	1.2371
4.0000E+08	0.000421	0.000415	1.4458
6.0000E+08	0.000362	0.000360	0.5556
8.0000E+08	0.000311	0.000303	2.6403
1.0000E+09	0.000267	0.000267	0.0000

where

$\gamma_j(t)$ = concentration of j-th decay heat group

E_j = yield fraction for j-th group

$n(t)$ = normalized reactor power.

Assuming a constant power level, initial values for the γ_j's are obtained from the steady state solution for Equation V.1-18, i.e.,

$$\gamma_{jo} = \frac{E_j}{\lambda_j} \quad . \tag{V.1-20}$$

The total power in the core is then given by

$$P(t) = P_o \left\{ n(t)\, E_f + \sum_{j=1}^{11} \lambda_j \gamma_j \right\} \tag{V.1-21}$$

where

E_f = 0.93 if decay heat is present
= 1.0 otherwise.

1.3 Decay of Actinides

The energy release from fission product decay may be supplemented by including the important radioactive actinides, $^{239}U_{92}$ and $^{239}Np_{93}$, produced by radiative neutron capture in $^{238}U_{92}$. The decay heat contributions from these isotopes are given in the ANS standard[V.1-2] for infinite operating time as

$$\frac{P(^{239}U)}{P_o} = A_1 C \frac{\sigma_{25}}{\sigma_{f25}} e^{-\lambda_1 t} \tag{V.1-22}$$

and

$$\frac{P(^{239}Np)}{P_o} = B_1 C \frac{\sigma_{25}}{\sigma_{f25}}\left[B_2\left(e^{-\lambda_2 t} - e^{-\lambda_1 t}\right) + e^{-\lambda_2 t}\right] \qquad \text{(V.1-23)}$$

where

$\frac{P(^{239}U)}{P_o}$ = normalized decay power from ^{239}U

$\frac{P(^{239}Np)}{P_o}$ = normalized decay power from ^{239}Np

λ_1 = decay constant for ^{239}U

λ_2 = decay constant for ^{239}Np

A_1, B_1, B_2 = constants

C = conversion ratio, atoms of ^{239}Pu produced per atom ^{235}U consumed

σ_{25} = effective absorption cross section of ^{235}U

σ_{f25} = effective fission cross section of ^{235}U.

Constants in Equations V.1-22 and V.1-23 are specified as

$A_1 = 2.23 \times 10^{-3}$

$B_1 = 2.17 \times 10^{-3}$

$B_2 = 7.0 \times 10^{-3}$

$\lambda_1 = 4.91 \times 10^{-4}\ sec^{-1}$

$\lambda_2 = 3.41 \times 10^{-6}\ sec^{-1}$.

1356 194

Summing Equations V.1-21 and V.1-22 and defining appropriate E_j's puts them in the same form as Equation V.1-18, i.e.,

$$\Gamma_{act} = \sum_{j=1}^{2} E_{j_{act}} e^{-\lambda_j t} \quad . \qquad \text{(V.1-24)}$$

These may then be included in the decay heat calculations, Equations V.1-19 and V.1-21.

2.0 METAL-WATER REACTION

A subroutine provided in RETRAN calculates the amount of heat generated when the fuel rod cladding temperature and steam conditions are appropriate for the occurrence of an exothermic metal-water reaction. The reaction calculated is the reaction between zirconium and steam and is expressed as

$$Zr + 2\ H_2O \rightarrow ZrO_2 + 2\ H_2 \quad .$$

When sufficient steam is available, the rate of this reaction is assumed to follow the parabolic rate law of Baker and Just.[V.2-1] When less steam is available than would be consumed by a reaction following the parabolic rate law, a steam-limited rate law is assumed in which all available steam reacts. Equation V.2-1 is a mathematical statement of the parabolic rate law:

$$-\frac{dr}{dt} = \left(\frac{0.0615}{RO - r}\right) \exp\left(-\frac{41200}{T}\right) \qquad (V.2\text{-}1)$$

where

r = radius of the reacting metal-oxide interface, in.

RO = initial rod radius, in.

T = absolute temperature at the reacting metal-oxide interface, °R

t = time, sec.

Integration of Equation V.2-1 over a time step gives

$$-\int_{r1}^{r_2} (RO - r)\, dr = \int_{t1}^{t_2} 0.0615 \exp\left(-\frac{41200}{T}\right) dt. \qquad (V.2\text{-}2)$$

If the expression, $0.0615 \exp\left(-\frac{41200}{T}\right)$, is assumed to be constant during the time step, then

$$-\int_{r_1}^{r_2} (RO - r)\, dr = 0.0615 \exp\left(-\frac{41200}{T}\right) \Delta t \qquad (V.2\text{-}3)$$

where $\Delta t = t_2 - t_1$ is the time-step size in seconds. A new variable $r' = RO - r$ and its differential $dr' = dr$ are substituted into Equation V.2-3 to obtain

$$\int_{DRP}^{DRP1} r'dr' = 0.0615 \exp\left(-\frac{41200}{T}\right) \Delta t \qquad (V.2\text{-}4)$$

where

DRP1 = the depth the reaction has penetrated the cladding at the end of a time step, in.

DRP = the depth the reaction has penetrated the cladding at the start of a time step, in.

Integration of Equation V.2-4 gives

$$\frac{DRP1^2 - DRP^2}{2} = 0.0615 \exp\left(-\frac{41200}{T}\right) \Delta t \qquad (V.2\text{-}5)$$

which reduces to

$$DRP1^2 - DRP^2 = 0.123 \exp\left(-\frac{41200}{T}\right) \Delta t \qquad (V.2\text{-}6)$$

A new variable is defined as

$$AP = DRP1^2 - DRP^2 = 0.123 \exp\left(-\frac{41200}{T}\right) \Delta t \qquad (V.2\text{-}7)$$

Solving for the unknown DRP1 in terms of DRP and AP gives

$$DRP1 = (DRP^2 + AP)^{1/2} \quad . \qquad (V.2\text{-}8)$$

The mass of zirconium reacted per unit length during the time step is

$$MZR = \pi \rho_{zr} [(RO - DRP)^2 - (RO - DRP1)^2] \qquad (V.2\text{-}9)$$

where

ρ_{zr} = the density of zirconium (0.231 $lb_m/in.^3$)

$$MZR = \pi \rho_{zr}[RO^2 - 2\ RO\ (DRP) + DRP^2 - RO^2 + 2\ RO\ (DRP1) - DRP1^2]$$

$$= \pi \rho_{zr}[2\ RO\ (DRP1 - DRP) - (DRP1^2 - DRP^2)]$$

$$= \pi \rho_{zr}[2\ RO\ (DRP1 - DRP) - AP] \quad . \qquad (V.2\text{-}10)$$

The heat of reaction is approximately 2800 Btu per pound of zirconium reacted. Therefore,

$$QMWR = \frac{2800\ MZR}{\Delta t} \qquad (V.2\text{-}11)$$

where QMWR = a heat rate of Btu per second per inch length of rod. The stoichiometric mass of steam required for the parabolic rate law to apply is

$$MSR = 0.395\ MZR \quad . \qquad (V.2\text{-}12)$$

If the amount of steam (MSR) is greater than the amount of steam available (MSTA) (steam limited condition), all available steam is assumed to react. Consequently,

$$MZR = \frac{MSTA}{0.395} \qquad (V.2\text{-}13)$$

and the steam-limited reaction heat is computed through use of Equations V.2-11 and V.2-13. The depth the reaction has penetrated the cladding (DRP1) corresponding to the steam-limited condition is computed by rearranging Equation V.2-9 as follows:

$$DRP1 = RO - \left[(RO - DRP)^2 - \frac{MZR}{\pi \rho_{zr}}\right]^{1/2} \quad . \qquad (V.2\text{-}14)$$

The consumption of steam and the evolution of hydrogen during the metal-water reaction are not accounted for in the mass and momentum equations.

3.0 DIRECT MODERATOR HEATING

Direct energy deposition in the moderator is permitted in any core section where a core section is defined as a power generating heat conductor. In RETRAN, a specified fraction of the core power, QFRAC, is allocated to each core section. This concept is extended by specifying that this fraction is further split between the metal and moderator associated with the core section. The actual energy deposition in the moderator is weighted with respect to a function of density so that the moderator fraction should be specified with respect to the initial value of the weighting function.

For each core section, the direct moderator heating may be split between a prompt term and a delay power term. The user specifies the fraction of QFRAC allocated to each term. Thus, if $QPMOD_k$ is the prompt fraction, then $QPMOD_k$*$QFRAC_k$ is the fraction of total power released promptly in the moderator for core section k. Similarly, $QDMOD_k$*$QFRAC_k$ is the fraction of the total delayed power released in the moderator for core section k.

The net direct moderator heating rate for a given core section, k, is defined as the sum of the prompt and delayed power contributions and is given by

$$P_{m_k}(t) = P_0\ QFRAC_k\ f(\rho_k)[QPMOD_k\ n(t)\ E_f + QDMOD_k \sum_{j=1}^{N_1} \lambda_j \gamma_j] \quad (V.3\text{-}1)$$

where the density weighting function $f(\rho_k)$ is defined as

$$f(\rho_k) = \frac{\rho_k(t)}{\rho_k(0)} \quad (V.3\text{-}2)$$

$\rho_k(0)$ = the initial moderator density for core section k

$\rho_k(t)$ = the moderator density for core section k at time t.

An alternate form of the weighting may be used at the user's option, where $f(\rho_k)$ is a user supplied tabular function of the moderator density. The terms used in

Equation V.3-1, but not defined locally, are discussed in detail in Section VI (note the similarity between Equations V.1-21 and V.3-1).

The power generated internal to a core section conductor, or the conductor heating rate, is defined as

$$P_{C_k}(t) = P_0 \, QFRAC_k \, [1 - f(\rho_k) \, QPMOD_k] \, n(t) \, E_f$$

$$+ [1 - f(\rho_k) \, QDMOD_k] \sum_{j=1}^{N} \lambda_j \gamma_j \qquad \text{(V.3-3)}$$

Through use of the direct moderator heating model described above, gamma and neutron heating of structural materials and their associated fluid volumes can be modeled by designating the structure as a core section and providing the appropriate values of QFRAC, QPMOD, QDMOD and $f(\rho_k)$.

VI. SYSTEM COMPONENT MODELS

VI. SYSTEM COMPONENT MODELS

The following sections describe the system component models contained in the RETRAN code package. The system component models include centrifugal pumps, valves, heat exchangers, and trip controls.

1.0 CENTRIFUGAL PUMPS

RETRAN contains a pump model which describes the interaction between a centrifugal pump and the primary system fluid. A standard RETRAN control volume is identified as a pump, with the pump behavior calculated through the use of pump characteristic curves, frequently referred to as four-quadrant curves. Modeling the pump as a volume rather than as a junction, eliminates potential instabilities due to rapidly oscillating flows and radically different thermodynamic states of adjacent control volumes.

The pump characteristic curves are empirically developed by the pump manufacturer and uniquely define head and torque response of the pump as functions of volumetric flow and pump speed. A typical set of four-quadrant curves is given in Figure VI.1-1. The four-quadrant curves can be converted to a simpler form by the development of homologous curves where the head and torque ratios (actual value to rated value) are input as functions of the pump speed and volumetric flow ratios.[VI.1-1] The developed homologous curves are for single-phase conditions. Typical homologous curves are shown in Figure VI.1-2 for the head and Figure VI.1-3 for torque. The nomenclature used in the following figures and pump equations is as follows:

- H = head
- I = moment of inertia
- $M(\alpha)$ = head multiplier
- $N=\omega$ = angular speed
- Δp_p = differential pressure
- Q = volumetric flow
- t = time
- Δt = time step size
- T = torque
- ρ = density

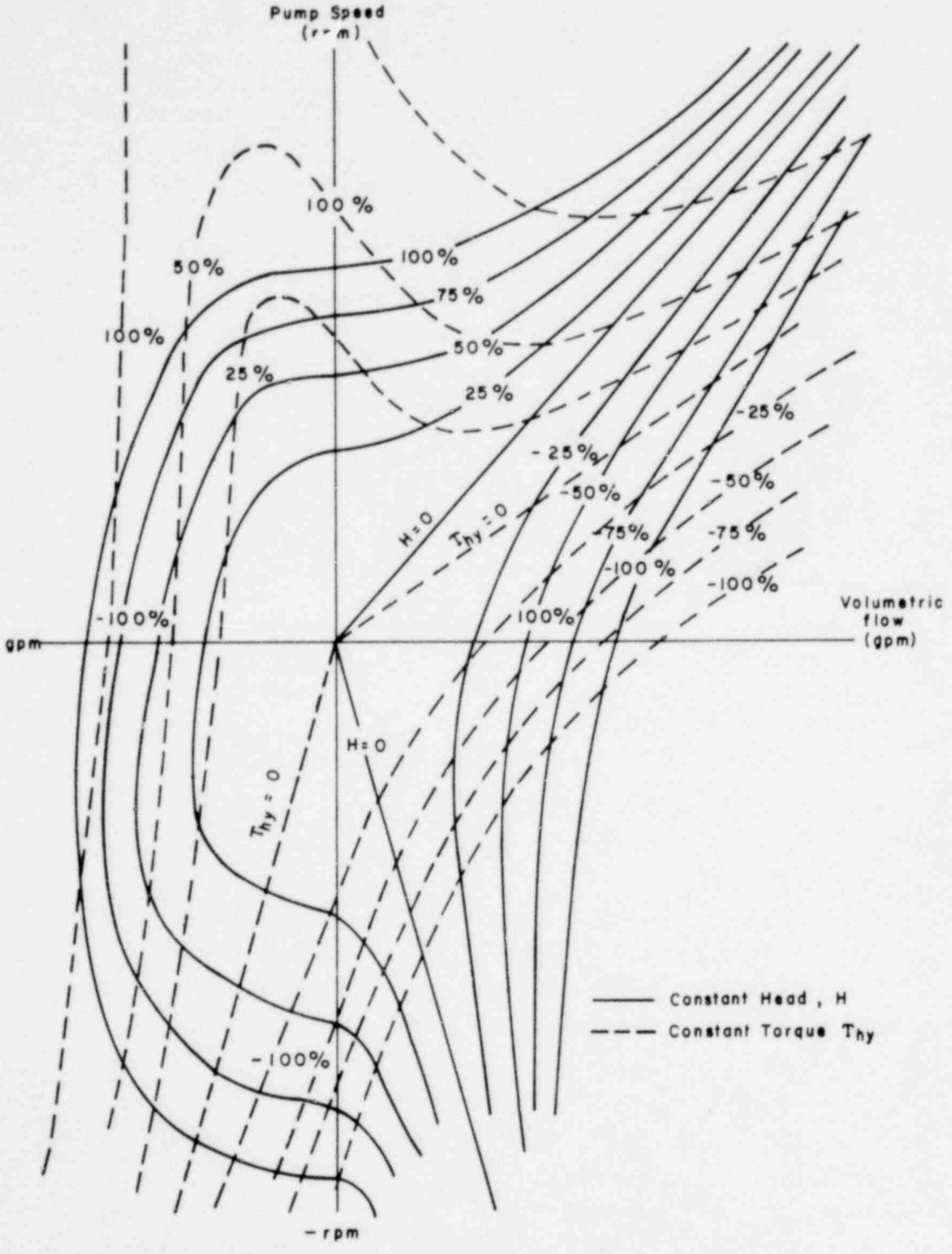

Figure VI.1-1 Four-Quadrant Pump Characteristic Curves

1356 204

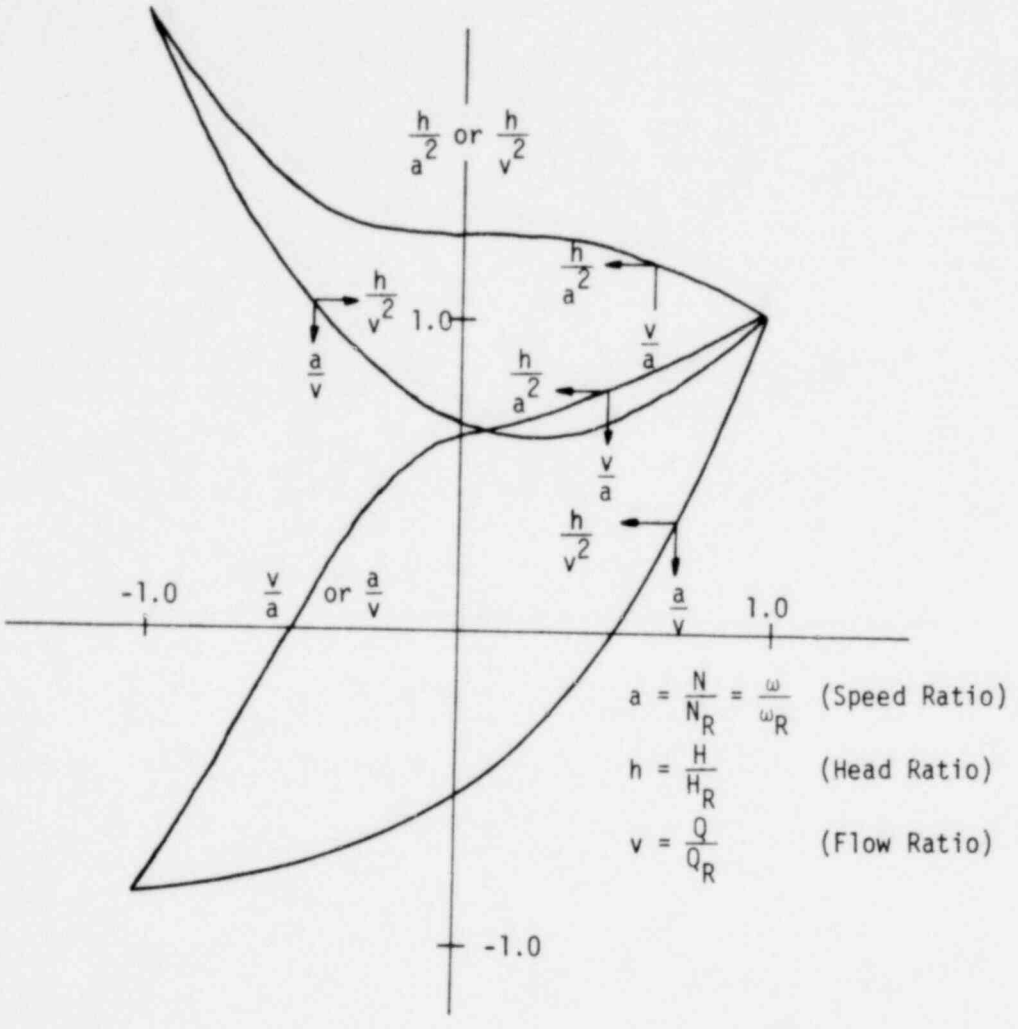

Figure VI.1-2 Homologous Pump Head Curves

1356 205

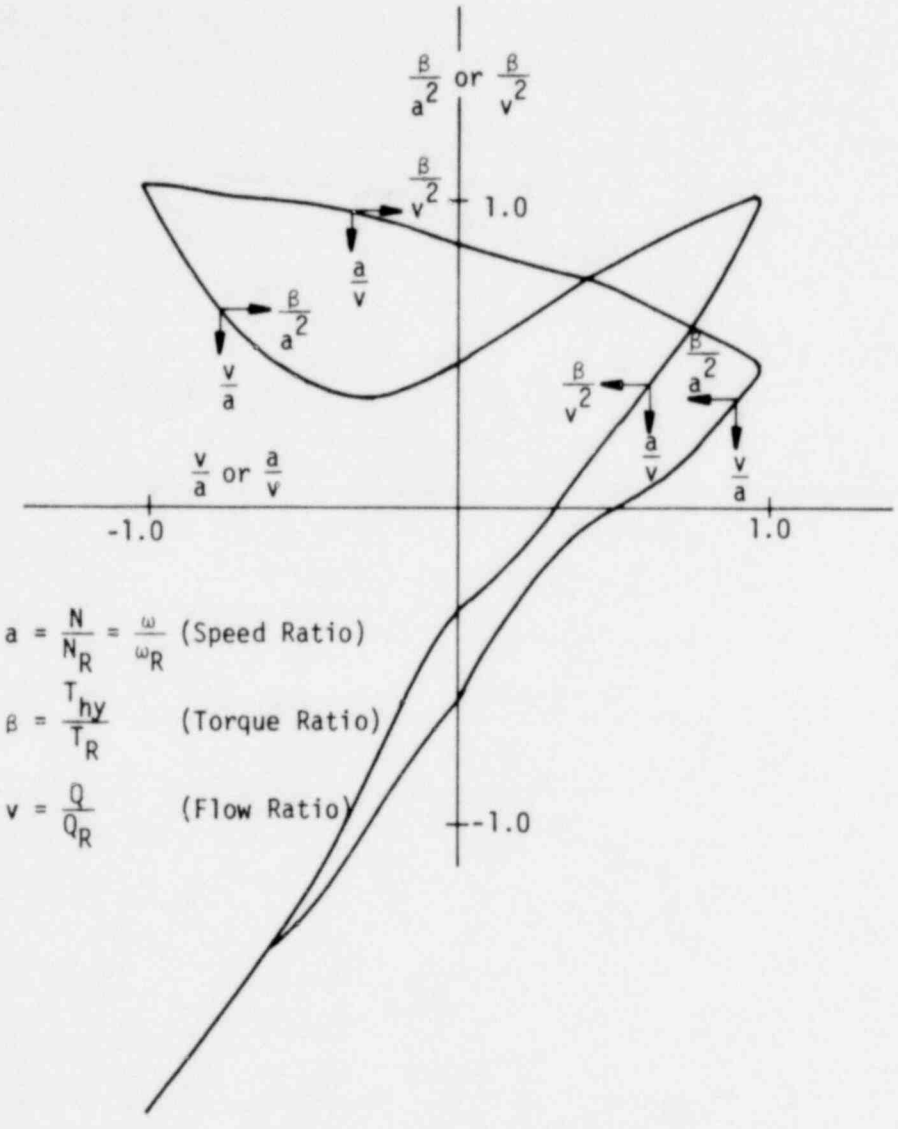

Figure VI.1-3 Homologous Pump Torque Curves

1756 206

subscript 1 = single-phase value
subscript 2 = two-phase value
subscript fr = friction
subscript hy = hydraulic
subscript R_a = rated operating value.

The volume pump model allows the user the option of accounting for cavitation or two-phase degradation effects on pump response. The user must supply a separate set of homologous two-phase curves for head and torque which are in the form of difference curves. Difference curves are used because in the analysis of available two-phase pump data, it was noted that when the fluid being pumped had a void fraction between 0.2 and 0.9, little head was developed by the pump being tested. Outside this range of void fraction, the pump-developed head ranged from zero to undegraded single-phase performance. The limited available data indicate pump performance in the void fraction range 0.2 to 0.9 is significantly degraded from single-phase behavior. To consider the degraded performance, a set of dimensionless homologous curves was fitted to the head data in the fully-degraded void fraction range, and the difference between the undegraded single-phase and the fully degraded two-phase head was expressed as a function of the standard pump model arguments (v/a or a/v).

To consider the ranges of void fraction where the pump was able to develop head (0 to 0.2 and 0.9 to 1.0), a multiplier as a function of void fraction was employed. The two-phase multiplier is a multiplier on the degradation curve where α denotes void fraction and a denotes speed ratio. The multiplier varied from 0 to about 1.0 as the void fraction varied from 0 to 0.2, and the multiplier varied from about 1.0 to 0 as the void fraction varied from 0.9 to 1.0.

There is a limited amount of available two-phase pump data. Pumps tested consist mainly of pumps of low specific speed and small scale pumps. Table VI.1-1 presents the Westinghouse Canada Ltd. (WCL) and Semiscale pump characteristics. Note, the specific speeds are much smaller than those for a reactor primary system pump.

The RETRAN pump model is the same as the pump model presented in the RELAP4 manual[VI.1-2] except that a motor torque option, pump stop option, and dimensionless head ratio difference data have been built into pump curve Set 4 for the two-phase model. These modifications are described in the following sections.

TABLE VI.1-1

PUMP CHARACTERISTICS

Pump	Flow (gpm)	Head (ft)	Speed (rpm)	Specific Speed
WCL	280	500	3560	550
Semiscale	189	192	3560	926

1.1 Two-Phase Flow Effects

Available pump data from the 1-1/2 Loop Model Semiscale and Westinghouse Canada Limited experiments were used in developing the two-phase pump data for RELAP4. This same pump data is used in RETRAN. Assumptions inherent in the pump model for two-phase flow include:

- The head multiplier $M(\alpha)$, that was determined empirically for the normal operating region of the pump, is also valid as an interpolating factor in all other operating regions.

- The relationship of the two-phase to the single-phase behavior of the semiscale pump is applicable to large reactor pumps. This assumes an independent pump specific speed for the pump model for two-phase flow.

The single-phase pump head (dimensionless) curve for the Semiscale pump is shown in Figure VI.1-4.

The two-phase pump head curves shown in Figure VI.1-5 represent complete pump characteristics for the Semiscale pump while operating under two-phase conditions when the average of the void fractions of the pump inlet and outlet mixtures is between 0.2 and 0.9. The lines drawn through the data were determined by least square polynomial fits to the data using known constraints.

A comparison of the two-phase data of Figure VI.1-5 with the single-phase data in Figure VI.1-4 shows that the dimensionless head ratio (h/v^2 or h/a^2) is significantly less than the single-phase dimensionless head ratio for the normal pump operation region (HAN and HVN). For negative ratios of v/a, such as those which occur in the HAD region, the pump flow becomes negative. When the pump flow is negative, the two-phase dimensionless head ratio is greater than the single-phase dimensionless head ratio. Two-phase flow friction losses are generally greater than single-phase losses, and friction is controlling in this energy dissipation region (HAD). The other regions of the two-phase dimensionless head ratio data show similar deviations from single-phase data.

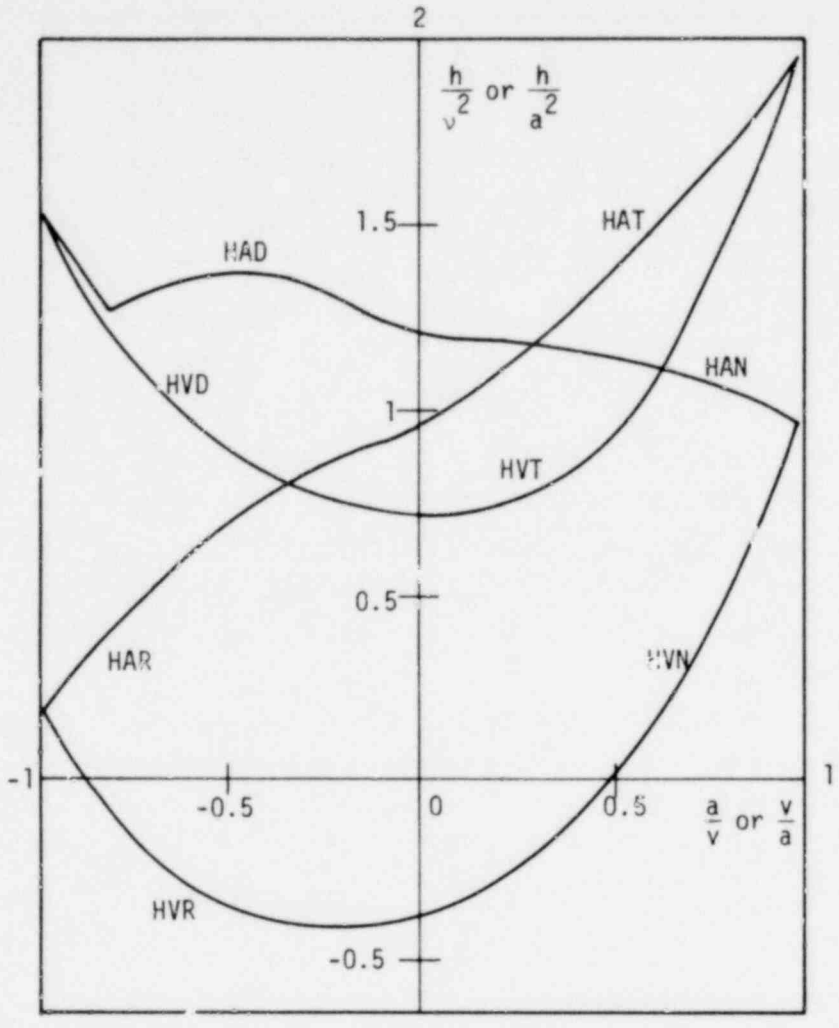

$h = H/H_R$

$\nu = Q/Q_R$

$a = N/N_r = \omega/\omega_R$

Normal Pump	(+Q,+N)	HAN, HVN
Energy Dissipation	(-Q,+N)	HAD, HVD
Normal Turbine	(-Q,-N)	HAT, HVT
Reverse Pump	(+Q,-N)	HAR, HVR

Figure VI.1-4 Single-Phase Head Curves for 1-1/2 Loop MOD-1 Semiscale Pumps

1256 210

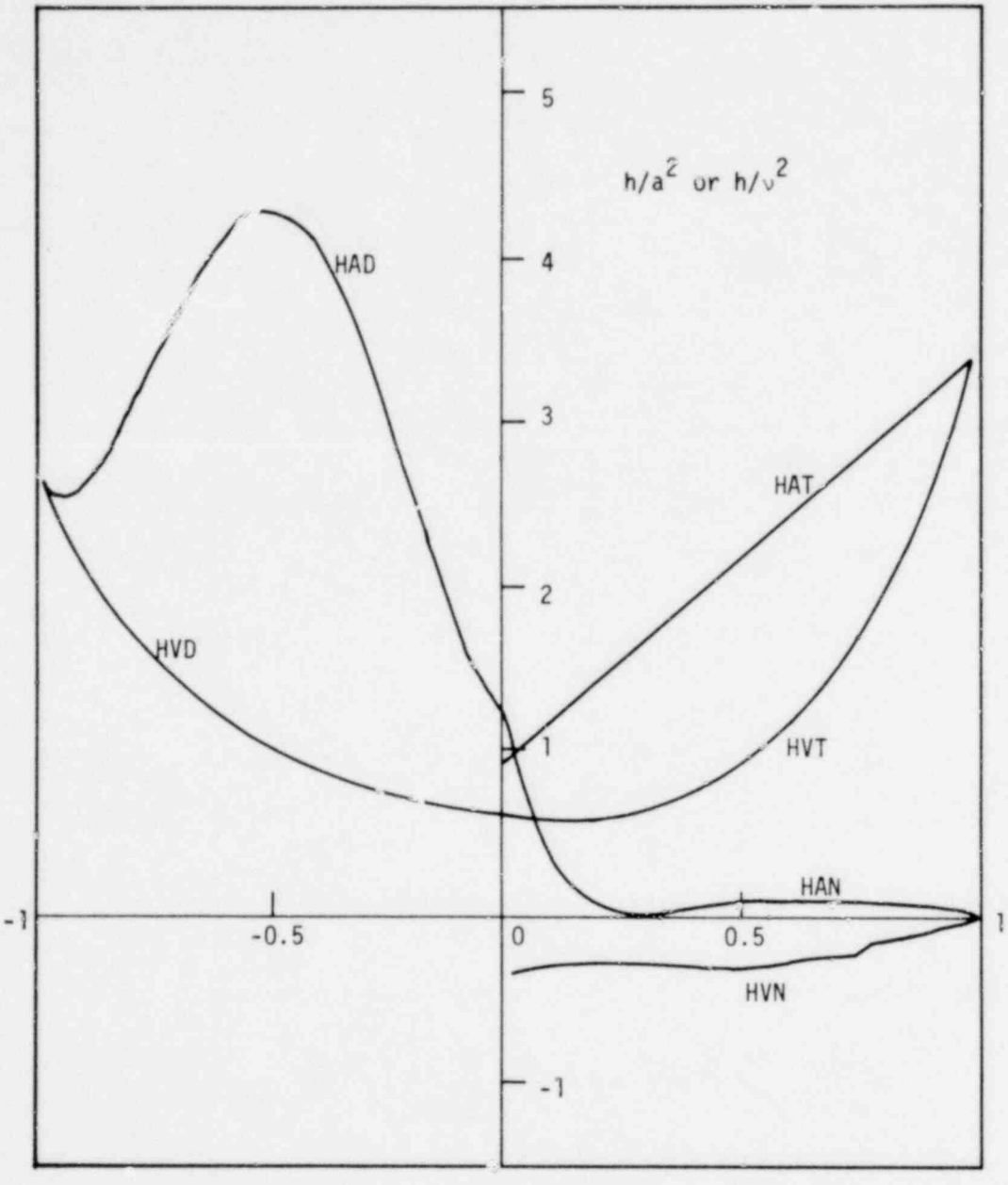

Figure VI.1-5 Two-Phase Homologous Head Curves for 1-1/2 Loop MOD-1 Semiscale Pump

Table VI.1-2 shows the difference between the single-phase and the two-phase dimensionless head ratio data as a function of v/a and a/v for the various pumping regions shown in Figures VI.1-4 and VI.1-5. The differences shown in Table VI.1-2 are for the eight curve types used in RETRAN for determining pump head.

The head multiplier, $M(\alpha)$, and void fraction, α, data shown in Table VI.1-3 were obtained in the following manner. The Semiscale and WCL pump data[VI.1-3] were converted to dimensionless head ratios of h/a^2 or h/v^2. Values of the dimensionless head ratios were obtained for those pump speeds and volumetric flow rates which were within 50% of the rated speed and flow rate for the pumps. The difference between the single-phase and two-phase dimensionless ratios was developed as a function of the average of the void fractions of the pump inlet and outlet mixtures. The difference between the single-phase dimensionless ratios was then normalized to a value between 0 and 1.0 and the normalized result was tabulated as a function of the void fraction.

The two-phase pump model in RETRAN calculates the pump head and torque as follows:

$$H = H_1 - M(\bar{\alpha})\ (H_1 - H_2) \qquad \text{(VI.1-1)}$$

where

$$H_1 - H_2 = \left(\frac{h}{a^2}\Big|_1 - \frac{h}{a^2}\Big|_2\right) a^2\, H_{R_a} \qquad \text{(VI.2-2)}$$

or

$$H_1 - H_2 = \left(\frac{h}{v^2}\Big|_1 - \frac{h}{v^2}\Big|_2\right) v^2\, H_{R_v} \qquad \text{(VI.1-3)}$$

and

$$T = T_1 - M(\bar{\alpha})\ (T_1 - T_2) \qquad \text{(VI.1-4)}$$

1256 212

TABLE VI.1-2

SEMISCALE DIMENSIONLESS HEAD RATIO DIFFERENCE
(SINGLE-PHASE MINUS TWO-PHASE) DATA

$x = v/a$ or a/v

$y = (\frac{h}{a^2})_1 - (\frac{h}{a^2})_2$ or $(\frac{h}{v^2})_1 - (\frac{h}{v^2})_2$

Curve Type	x	y	Curve Type (Continued)	x (Continued)	y (Continued)
1 (HAN)	0.00	0.00	4 (HVD)	-1.00	-1.16
	0.10	0.83		-0.90	-0.78
	0.20	1.09		-0.80	-0.50
	0.50	1.02		-0.70	-0.31
	0.70	1.01		-0.60	-0.17
	0.90	0.94		-0.50	-0.08
	1.00	1.00		-0.35	0.00
				-0.20	0.05
2 (HVN)	0.00	0.00		-0.10	0.08
	0.10	-0.04		0.00	0.11
	0.20	0.00			
	0.30	0.10	5 (HAT)	0.00	0.00
	0.40	0.21		0.20	-0.34
	0.80	0.67		0.40	-0.65
	0.90	0.80		0.60	-0.93
	1.00	1.00		0.80	-1.19
				1.00	-1.47
3 (HAD)	-1.00	-1.16			
	-0.90	-1.24	6 (HVT)	0.00	0.11
	-0.80	-1.77		0.10	0.13
	-0.70	-2.36		0.25	0.15
	-0.60	-2.79		0.40	0.13
	-0.50	-2.91		0.50	0.07
	-0.40	-2.67		0.60	-0.04
	-0.25	-1.69		0.70	-0.23
	-0.10	-0.50		0.80	-0.51
	0.00	0.00		0.90	-0.91
				1.00	-1.47
			7 (HAR)	-1.00	0.00
				0.00	0.00
			8 (HVR)	-1.00	0.00
				0.00	0.00

TABLE VI.1-3

HEAD MULTIPLIER AND VOID FRACTION DATA

α	$M(\alpha)$
0.00	0.00
0.10	0.00
0.15	0.05
0.24	0.80
0.30	0.96
0.40	0.98
0.60	0.97
0.80	0.90
0.90	0.80
0.96	0.50
1.00	0.00

where

a = angular speed ratio

H = head

h/a^2 = dimensionless head ratio

h/v^2 = dimensionless head ratio

$M(\bar{\alpha})$ = head multiplier on difference curve

T = torque

v = volumetric flow ratio

$\bar{\alpha}$ = average volume void fraction

subscript 1 = single-phase value

subscript 2 = two-phase value

subscript R_a = rated operating value.

The differential pressure change, Δp_p, across the pump is dependent upon the head value, H, and the average pump volume density ($\bar{\rho}$). Thus, the pressure change is given by

$$\Delta p_p = \rho H \quad . \tag{VI.1-5}$$

The pump torque is used to calculate pump speed after the pump has shut off. The speed is calculated by the equation

$$I \frac{d\omega}{dt} = T \tag{VI.1-6}$$

or

$$\omega^{(t+\Delta t)} = \omega^{t} - \frac{T\Delta t}{I} \tag{VI.1-7}$$

where

I = moment of inertia

ω = angular speed

T = total torque.

The rate of energy addition to the pump fluid is given by ωT.

The total pump torque is calculated by considering the hydraulic torque from the homologous pump curves and the pump frictional torque. The total torque is given by

$$T = T_{hy} \frac{\rho}{\rho_r} + \sum_{i=1}^{4} (T_{fr})_i \left[\frac{|\omega|}{\omega_{R_a}}\right]^{i-1} \qquad \text{(VI.1-8)}$$

or

$$T = T_{hy} + T_{fr} \qquad \text{(VI.1-9)}$$

where

T_{hy} = hydraulic torque

$(T_{fr})_i$ = i^{th} coefficient of frictional torque.

The frictional torque is in the form of a cubic equation. The value of the frictional torque is also dependent on the sign of the pump speed. An option is available to specify whether or not reverse rotation of the pump is allowed.

The RETRAN pump model has been modified to include the influence of the electric drive motor on the speed behavior of the pump while the motor remains connected to its power source. The effect of the motor is incorporated into the pump model by adding the value of motor torque, T_m, to the torque summation

$$T = - T_{hy} - T_{fr} + T_{m} \quad , \qquad \text{(VI.1-10)}$$

where the sign of the motor torque is opposite to that of the hydraulic and frictional torque for normal operating conditions.

The motors used to drive reactor primary system pumps are induction-type machines. At constant voltage the motor torque is an explicit function of speed. This torque-speed relationship is normally available from the motor manufacturer. Motor torque is supplied to the RETRAN model as a tabular function of torque vs speed as defined by the manufacturer's data. A typical torque-speed curve for an induction motor is shown in Figure VI.1-6.

The capability to simulate a pump with a locked rotor is included in RETRAN. This option provides for simulating the lockup of the pump rotor as a function of input elapsed time, maximum forward speed, or maximum reverse speed. At the time the rotor locks, and at all times thereafter, the pump speed is set equal to zero.

Four sets of single-phase head and torque data may be used as input to RETRAN. The pump model has built-in single-phase pump data for both a Bingham Pump Company pump with a specific speed of 4200 (Curve Set 1) and a Westinghouse Electric Corporation pump with a specific speed of 5200 (Curve Set 2). If the two-phase option is selected, the difference curves are input into Curve Set 4.

Each pump curve set is divided into eight types of input data depending upon the values of the speed ratio (a) and the flow ratio (v). The independent variable is either

$$\frac{h}{a^2}, \frac{\beta}{a^2}, \frac{h}{v^2}, \text{ or } \frac{\beta}{v^2} .$$

The definition of each type of input data is as shown in Table VI.1-4.

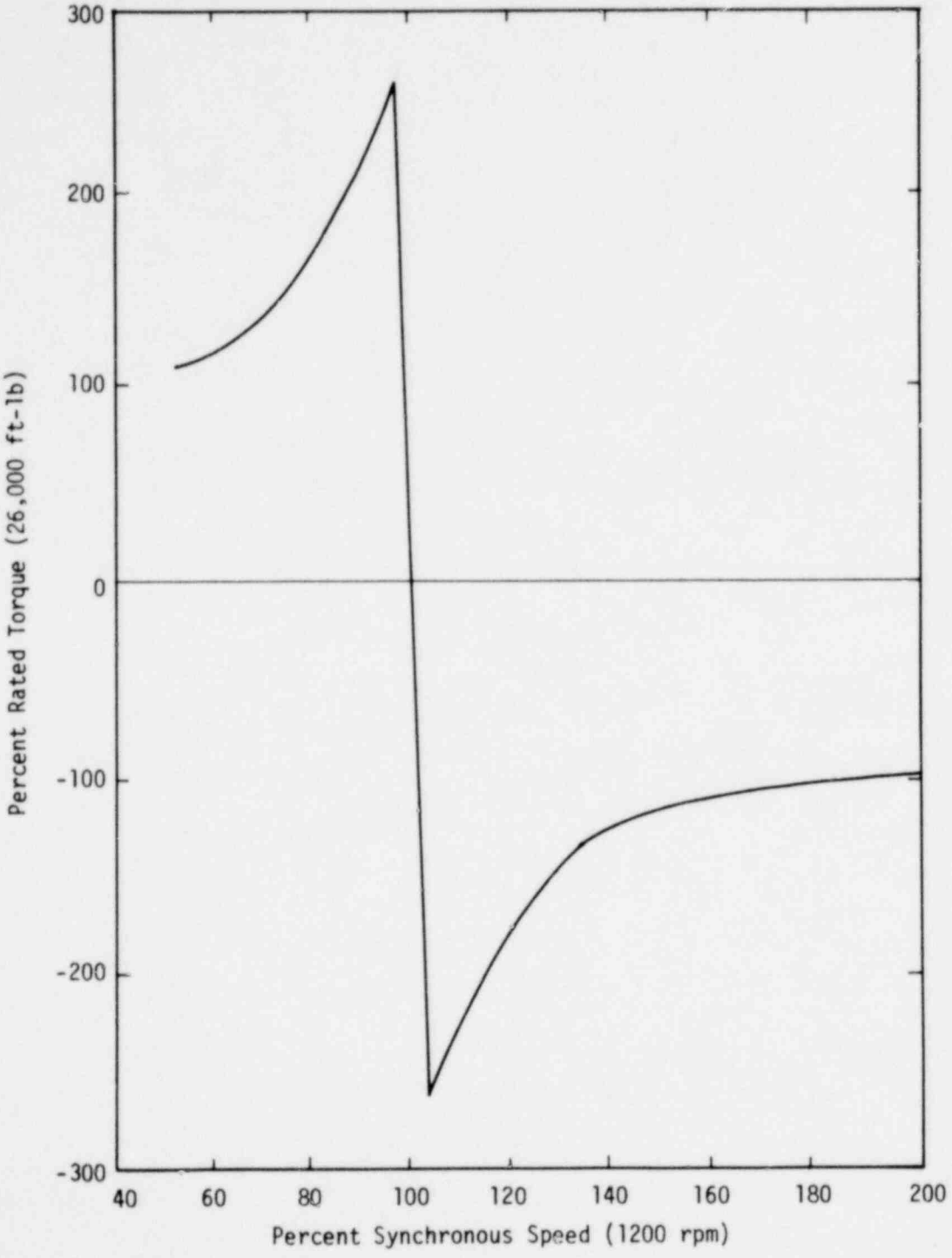

Figure VI.1-6 Torque Versus Speed Type 93A Pump Motor (Rated Voltage)

1256 218

TABLE VI.1-4

PUMP CURVE INPUT DATA

Type	a	v	v/a	Independent Variable	Dependent Variable	
					Head	Torque
1	>0	$\geq$0	$\leq$1	v/a	h/a^2	β/a^2
2	>0	$\geq$0	>1	a/v	h/v^2	β/v^2
3	>0	<0	$\geq$-1	v/a	h/a^2	β/a^2
4	>0	<0	<-1	a/v	h/v^2	β/v^2
5	$\leq$0	$\leq$0	$\leq$1	v/a	h/a^2	β/a^2
6	$\leq$0	$\leq$0	>1	a/v	h/v^2	β/v^2
7	$\leq$0	>0	$\geq$-1	v/a	h/a^2	β/a^2
8	$\leq$0	>0	<-1	a/v	h/v^2	β/v^2

1756 219

2.0 VALVES

RETRAN has models for simple valves, check valves, and inertial valves. The simple on-off valves can be opened or closed subject to a user-specified trip condition. The check valves are distinguished from inertial valves in that the valve gates of the inertial valves have an inertia controlled rate of opening for a given pressure drop across the valve.

In the momentum equation, Equation II.2-23, the pressure drop across a valve can be treated in either of two ways. In the first case, the pressure drop is computed from a form loss term. For a completely closed valve, the loss coefficient is set equal to a large value. In the second case, the pressure drop is computed as a conventional friction loss, with the effect of the valve entering the friction term through the junction flow area.

2.1 Check Valves

Two types of check valves are modeled in RETRAN, one which exhibits a hysteresis behavior and one which does not. Both types of check valves are controlled by flow dependent pressure drops of the form

$$\Delta P = \frac{(CV)_i W_i |W_i|}{\rho_i} \qquad \text{(VI.2-1)}$$

The characteristic pressure versus flow curves for each of these check valves are shown in Figure VI.2-1.

The coefficient, $(CV)_i$, in Equation VI.2-1 can assume one of three values for a given valve, depending on the direction of flow through the valve and whether the valve is open or virtually closed. For the case of reverse flow through an open valve, the valve will remain open until the pressure drop equals or exceeds the back pressure, P_{cv}, required to close the valve. After a valve closes, $(CV)_i$ assumes a value such that the pressure drop across the valve is representative of small leakage flow.

1256 220

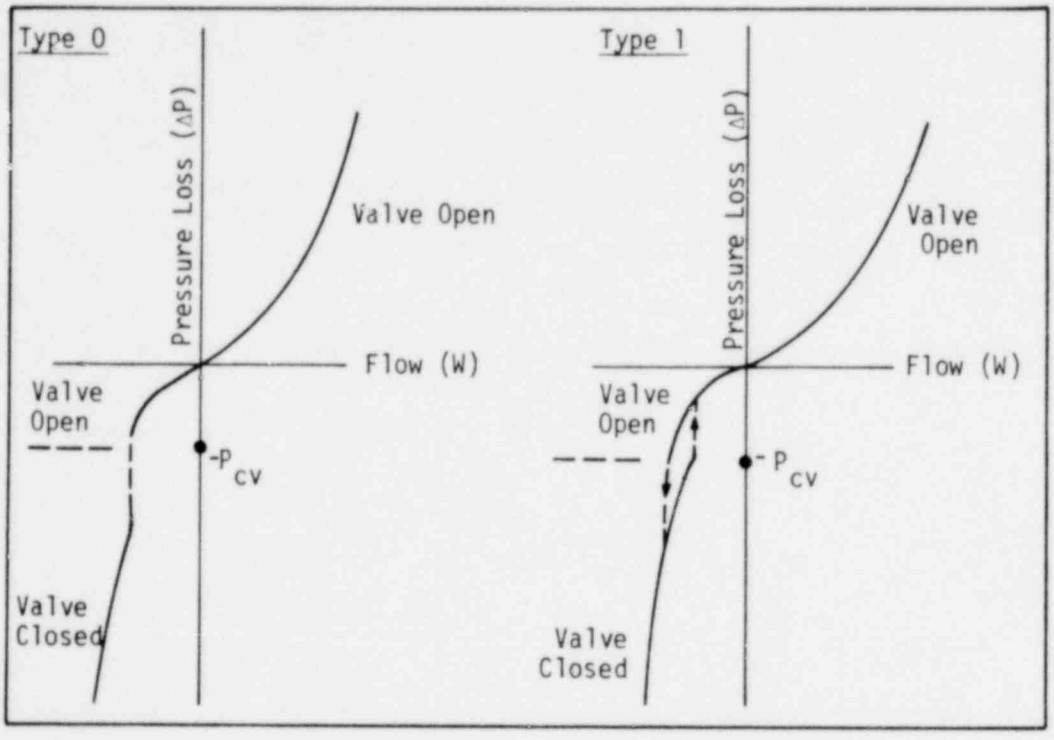

Figure VI.2-1 Check Valve Characteristic Curves

1356 221

The pressure drop across a valve can also be computed by changing the junction flow area as a function of time. This option is initiated with a trip condition at a specified time. The junction area is given by

$$A_i(t) = C(t)\, A_i(0) \qquad \text{(VI.2-2)}$$

where

$C(t)$ = rate of valve opening (closing)

$A_i(0)$ = junction area for valve fully opened.

2.2 Inertial Valves

Inertial valves in RETRAN are assumed to have valve gates which are hinged on each side and which open from the center. The differential pressure across the valve acts as a torque on the gates, and the gate angle at any time is found by integrating the equation of motion. A viscous damping coefficient may optionally be supplied for the equation of motion. Once the gates reach a rotation of 90 degrees they are latched and remain fully open.

The equation of motion for the valve gate may be written as

$$I\,\ddot{\theta}(t) = AP(t) - K\,\dot{\theta}(t) \qquad \text{(VI.2-3)}$$

where

θ = opening angle in degrees

I = moment of inertia (lb_m-ft^2) = $\int x^2\, dm$

A = area x moment arm (ft^3) = $\int x\, dA$

P = differential pressure (lb_f/ft^2) ($P = P_{in} - P_{out} - P_{cv}$)

K = damping constant.

1356 222

In the expression for differential pressure, P_{cv} is the back pressure tending to hold the gates shut.

Equation VI.2-3 can also be written in terms of the angular velocity, $\omega = \dot{\theta}$, as

$$I\,\dot{\omega}(t) + K\,\omega(t) = AP(t). \qquad \text{(VI.2-4)}$$

The solution to Equation VI.2-4 is of the form

$$\omega(t)e^{\frac{K}{I}t} = \frac{A}{I}\int_{t_o}^{t} P(\tau)\, e^{\frac{K}{I}}\, d\tau + \omega_o \qquad \text{(VI.2-5)}$$

where

t_o = time at beginning of time step

ω_o = angular velocity at time t_o.

The pressure term in Equation VI.2-5 is constant over the time step so Equation VI.2-5 can be integrated to give

$$\omega(t) = \omega_o e^{-\frac{K}{I}t} + \frac{AP(t)}{I}\left(1 - e^{-\frac{K}{I}t}\right). \qquad \text{(VI.2-6)}$$

The angle of opening of the gates is, from integration of Equation VI.2-6,

$$\theta(t) = \theta + \omega_o t + \left[\frac{AP(t)}{K} - \omega_o\right]\left[t - \frac{I}{K}\left(1 - e^{-\frac{K}{I}t}\right)\right] \qquad \text{(VI.2-7)}$$

where θ_o = angle of opening at time, t_o.

For the case of no damping ($K \to 0$), Equation VI.2-7 approaches

$$\theta(t) = \theta_o + \omega_o t + \frac{AP(t)}{2I}\, t^2. \qquad \text{(VI.2-8)}$$

The effective junction flow area is then found from a table of normalized area versus angle values.

1356 223

3.0 HEAT EXCHANGERS

3.1 Conduction Based Heat Exchanger Models

The most physically realistic method of modeling a heat exchanger in RETRAN is by use of a heat conductor, usually a hollow cylinder to represent a heat exchanger tube, with fluid volumes on both the inside (primary side) and the outside (secondary side). This method of modeling a heat exchanger is simply a direct application of the RETRAN heat conduction model where the conductor has a control volume on the left and right sides. (See Section VIII.2).

A second, more simplistic, option exists in RETRAN as an alternative for heat exchanger modeling. This option takes the form of a special boundary condition used in conjunction with the heat conduction model. This boundary condition is applied to the secondary side of a heat exchanger conductor and is specified as fraction of total power to be removed by the conductor (Q_o) in steady-state initialization, together with a constant convective heat transfer coefficient (h_c). These conditions are sufficient to determine a known heat flux boundary condition to be applied to the steady-state heat conduction equation, which in turn uniquely determines an effective secondary side fluid temperature via the equation

$$T_{sec} = T_w - \frac{Q_o}{A\ h_c} \qquad \text{(VI.3-1)}$$

where

T_{sec} = constant temperature of fluid on secondary side of heat exchanger

T_w = wall surface temperature

A = heat transfer area.

During the transient calculation, T_{sec} and h_c are held constant to provide the secondary side boundary condition for the transient heat conduction equation. This special boundary condition can be applied to at most one side of each heat conductor modeled.

1256 224

3.2 Nonconduction Heat Exchanger Models

This model accounts for heat removal or addition to a RETRAN fluid volume by means other than conduction. This option provides seven models to simulate various types of heat sources or sinks. The enthalpy transport model may be used in conjunction with a nonconduction heat exchanger if a continuous enthalpy profile through the volume is desired.

3.2.1 Flow and/or Temperature-Dependent Heat Exchangers

The heat exchanger data cards supply a constant or time variant secondary sink temperature, T_{sec}, a constant effective heat transfer coefficient, h_c, and the fraction of total thermal power generated which the heat exchanger removes. From the latter, the initial heat removal rate, Q_o, is calculated. If the input value of h_c is zero, h_c is then calculated for flow and temperature dependent heat exchangers as

$$h_c = Q_o \left(\frac{1}{W_o}\right)\left(\frac{1}{T_{pri_o} - T_{sec_o}}\right) \qquad \text{(VI.3-2)}$$

where

W_o = initial average volume flow

T_{pri_o} = initial volume fluid temperature.

For the case of a temperature-dependent heat exchanger, if h_c is input as zero, h_c is then calculated as

$$h_c = Q_o \left(\frac{1}{T_{pri_o} - T_{sec_o}}\right) . \qquad \text{(VI.3-3)}$$

In the transient calculation, the updated values of W, T_{pri}, and T_{sec} (if time dependent) are used to calculate the heat removal rate for flow and temperature-dependent heat exchanger and for temperature-dependent heat exchanger, respectively, as

$$Q = h_c W (T_{pri} - T_{sec}) \qquad \text{(VI.3-4)}$$

and

$$Q = h_c (T_{pri} - T_{sec}) \qquad \text{(VI.3-5)}$$

3.2.2 Time-Dependent Heat Exchangers

This model uses an input table of normalized thermal-power versus time, or power in megawatts versus time supplied by the heat exchanger data cards. The normalized power represents that fraction of total thermal power generated, i.e., power generated in the core sections and by the pumps, which the heat exchanger is removing. Heat sources are modeled by supplying negative values of normalized thermal power or power in the tables.

3.2.2 Pressurizer Heater Model

This model is described in Section VII.3.3.

3.2.3 Heat Exchanger Controlled by the Control System

By combining the heat exchanger model with the control system models, the user is given the flexibility to specify the heat removal rate as an arbitrary function of any system parameter which can be monitored by the control system. For example, it is possible to model a heat exchanger whose heat removal rate is determined by an algebraic or differential equation involving pressure, temperature, and flow. The equation would be specified by using the control system models, and the heat removal rate is equal to the output of the control block designated by the user. The units of power may be chosen to be either normalized total thermal power or megawatts.

1356 226

4.0 TRIP CONTROLS

The trip controls model the trip logic of reactor systems, initiate transient events, and specify conditions for termination a RETRAN simulation. Trip logic of arbitrary complexity can be modeled by using AND trips, OR trips, and trips on high and low setpoints. Switching control systems, also known as "bang-bang" control systems, are modeled using normal and reset trips. Functional trips are modeled by using the control system to combine several systems parameters in algebraic, differential, or integral functions.

4.1 Standard Trips

The data consists of NTRP cards, where NTRP is a number greater than or equal to 1. Each card specifies a signal to be monitored, a high or low setpoint, a delay, and a trip identifier (IDTRP). When the signal reaches the setpoint value, the trip is actuated after the specified delay. The action initiated by the trip is specified by IDTRP.

The signals which can be monitored by the trip controls are:

(1) elapsed problem time

(2) normalized reactor power

(3) reactor period

(4) average pressure in any volume

(5) mixture level in any volume

(6) liquid level in any volume

(7) water temperature in any volume

(8) metal temperature in any core volume

(9) mass flow at any junction

(10) temperature of any node of any conductor

(11) output of any control block

The action initiated by the trip is determined by input data associated with those component models which are subject to control by trips. For example, if an initially closed valve is to open when a trip is actuated, the input data for that valve must refer to IDTRP, the trip identifier. IDTRP = 1 is reserved for problem termination. When the condition specified by any card with IDTRP = 1 is satisfied, the RETRAN simulation is terminated. The first card of trip data must be a problem termination card monitoring elapsed time. The actions which can be controlled by the trip controls are:

(1) problem termination

(2) opening initially closed valves

(3) closing initially open valves

(4) fill water injection (or removal)

(5) pump shutoff

(6) reactor scram

(7) off and on switching of a simplified heat exchanger

4.2 OR Trips

A trip can be activated if any one of a number of conditions is met. This is called an OR trip. For example, if a reactor scram is to occur in a PWR when either the pressurizer pressure is low or when the pressurizer pressure is high, two trip cards are needed to model the trip for the scram. One will specify a trip on a low pressure setpoint. The other will specify a trip on a high pressure setpoint. When either condition is met, the trip will be actuated.

4.3 Multiple Actions

The input for several different component models may refer to the same IDTRP. The effect is to model multiple actions which are initiated simultaneously when the trip is actuated.

4.4 Coincidence Trips

The coincidence trip, also called an AND trip, is a trip which occurs only after both of two conditions have been satisfied. For example, a PWR may trip a safety injection system when there is low pressure and low level in the pressurizer. Cascading coincidence trips allows modeling of trips which are activated when all of several conditions are met. The ability to model AND and OR trips together allows modeling trip logic of arbitrary complexity. For example, it is possible to model a "majority gate," where a trip is actuated only when at least two out of three conditions are met.

4.5 Indirect Trip

An indirect trip is defined to be a trip which is actuated, with possibly an additional delay, by another trip. Consider a system which trips the turbine whenever the reactor is scrammed. The reactor scram could be tripped by a number of different signals, say, six signals. The reactor scram trip logic could be modeled using six cards. If an indirect trip is used, only one additional trip card would be required to model the turbine trip. By assigning different delays to each trip card, indirect trips allow a trip condition to initiate several actions at different times. Thus, indirect trips can model a sequence of events, all triggered by the same trip.

4.6 Reset Trips

Reset trips specify conditions under which previously activated trips are to be reset. For example, an initially closed valve that was opened by a trip can be reclosed by a reset trip. A reset trip used in this way is sometimes called a "reverse" trip or an "off" trip. Trips whose setpoint threshhold has been crossed, but whose delay time has not yet expired can also be reset. An indirect trip used in this way is sometimes called a "blocking" trip.

When a reset and normal trip are used together, the trips could alternately be activated by system conditions. In the example given above, the valve may be opened and closed repeatedly as required by the trip conditions. Thus, "bang-bang" control systems can be modeled using the trip controls.

4.7 Control System Trips

A control system trip is simply a trip which monitors the output signal of a control block used in the control system model. Control system trips greatly increase the capability of the trip logic by allowing the modeling of trips that are an algebraic, differential, or integral function of various system parameters. This type of control system trip is also called a functional trip.

VII. OPERATIONAL TRANSIENT MODELS

Some of the modeling assumptions made in analyzing the blowdown transients are not valid for the less severe operational plant transients. The models described in this section are models which have been included in the RETRAN code to account for these assumptions and to provide the capability to analyze operational plant transients in Pressurized Water Reactors (PWR) and Boiling Water Reactors (BWR). The feedback of various plant systems is more important for the operational transients than for the blowdown transient. A control system model has been developed to model this feedback in more detail. Models to account for transport delay and a more accurate pressurizer response have also been included. A DNB model is provided to perform subchannel analysis during the system analysis.

1.0 CONTROL SYSTEM MODELS

The response of various plant systems may have a large effect on the overall system response depending on the particular transient being analyzed. For example, in a BWR loss of feedwater heater transient, an accurate simulation of the feedwater flow response is necessary because of its large effect on the reactivity feedback.

The control system models allow RETRAN to model a variety of reactor control systems. The block-structured input of the models allows the user to prepare input from a block diagram of the control system. The set of fundamental blocks, the provision for arbitrary interconnection of these blocks, and the availability of any plant variable to be used as an input all give the user the flexibility to model complex control systems.

The fundamental blocks available to the user include analog computer elements, such as integrators, differentiators, delays, and weighted summers; arithmetic blocks, such as multipliers, dividers, logarithmic and exponentiation blocks; and nonlinear blocks, such as function generators, velocity limiters, and amplitude limiters. This selection of blocks allows the user to simulate the dynamics of linear control systems and the effects of both soft and hard nonlinearities.

Interconnection of these control blocks permits simulation of commonly used controllers, such as a proportional-integral-derivative (PIC) controller, or, in fact, any arbitrary transfer function desired by the user. When used with the trip logic model, the control system models can easily model hysteresis.

Input to the control system may be any variable for which a minor edit may be specified. This includes, but is not limited to, temperatures, pressures, flows, or levels anywhere in the system being modeled.

The parameters which may be controlled by the control system models are

- fill flux
- pressure of the fill fluid

- specific enthalpy of the fill fluid
- reactivity insertion
- valve area
- pump speed
- pump motor torque
- heat exchanger heat removal rate.

1.1 Model Description

Table VII 1-1 defines the nomenclature that is used to describe the control system model. The letter "x" refers to signals related to the input of a control block and "y" refers to signals related to the output of a control block. The letter "h" refers to time step intervals. A scale factor "G" is used by all control blocks.

Table VII.1-2 presents the mathematical definition for each control block. The output is expressed either explicitly, as a function of the input, or implicitly, as the solution of a differential equation where the input is a given function of time. In addition, Table VII.1-2 briefly describes the numerical approximations used by the RETRAN coding to represent the control block.

The object of a control system model is to determine the output of a system given the input and information characterizing the system. The input is a given function of time. The output is a function of time to be determined.

When the input and output time functions can be related by a linear differential equation, the system is said to be linear. If information concerning the state of the system in terms of the initial output is known, the differential equation can be solved for the output given an arbitrary input. The DER, INT, LAG and LLG control blocks represent systems which are linear. RETRAN solves the differential equation characterizing these blocks by using a backward difference approximation to the first derivative. Solving the resulting difference equation

TABLE VII.1-1

CONTROL SYSTEM MODEL NOMENCLATURE

$F_m[\ ]$	=	functional relation defined by the user via pairs of values of the independent and dependent variables in area vs. time Table m.
g_1, g_2	=	user specified gains which apply to input 1 and input 2 respectively; these gains are used by SUM block only
G	=	user specified value for the overall gain of a control block
h_i	=	$t_i - t_{i-1}$, the i^{th} time interval
i	=	subscript used to denote values evaluated at i^{th} value of time
IDC	=	control block identification number
m	=	Time Dependent Area Table index; only the FNG block uses m
n	=	user specified integer value denoting the number of samples taken and saved per delay interval; only the DLY block uses n
s	=	complex frequency in radians per second
t	=	time in seconds
t'	=	dummy variable representing time
t_i	=	i^{th} value of time
t_{i-1}	=	$(i-1)^{th}$ value of time
T	=	Delay time interval; T is used by DLY block only
v_{down}	=	user specified maximum negative rate of change for control block output, maximum "downward slew rate"; only the VLM block uses v_{down}
v_{up}	=	user specified maximum positive rate of change for control block output, maximum "upward slew rate"; only the VLM block uses v_{up}
x_i	=	value of $x_1(t)$ when $t=t_i$
x_0	=	value of $x_1(t)$ when $t=0$
$x_1(t)$	=	input 1 of control block represented as a function of time
$x_2(t)$	=	input 2 of control block represented as a function of time

TABLE VII.1-1 (Cont'd.)

$y(t)$	=	output of control block represented as a function of time
y_i	=	value of y(t) when $t=t_i$
y_{i-1}	=	value of y(t) when $t=t_{i-1}$
y_{max}	=	user specified maximum value of y(t)
y_{min}	=	user specified minimum value of y(t)
y_0	=	value of y(t) when t=0
t_1	=	lead time constant
t_2	=	lag time constant

1756 236

TABLE VII.1-2

MODELS FOR CONTROL BLOCKS

Symbol	Descriptive Name	Mathematical Definition	Numerical Approximation Used by RETRAN
DER	Differentiator	$y(t) = G \cdot \frac{dx(t)}{dt}$	$y_i = G \cdot \frac{x_i - x_{i-1}}{h_i}$
DIV	Divider	$y(t) = G \cdot \frac{x_1(t)}{x_2(t)}$	$y_i = G \cdot \frac{x_1(t_i)}{x_2(t_i)}$
DLY	Time delay	$y(t) = y_0$ for $0 \leq t \leq T$ $= G \cdot (t-T)$ for $t > T$	Numerical approximation used is described in this section.
FNG	Function generator	$y(t) = G \cdot F_m[x(t)]$	$y_i = G \cdot F_m[x_i]$ where $F_m[\cdot]$ represents linear interpolation over a table of ordered pairs of independent and dependent variables.
INT	Integrator	$y(t) = y_0 + G \cdot \int_0^t x(t')\, dt'$	$y_i = y_{i-1} + G \cdot x_i \cdot h_i$ with y_0 given.
LAG	Lag compensation	$y(t) + \tau_2 \cdot \frac{dy(t)}{dt} = G \cdot x(t)$ with $y(0) = y_0$	$y_i = \frac{G \cdot x_i + \frac{\tau_2 \cdot y_{i-1}}{h_i}}{1 + \frac{\tau_2}{h_i}}$

TABLE VII.1-2 (Cont'd)

MODELS FOR CONTROL BLOCKS

Symbol	Descriptive Name	Mathematical Definition	Numerical Approximation Used by RETRAN
LLG	Lead-lag	$y(t) + \tau_2 \cdot \frac{dy(t)}{dt} = G\, x_1(t) + \tau_1 \cdot \frac{dx_1(t)}{dt}$ with $y(0) = y_0$	$\frac{G \cdot x_i + \frac{\tau_1 \cdot (x_i - x_{i-1})}{h_i} + \frac{\tau_2 \cdot y_{i-1}}{h_i}}{(1 + \frac{\tau_2}{h_i})}$ with y_0 given
MUL	Multiplier	$y(t) = x_1(t) \cdot x_2(t)$	$y_i = x_1(t_i) \cdot x_2(t_i)$
LN	Natural logarithm	$y(t) = \ln [x(t)]$	$y_i = \ln [x_i]$
MAX	Maximum	$y(t) = \max [x_1(t), x_2(t)]$	$y_i = \max [x_1(t_i), x_2(t_i)]$
MIN	Minimum	$y(t) = \min [x_1(t), x_2(t)]$	$y_i = \min [x_1(t_i), x_2(t_i)]$
SUM	Weighted summer	$y(t) = G \cdot [g_1 \cdot x_1(t) + g_2 \cdot x_2(t)]$	$y_i = G \cdot [g_1 \cdot x_1(t_i) + g_2 \cdot x_2(t_i)]$
VLM	Velocity limiter	$y_i = y_{down}$ if $G \cdot x_i < y_{down}$; $= y_{up}$ if $G \cdot x_i > y_{up}$; $= G \cdot x_i$ otherwise; where $y_{down} = y_{i-1} - h_i \cdot v_{down}$, $y_{up} = y_{i-1} + h_i \cdot v_{up}$	Same as mathematical definition

TABLE VII.1-2 (Cont'd)

MODELS FOR CONTROL BLOCKS

Symbol	Descriptive Name	Mathematical Definition	Numerical Approximation Used by RETRAN
XPO	Exponentiation	$y_i = [x_1(t)]^{X2(t)}$	$y_i = [x_1(t_i)]^{x2(ti)}$

for y_i in terms of x_i, x_{i-1}, y_{i-1}, and h_i represents an explicit formula for calculating the output of each block for each time step. This formula applies as long as the linear difference equation is a good approximation to the differential equation and the differential equation accurately represents the actual hardware.

In reality the input-output relation of the hardware can be represented by a linear system over only a finite range of output values. To model this nonlinear characteristic RETRAN assumes that a control block is linear whenever its output is greater than y_{min} and less than y_{max}. If the linear model predicts an output greater than y_{max}, then the output is assumed to be equal to y_{max}. If the linear model predicts an output less than y_{min}, then the output is y_{min}. The user specifies the parameters y_{min} and y_{max}. In addition, RETRAN provides nonlinear control blocks such as the FNG and VLM blocks to allow the user to model other types of nonlinear behavior which may be in the hardware.

The numerical approximations used for the control blocks are straight-forward. The DER, INT, LAG, and LLG blocks were discussed above. The DIV, LN, MAX, MIN, MUL, SUM, and XPO blocks simply take the inputs at time t_i and perform the operations indicated by their names to calculate the output. The FNG block takes the input at time t_i and linearly interpolates over the user-supplied table to calculate the output. The VLM block calculates the maximum and minimum values the output may have without exceeding the user-specified rate limitations and calculates the output according to the conditions described in Table VII.1-2.

The method used to model the DLY block is conceptually simple, but difficult to describe symbolically. The details are described here to explain the significance of the n parameter required by the DLY block. The DLY block stores the values of the input for the past T seconds. The output of the DLY block at time t_i is the input that it had at time (t_i-T) multiplied by the scale factor G. The manner in which the DLY block stores the input values is to make a piecewise continuous function out of the input, sample the input at fixed time intervals equal to (t/n), and save each sample for the previous T seconds. Thus, n is equal to the number of samples of the input the DLY block has stored over the past T seconds. A larger value of n results in a more accurate representation of the past input at the cost of more storage. It is the responsibility of the user to choose the smallest value of n consistent with acceptable accuracy.

1356 240

2.0 TRANSPORT DELAY MODEL

The timing of temperature changes in the primary system can be very important in the simulation of plant transients for both BWRs and PWRs because of the effects of reactivity feedback and/or steam generator heat removal on the system transient response. Temperature changes move through some regions (such as piping) essentially as a front, that is, the incoming fluid does not mix with the fluid within the particular region but only displaces it. The standard RETRAN method for determining the junction enthalpy is to homogeneously mix incoming fluid with the contents of a particular region; thus, the outlet enthalpy begins to respond immediately to changes in the inlet. This is the type of response that best represents a plenum. Other options available in RETRAN to affect the determination of junction enthalpy (out of a volume) include a vapor-liquid separation model and an enthalpy transport model to more appropriately model heated sections. The RETRAN solution, taking the number of nodes (control volumes) to a theoretical infinite number, would account for the transport phenomena. However, there are realistic limitations on problem run time and size such that an approximate submodel is necessary to keep track of the enthalpy movement within a region. The transport delay model is intended to serve this purpose and is not designed to solve the transport problem in the most general sense.

The transport delay model considers the movement of fluid through a region as a slug. In other words, the fluid coming into a region at time (t) leaves that region at time ($t + \tau$) where τ represents the time required to transport that fluid through the volume. Thus, the timing of feedback effects either from the core or the steam generator are properly modeled.

2.1 General Approach and Assumptions

The transport of fluid through a region with one inlet, one outlet and with the flow always moving in the same direction is not a particularly difficult problem to fit into RETRAN. However, to appropriately cover situations such as a single-loop pump coastdown (or locked rotor), a variety of junctions into and out of a volume, and flow reversals present significantly more difficulties in modelling. The overall approach and objective of the transport delay model include:

(1) The ability to define the enthalpy distribution spatially (one-dimensionally) within the volume such that major flow reversals will be handled appropriately.

(2) The ability to model several junctions into and out of a given "transport" volume.

(3) The ability to handle flow oscillations such as might occur intermittently due to numerics or other problems.

In order to accomplish the aforementioned objectives, a mesh is defined by which the enthalpy distribution within the volume is maintained. The mesh is defined by user input for each volume which is to be treated as a "transport" volume. This mesh divides the volume into equal segments of mass, which are then used to define the enthalpy distribution within the volume and the movement of temperature changes through the volume.

2.2 Detailed Description and Solution Technique

The enthalpy of each mass interval defined for each transport volume are updated according to the mass flow and energy into the volume during each time step. The enthalpy associated with each mesh is shifted in the volume by the mass that has moved into the volume during that time step. The junction flow rates into a "transport" volume are integrated and summed to indicate the shift in the distribution. Similarly, the integrated average enthalpy is attached to the new mass in the "transport" volume. Because of the variety of geometries and transient situations that may be simulated, a primary flow direction is defined which is used to indicate the direction of shift in enthalpy distribution. In other words, if the primary flow is positive, the junctions on the inlet side of the volume are integrated for the shift and, similarly, the outlet end, if the primary flow is negative. The primary inlet and outlet junctions are those junctions with the largest absolute flow rates at initial conditions and are assumed to be in the same direction.

The mesh enthalpy for each of the mesh intervals is maintained until sufficient mass has been accumulated in the volume to shift an entire mesh interval. Given this approach, the new mesh enthalpy for the leading mesh is the integrated

average of the inlet enthalpy over the transient time period required to accumulate the mass of one mesh. This new mesh enthalpy is then shifted through the volume as the transient progresses.

If the primary flow is positive, the shift is performed from volume inlet to outlet and vice versa for negative flow. In RETRAN, there may arise situations where particular junctions flow counter to the primary direction. When this occurs on the inlet side of a "transport" volume (with positive flow) it is considered in the summation for the shift. However, on the outlet side, the mesh enthalpy is adjusted to account for junctions counter to the primary direction. The same approach is used if the primary flow direction is negative.

The determination of the outlet junction enthalpy(s) from the "transport" volume is based on the enthalpy of the outlet mesh interval. If more than one interval is affected, the outlet enthalpy is the mass average of the interval enthalpy. The mass moved out of a "transport" volume is extrapolated from the two previous time steps to estimate the current time step junction enthalpy.

Given the general approach of the transport model, it is conceivable that the integrated average enthalpy in the "transport" volume would not equal the average enthalpy from the overall volume mass and energy balance. This is rectified by normalizing the mesh enthalpies after each shift to the volume average enthalpy. Thus, if heat conductors are considered in volumes which are to be treated as "transport" regions, the enthalpy distribution will be shifted up or down as the heat transfer is reflected in the volume averaged enthalpy. The heat transfer calculations continue to use the volume average conditions to determine the heat transfer rate.

3.0 PRESSURIZER MODEL

The simulation of PWR plant transients, such as the loss of reactor coolant flow, uncontrolled rod withdrawal, and loss of feedwater flow, requires a model of the pressurizer that considers the physical processes taking place during these types of transients. A standard RETRAN state solution of the pressurizer would assume that all of the contents are in thermal equilibrium. However, the pressurizer, rather than behaving in an equilibrium manner, has two somewhat distinct regions such that a state solution of the whole volume is not a proper representation of the physical process. Non-equilibrium between pressurizer regions is particularly necessary when the transient involves a surge of subcooled liquid into the pressurizer.

Various pressurizer models have been used to describe the thermodynamic processes and non-equilibrium conditions between the regions.[VII.3-1 through VII.3-5] Several of these approaches, beginning with the TOP's model [VII.3-11] in 1965 apply separate mass and energy conservation equations to a "liquid" and a "vapor" region within the pressurizer. The heat and mass transfer interfaces with the pressurizer walls, between regions, and with the spray are then described with different models and varying degrees of detail depending on the author's assumptions.

3.1 General Approach and Assumptions

The RETRAN pressurizer model defines two separate thermodynamic regions which are not required to be in thermal equilibrium. The two regions are termed a "liquid" and a "vapor" region, although each region may contain both liquid and vapor. Each region thermodynamic state solution is determined from a distinct mass and energy balance on that region. Hence, the thermodynamic state for each region is determined without restrictions as to the other. In other words the vapor region can be superheated and the liquid region subcooled, both saturated, vapor region saturated and liquid region subcooled, and so on. However, should the pressure rise above the critical point, all further calculations are performed using a single region equilibrium approach.

The mass and energy balance provides the total mass and energy in each region as a function of time through the transient. The solution of the thermodynamic state in each region then involves the determination of each region volume (constrained that the sum equals the total volume) such that the calculated pressure is equal in each region.

Included at the interface between the liquid and vapor regions is a flashing model which describes the movement of vapor from the liquid to vapor region and a rainout model which describes the movement of liquid from the vapor region to the liquid region. Heat transfer between the regions is omitted as it is not considered significant relative to the other phenomena. The present pressurizer model does not allow heat conductors to be specified in the pressurizer as their contribution is typically a second order effect in most transients. The pressurizer safety and relief valves are modeled as junctions from the vapor region and can be modeled using standard "fill" junction options or in conjunction with the control system models as described in Section VII.1.

3.2 Mass and Energy Equations

The fluid mass and energy equations are basically the same as those discussed in Sections II and III. The primary difference is that the rate of change of mass and energy is determined for each region of a non-equilibrium volume. Several terms are included in the equations which account for specific phenomena and equipment unique to the pressurizer. The following equations are written for each liquid and vapor region of non-equilibrium volume "i".

3.2.1 Liquid Region Mass Equation

$$\frac{dM_\ell}{dt} = \sum_j W_{ij}^{(\ell)} + W_r - W_{f\ell} + W_{sp} + W_{cs} \qquad \text{(VII.3-1)}$$

where

M_ℓ = Mass in liquid region

$W_{ij}^{(\ell)}$ = Flows from junction j into the liquid region of volume i

W_r = Rainout of liquid droplets from the vapor region to the liquid region

$W_{f\ell}$ = Flashing of vapor from the liquid region to the vapor region

W_{sp} = Mass flow rate of spray into non-equilibrium volume if special spray option selected (details in Section VII.3-3)

W_{cs} = Mass flow rate from the vapor region of mass condensing on the spray if special spray option selected.

3.2.2 Vapor Region Mass Equation

$$\frac{dM_v}{dt} = \sum_j W_{ij}^{(v)} + W_{f\ell} - W_r - W_{cs} \qquad \text{(VII.3-2)}$$

where

M_v = Mass in vapor region

$W_{ij}^{(v)}$ = Flows from junction j into the vapor region of volume i.

3.2.3 Liquid Region Energy Equation

$$\frac{dU_\ell}{dt} = \sum_j W_{ij}^{(\ell)} h_{ij} + W_r h_f - W_{f\ell} h_g + (W_{sp} + W_{cs}) h_f + Q_h - P\dot{V}_\ell \qquad \text{(VII.3-3)}$$

where

U_ℓ = Internal energy of the liquid region

1356 24

h_f, h_g = Saturated fluid and gas enthalpy at volume pressure

Q_h = Heat input rate of pressurizer heaters

P = Transient pressure of the non-equilibrium volume i

$\dot{V}_\ell$ = Time rate of change of liquid region volume.

3.2.4 Vapor Region Energy Equation

$$\frac{dU_v}{dt} = \sum_j W_{ij}^{(v)} h_{ij} + W_{f\ell} h_g - W_r h_f - W_{cs} h_v + P\dot{V}_\ell \qquad \text{(VII.3-4)}$$

where

h_v = Enthalpy of gas in vapor region.

3.3 Region Interface Models

The region interface models are presented in the following sections. These models include the pressurizer spray model, the pressurizer heaters model, the rainout model, and the flashing model.

3.3.1 Pressurizer Spray

The effects of spray on the pressurizer response can be modeled in one of two ways in RETRAN. The first is simply the specification through input that the spray junction is in the vapor region. This option desuperheats the vapor region. The second option is a special option spray which involves the removal of mass and energy from the vapor region but does not desuperheat the region. This option assumes that the spray, in falling through the atmosphere, condenses vapor from that region such that the result is a saturated liquid being deposited in the liquid region. The spray plus condensed mass is deposited directly in the liquid region without a time delay. The following equation defines the quantity of mass condensed on the spray:

$$W_{cs} = W_{sp}\left[\frac{h_f - h_{sp}}{h_v - h_f}\right] \qquad \text{(VII.3-5)}$$

where

W_{sp} = Mass flow rate of the spray junction

h_f = Saturated liquid enthalpy at the volume pressure

h_{sp} = Enthalpy of the spray

h_v = Enthalpy of gas in the vapor region

The pressurizer spray is controlled through the definition of appropriate trips to turn the spray on and off and by a control system (if required) to modulate the spray after the valve is open.

3.3.2 Pressurizer Heaters

The energy input to the liquid region of each pressurizer heater is simulated by a first order differential equation as each heater is turned on or off through the trip inputs. The following equation describes the heater performance:

$$\frac{\tau dq_o}{dt} + q_o = q_{in} \qquad \text{(VII.3-6)}$$

where

τ = time constant relating electrical input to the element to thermal output to the liquid region fluid

q_o = heat input to the liquid region

q_{in} = electrical input to the heaters

The total energy input to the fluid region is the sum of "q_o" for each of the heaters modeled.

1256 248

3.3.3 Rainout Model

The rainout of liquid droplets from the vapor to the liquid region is modeled in the pressurizer model. Other phenomena such as interfacial condensation and condensation on the pressurizer vessel walls are assumed to be second order effects. The vapor region is assumed to be homogeneous and the rainout mass flow rate is calculated as

$$W_r = V_r A (1 - \alpha) \rho \qquad \text{(VII.3-7)}$$

where

W_r = rainout mass flow rate

V_r = liquid droplet rainout velocity

A = cross sectional area of the volume

α = Void fraction of the vapor region

ρ = liquid density in the vapor region.

The droplet rainout velocity is an input parameter for any volume specified to use a non-equilibrium solution and is assumed to be constant during the transient.

3.3.4 Flashing Model

The movement of vapor from the liquid region to the vapor region is modeled using the Wilson[VII.3-6] bubble velocity model and the bubble density gradient parameter as currently used in RETRAN and described in Section III. Surface evaporation is assumed to be an insignificant effect relative to the mass and energy movement accomplished by flashing. The equation representing the vapor movement is

$$W_{f\ell} = V_B (\rho_{gb})_{z_m} A \qquad \text{(VII.3-8)}$$

where

$W_{f\ell}$ = vapor mass flow rate from liquid region to vapor region

V_B = vapor bubble velocity as determined from the relationships defined by Wilson, et al.[VII.3-6)

A = Cross-sectional area of the volume

$(\rho_{gb})_{z_m}$ = Void fraction of the liquid region at the mixture surface times the vapor density (See Section III).

The user is required to specify the desired bubble gradient constant.

3.4 Solution Technique

As discussed previously, there is a unique mass and energy balance on each of the two regions within the pressurizer and thus, there is a thermodynamic state solution for each region. The basic problem in the solution for the transient pressurizer pressure is in the determination of the volume associated with each region as the solution is advanced, such that the resulting state pressure for each region is equal. In order to accomplish the solution, the following procedure is used:

(1) The specific volume of the liquid region is extrapolated linearly from the two previous time steps and, along with the updated mass in that region, establishes an initial liquid region volume.

(2) Using this volume, the thermodynamic state of each region is calculated and, if the difference in the predicted pressure for each region is less than the convergence criteria, the sequence is exited.

(3) If the difference in pressure is greater than the convergence criteria, the volumes are adjusted using the $\frac{\partial r}{\partial P}\Big|_h$ for each region. A linear equation is written for each region and the two solved simultaneously for the volume that would cause the pressure in

each region to be equal. These new volumes are then used in the state solution and the convergence criteria checked again. This process is repeated until convergence is achieved.

(4) A special situation exists when crossing phase lines such that the above approach will not always converge; therefore, when the solution has not converged in more than three iterations, the aforementioned solution technique is used in combination with interval halving to accomplish convergence.

Presently the pressurizer model uses a criteria for convergence between the liquid and vapor pressures of 0.1 psi. The sensitivity of the transient predictions have been examined with a 0.05 criteria and no systematic error or noticeable differences were found over a 600 second transient. Using the above approach, the region pressure convergence will normally be achieved in one iteration and many times using the extrapolated specific volume the first time through the subroutine (no iterations).

4.0 AUXILIARY DNB MODEL

When studying the various operational transients, the majority of these cases involve thermal-hydraulic conditions in which departure from nucleate boiling (DNB) does not occur. For some of these types of transients a single hot subchannel model is sufficient. The auxiliary DNB model provides for the analysis of a hot subchannel with determination of the DNB ratio as a function of channel position.

The models and the approach taken are oriented toward pressurized water reactors (PWR). The PWR CHF correlations available are the B&W-2[VII.4-1] or the W-3[VII.4-2]. Two additional correlations, Barnett[VII.4-3] and Jansen-Levy[VII.4-4], have been added for boiling water reactor (BWR) analysis. The model also includes the MacBeth CHF correlation[VII.4-5] which may be applied to either a PWR or BWR.

4.1 Model Description

The principal consideration in modeling for an auxiliary DNB calculation was to minimize computer running time while reducing as much as practical the conservatism with respect to a more detailed analysis. The present RETRAN model employs an enthalpy rise calculation, for every six inches, through the hot subchannel. The heat flux as a function of axial position is developed from the core heat conductor data as determined within RETRAN. Solving for fluid enthalpy allows for determination of local quality. This and other local condition parameters are then used to determine the critical heat flux, thus the DNB ratio as a function of axial position. A summary of the model is presented in Table VII.4-1, while details are described in the following paragraphs.

4.1.1 Heat Flux Estimate

The heat flux values used in the fluid energy equation and for the DNBR calculation are developed in the following manner. Average heat flux values (q''_{core} (z,t)) are obtained from the core heat conductor solutions in RETRAN. A fit to a power series is developed describing the hot rod flux, ($q''_{hot\ rod}$ (z,t)), as corrected for a detailed axial power profile and heat flux factors.

TABLE VII.4-1

AUXILIARY DNB MODELING

Model	Formation
Subchannel Array	Single channel, normalized to multiple subchannel array
Turbulent Cross Flow Mixing	Rogers and Rosehart correlation
Heat Flux Factors and Flow Redistribution Factors	Input from design assumptions or detailed hydraulic analysis
Engineering Enthalpy Rise Factor	Output at initialization of RETRAN
CHF Correlations	PWR B&W-2, W-3 or MacBeth correlations BWR Barnett, Janssen-Levy, or MacBeth correlations
Non-Uniform Axial Power Shape Correction	B&W or Westinghouse available, values vary with time and position
Grid Spacer Mixing and Cold Wall Effects on CHF	Westinghouse correlations available
DNB Calculation	Calculated at every three-inch interval between input axial limits
Subchannel Mass Velocity	Varies with time and position as interpolated from RETRAN

1756 253

$$q''_{\text{hot rod}}(z,t) = F_Q^{ENG} F_R^N F_Q^{UNC} \left[F_z^N (z,t) \right] \left[\bar{q}''_{\text{core}}(t) \right] \quad f \quad \text{(VII.4-1)}$$

where

F_Q^{ENG} = Engineering heat flux factor

F_R^N = Total radial x local nuclear heat flux factor

F_Q^{UNC} = Uncertainity factor on heat flux

$F_z^N (z,t)$ = Variable for axial nuclear heat flux factor

f = Fraction of power generated within the fuel rod

$\bar{q}''_{\text{core}}(t)$ = Average RETRAN core heat flux

$F_z^N (z,t)$ is approximated as:

$$F_z^N (z,t) = \left(\frac{q''_{\text{core}}(z,t)}{\bar{q}''_{\text{core}}(t)} \right) \left(\frac{\bar{q}''_{\text{core}}(0)}{q''_{\text{core}}(z,0)} \right) \left(\frac{q''_{\text{hot rod}}(z,0)}{\bar{q}''_{\text{hot rod}}(0)} \right) . \quad \text{(VII.4-2)}$$

In the above expression the last term is $F_z^N (z,0)$ as defined by detailed user input. $q''_{\text{core}}(z,t)$ is given as:

$$q''_{\text{core}}(z,t) = C_1 + C_2 z + \ldots + C_m z^{m-1}$$

where:

m = number of core volumes

C_i = Constants, normalized to $\bar{q}''_{\text{core}}$ from RETRAN.

4.1.2 Hot Channel Calculation

When the transient variation in fluid enthalpy is generally small, as an approximation, the steady state fluid energy equation is used to develop subchannel local quality.

$$G_{DNB} \frac{\partial h}{\partial z} = \frac{\pi D_{he}}{Af} q''_{hot\ rod}(z, t) \times FDELH \qquad (VII.4\text{-}3)$$

where

FDELH = Channel enthalpy adjustment factor to account for the effects of turbulent cross flow enthalpy mixing.

If more severe transients, such as anticipated transients without scram or very rapid fluid changes are considered, then the above expression may not prove adequate. If such is the case, then the complete transient energy equation should be used with its internal time step control logic.

For the energy equation the following definitions of mass flux are used

$$G_{DNB} = G_{HOT\ BUNDLE}(z,t) = \left(\frac{W_{core}(z,t)}{A_{core}} \right) \times FDHCOR \qquad (VII.4\text{-}4)$$

where:

FDHCOR = Accounts for the reduction effects of bypass flow, plenum mixing, etc. as associated with the hot bundle.

4.1.3 Correlations and Usage

Critical heat flux correlations used are either the B&W-2, W-3, or MacBeth correlations for a PWR and Barnett, Janssen-Levy or MacBeth correlation for a BWR. This value, $q''_{CHF,\ uniform}$, can be corrected as follows:

$$q''_{CHF,CORR}(z) = q''_{CHF,UNIFORM}(z) \left[\left(\frac{1}{F_{CNU}} \right) (1.0 - F_{cw})(F_s) \right]. \qquad (VII.5\text{-}8)$$

The correction factors adjust for the following effects[VII.4-7, to VII.4-9] non-uniform axial power shape; cold wall effects of guide tubes; and grid spacer effects. Correlations for the grid spacer correction factors include the following three options,

Option 1: $$F_s = 1.0 + 0.03 \left(\frac{G_{\text{HOT BUNDLE}}(z,t)}{10^6}\right)\left(\frac{TDC}{0.019}\right)^{0.35} \quad \text{(VII.4-6)}$$

Option 2: $$F_s^R = (1.445 - .0371L)\left(\frac{9}{225.895}\right)^{.5}[e^{(x+.2)^2} - .73] + K_s \frac{G}{10^6}\left(\frac{TDC}{.019}\right)^{.35} \quad \text{(VII.4-7)}$$

Option 3: $$F_s^L = 0.986\, F_s^R \quad \text{(VII.4-8)}$$

where

TDC = Thermal diffusion coefficient for grid spacer mixing effect

K_s = Axial grid spacing factor

L = Heated length.

The correction factor which accounts for cold wall effects is

$$F_{cw} = R^*\left[13.76 - 1.372\, e^{1.78x} - 4.732\left(\frac{G_{\text{HOT BUNDLE}}(z,t)}{10^6}\right)^{-0.0535} - 0.0619\left(\frac{P_r}{10^3}\right)^{0.14} - 8.509\, D_{he}^{0.107}\right] \quad \text{(VII.4-9)}$$

where

P_r = Pressure given at the nodal point (psia)

x = Local thermodynamic quality given at the nodal point

$R^* = 1.0 - \frac{D_{hy}}{D_{he}}$.

The correction factor used to account for a non-uniform axial power shape is

$$F_{CNU}(Z_I) = \frac{RC \int_{Z_o}^{Z_I} q''_{hot\ rod}(z)\, e^{-C(Z_I - z)}\, dz}{q''_{hot\ rod}(Z_I)\,[1.0 - \exp(-CZ_I)]} \qquad \text{(VII.4-10)}$$

where

$$C = S(1 - x)^T (G_{HOT\ BUNDLE}/10^6)^{-U} \quad . \qquad \text{(VII.4-11)}$$

For the B&W correlation:

R = 1.02508, T = 7.82293
S = 0.2486, U = 0.45758
Z_I = Pt. of calc., Z_o = 0.000

For the Westinghouse correlation:

R = 1.000, T = 4.31
S = 0.15, U = 0.478
Z_I = Pt. of calc., Z_o = 0.000

The integral within the F_{CNU} correlation is evaluated using Lagrangian interpolation, which develops the following expression.

$$\int_{Z_0}^{Z_I} q''_{hot\ rod}(z)\, e^{-C(Z_I - z)}\, dz = \frac{1}{C} \sum_{i=1}^{I} \left\{ q''(z_i) - \frac{1}{C} \frac{q''(z_i) - q''(z_{i-1})}{z_i - z_{i-1}} \right.$$

$$\left. - e^{-C(z_i - z_{i-1})} \left[q''(z_{i-1}) - \frac{1}{C} \frac{q''(z_i) - q''(z_{i-1})}{z_i - z_{i-1}} \right] \right\} \quad . \qquad \text{(VII.4-12)}$$

The DNBR is evaluated at every three inches up the hot channel and at every specified time step. Output consists of DNBR at several locations, the lowest channel position of interest, the hot spot location, and at the point of minimum DNBR.

1356 257

VIII. NUMERICAL SOLUTION METHODS

1.0 FLUID FLOW

The fluid flow equations developed in Section II constitute a set of coupled non-linear differential equations. In general, these equations cannot be solved in closed form. Numerical methods must be used to generate solutions. This section describes the numerical solution methods used in RETRAN to solve these differential equations.

1.1 Numerical Formulation

In order to solve the partial differential equations described in the previous sections, these equations are usually approximated by algebraic equations. The algebraic equations may be obtained by two different routes. The first method uses finite difference representations of the partial differential equations. The second method derives the equations by use of a tube and tank approach. The resultant equations can be identical in both cases if conservation-law-form differential equations are used with the first method and if the proper perspective is maintained when using the tube and tank model to represent certain geometries such as a straight pipe.

The tube and tank model assumes that a straight pipe is made up of several tanks interconnected by tubes. Energy and mass balances are performed on the tanks and momentum equations are solved to obtain the flow in the tubes. Early versions of these models represented the flow in the tubes with orifice equations. An orifice equation may be considered as an approximation to a momentum equation obtained by retaining only the pressure gradient and friction factor terms. In order to apply the tube and tank model correctly it is necessary to assume that (1) the opening connecting two tanks must be in the same physical location, and (2) the tubes are physically overlaid on the tanks and represent flow from the center of one volume to the center of another.

The first of these restrictions does not allow models which consider the pipe connecting two tanks to be able to connect the exit of one tank at a different physical location to the entrance of another tank. In order to represent such a system correctly, it would be necessary to solve the energy and continuity

equation for the pipe as well as the momentum equation. The second restriction requires the tubes to cover the same region as the tanks. This is equivalent to using the same control volume for the continuity and energy equations but an offset control volume for the momentum equation. When these restrictions are observed, the numerical technique is similar to the well known MAC methodology.[VIII.1-1]

The continuity and energy equations are obtained from balances over a control volume (tank) and the momentum equation is obtained from a balance over a junction control volume (tube).

1.1.1 Finite Difference Equations

The basic finite difference equations are presented in this section for the fundamental variables, total mass, M, flow rate, W, and total fluid internal energy, U. These equations are the numerical representations of the integrated stream-tube fluid equations derived in Section II.1. For reasons of clarity, only the compressible single-stream flow with momentum flux form of the flow equation is considered. The basic mesh layout and location of major variables are shown in Figure VIII.1-1.

1.1.1.1 Explicit Formulation

The explicit formulation of the RETRAN finite difference equations is based upon the FLASH-4 technique developed by Porsching et al.[VIII.1-2] The essence of the technique can be explained as follows.

Systems of ordinary differential-difference equations representing a semi-discretized approximation to sets of governing partial differential equations may be expressed as

$$\frac{dY}{dt} = F(Y) \qquad \text{(VIII.1-1)}$$

where Y is a column vector of nodal variables and F is a column vector of functions (F_1, F_2, . . . F_N) and N is the number of independent variables and nodes combined. The vector F(Y) may be linearized about a vector of guesses, Y_o as

1256 240

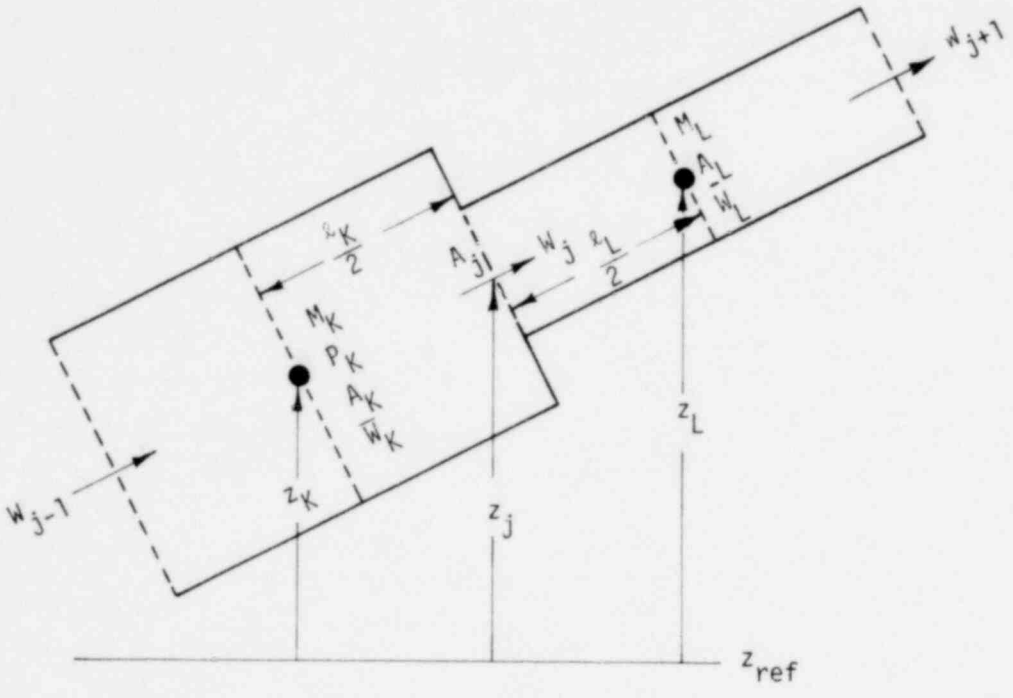

Figure VIII.1-1 Typical Computational Mesh For Two Junctions on a Volume

$$F(Y) = F(Y_o) + J(Y_o)\,(Y-Y_o) \qquad \text{(VIII.1-2)}$$

where the Jacobian matrix J is given by

$$J(Y_o) = \left(\frac{\partial F_i}{\partial Y_j}\right)_{Y_o} \quad . \qquad \text{(VIII.1-3)}$$

Combination of Equations VIII.1-1 and VIII.1-2 produces

$$\frac{dY}{dt} = F(Y_o) + J(Y_o)\,(Y-Y_o) \quad . \qquad \text{(VIII.1-4)}$$

Equation VIII.1-4 represents a system of <u>linear</u> coupled ordinary differential equations which may be solved by matrix methods.

A first order accurate finite difference approximation to Equation VIII.1-4 may be written as

$$\frac{Y^{n+1} - Y^n}{t^{n+1} - t^n} = F(Y_o) + J(Y_o)\,(Y^{n+1} - Y_o) \qquad \text{(VIII.1-5)}$$

where Y^{n+1} and Y^n are the values of Y at time levels t^{n+1} and t^n respectively. If Y_o is chosen to be equal to Y^n, Equation VIII.1-5 becomes

$$\frac{Y^{n+1} - Y^n}{t^{n+1} - t^n} = F(Y^n) + J(Y^n)\,(Y^{n+1} - Y^n) \quad . \qquad \text{(VIII.1-6)}$$

Equation VIII.1-6 may be rearranged to solve for $Y^{n+1} - Y^n$ as

$$\Delta Y^n \equiv Y^{n+1} - Y^n = (t^{n+1} - t^n)\,F(Y^n)\,[I - (t^{n+1} - t^n)\,J(Y^n)]^{-1} \qquad \text{(VIII.1-7)}$$

where I is the identity matrix.

Porsching et al.,[VIII.1-2] refers to Equation VIII.1-7 as an <u>implicit</u> numerical procedure and proves consistency and unconditional stability. Equation VIII.1-7

is actually an explicit numerical procedure on the time scale because the incremental quantity ΔY^n may be solved for explicity using only old time values of Y^n in the matrix J. Equation VIII.1-6, however, is implicit since it is of the form $\Delta Y = G(\Delta Y)$. In practice the entire matrix is not inverted as will be shown later.

In Figure VIII.1-1, the locations of the major variables are indicated. Although only two junctions have been assigned to each volume as indicated, the code allows many more. The concept of initial and terminal nodes or control volumes seems to be attributable to Porsching et al., who thought of each link or junction as having a definite beginning and a definite end as shown in Figure VIII.1-2. As shown in Figure VIII.1-1, and as discussed previously, the inlet and outlet of the junctions are actually at the same positions. Thus, the junction is in actuality a point. Distinctly different flow areas may be assigned to the nodes and junctions as shown in Figure VIII.1-1.

Use of the concept of links between nodes, allows an initial or "from" volume and a terminal or "to" volume to be assigned to each junction, as input to the code. This assignment means that the nominal direction of positive flow for W_j is from volume K to volume L. In more mathematical language, volume i has associated with it two sets of junctions, I_i and T_i. The set I_i is the set of junctions for which volume i is the initial node and the set T_i is the set of junctions for which volume i is the terminal node. A given junction j can belong to only one of the two sets. The set changes during a transient depending on the sign of W_j. For example, if W_j is negative and volume K is the initial or "from" volume, and L is the terminal or "to" volume, flow is from volume L to volume K. Junction j would then belong to sets I_K and T_L. The use of these two sets of junctions greatly simplifies the differential equation representations for total mass and energy for a network.

The semi-discretized representation of the RETRAN field equations will now be given for the conservation of mass, momentum and energy to illustrate the application of the FLASH technique.

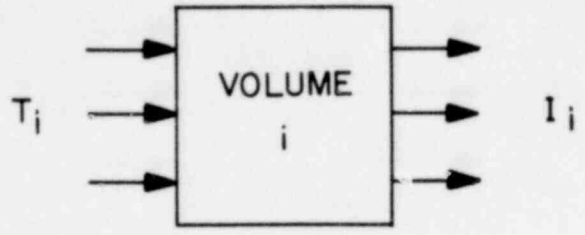

VOLUME i IS THE TERMINAL NODE FOR A SET OF JUNCTIONS T_i AND THE INITIAL NODE FOR A SET OF JUNCTIONS I_i.

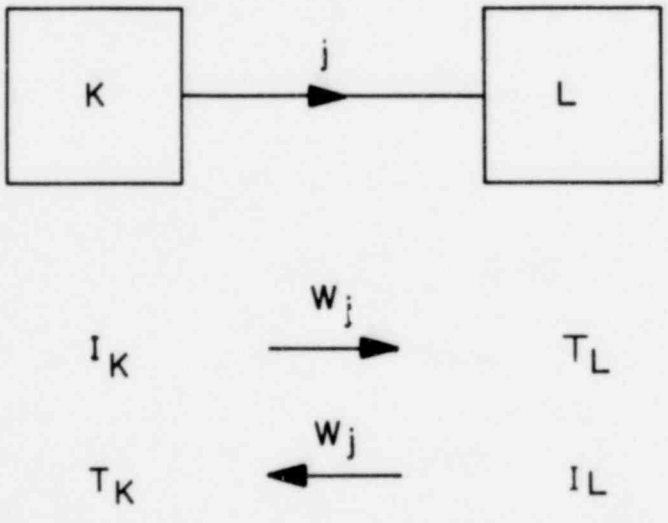

JUNCTION j IS ASSIGNED TO THE TERMINAL AND INITIAL NODE SETS ACCORDING TO JUNCTION FLOW DIRECTION.

Figure VIII.1-2 Junction Terminal and Initial Node Assignment

1256 264

CONSERVATION OF MASS

$$\frac{dM_i^{n+1}}{dt} = \sum_{j\varepsilon T_i} W_j^{n+1} - \sum_{j\varepsilon I_i} W_j^{n+1} + \sum_{j>k} W_{j_{FILL}}^{n} \qquad \text{(VIII.1-8)}$$

$$(i = 1, 2, \ldots, NVOL)$$

where M_i^{n+1} = total mass in volume i at time t^{n+1}, lb

W_j^{n+1} = mass flow into or out of volume i from junction j at time level t^{n+1}, lb/s

and

W_{jFILL}^{n} is a prescribed fill mass flow, either positive or negative from time level t^n.

The symbolism $j\varepsilon T_i$ or I_i means that junction j is a member of the set T_i or I_i as explained above. Equation VIII.1-8 states that the rate of change of mass is equal to the sum of the flow rates into the control volume.

CONSERVATION OF MOMENTUM

$$I_j \frac{dW_j^{n+1}}{dt} + \left\{\frac{K_j S_{gn}(W_j)}{2\rho_j[A_j(t)]^2}\right\}^n (W_j^2)^{n+1} = \left[\frac{\bar{W}_K^2}{\bar{\rho}_K A_K^2} - \frac{\bar{W}_L^2}{\bar{\rho}_L A_L^2}\right]^n + \mathcal{F}_j^n (W_j^2)^{n+1}$$

$$- \left[\frac{f_K \ell_K \bar{W}_K |\bar{W}_K|}{D_{hy_K} \bar{\rho}_K A_K^2} \phi_{tp_K}^2 + \frac{f_L \ell_L \bar{W}_L |\bar{W}_L|}{D_{hy_K} \bar{\rho}_L A_L^2} \phi_{tp_L}^2\right]^n + (p_K - p_L)^{n+1}$$

$$- \left[\int_K^j \rho \, dz + \int_j^L \rho \, dz\right] g, \qquad \text{where } (j \;\; 1, 2, \ldots, k) \; . \qquad \text{(VIII.1-9)}$$

The first term in Equation VIII.1-9 represents the rate of change of momentum. The second and fifth term represent friction, the first being a junction friction associated with area changes and the second being the fanning friction for the

two volumes. The third and fourth term account for the momentum flux or spatial acceleration term due to compressibility and area changes respectively. The sixth term represents the pressure difference between two volumes and the last term represents gravity head change between two volumes.

The $\mathcal{J}_j$ factor which accounts for junction momentum flux change due to area change has been derived for the compressible flow case to be:

$$\mathcal{J}_j^n = \frac{1}{2\rho_{j_o}} \left(\frac{1}{A_L^2} - \frac{1}{A_K^2} \right) \frac{2\left[\frac{\rho}{\rho_o} \left(\frac{M^2}{M_o^2} + \frac{1}{M_o^2} \right) - \left(1 + \frac{1}{M_o^2} \right) \right]}{A_o^2 \left[\frac{1}{A^2} - \frac{1}{A_o^2} \right]} \quad . \qquad \text{(VIII.1-9a)}$$

The parameters ρ, ρ_o, M, M_o, A and A_o which are inlet and outlet values of density, mach number and area at the junction and depend on the flow direction. The relations between them are

$$\frac{\rho}{\rho_o} = \exp\left[-(M^2 - M_o^2)/2\right] \quad . \qquad \text{(VIII.1-9b)}$$

and

$$\left(\frac{A_o}{A} \right)^2 = \left(\frac{M}{M_o} \right)^2 \exp\left[-(M^2 - M_o^2)\right] \quad . \qquad \text{(VIII.1-9c)}$$

The assumptions required to arrive at Equations VIII.1-9b and VIII.1-9c are:

(1) steady frictionless isentropic flow

(2) constant sonic velocity across the area change.

In the limit of incompressible flow, $\mathcal{J}_j$ becomes

$$\mathcal{J}_j = \frac{1}{2\rho_o} \left(\frac{1}{A^2} - \frac{1}{A_o^2} \right) . \qquad \text{(VIII.1-9d)}$$

In the case of homogeneous flow (no separation) the gravity term becomes

$$-\left[\int_K^j \rho\, dz + \int_j^L \rho\, dz\right] g = [\bar{\rho}_K(z_K - z_j) - \bar{\rho}_L(z_L - z_j)]g \ . \quad \text{(VIII.1-9e)}$$

Equation VIII.1-9 may be rewritten concisely as:

$$I_j \frac{dW_j^{n+1}}{dt} = MF_K^n - MF_L^n - (F_{fK} + F_{fL})^n - F_{fj}^{n+1} + MF_j^{n+1} + (p_K - p_L)^{n+1}$$

$$+ (P_{Kg} - P_{Lg})^n \ , \quad \text{where } j = 1, 2, \ldots, k \ . \quad \text{(VIII.1-10)}$$

In Equations VIII.1-9 and VIII.1-10 above

A_i = flow area of volume i, ft^2

$A_j(t)$ = flow area of junction j (possibly time dependent), ft^2

D_{h_i} = hydraulic diameter of flow area A_i, ft

F_{fi} = Fanning friction pressure loss within each half-volume, $V_i/2$,

$$= \frac{f_i \rho_i \bar{W}_i |\bar{W}_i|}{D_{h_i} \bar{\rho}_i A_i^2} \ , \text{ psi}$$

F_{fj} = junction friction pressure caused by form drag losses and area changes

$$= \frac{K_j W_j |W_j|}{2\rho_j [A_j(t)]^2} \ , \text{ psi}$$

f = Fanning friction factor, dimensionless

g = gravitational constant = 32.174 ft/s^2

1756 267

I_j = geometric "inertia" for junction j

$$= \frac{\ell_K}{2A_K} + \frac{\ell_L}{2A_L} \text{ , } ft^{-1}$$

K_j = junction friction coefficient, dimensionless

ℓ_i = length of volume i, ft

M_j = junction Mach number, dimensionless

MF_i = momentum flux of volume center

$$= \bar{W}_i^2 / (\bar{\rho}_i A_i^2)$$

MF_j = momentum flux due to area change,

$$= \mathcal{J}_i W_j^2$$

p_i = thermodynamic pressure at volume V_i center, psi

P_{Kg} = gravity pressure differential from the center of volume K to junction j, psi

P_{Lg} = gravity pressure differential from junction j to the center of volume L, psi

V_i = displacement of volume i, ft^3

$\bar{W}_i$ = average mass flow for volume i, lb/s

z_i = volume center heights above reference height z_{ref}, ft

z_j = junction height above reference height z_{ref}, ft

$\bar{\rho}_i$ = fluid density in volume i, lb/ft^3

ρ_j = fluid density at junction j, lb/ft^3

$\Phi^2_{tp_i}$ = two phase flow friction multiplier, dimensionless

CONSERVATION OF ENERGY

$$\frac{dU_i^{n+1}}{dt} = - \frac{\ell_i}{2A_i}\left[\frac{d}{dt}\left(\frac{\bar{W}_i^2}{\bar{\rho}_i}\right)\right]^n + \sum_{j\varepsilon T_i} W_j^{n+1}\left\{h_j^n + \frac{1}{2}\left[\left(\frac{W_j}{\rho_j A_i}\right)^2\right]^n + g(z_j - z_i)\right\}$$

$$- \sum_{\substack{j\varepsilon I \\ i}} W_j^{n+1}\left\{h_j^n + \frac{1}{2}\left[\left(\frac{W_j}{\rho_j A_j}\right)^2\right]^n + g(z_j - z_i)\right\} + \sum_{j>K} W^n_{j_{FILL}}\, h^n_{j_{FILL}} + Q_i^n \qquad \text{(VIII.1-11)}$$

where

h_j = specific fluid enthalpy of junction j, Btu/lb

$h_{j_{FILL}}$ = prescribed fill junction enthalpy, Btu/lb

U_i = total internal energy, Btu

Q_i = rate of heat energy transferred into volume i, Btu/s

The first term represents the rate of change of internal energy. The second term represents the energy added or subtracted at the fill junction. The last term represents the heat addition in a control volume.

The specific internal energy, u_i, is by definition the ratio of the total internal energy, U_i, to the total mass, M_i,

$$u_i = \frac{U_i}{M_i} \qquad \text{(VIII.1-12)}$$

and the average fluid density $\bar{\rho}_i$ is

$$\bar{\rho} = \frac{M_i}{V_i} \quad . \qquad \text{(VIII.1-13)}$$

The thermodynamic or static pressure is obtained from the steam tables with a call of the form

$$p_i = P_{eos}\ (u_i, \bar{\rho}_i) \quad . \qquad \text{(VIII.1-14)}$$

The tables themselves are constructed using temperature and specific volume as variables. The state properties calculation are discussed in Section VIII.1.1.1.2.

Due to the scalar nature of the mass and energy, their respective equations can represent junctions from many directions. The vector nature of the momentum

equations requires assumptions on the directional momentum flux terms and, in fact, the cross product terms are neglected. The momentum equation can only connect two volumes but one volume may have many junctions. By appropriate specification of input, the RETRAN code can represent flow in two or three dimensions. The resulting equations represent multi-dimensional flow with the approximation that the cross product terms in the momentum equations are neglected.

To evaluate the terms involving the volume average flow rate, $\bar{W}_i$, the following is used:

$$\bar{W}_i = \left(\sum_{j \varepsilon T_i} W_j + \sum_{j \varepsilon I_i} W_j \right) \Big/ 2 \qquad \text{(VIII.1-15)}$$

which assumes that all junction directions are the same.

Equation VIII.1-15 states that the flow in volume i is the simple average of all inlet and outlet flows.

The junction enthalpy, h_j and kinetic energy, $1/2\ (W_j/\rho_j A_i)^2$ in the energy equation are evaluated immediately upstream of the actual junction flow area, A_j, that connects one volume to another volume or flow source, where A_i is the flow area of the doner volume. The junction enthalpy and kinetic energy are determined by the fluid properties of the source of flow, W_j. For example, if W_j is negative, that is, if W_j is a flow out of volume k, then h_j and W_j are determined by the properties of volume k. Hence, the junction enthalpy and kinetic energy with respect to the source volume are:

$$h_j + \frac{1}{2} [W_j/\rho_j A_K]^2 + Z_j = h_K + \frac{1}{2} (\bar{W}_K/\bar{\rho}_K A_K)^2 + Z_K + \Delta h_{Q,s_{Kj}} ; \; W_j \geq 0 \qquad \text{(VIII.1-16a)}$$

$$h_j + \frac{1}{2} [W_j/\rho_j A_L] + Z_j = h_L + \frac{1}{2} (\bar{W}_L/\bar{\rho}_L A_L)^2 + Z_L + \Delta h_{Q,s_{Lj}} ; \; W_j < 0 \qquad \text{(VIII.1-16b)}$$

where

h_i = enthalpy of source volume i, i = K,L,

$\Delta h_{Q,s_{ij}}$ = junction enthalpy change from center of volume to junction due to heating within source volume i, or enthalpy change due to phase separation at junction j within source volume i.

The concept of "borrowing" volume quantities and donating them to a junction (or vice versa) is called donor cell.[VIII.1-3]

The rate of enthalpy increase due to heating within volume i at junction j is modeled by the equation

$$M_i^n \left[\frac{dh_j}{dt}\right]^{n+1} + [(\Delta h_i)_q \ |\bar{W}_i + W_j|]^n = Q_i^n \qquad \text{(VIII.1-17a)}$$

The heating model, Equation VIII.1-17a, is applicable only for a single-path volume with one inlet and one outlet junction and for homogeneous fluid with no phase separation. This model is obtained from the integral mass and energy conservation equations applied to the half-volume that represents the outlet side of a heated RETRAN control volume. Kinetic and potential energy changes are neglected and pressure is assumed to be independent of time.

For steady flow, $\Delta h_{Qi} = Q_i/2\bar{W}_i$ is the proper limit for heating with negligible pressure changes. The heating model also has the numerical property that the junction enthalpy changes smoothly when the flow direction reverses. Without the heating model, the junction enthalpy is defined strictly by the source volume conditions and the junction enthalpy is permitted to change discontinuously during a flow reversal when the source volume changes. Thus, the heating model is physically reasonable during a flow reversal for a volume representing a single flow path channel. The standard junction enthalpy defined by the source volume can be discontinuous during flow reversals and is physically reasonable in unheated volumes in which the fluid is well mixed.

The heating model is optional and is controlled by the input data for the junction description. Likewise, use of the separation model is optional and is controlled by the input data for both the junction and volume descriptions.

The junction density is also obtained by use of the doner cell concept. First the junction pressure defined as

$$p_j = p_K - P_{Kg} - F_{fK} \qquad W_j \geq 0 \qquad \text{(VIII.1-17b)}$$

$$p_j = p_L - P_{Lg} - F_{gL} \qquad W_j < 0 \qquad \text{(VIII.1-17c)}$$

is computed. The junction enthalpy h_j is computed from Equation VIII.1-16a or VIII.1-16b depending on the flow direction together with the heating or separation model.

The junction density is then computed from a pressure-enthlapy state relation as

$$v_j = v(p_j, h_j) \qquad \text{(VIII.1-17d)}$$

where

$$v_j = 1/\rho_j \qquad \text{(VIII.1-17e)}$$

Equations VIII.1-8, VIII.1-10, VIII.1-11 and VIII.1-14 are now cast into the FLASH form. It should be emphasized that this technique transforms this system of non-linear coupled ordinary differential equations into another, different, system of linear coupled differential equations. The transformed set is subsequently differenced, rearranged and solved for an array of flow changes.

Let,

$$Y = \begin{bmatrix} W_1 \\ \vdots \\ W_j \\ \vdots \\ W_k \\ M_1 \\ \vdots \\ M_i \\ \vdots \\ M_{NVOL} \\ U_1 \\ \vdots \\ U_i \\ \vdots \\ U_{NVOL} \end{bmatrix} \qquad \text{(VIII.1-18)}$$

be a vector of length k+2NVOL representing the dependent variables. Equations VIII.1-8, VIII.1-10, and VIII.1-11 may be compactly written as

$$\frac{dY}{dt} = \begin{bmatrix} \vdots \\ I_j^{-1}(p_K - p_L)^{n+1} - I_j^{-1}F_j^{n+1} + I_j^{-1}MF_j^{n+1} \\ \vdots \\ \sum_{j\varepsilon T_i} W_j^{n+1} \quad \sum_{j\varepsilon I_i} W_j^{n+1} \\ \vdots \\ \sum_{j\varepsilon T_i} W_j^{n+1} e_j^n - \sum_{j\varepsilon I_i} W_j^{n+1} e_j^n \end{bmatrix} + \begin{bmatrix} \vdots \\ I_j^{-1}(MF_K - MF_L) \\ -I_j^{-1}(F_{fK} + F_{fL}) + I_j^{-1}(P_{Kg} - P_{Lg}) \\ \vdots \\ \sum_{j>k} W_{j_{FILL}} \\ \vdots \\ -\frac{\ell_i}{2A_i}\frac{d}{dt}\frac{\bar{W}_i^2}{\bar{\rho}_i} + Q_i \\ + \sum_{j>K} W_{j_{FILL}} h_{j_{FILL}} \end{bmatrix}^n \qquad \text{(VIII.1-19)}$$

where

$$e_j = h_j + \frac{1}{2}\left[\frac{W_j}{\rho_j A_j(t)}\right]^2 + z_j - z_i \qquad \text{(VIII.1-20)}$$

Equation VIII.1-19 may be considered to be of the form

$$\frac{dY}{dt} = f^{n+1} + g^n \,. \qquad \text{(VIII.1-21)}$$

For more flexibility, Equation (VIII.1-22) is written in final form as

$$\frac{dY}{dt} = \theta f^{n+1} + (1 - \theta)f^n + g^n \qquad \text{(VIII.1-22)}$$

where θ is a user-supplied dimensionless constant representing the "implicit-explicit" proportion multiplier. When $\theta = 0$, a completely explicit numerical scheme is produced. When $\theta = 0.5$, the Crank-Nicolson[VIII.1-4] scheme results and when $\theta = 1$, the "fully implicit" numerical scheme is produced.

Equation VIII.1-22 is linearized according to Equation VIII.1-4 as

$$\frac{dY}{dt} = \theta \left(\frac{\partial f_i}{\partial Y_j} \right) \Bigg|_{Y_n} (Y^{n+1} - Y^n) + E^n \qquad \text{(VIII.1-23a)}$$

or

$$\frac{dY}{dt} = \theta \begin{bmatrix} \frac{\partial f_1}{\partial Y_1} & \cdots & \frac{\partial f_1}{\partial Y_{k+2NVOL}} \\ \vdots & \vdots & \vdots \\ \frac{\partial f_{k+2NVOL}}{\partial Y_1} & \cdots & \frac{\partial f_{k+2NVOL}}{\partial Y_{k+2NVOL}} \end{bmatrix}^n \begin{bmatrix} (Y^{n+1} - Y^n)_1 \\ \vdots \\ (Y^{n+1} - Y)^n_{k+2NVOL} \end{bmatrix} + \begin{bmatrix} E_1 \\ \vdots \\ E_{k+2NVOL} \end{bmatrix}^n \qquad \text{(VIII.1-23b)}$$

where $E^n = (1 - \theta) f^n + g^n$. (VIII.1-23c)

In order to compute the $\partial f_i / \partial y_i$ according to the FLASH technique, it is assumed that the variables are independent of each other. Therefore such terms as

$$\frac{\partial \left(\sum_{j \varepsilon T_i} W_j^{n+1} \right)}{\partial W_j^{n+1}} = +1 \; ; \quad \frac{\partial \left(\sum_{j \varepsilon I_i} W_j^{n+1} \right)}{\partial W_j^{n+1}} = -1 \qquad \text{(VIII.1-24)}$$

or

$$\frac{\partial (p_K - p_L)^{n+1}}{\partial W_j} = 0 \ . \qquad \text{(VIII.1-25)}$$

Derivatives of flows with respect to mass and internal energy are set to zero as:

$$\frac{\partial \left(\sum_{\substack{j \varepsilon T_i \\ \text{or } I_i}} W_j^{n+1} \right)}{\partial M_i^{n+1}} = 0 \qquad \text{(VIII.1-26)}$$

and

$$\frac{\partial \left(\sum_{\substack{j \varepsilon T_i \\ \text{or } I_i}} W_j \right)}{\partial U_i^{n+1}} = 0 \qquad \text{(VIII.1-27)}$$

The derivative of the junction friction is:

$$I_j^{-1} \frac{\partial F_{fj}^{n+1}}{\partial W_j} = \frac{K_j^n S_{gn} (W_j^n) W_j^{n+1}}{I_j \rho_j^n [A_j(t)]^2} \ . \qquad \text{(VIII.1-28)}$$

and the derivative of the junction momentum flux is

$$I_j^{-1} \frac{\partial MF_j^{n+1}}{\partial W_j} = 2 W_j^{n+1} \mathcal{J}_j^n \qquad \text{(VIII.1-29)}$$

Equations VIII.1-28 and VIII.1-29 may be combined as

$$- I_j^{-1} \frac{\partial F_{fj}^{n+1}}{\partial W_j} + I_j^{-1} \frac{\partial MF_j^{n+1}}{\partial W_j} = F_j^{n+1} \qquad \text{(VIII.1-30a)}$$

where

$$F_j^n = I_j^{-1}\left\{ - \frac{K_j S_{gn}(W_j^n)}{\rho_j^n [A_j(t^n)]^2} + 2\mathcal{J}_j^n \right\} W_j^n \qquad \text{(VIII.1-30b)}$$

Carrying out the differentiation as just explained, the linearized version of Equation VIII.1-19 is

$$\frac{d}{dt}\begin{bmatrix} \vdots \\ W_j \\ \vdots \\ M_i \\ \vdots \\ U_i \\ \vdots \end{bmatrix}^{n+1} = \theta \begin{bmatrix} \vdots & & \vdots & & \vdots \\ \cdots F_j \cdots I_j^{-1}\frac{\partial p}{\partial M}_K & \cdots & I_j^{-1}\frac{\partial p}{\partial M}_L \cdots & \cdots & I_j^{-1}\frac{\partial p}{\partial U}_K \cdots I_j^{-1}\frac{\partial p}{\partial U}_L \cdots \\ \vdots & & \vdots & & \vdots \\ \cdots \pm 1 \cdots & & 0,0 & \cdots & 0,0 \cdots \\ \vdots & & \vdots & & \vdots \\ \cdots \pm e_j \cdots & & 0,0 & \cdots & 0,00 \cdots \\ \vdots & & \vdots & & \vdots \end{bmatrix}^{n} \begin{bmatrix} \vdots \\ W_j^{n+1} - W_j^n \\ \vdots \\ M_K^{n+1} - M_K^n \\ M_L^{n+1} - M_L^n \\ \vdots \\ U_K^{n+1} - U_K^n \\ U_L^{n+1} - U_L^n \\ \vdots \end{bmatrix} + \begin{bmatrix} \vdots \\ E_j \\ \vdots \\ E_{k+i} \\ \vdots \\ E_{k+NVOL+i} \\ \vdots \end{bmatrix}$$

(VIII.1-31)

In order to clearly see the structure of each general linearized flow, mass and energy equation, Equation VIII.1-31 is expanded as

1356 276

$$\frac{dW_j^{n+1}}{dt} = \theta\left[F_j^n\left(W_j^{n+1} - W_j^n\right) + I_j^{-1}\left(\frac{\partial p}{\partial M}\right)_K^n\left(M_K^{n+1} - M_K^n\right) - I_j^{-1}\left(\frac{\partial p}{\partial M}\right)_L\left(M_L^{n+1} - M_1^n\right)\right.$$

$$\left. + I_j^{-1}\left(\frac{\partial p}{\partial U}\right)_K\left(U_K^{n+1} - U_K^n\right) - I_j^{-1}\left(\frac{\partial p}{\partial U}\right)_L\left(U_L^{n+1} - U_L^n\right)\right] + E_j^n \qquad \text{(VIII.1-32)}$$

where $j = 1, 2, \ldots, k$

$$\frac{dM_i^{n+1}}{dt} = \theta\left[\sum_{j\varepsilon T_i}\left(W_j^{n+1} - W_j^n\right) - \sum_{j\varepsilon I_i}\left(W_j - W_j^n\right)\right] + E_{k+i}^n \qquad \text{(VIII.1-33)}$$

where $j = 1, 2, \ldots, NVOL$

and

$$\frac{dU_i^{n+1}}{dt} = \theta\left[\sum_{j\varepsilon T_i} e_j^n\left(W_j^{n+1} - W_j^n\right) - \sum_{j\varepsilon T_i} e_j^n\left(W_j^{n+1} + W_j^n\right)\right] + E_{k+NVOL+i}^n$$

(VIII.1-34)

where $j = 1, 2, \ldots, NVO$.

Next the time derivatives in Equations VIII.1-32 through VIII.1-34 are forward differenced as:

$$\frac{dY^{n+1}}{dt} = \frac{Y^{n+1} - Y^n}{t^{n+1} - t^n} = \frac{\Delta Y^n}{\Delta t^n} . \qquad \text{(VIII.1-35)}$$

After carrying out the indicated differencing, Equations VIII.1-32 through VIII.1-34 may be rearranged as

$$(1 - \theta\,\Delta t\,F_j^n)\,\Delta W_j^n = \Delta t\,\theta\left[I_j^{-1}\left(\frac{\partial p}{\partial M}\right)_K^n \Delta M_K^n - I_j^{-1}\left(\frac{\partial p}{\partial M}\right)^n \Delta M_L^n\right]$$

$$+\,\Delta t\,\theta\left[I_j^{-1}\left(\frac{\partial p}{\partial U}\right)_K^n \Delta U_K^n - I_j^{-1}\left(\frac{\partial p}{\partial U}\right)_L^n \Delta U_L^n\right] + \Delta t\,E_j^n \qquad \text{(VIII.1-36)}$$

$$\Delta M_i^n = \theta\,\Delta t\left(\sum_{j\varepsilon T_i} \Delta W_j^n - \sum_{j\varepsilon I_i} \Delta W_j^n\right) + \Delta t\,E_{k+1}^n \qquad \text{(VIII.1-37)}$$

and

$$\Delta U_i^n = \theta\,\Delta t\left(\sum_{j\varepsilon T_i} e_j^n\,\Delta W_j^n - \sum_{j\varepsilon I_i} e_j^n\,\Delta W_j^n\right) + \Delta t\,E_{k+NVOL+i}^n \qquad \text{(VIII.1-38)}$$

Equations VIII.1-36 through VIII.1-38 constitute a coupled linear system of k+2NVOL unknowns involving ΔW_j^n, ΔM_i^n and ΔU_i^n. Because of the simple form of the differenced mass and energy equations, they may be used to eliminate ΔM_i^n and ΔU_i^n in the flow equations as:

$$(1 - \theta\Delta t\,F_j^n)\,\Delta W_j^n = \theta\,\Delta t\,I_j^{-1}\left[\left(\frac{\partial p}{\partial M}\right)_K^n \theta\,\Delta t\left(\sum_{j\varepsilon T_K} \Delta W_j^n - \sum_{j\varepsilon I_K} \Delta W_j^n\right)\right.$$

$$\left. + \left(\frac{\partial p}{\partial M}\right)_K^n \Delta t\,E_{k+K}^n\right] - \theta\,\Delta t\,I_j^{-1}\left[\left(\frac{\partial p}{\partial M}\right)_L^n \theta\,\Delta t\left(\sum_{j\varepsilon T_L} \Delta W_j^n - \sum_{j\varepsilon I_L} \Delta W_j^n\right)\right.$$

$$\left. + \left(\frac{\partial p}{\partial M}\right)_L^n \Delta t\,E_{K+L}^n\right] + \theta\,\Delta t\,I_j^{-1}\left[\left(\frac{\partial p}{\partial U}\right)_K^n \theta\,\Delta t\left(\sum_{j\varepsilon T_K} e_j \Delta W_j^n - \sum_{j\varepsilon I_K} e_j\,\Delta W_j^n\right)\right.$$

$$\left. + \left(\frac{\partial p}{\partial U}\right)_K^n \Delta t\,E_{k+NVOL+K}^n\right] - \theta\,\Delta t\,I_j^{-1}\left[\left(\frac{\partial p}{\partial U}\right)_L^n \theta\,\Delta t\left(\sum_{j\varepsilon T_L} e_j\,\Delta W_j^n - \sum_{j\varepsilon I_L} e_j\,\Delta W_j^n\right)\right.$$

$$\left. + \left(\frac{\partial p}{\partial U}\right)_L^n \Delta t\,E_{k+NVOL+L}^n\right] + \Delta t\,E_j^n\,. \qquad \text{where } j = 1, 2, \ldots, k \qquad \text{(VIII.1-39)}$$

1256 278

Equation VIII.1-39 can be arranged into the form

$$A^n \Delta W^n = B^n \qquad \text{(VIII.1-40)}$$

where A is a kxk matrix and B is a column vector of length k. The diagonal elements of A have the forms, assuming positive flow from volume K to volume L

$$A^n_{jj} = 1 - \theta\ \Delta t\ F^n_j + (\theta\ \Delta t)^2 C^n_{dj} \qquad \text{(VIII.1-41)}$$

where

$$C^n_{dj} = I_j^{-1}\left[\left(\frac{\partial p}{\partial M}\right)_K + \left(\frac{\partial p}{\partial M}\right)_L + \left(\frac{\partial p}{\partial U}\right)_K e_j + \left(\frac{\partial p}{\partial U}\right)_L e_j\right]^n \qquad \text{(VIII.1-42)}$$

The elements of B^n have the form

$$B^n_j = \Delta t\ E^n_j + \theta\ (\Delta t)^2\ I_j^{-1}\left[\left(\frac{\partial p}{\partial M}\right)^n_K E^n_{k+k} - \left(\frac{\partial p}{\partial M}\right)^n_L E^n_{k+L}\right]$$

$$+ \theta(\Delta t)^2\ I_j^{-1}\left[\left(\frac{\partial p}{\partial U}\right)^n_K E^n_{k+NVOL+K} - \left(\frac{\partial p}{\partial U}\right)^n_L E^n_{k+NVOL+L}\right] \qquad \text{(VIII.1-43)}$$

The off-diagonal terms $A_{j\ell}$, $j \neq \ell$ have different forms depending upon whether $\ell \varepsilon T_k$, I_k, T_L or I_L. Except for the degenerate case where ℓ is not a member of any of the sets and $A_{j\ell} = 0$, the form of the $A_{j\ell}$ is

$$A^n_{j\ell} = (\Delta t\ \theta)^2\ C^n_{o\ell}\ ,\ \ell \neq j. \qquad \text{(VIII.1-44)}$$

A general form for C_{cj} is obtained for the case εI_K and T_L (flow from volume K to volume L).

In this case:

$$C_{o\ell}^{n} = I_j^{-1}\left[\left(\frac{\partial p}{\partial M}\right)_K + \left(\frac{\partial p}{\partial M}\right)_L + \left(\frac{\partial p}{\partial U}\right)_K e_\ell + \left(\frac{\partial p}{\partial U}\right)_L e_\ell\right]^n \qquad \text{(VIII.1-45)}$$

The numerical calculation for ΔW_j^n is discussed in a later subsection of Section VIII. After the ΔW_j^n's are computed from Equation VIII.1-39, they are substituted into Equations VIII.1-37 and VIII.1-38 to obtain updated volume masses and energies.

1.1.1.2 State Properties

Tables of steam and water properties were generated by use of the ASTEM package [VIII.1-7] which uses the 1967 International Formulation Committee (IFC) formulation for industrial use of the properties of steam[VIII.1-5,VIII.1-6]. STH2ØG then writes these tables on a data set in the proper format for RETRAN. Properties stored in the tables as functions of pressure and temperature include specific volume, internal energy, coefficient of thermal expansion, isothermal compressibility, and the isopiestic heat capacity. The data spacing in the tables is variable permitting the density to be greatest where the most accuracy is required, but the tables must be regenerated to change the data distribution.

State properties in the data tables are in the SI units. The nomenclature used in this section and the units of the properties are:

T	Temperature	kelvin (K)
p	Pressure	pascal (Pa) = newton/meter^2(N/m^2) = joule/meter^3(J/m^3)
v	Specific volume	meter^3/kilogram (m^3/kg)
u	Specific internal energy	joule/kilogram (J/kg)
h	Enthalpy	joule/kilogram (J/kg)
$\beta = \frac{1}{v}\frac{\partial v}{\partial T}\|_p$	Coefficient of thermal expansion	kelvin^{-1} (K^{-1})
$\kappa = \frac{1}{v}\frac{\partial v}{\partial P}\|_T$	Isothermal compressibility	pascal^{-1} (Pa^{-1})
$c_p = \frac{\partial h}{\partial T}\|_p$	Isopiestic heat capacity	joule/kilogram-kelvin (J/kg-K)

f	Saturated liquid subscript
g	Saturated vapor subscript
sat	Saturated pressure subscript

The data file contains five tables packed into a single-dimensioned array. The first two tables are temperatures and pressures obtained from input data; the third table contains saturation properties as a function of the saturation temperatures in the temperature table; the fourth table is a separate saturation table as a function of the saturation pressures in the pressure table; and the fifth table is a two-dimensional table containing the single-phase properties as a function of the temperatures and pressures in the first two tables. The tables are written on a data set for use by other modules utilizing the subroutines. The tables are generated and stored using full word floating-point quantities where a full word is a 64-bit or 60-bit item for IBM and CDC machines respectively.

In the description of the tables, A is used for the array symbol, NT is the number of temperatures entered, and NP is the number of pressures entered into the table. NS is the number of input temperatures not above the critical temperature, and NS2 is the number of input pressures not above the critical pressure. The table storage is as follows:

(1) The temperatures in increasing order, as obtained from the input data, are stored in A(1) through A(NT). The temperature can be considered to be stored in any array dimensioned T(NT), where T(1) is equivalenced to A(1).

(2) The pressures in increasing order, as obtained from the input data, are stored in A(NT + 1) through A(NT + NP). The pressures can be considered to be stored in any array dimensioned P(NP), where P(1) is equivalenced to A(NT + 1).

(3) The saturation properties as a function of temperature are stored in A(NT + NP + 1) through A(NT + NP + NS*11). The saturation properties are stored as an array dimensioned B(11,NS), where B(1,1) is equivalenced to A(NT + NP + 1). The saturation values in B(N,1), $1 \leq N \leq 11$, are a function of the temperature in T(I). The correspondence between the B array and the saturation properties are:

B(1,I)	P	B(7,I)	v_g
B(2,I)	v_f	B(8,I)	u_g
B(3,I)	u_f	B(9,I)	β_g
B(4,I)	β_f	B(10,I)	κ_g
B(5,I)	κ_f	B(11,I)	c_{pg}
B(6,I)	c_{pf}		

(4) The saturation properties as a function of pressure are stored in A(NT + NP + NS*11 + 1) through A(NT + NP + NS*11 + NS2*11). The saturation values in C(N,J), $1 \leq N \leq 11$, are a function of the pressure in P(J). The correspondence between the C array and the saturation properties is the same as for the B array except that C(1,J) is the saturation temperature instead of the saturation pressure.

(5) The single-phase properties as a function of temperature and pressure are stored in A(NT + NP + NS*11 + NS2*11 + 1) through A(NT + NP + NS*11 + NS2*11 + NT*NP*5). The single-phase properties are stored as an array dimensioned D(5,NT,NP), where D(1,1,1) is equivalenced to A(NT + NP + NS*11 + NS2*11 + 1). The values D(N,I,J), $1 \leq N \leq 5$, are a function of the temperature in T(I) and the pressure in P(J). The correspondence between the D values and the properties are:

D(1,I,J)	v	D(4,I,J)	κ
D(2,I,J)	u	D(5,I,J)	c_p
D(3,I,J)	β		

The data containing the steam-water property data consists of two binary records. The first record contains NT, NP, NS, and NS2. The second record contains the A array which has NTOT elements, where NTØT = NT + NP + NS*11 + NT*NP*5.

The STH2ØI subroutine resides in the RETRAN source and is a special purpose subroutine used to retrieve the tables needed by the other STH2Ø subroutines. STH2ØI uses the first record of the state properties data set to initialize the STH2ØC common block. Additionally, STH2ØI reserves a block of central memory for the A array, and then moves the table from the state properties data set into the A array.

1356 282

The water property file resides on a disk and is brought into RETRAN by calling subroutine STH2ØI. This call is of the form CALL STH2ØI and must preceed any reference to the other water property subroutines. It need be executed only once unless the data array is destroyed. On CDC systems, the file has W-type records with I-type blocking, and on IBM systems the file has a VS record format with a maximum blocking of the 800 bytes.

The integer variable, IT, is set by the STH2Ø subroutines that can compute properties in the liquid, two-phase, and vapor states. IT is set to 1 for the liquid state, 2 for the two-phase state, 3 for the vapor state below the critical temperature, and 4 for the state above the critical temperature. Water above the critical pressure, but below the critical temperature, is considered to be in the liquid state.

S is an array of twenty-three floating-point words containing both input to and output from the subroutines. The assignment of properties to the S array is:

S(1)	T	S(13)	u_f
S(2)	P	S(14)	u_g
S(3)	v	S(15)	h_f
S(4)	u	S(16)	h_g
S(5)	h	S(17)	β_f
S(6)	β	S(18)	β_g
S(7)	κ	S(19)	κ_f
S(8)	c_p	S(20)	κ_g
S(9)	X(quality)	S(21)	c_{pf}
S(10)	P_{sat}	S(22)	c_{pg}
S(11)	v_f	S(23)	indices
S(12)	v_g		

S(6) through S(8) are undefined if IT is returned as 2. S(9) contains 0.0 if IT is returned as 1, contains the quality if IT is returned as 2, and contains 1.0 if IT is returned as 3 or 4. S(10) is the saturation pressure corresponding to the temperature in S(1) if IT is returned as 1 through 3 and is undefined if IT is returned as 4. S(11) through S(22) are undefined if IT is not returned as 2. The S array is used for working storage and undefined elements may be changed during subroutine execution. On entry, the indices in S(23) are used to start

the table search, if they are valid. On return, S(23) contains the indices obtained by the table search. Execution time can be minimized if the table indices returned are saved and used subsequently to start a table search. The subroutines do not fail when invalid indices are entered in S(23) because the table search will then start at the beginning of the table.

An error flag, ERR, is returned FALSE if the input quantities are within the range of the tables and TRUE otherwise.

CALL STH2ØØ (T, P, ERR) computes the saturation pressure P given the temperature T as input. The temperature must be in the range 273.16K $\leq$ T $\leq$ 647.30K. This subroutine does not use the A array and can be called before STH2Ø1 is called.

CALL STH2Ø1 (A, S, ERR) computes the saturated water properties given temperature and quality as input. The temperature is entered in S(1) and must be greater than or equal to either T(1) or C(1,1) and less than or equal to either T(NS) or C(1,NS2). The quality, X, is entered in S(9) and must be in the range 0.0 $\leq$ X $\leq$ 1.0. S(3) through S(5) returned values for the two-phase mixture and S(11) through S(22) return values for saturated liquid and saturated vapor. S(2) and S(10) are returned equal. IT would always be 2 for this call and thus is not included in the argument list.

CALL STH2Ø2 (A, S, ERR) computes saturated water properties given pressure and quality as input. The pressure is entered in S(2) and must be greater than or equal to the triple point pressure (611.2 Pa). The saturation temperature is returned in S(1) and the other elements of S are set as in STH2Ø1. STH2Ø2 is an entry point in the STH2Ø1 subroutine.

CALL STH2Ø3 (A, S, IT, ERR) computes single-phase water properties given temperature and pressure as input. The temperature, T, is entered in S(1) and must be within the range T(1) $\leq$ T $\leq$ T(NT). The pressure, P, is entered in S(2) and must be within the range 0 < P $\leq$ P(NP) for the vapor state and P(1) $\leq$ P $\leq$ P(NP) for the liquid state. IT is never set to 2 because temperature and pressure cannot determine a two-phase condition. The single-phase quantities are returned in S(3) through S(8), and S(9) is set to either 0.0 or 1.0 corresponding to the liquid or vapor state, respectively.

CALL STH2Ø4 (A, S, IT, ERR) computes water properties given temperature and specific volume as input. The temperature, T, is entered in S(1) and must be within the range $T(1) \leq T \leq T(NT)$. The range of specific volume depends on the state. If the temperature and specific volume indicate the liquid state, the resultant pressure, P, must be within the range $P(1) \leq P \leq P(NP)$. If the temperature and specific volume indicate the superheated state, the resultant pressure must be less than P(NP). S(6) through S(8) are undefined if IT is returned as 2. S(9) contains 0.0 if IT is returned as 1, contains the quality if IT is returned as 2, and contains 1.0 if IT is returned as 3 or 4. S(10) is the saturation pressure corresponding to the temperature in S(1) if IT is returned as 1 through 3 and is undefined if IT is returned as 4. S(11) through S(22) are undefined if IT is not returned as 2. The S array is used for working storage and undefined elements may be changed during subroutine execution.

Call STH2Ø5 (A, S, IT, ERR) computes water properties given pressure and enthalpy as input. The pressure, P, is entered in S(2) and must be within the range $P(1) \leq P \leq P(NP)$. The enthalpy, h, is entered in S(5). The operation range of STH2Ø5 is further bounded by the temperature range $T(1) \leq T \leq T(NT)$. On return from an STH2Ø5 call, IT is appropriately set to reflect the phase conditions. S(6) through S(8) are undefined if IT is returned as 2. S(9) contains 0.0 if IT is returned as 1, contains the quality if IT is returned as 2, and contains 1.0 if IT is returned as 3 or 4. S(10) is the saturation pressure corresponding to the temperature in S(1) if IT is returned as 1 through 3 and is undefined if IT is returned as 5. S(11) through S(22) are undefined if IT is not returned as 2. The S array is used for working storage and undefined elements may be changed during subroutine execution.

The STH2Ø1, STH2Ø2, STH2Ø3, STH2Ø4, and STH2Ø5 subroutines all use similar table search and interpolation procedures. Linear interpolation is always used for liquid properties and linear or reciprocal interpolation is used for vapor properties based on the perfect gas relations, $PV = RT$, $u = C_v T$, $h = C_p T$, $\beta = T^{-1}$, and $\kappa = P^{-1}$. For example, since $v = RTP^{-1}$, linear interpolation is used for the temperature dependence and reciprocal interpolation is used for the pressure dependence. The linear interpolation is

$$Y = Y_1 + \frac{(Z - Z_1)(Y_2 - Y_1)}{(Z_2 - Z_1)} \quad , \qquad \text{(VIII.1-46)}$$

and the reciprocal interpolation is

$$Y = Y_1 + \frac{(Z - Z_1)\, Z_2\, (Y_2 - Y_1)}{(Z_2 - Z_1)\, Z} \quad . \qquad \text{(VIII.1-47)}$$

The saturation pressure as a function of temperature is always computed using the K function of the IFC formulation. The STH2Ø0 subroutine is just this evaluation. Enthalpy values are always obtained from h = u + Pv.

For the STH2Ø1 subroutine, the saturation pressure is obtained from the K function. Both the saturated table as a function of temperature and the saturated table as a function of pressure are searched and the nearest bracketing values are used for interpolation. The saturated liquid properties are obtained by linear interpolation on temperature. The saturated vapor specific volume is obtained from

$$r = \frac{T - T_1}{T_2 - T_1} \quad , \quad v = \left[(1 - r)\, \frac{P_1}{T_1}\, v_1 + r\, \frac{P_2}{T_2}\, v_2 \right] \frac{T}{P} \quad . \qquad \text{(VIII.1-48)}$$

Linear interpolation on temperature is used for saturated vapor in ernal energy. The saturated vapor thermal expansion is obtained from reciprocal interpolation on temperature; the saturated vapor compressibility is obtained from reciprocal interpolation on pressure; and the saturated vapor heat capacity is obtained from linear interpolation on temperature. The two phase values of specific volume, internal energy, and enthalpy are obtained from the saturated liquid and vapor values and the quality, e.g.,

$$v = (1 - x)\, V_f + x v_g \quad . \qquad \text{(VIII.1-49)}$$

For the STH2Ø2 subroutine, the saturation temperature is estimated from the input pressure, using equations given in SHARE Program 1095 converted to SI units. The equations are given below with the values in parentheses being the original values for temperature in deg.F and pressure in lb_f/in^2.

$$C_1 \leq P < C_2 \qquad C_2 \leq P \leq C_4 \qquad \text{(VIII.1-50a,50b)}$$

$$T = \sum_{i=0}^{8} A_i \left[\ln(C_3 P) \right]^i \qquad T = \sum_{i=0}^{5} B_i \left[\ln(C_5 P) \right]^i \qquad \text{(VIII.1-51a,51b)}$$

$A_0 = 274.9043833(35.157890)$ $B_0 = 6669.352222(11545.164)$

$A_1 = 13.66254889(24.592588)$ $B_1 = -4658.899(-8386.0182)$

$A_2 = 1.176781611(2.1182069)$ $B_2 = 1376.536722(2477.7661)$

$A_3 = -.189693(-0.34144740)$ $B_3 = -201.9126167(-363.44271)$

$A_4 = 8.74535666 \times 10^{-2}(0.15741642)$ $B_4 = 14.82832111(26.690978)$

$A_5 = -1.7405225 \times 10^{-2}(-3.132958 \times 10^{-2})$ $B_5 = -0.4337434056(-0.78073813)$

$A_6 = 2.147682333 \times 10^{-3}(3.8658282 \times 10^{-3})$ $C_1 = 1378.951459(0.2)$

$A_7 = -1.383432444 \times 10^{-4}(-2.4901784 \times 10^{-4})$ $C_2 = 3102640.782(450.)$

$A_8 = 3.800086611 \times 10^{-6}(6.8401559 \times 10^{-6})$ $C_3 = 1.450377377 \times 10^{-3}(10.)$

$C_4 = 2.212 \times 10^{7}(3206.2)$ $C_5 = 1.450377377 \times 10^{-4}(1.0)$

The estimated temperature is then used by STH2Ø1 to compute the saturation pressure. If the computed pressure does not converge to within 1.0×10^{-4} Pa of the input pressure, the reciprocal of the temperature derivative of the K function is used to predict the new temperature to be used in the next pass thru STH2Ø1. STH2Ø2 is merely an extension o STH2Ø1, allowing saturation pressure calls to use the K function, thus improving the consistency between pressure-quality and temperature-quality steam table entries. STH2Ø1 and STH2Ø2 use a common, table search and interpolation procedure.

For the STH2Ø3 subroutine, the temperature and pressure tables are searched to bracket the input temperature and pressure, and the bracketing temperature and

pressure values and the corresponding values from the single phase table are used in a two-dimensional interpolation procedure. The two-dimensional interpolation procedure consists of two temperature interpolations, one for each bracketing pressure, followed by a pressure interpolation. When the temperatures and pressures bracket the saturation line, not all the single phase values are in the same phase. When this occurs, the appropriate saturation values are used in place of the single phase values that are in the wrong phase. Depending on how the temperatures and pressures bracket the saturation line, saturation values can be used in one or both temperature interpolations or may entirely replace one of the temperature interpolations. For determining whether the state is liquid or vapor, the input pressure is compared to the saturation pressure; the vapor state is assumed in the indeterminate case when the input pressure equals the saturation pressure. Linear interpolation on both temperature and pressure is used for the liquid state. For the vapor state, linear interpolation on temperature is used for all quantities except thermal expansion where reciprocal interpolation is used; for pressure interpolation, reciprocal interpolation is used for specific volume and compressibility and linear interpolation is used for the others.

When the input pressure is below the first pressure table entry and the temperature is such that the state is liquid, ERR is set TRUE. With the same pressure input, but with temperature such that the state is vapor, the water properties can be computed if the input temperature is bounded by the temperature table. For input temperatures above the saturation temperature corresponding to the first pressure table entry, the internal energy, thermal expansion, and heat capacity are obtained from temperature interpolation using the first pressure values and the specific volume and compressibility are given by

$$r = \frac{T - T_1}{T_2 - T_1} \quad , \quad v = \left[(1 - r) \frac{v_1}{T_1} + r \frac{v_2}{T_2} \right] \frac{P_1 T}{P} \quad , \quad \kappa = P^{-1} \quad . \quad \text{(VIII.1-52)}$$

Saturation values are used in place of the lower single phase values if the lower single phase values are in the liquid phase. For input temperatures below the saturation temperature corresponding to the first table pressure value, the saturation values corresponding to the input temperature are used for internal energy and heat capacity, the perfect gas laws $\beta = T^{-1}$ and $\kappa = P^{-1}$ are used for

thermal expansion and compressibility, and the specific volume is computed as for saturated vapor conditions in STH2Ø1 except that the temperature and pressure are not saturation values.

For STH2Ø4, the input specific volume is compared to the saturated liquid and vapor values corresponding to the input temperature to determine whether the state is liquid, two phase, or vapor. The interpolation procedure for two phase is similar to that for STH2Ø1 with the quality determined from

$$x = \frac{v - v_f}{v_g - v_f} . \qquad \text{(VIII.1-53)}$$

For single phase states, the temperature table is searched until the temperature is bracketed and then the specific volumes for the lower bracketing temperature are searched until the input specific volume is bracketed. Two temperature interpolations are made as in STH2Ø3, but because specific volume is not one of the table coordinates, the results of the temperature interpolations may not bracket the input specific volume. When this occurs, the table search is moved in the appropriate direction. When the temperature interpolations bracket the input specific volume, the specific volume interpolation is performed. The procedures for handling the saturation line, determining the state and type of interpolation and the handling of states with pressure below the first table pressure are similar to those in STH2Ø3 with specific volume and pressure exchanging roles.

For STH2Ø5, the input pressure is used with a quality of 0.5 in a call to STH2Ø2. If the input enthalpy lies between h_f and h_g (returned from STH2Ø2), the two-phase properties are computed, IT is set to 2 and a return made.

Single phase properties are computed with a temperature iteration and STH2Ø3, where the appropriate value of IT is determined using the input enthalpy and, h_f and h_g returned from the initial call to STH2Ø2. The input pressure, the temperature estimate from the previous temperature iteration, and the phase index are then used in a call to STH2Ø3. If the enthalpy returned from STH2Ø3 is not converged to the input enthalpy a new temperature estimate is made and a new iteration performed. This iterative procedure is continued until

$$\left[\frac{h_3 - h_I}{h_I}\right] \leq \varepsilon$$

where

h_I = input enthalpy

h_3 = enthalpy returned from STH2Ø3

ε = convergence parameter.

If a convergent solution is not reached in 20 iterations, an error message is written and ERR set TRUE.

1.1.1.3 Phase Separation (Bubble Rise) Model

The phase separation model was described and derived in Section III-1. The numerical treatment is completely explicit. There is no attempt to incorporate the model into the matrix flow solution. First the bubble mass is updated as

$$(M_{gb})_i^{n+1} - (M_{gb})_i^n = (M_g)_i^{n+1} - (M_g)_i^n - \Delta t \left[\sum_{j\varepsilon T_i} \Psi_j x_j W_j \right.$$

$$\left. \sum_{j\varepsilon I_i} \psi_j x_j W_j \right]^n - \Delta t[Av_{bub}(\rho_{gb})\ z_m]_i^n \quad . \qquad \text{(VIII.1-54)}$$

If M_{gb}^{n+1} is negative, it is set to zero. The new value of the average steam volume fraction in the mixture is computed as

$$(\alpha_{gm})_i^{n+1} = (M_{gb})_1^{n+1} / (\rho_g V_m)_i^n \qquad \text{(VIII.1-55)}$$

Depending on whether $(\alpha_{gm})_i^{n+1}$ is greater or less than 0.5, the proper functional forms of the parameters m and b from Section III-1 are chosen and the new mixture level is computed as

$$(z_m)_i^{n+1} = \frac{(M_{gb})_i^{n+1}}{A\left(\frac{m_i^{n+1}}{2} + b_i^{n+1}\right)} \qquad \text{(VIII.1-56)}$$

The bubble density at $z=z_m$, $(\rho_{gb})_{z_m}$ is then updated as

$$[(\rho_{gb})z_m]_i^{n+1} = b_i^{n+1} \qquad \text{(VIII.1-57)}$$

1.1.2 Boundary Conditions

This section outlines dependent variables which may be externally manipulated in the RETRAN code. By external manipulation of the variable, we mean that it may be controlled by the user as input to the code. These prescriptions might be thought of as "boundary conditions" in the sense that the prescribed variables occur as values at the boundaries of volume or junction nodes. Several of the many options available to the user are described below.

1.1.2.1 Critical Flow

The critical or "choked" flow options available to the user are:

(1) Sonic or "self" choking

(2) Extended Henry-Fauske

(3) Henry-Fauske

(4) Moody

These options act as upper bounds on the junction flow. If the flow exceeds the value returned from the option desired, the friction is adjusted in the manner discussed in Volume III. Except for the sonic choking option the options are preprogrammed as tables. The sonic option uses the local HEM speed of sound. An input junction coefficient may serve to raise or lower the table output uniformly.

1.1.2.2 Fill Junctions

As indicated previously in Section VII-1, the "normal" junctions comprise the solution space for the unknown flows, W_j. In addition to the flows, there are (NJUN-k) "fill" junctions, W_{jFILL}, where NJUN is the total number of junctions. A fill junction is a boundary condition whereby a flow is prescribed either positive or negative as

$$W_j^{n+1} = W_{j_{FILL}}^{n+1} \qquad j > k \qquad \text{(VIII.1-58)}$$

The W_{jFILL} junction is a user input tabular function of time or pressure. If the fill is positive, the junction enthalpy must be prescribed as

$$h_j^{n+1} = h_{j_{FILL}}^{n+1} \qquad \text{(VIII.1-59)}$$

1.1.2.3 Time-Dependent Volumes

The option of using special boundary volumes with explicit time-dependent fluid boundary conditions is intended primarily for performing detailed calculations on part of a reactor system using results of previous RETRAN calculations as boundary conditions. This option allows RETRAN to perform a detailed core calculation similar to that performed by THETA1-B[VIII.1-8] which was formerly used to provide a detailed core calculation in conjunction with RELAP3.[VIII.1-9] For a detailed core calculation, the special boundary volumes may be chosen independently to have fluid conditions described as an explicit function of time. The fluid conditions in such boundary volumes are unaffected by the course of the detailed transient being calculated. The necessary fluid boundary data may be provided either as tabular data on input cards or by automatic retrieval from a data tape created during a previous RETRAN calculation. Performing detailed calculations on part of a system by using special boundary volumes saves computer time as compared to modeling the complete system. A detailed calculation can be performed on any portion of the reactor system, such as a pump, by using special boundary volumes.

1756 292

The time-dependent volume option is controlled by an index (IREAD) on a Volume Data Card. A positive index for any volume requires that pressure, temperature, quality, and mixture level as functions of time be supplied on the Time-Dependent Volume Data Cards. A negative index causes the data to be retrieved from a RETRAN data tape. The data retrieved from tape are those for the volume number corresponding to the negative index. The volume numbers used for the detailed calculation need not correspond to the volume numbers on the RETRAN data tape. A zero index turns the option off for any volume. Since the average volumetric flow is not prescribed, the volume momentum flux term is zero for a time-dependent volume.

The geometric detail of a time-dependent volume is required input just as for a normal volume. Fluid conditions are required as a function of time and include pressure, temperature, quality, and mixture level. The geometric detail plus these four time-dependent functions provide sufficient information to define completely the fluid conditions in a volume. For each time step, the data supplied on either cards or tape is interpolated to obtain current fluid conditions. To perform calculations for a single core channel, a RETRAN problem would be set up with the upper and lower volumes defined as time-dependent volumes. The data would be retrieved from the volumes representing the upper and lower plenums in a RETRAN calculation of the entire primary loop. The power history would also be retrieved from the previous calculation.

1.1.2.4 Valves

Generally valves are controlled by flow-dependent pressure losses of the form $(CVi)W\,W/\rho$. For example, three regions of operation are defined for a check valve:

(1) CV1 is used for positive flow with the valve open

(2) CV2 is used for negative flow with the valve open

(3) CV3 is used for negative flow with valve almost closed.

For positive flow, the valve remains open and sustains a pressure loss proportional to CV1. For negative flow, the valve remains open if the pressure loss, which

is proportional to CV2, is less than the back pressure, P_{CV}, required to close the valve.

After the valve closes, the pressure loss is proportional to CV3 for small leakage flows. The hysteresis difference between Type 0 and Type 1 check valves is apparent in Figure VI.2-1. Type 0 check valves open in exactly the reverse sequence of the closing sequence. A Type 0 valve opens when negative flow has decreased to a value such that the pressure loss for the open phase is less than the loss required to keep the valve closed. A Type 1 valve reopens only when the pressure loss developed across the valve in the closed position is less than the required back pressure.

A time-dependent area may be associated with a valve. The normalized junction area for any time step is interpolated from an input table of area-versus-time. The junction area used during the time step is then given by

$$A = A(t)*AJUN*F(t) \qquad \text{(VIII.1-60)}$$

where

A(t) = time dependent junction area

AJUN = total junction area

F(t) = normalized time dependent area $(0 \leq F(t) \leq 1)$

t = time

1.2 Solution Methods

The solution of RETRAN is governed by the following mass, energy and momentum conservation equations:

$$\frac{dM}{dt} = f_M(W) \qquad \text{(VIII.1-61)}$$

1356 294

$$\frac{dU}{dt} = f_U (H, W) \qquad \text{(VIII.1-62)}$$

$$\frac{dW}{dt} = f_W (p, W) \qquad \text{(VIII.1-63)}$$

where

M = fluid mass
U = fluid internal energy
W = mass flow rate
H = enthalpy
p = thermodynamic pressure

with the thermodynamic pressure defined by the water state-property relation in terms of specific internal energy and density. In this Section it will be shown how the numerical solution technique, the computational flow path, and various computational features of the physical models are modified to optimize the performance of the code.

1.2.1 Explicit Solution

1.2.1.1 Explicit Equations

The numerical technique employed in the solution of the three sets of conservation equations is based on a first order Taylor series expansion, in time, of the time rate of change of mass, energy and flow.

That is,

$$f(y, t + \Delta t) = f(y, t) + \left(\frac{\partial f}{\partial t}\right)_t \Delta t \qquad \text{(VIII.1-64)}$$

where $y = [W_j, M_i, U_i]$ and with j being the junction index and i the volume index.

From Equations VIII.1-61 to VIII.1-63, one obtains

$$f(y,\ t) = \frac{dy}{dt} \qquad \text{(VIII.1-65)}$$

or

$$f_y = \left[\frac{dW_i}{dt} ,\ \frac{dM_i}{dt} ,\ \frac{dU_i}{dt} \right] . \qquad \text{(VIII.1-66)}$$

Application of the chain rule for differentials to Equation VIII.1-66 results in

$$\left(\frac{\partial f_y}{\partial t} \right)_t = \left(\frac{\partial f_y}{\partial W_j} \right) \frac{dW_j}{dt} + \left(\frac{\partial f_y}{\partial m_i} \right) \frac{dM_i}{dt} + \left(\frac{\partial f_y}{\partial U_i} \right) \frac{dU_i}{dt}$$

$$= J(y^n)\ \frac{\Delta y}{\Delta t} \qquad \text{(VIII.1-67)}$$

Differencing Equation VIII.1-65 gives

$$\frac{\Delta y^{n+1}}{\Delta t} = f^{n+1} \quad . \qquad \text{(VIII.1-68a)}$$

Substitution of Equation VIII.1-64 into Equation VIII.1-67 results in

$$\frac{\Delta y^{n+1}}{\Delta t} = f^n + \left(\frac{\partial f}{\partial t} \right)_t \Delta t = f^n + J(y^n)\ \frac{\Delta y^{n+1}}{\Delta t}\ \Delta t \quad . \qquad \text{(VIII.1-68b)}$$

Hence

$$\Delta y^{n+1} = f^n\ \Delta t + J(y^n)\ \Delta y^{n+1}\ \Delta t \qquad \text{(VIII.1-68c)}$$

where

$$y^n = y(t^n) \qquad \text{(VIII.1-69)}$$

$$y^{n+1} = y(t^{n+1}) = y(t^n + \Delta t) \qquad \text{(VIII.1-70)}$$

$$\Delta y^{n+1} = y^{n+1} - y^n \qquad \text{(VIII.1-71)}$$

and the Jacobian matrix, $J(y^n)$, is

$$J(y^n) = \begin{bmatrix} \frac{\partial f_W}{\partial W_i} & \frac{\partial f_W}{\partial M_i} & \frac{\partial f_W}{\partial U_i} \\ \frac{\partial f_M}{\partial W_i} & \frac{\partial f_M}{\partial M_i} & \frac{\partial f_M}{\partial U_i} \\ \frac{\partial f_U}{\partial W_j} & \frac{\partial f_U}{\partial M_i} & \frac{\partial f_U}{\partial U_i} \end{bmatrix} \qquad \text{(VIII.1-72)}$$

The solution to this system of linear simultaneous equations can be expressed explicitly in terms of values evaluated in the previous time step:

$$\Delta y^{n+1} = [I - J(y^n)\Delta t]^{-1} f^n \Delta t \qquad \text{(VIII.1-73)}$$

where I is the identity matrix.

The numerical equations describing changes in mass and energy are eliminated in the solution scheme before a reduced set of equations in ΔW_j^{n+1} is solved. The quantities f^n and $J(y^n)$ are computed from the conservation equations and the state properties of water.

1.2.1.2 Computational Flow Path

The flow diagram for the explicit solution is shown in Figure VIII.1-3. The time step selection is based upon a built-in iterative integration accuracy algorithm for the numerical equations in junction flow, W_j. The computation is explicit in the sense that, at every iteration, all the coefficients are evaluated in terms of old time values. Accuracy is estimated from two consecutive integrations of the flow equations for the incremental changes in junction flow, ΔW_j.

The explicit iterative method allows the time step to be increased or decreased depending upon the behavior of the flow solution. If nonlinear behavior is

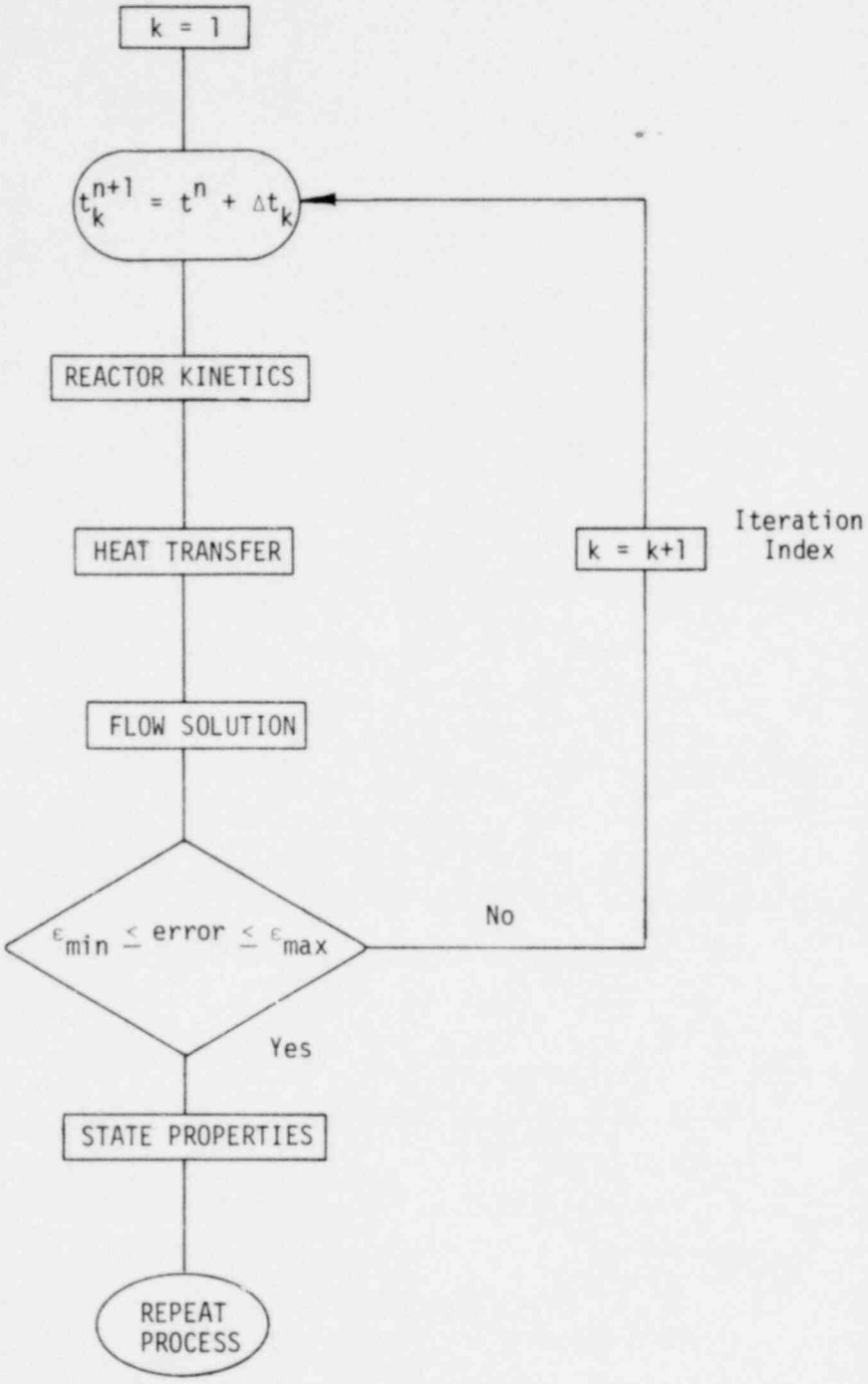

Figure VIII.1-3 Flow Diagram for Explicit Solution

1756 298

detected, the time step size is decreased until the solution has converged within the specified accuracy requirements. However, if the flow solution behaves in a linear manner the time step size is increased until the solution falls within the required accuracy.

The first iteration uses information from the previously converged flow solution for a linear prediction of the next incremental change in junction flow. The ΔW_j's are then calculated using the same time step size as the previous converged flow solution. The error in the calculated ΔW_j for the first iteration, k = 1, is then defined as

$$\varepsilon_j^k = \frac{A_{2_j}^k}{A_{1_j}^k} \left(\frac{\Delta W_j^k}{\sum_{NJUN} \Delta W_j^k} \right) \qquad \text{(VIII.1-74)}$$

where

$$A_{2_j}^k = \frac{1}{2} \Delta t^k \quad |\Delta W_j^k - \Delta W_j^1| \qquad \text{(VIII.1-75)}$$

ΔW_j^1 = Converged ΔW_j for previous time step

$$A_{1_j}^k = \bar{W}_j \Delta t^1 \qquad \text{(VIII.1-76)}$$

$\bar{W}_j^k$ = $|W_j|$ Averaged over all previous time.

Both upper and lower limits for the convergence criteria are defined. If the calculated error for any junction falls above the upper limit, the time step size is decreased. If all calculated errors are below the lower error limit the time step is increased. If one or more calculated errors in the flow solution are within the error band with none exceeding the upper error limit, the flow solution and time step size are accepted.

If all errors in the calculated ΔW_j^k's are below the convergence criteria the time step size is doubled and ΔW_j^{k+1}'s are calculated. The error calculation for time step advancement is defined as

$$\varepsilon_j^{k+1} = \frac{A_{2_j}^{k+1}}{A_{1_j}^{k+1}} \left(\frac{\Delta W_j^{k+1}}{\sum \Delta W_j^{k+1}} \right) \qquad \text{(VIII.1-77)}$$

where

$$A_{2_j}^{k+1} = \frac{1}{2} \Delta t^{k+1} \quad \Delta W^{k+1} - 2\Delta W^k \qquad \text{(VIII.1-78)}$$

$$A_{1_j}^{k+1} = \bar{W}_j \Delta t^1 \qquad \text{(VIII.1-79)}$$

If any errors in the ΔW_j^k's are above the upper limit of the convergence criteria, the time step is halved and the ΔW_j^{k+1}'s are calculated. The error for this case is defined as :

$$\varepsilon_j^{k+1} = \frac{A_{2_j}^{k+1}}{A_{1_j}^{k+1}} \left(\frac{\Delta W_j^{k+1}}{\sum \Delta W_j^{k+1}} \right) \qquad \text{(VIII.1-80)}$$

where

$$A_{2_j}^{k+1} = \frac{1}{2} \Delta t^{k+1} \quad \left| \Delta W^{k+1} - \frac{1}{2} \Delta W^k \right| \qquad \text{(VIII.1-81)}$$

$$A_{1_j}^{k+1} = \bar{W}_j \Delta t^1 \qquad \text{(VIII.1-82)}$$

In order to prevent a large change between time steps used for two consecutive flow solutions, A_{1j}^{k+1} is fixed while A_{2j}^{k+1} is allowed to vary with each new Δt within the explicit iteration. This technique serves as a time step stabilizer and prevents a large change in time step size from one point to the next.

A check is made to detect a trip. To insure numerical stability the calculations are made to cross the trip point with a minimum number of time steps. The time step size is reduced if necessary so the trip setpoint is not passed over by a large time step before it is tripped.

1.2.2 Computational Efficiency

1.2.2.1 Numerical Efficiency

A causality concept is formulated and implemented into RETRAN to reduce computational effort in time consuming calculational blocks. This concept is based on the idea that the frequency at which fluid volumes or heat conductors need to be treated is inversely proportional to the time constants for which physical changes occur in fluid volumes and heat conductors. This follows from the observation that certain volumes that undergo large changes will cause subsequent changes in other volumes and only these causal volumes, which dictate time step selection, need be treated at each time step.

A control volume is designated causal if its change in pressure, Δp_i, due to change in mass and energy is greater than a prescribed limit. That is, if

$$\left| \frac{\Delta p_i}{p_i} \right| > \varepsilon_c \qquad \text{(VIII.1-83)}$$

then the i^{th} volume is causal.

A noncausal volume, on the other hand, should also be treated at a later time. A credit equal to the cumulative change in mass and energy is given to each noncausal volume. This credit is added to each noncausal volume before checking to see if it is causal at a new time step.

When only the causal volumes are treated at each time step in the lengthy state properties computational block, the computational effort is significantly reduced without noticeably affecting the accuracy of the computational outcome. The savings in computational time is proportional to the fraction of noncausal volumes that can be skipped.

The causal conductor concept is based on the observation that, in many problems, the time constant for heat transfer is greater than the time constant for hydrodynamic changes. Thus, it is possible for heat transfer calculations to be performed less frequently than every hydrodynamic time step without significantly affecting the computational results.

In the present version of RETRAN, a heat conductor will be designated "causal" (i.e., sent through the heat conduction solution during the current time step) by meeting any of the following conditions:

(1) An adjacent fluid volume average flow or bulk temperature changes by more than a prescribed limit.

(2) The total power changes by more than a prescribed limit (for core conductors).

(3) A transition in heat transfer regimes is detected.

(4) A conductor approaches CHF.

(5) An adjacent fluid volume bulk temperature crosses the conductor wall temperature.

(6) If the conductor has been "non-causal" (not treated) for more than one second.

A method has been developed to keep track of a non-causal conductor's history. The method is important, since once a conductor has been designated non-causal, there has to be a mechanism to reactivate the conductor as causal.

As an example of how the non-causal history or "credit" is determined, consider the simplified example of a single fluid volume with one conductor. Assign the criterion that if the volume average flow changes by more than 10%, the conductor must be designated causal (assume that initially the conductor is non-causal).

As the flow plot (Figure VIII.1-4) indicates, the required 10% change may take several time steps during which the conductor will remain non-causal. However, during the first time step, the flow changes 1/4 of the required amount. That change will be stored as credit. Initially all conductors are assigned a credit value of 1.0. In this example, after the first time step, the conductor is still non-causal, but its credit has been reduced to 0.75, reflecting the flow change for that time step relative to the allowed 10% criterion. Each of the remaining time steps continues to reduce the noncausal credit until it becomes

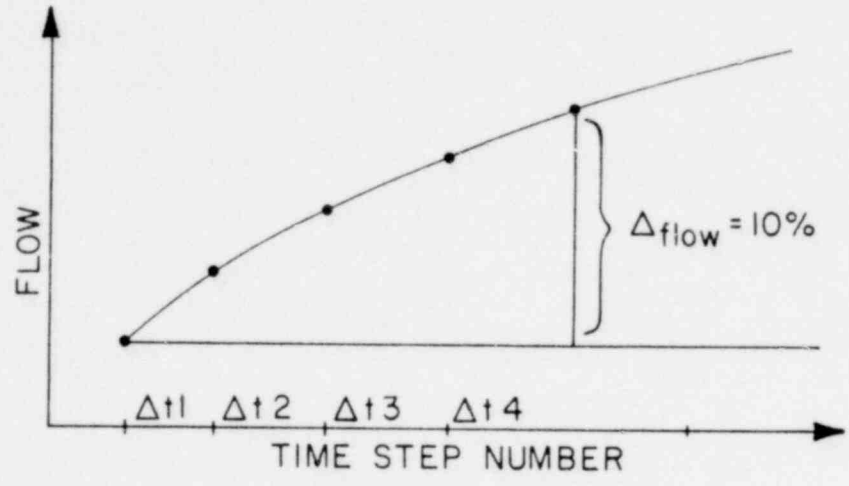

(a) Flow History

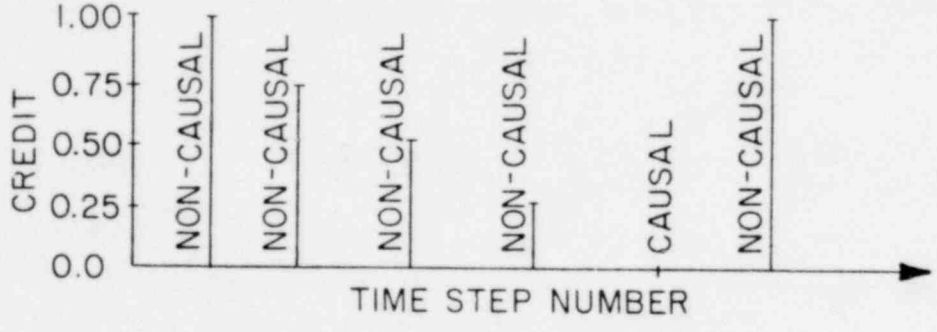

(b) Credit History

Figure VIII.1-4 Causal Credit Memory Technique

less than or equal to zero. The conductor is then declared causal, sent through the conduction solution, and reassigned a credit of 1.0 as the process cycles again. In this example, the conductor time step size is four times the hydrodynamic time step size.

In RETRAN, the same credit memory technique is used for each conductor. The only difference is that changes in bulk fluid temperature and total power (if the conductor is a core conductor) are also scanned. The credit considered is the maximum of the three parameters.

2.0 SOLUTION METHOD FOR HEAT CONDUCTION EQUATIONS

The numerical equations are derived from Equation IV.1-3 by integration over a discrete set of mesh points.

Temperatures are calculated at each mesh point. Mesh spacing is arbitrary with the exception that mesh points must be on material interfaces including exterior boundaries. Geometry is included implicitly according to the choice of gradient operator and differentials for surface and volume. Figure VIII.2-1 illustrates a typical mesh layout. Numbering begins at the left surface and proceeds to the right. An expanded view of three mesh points centered on the i^{th} one is shown in Figure VIII.2-2. The subscripts i are the mesh number, r and ℓ are, respectively, the half values to the right and left of the i^{th} mesh point. Where temperature dependent, the material properties k_{ri}, $k_{\ell i}$, $(C_p)_{ri}$, $(C_p)_{\ell i}$ are evaluated at temperature T_i.

The numerical approximation to Equation IV.1-3 is obtained by integrating over the volume about each mesh point. For the i^{th} mesh point this is given by

$$\int_{V_i} \rho C_p \frac{\partial T}{\partial t}\, dV = \int_{V_i} \tilde{\nabla}\cdot k\tilde{\nabla}T dV + \int_{V_i} Q\, dV \qquad \text{(VIII.2-1)}$$

Converting the volume integral of the temperature gradient to a surface integral using the divergence theorem results in

$$\int_{V_i} \rho C_p \frac{\partial T}{\partial t}\, dV = \int_{S_i} k\tilde{\nabla}T\cdot d\hat{A}_i + \int_{V_i} Q\, dV. \qquad \text{(VIII.2-2)}$$

Assuming the material properties and temperatures in half mesh interval in Figure VIII.2-2 are constant over a time interval Δt, then

$$[(\rho C_p)_{\ell i} h^{v}_{\ell i} + (\rho C_p)_{ri} h^{v}_{ri}] \frac{\partial T_i}{\partial t} = k_{\rho i}\tilde{\nabla}T_{\ell i}\cdot\tilde{n}_{\ell} h^{s}_{\ell i} + k_{ri}\tilde{\nabla}T_{ri}\cdot\tilde{n}_{ri} h^{s}_{ri} + Q_{\ell i} h^{v}_{\ell i} + Q_{ri} h^{v}_{ri} \qquad \text{(VIII.2-3)}$$

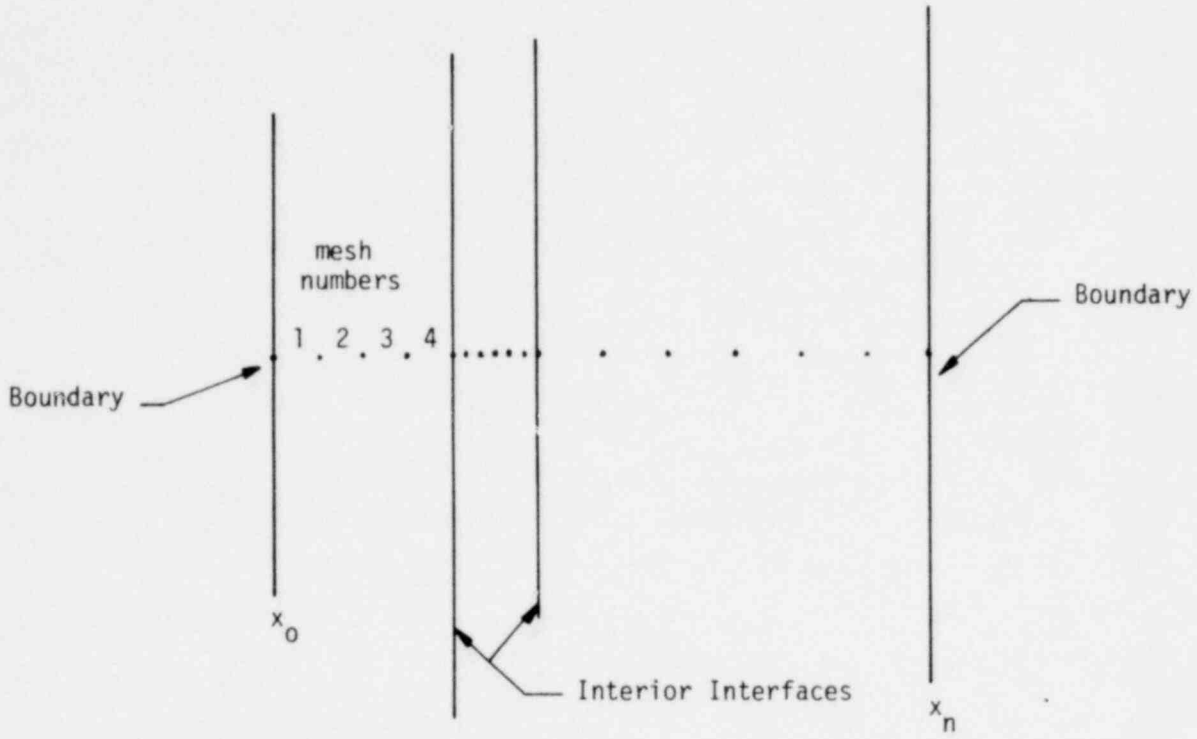

Figure VIII.2-1 Mesh Point Structure

1256 306

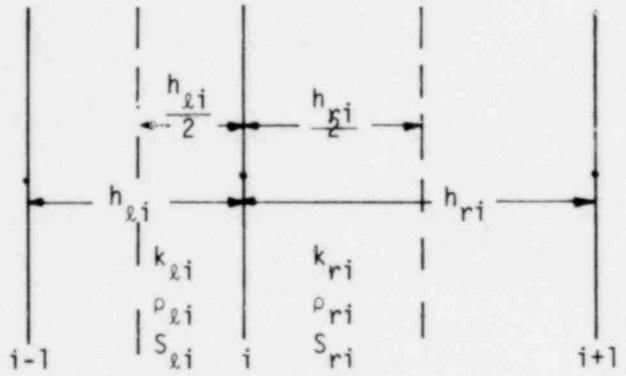

Figure VIII.2-2 Expanded Mesh Point Structure

1756 307

where

$h^v_{\ell i}$ = volume weight on left half mesh interval at point i

h^v_{ri} = volume weight on right half mesh interval at point i

$h'^s_{\ell i}$ = surface weight at $x_i - \frac{h_{\ell i}}{2}$

h'^s_{ri} = surface weight at $x_i + \frac{h_{ri}}{2}$

$\tilde{n}_\ell$ = unit normal vector at left surface

$\tilde{n}_r$ = unit normal vector at right surface

The exact expressions for the surface and volume weights depend upon the geometry. The two most common coordinate systems are rectangular and cylindrical. The expressions for h^v and h^s in these two systems are as follows:

Rectangular

$$h^v_{\ell i} = \int_{x_i - \frac{h_{\ell i}}{2}}^{x_i} dx = \frac{h_{\ell i}}{2} \qquad h^v_{ri} = \int_{x_i}^{x_i + \frac{h_{ri}}{2}} dx = \frac{h_{ri}}{2} \qquad \text{(VIII.2-4a,4b)}$$

$$h'^s_{\ell i} = \int_{S_\ell} dA = 1 \qquad h'^s_{ri} = \int_{S_r} dA = 1 \qquad \text{(VIII.2-4c,4d)}$$

Cylindrical

$$h^v_{\ell i} = 2\pi \int_{x_i - \frac{h_{\ell i}}{2}}^{x_i} r\,dr = 2\pi \frac{h_{\ell i}}{2} \left(x_i - \frac{h_{\ell i}}{4}\right) \qquad \text{(VIII.2-5a)}$$

$$h^{v}_{ri} = 2 \int_{x_i}^{x_i + \frac{h_{ri}}{2}} r\,dr = 2\pi \frac{h_{ri}}{2} \left(x_i + \frac{h_{ri}}{4}\right) \qquad \text{(VIII.2-5b)}$$

$$h'^{s}_{\ell i} = \int_{S_\ell} r\,d\theta = 2\pi\left(x_i - \frac{h_{\ell i}}{2}\right) \qquad \text{(VIII.2-5c)}$$

$$h'^{s}_{ri} = \int_{S_r} r\,d\theta = 2\pi \left(x_i + \frac{h_{ri}}{2}\right) \qquad \text{(VIII.2-5d)}$$

The gradient terms are given by

$$(\tilde{\nabla} T_i \cdot \tilde{n})_\ell = \frac{T_{i-1} - T_i}{h_{\ell i}} \qquad \text{(VIII.2-6)}$$

$$(\tilde{\nabla} T_i \cdot \tilde{n})_r = \frac{T_{i+1} - T_i}{h_{ri}} \qquad \text{(VIII.2-7)}$$

and the time derivative by

$$\frac{\partial T_i}{\partial t} = \frac{T_i^{m+1} - T_i^{m}}{\Delta t} \qquad \text{(VIII.2-8)}$$

Defining new surface weights h^s by

$$h^{s}_{\ell i} = h'^{s}_{\ell i} \frac{1}{h_{\ell i}} \qquad \text{(VIII.2-9a)}$$

$$h^{s}_{ri} = h'^{s}_{ri} \frac{1}{h_{ri}} \qquad \text{(VIII.2-9b)}$$

Equation VIII.2-3 can be written as

$$\left\{(\rho C_p)_{\ell i} h^v_{\ell i} + (\rho C_p)_{ri} h^v_{ri}\right\}\left(\frac{T_i^{m+1} - T_i^m}{\Delta t}\right) = k_{\ell i} h^s_{\ell i}(T_{i-1} - T_i)$$
$$+ k_{ri} h^s_{ri}(T_{i+1} - T_i) + Q_{\ell i} h^v_{\ell i} + Q_{ri} h^v_{ri} \qquad \text{(VIII.2-10)}$$

At the left boundary, for all geometries

$$h^v_{\ell i} = 0 \qquad \text{(VIII.2-11)}$$

and $h^s_{\ell 1}$ is given by

Rectangular $$h^s_{\ell 1} = 1 \qquad \text{(VIII.2-12a)}$$

Cylindrical $$h^s_{\ell 1} = 2\pi x_1 \qquad \text{(VIII.2-12b)}$$

At the right boundary, for all geometries

$$h^v_{rN} = 0 \qquad \text{(VIII.2-13)}$$

and h^s_{rN} is given by

Rectangular $$h^s_{rN} = 1 \qquad \text{(VIII.2-14a)}$$

Cylindrical $$h^s_{rN} = 2\pi x_N \qquad \text{(VIII.2-14b)}$$

Letting the right side of Equation VIII.2-10 be represented by δ and defining

$$G_i = \frac{(\rho C_p)_{\ell i} h^v_{\ell i} + (\rho C_p)_{ri} h^v_{ri}}{\Delta t} \qquad \text{(VIII.2-15)}$$

gives

$$G_i^{m+1/2}\,(T_i^{m+1} - T_i^m) = \delta_i^m \qquad \text{(VIII.2-16)}$$

1256 310

which is an explicit formulation for T_i^{m+1} in terms of T_i^m.

An implicit formula can be written as

$$G_i^{m+1/2} (T_i^{m+1} - T_i^m) = \omega \delta_i^{m+1} + (1 - \omega) \delta_i^m \qquad \text{(VIII.2-17)}$$

where ω is a parameter between 0 and 1. A value for ω of 1/2 leads to the Crank-Nicolson implicit equations.

The variable $G^{m+1/2}$ implies that G is a quantity averaged over T^m and T^{m+1}. Material properties evaluated at T^{m+1} require iteration of the solution. Where such iteration is not carried out properties are evaluated at T^m.

Equation VIII.2-17 for the left boundary is given by (for $\omega = 1/2$)

$$G_1^{m+1/2} (T_1^{m+1} - T_1^m) = - 1/2\ h_{\ell 1}^s \dot{q}_{\ell w}^{m+1} + 1/2\ h_{ri}^{m+1} h_{ri}^s\ (T_2^{m+1} - T_1^{m+1}) \qquad \text{(VIII.2-18a)}$$

$$+ 1/2\ h_{r1}^v Q_{r1}^{m+1} - 1/2\ h_{\ell 1}^s \dot{q}_{\ell w}^m + 1/2\ k_r^m h_{r1}^s\ (T_2^m - T_1^m) + 1/2\ h_{r1}^v Q_{r1}^m$$

or rearranging

$$(G_1^{m+1/2} + 1/2\ k_{ri}^{m+1} h_{ri}^s) T_1^{m+1} - 1/2\ k_{r1}^{m+1} h_{r1}^s T_2^{m+1} + 1/2\ h_{\ell 1}^s \dot{q}_{\ell w}^{m+1} \qquad \text{(VIII.2-18b)}$$

$$= - 1/2\ h_{\ell 1}^s \dot{q}_{\ell w}^m + 1/2\ k_r^m h_{r1}^s (T_2^m - T_1^m) + 1/2\ h_{r1}^v (Q_{r1}^{m+1} + Q_{r1}^m) + G_1^{m+1/2}\ T_1^m \ .$$

The equation for the central mesh points becomes

$$G_i^{n+1/2} (T_i^{m+1} - T_1^n) = 1/2\ K_{\ell i}^{m+1} h_{\ell i}^s (T_{i-1}^{m+1} - T_i^{m+1}) + 1/2\ K_{ri}^{m+1} h_{ri}^s (T_{i+1}^{m+1} - T_i^{m+1})$$

$$+ 1/2\ h_{ri}^v Q_{ri}^{m+1} + 1/2\ h_{\ell i}^v A_{\ell i}^{m+1} + 1/2\ k_{\ell i}^m h_{\ell i}^s (T_{i-1}^m - T_i^m)$$

$$+1/2\ k_{ri}^m h_{ri}^s (T_{i+1}^m - T_i^m) + 1/2\ h_{ri}^v Q_{ri}^m + 1/2\ h_{\ell i}^v A_{\ell i}^m \qquad \text{(VIII.2-19)}$$

or rearranging

$$- 1/2\ k_{\ell i}^{m+1} h_{ri}^{s} T_{i-1}^{m+1} + (G_i^{m+1/2} + 1/2\ k_{\rho i}^{m+1} h_{\rho i}^{s} + 1/2\ k_{ri}^{m+1} h_{ri}^{s}) T_i^{m+1}$$

$$- 1/2\ k_{ri}^{m+1} h_{ri}^{s} T_{i+1}^{m+1} = G_i^{m+1/2}\ T_i^m + 1/2\ k_{\ell i}^{m} h_{\ell i}^{s} (T_{i-1}^m - T_i^m)$$

$$+ 1/2\ k_{ri}^{m} h_{ri}^{s} (T_{i+1}^m - T_i^m) + 1/2\ h_{\ell i}^{v} (Q_{\ell i}^{m+1} + Q_{\ell i}^{m}) + 1/2\ h_{ri}^{v} (Q_{ri}^{m+1} + Q_{ri}^{M}) \quad . \tag{VIII.2-20}$$

For the right boundary, Equation VIII.2-17 is given by

$$G_N^{m+1/2} (T_N^{m+1} - T_N^m) = 1/2\ k_{\ell N}^{m+1} h_{\ell N}^{s} (T_{N-1}^{m+1} - T_N^{m+1}) - 1/2\ h_{rN}^{w} \dot{g}_{rw}^{m+1}$$

$$+ 1/2\ h_{\ell N}^{v} Q_{\ell N}^{m+1} + 1/2\ k_{\ell N}^{m} h_{\ell N}^{s} (T_{N-1}^m - T_N^m) - 1/2\ h_{rN}^{s} \dot{q}_{rw}^{m} + 1/2\ h_{\ell N}^{v} Q_{\ell N}^{m} \tag{VIII.2-21}$$

or, rearranging

$$- 1/2\ k_{\ell N}^{m+1} h_{\ell N}^{s} T_{N-1}^{m+1} + (G_N^{m+1/2} + 1/2\ k_{\ell N}^{m+1} h_{\ell N}^{s}) T_N^{m+1} + 1/2\ h_{rN}^{s} \dot{q}_{rw}^{m+1} = G_N^{m+1/2}\ T_N^m$$

$$+ 1/2\ k_{\ell N}^{m} h_{\ell N}^{s} (T_{N-1}^m - T_N^m) - 1/2\ h_{rN}^{s} \dot{q}_{rw}^{m} + 1/2\ h_{\ell N}^{v} (Q_{\ell N}^{m+1} + Q_{\ell N}^{m}) \quad . \tag{VIII.2-22}$$

Equations VIII.2-18 through VIII.2-22 for the time-dependent problem can be put into matrix form by defining the following variables:

$$b_1^{m+1} = G_1^{m+1/2} - c_1^{m+1} \tag{VIII.2-23a}$$

$$c_1^{m+1} = -1/2\ k_{r1}^{m+1} h_{r1}^{s} \tag{VIII.2-23b}$$

$$\rho_1^{m+1} = -1/2\ h_{\ell 1}^{s} \tag{VIII.2-23c}$$

$$d_1 = G_1^{m+1/2}\ T_1^m + 1/2\ k_{r1}^{m} h_{r1}^{2} (T_2^m - T_1^m)$$

$$- 1/2\ h_{\ell 1}^{s} \dot{q}_{\ell w}^{m} + 1/2\ h_{r1}^{v} (Q_{r1}^{m+1} + Q_{r1}^{m}) \tag{VIII.2-23d}$$

$$a_i^{m+1} = -\ 1/2\ k_{\ell i}^{m+1} h_{\ell i}^{s} \qquad \text{(VIII.2-23e)}$$

$$b_i = G_i^{m+1/2} - a_1^{m+1} - c_1^{m+1} \qquad \text{(VIII.2-23f)}$$

$$c_i = -\ 1/2\ k_{ri}^{m+1} h_{ri}^{s} \qquad \text{(VIII.2-23g)}$$

$$d_i = G_i^{m+1/2}\ T_i^m + 1/2\ k_{\ell i}^m h_{\ell i}^s (T_{i-1}^m - T_i^m) + 1/2\ k_{ri}^m h_{ri}^s (T_{i+1}^m - T_i^m)$$

$$+ 1/2\ h_{\ell i}^v (Q_{\ell i}^{m+1} + Q_{\ell i}^n) + 1/2\ h_{ri}^v (Q_{ri}^{m+1} + Q_{ri}^m) \qquad \text{(VIII.2-23h)}$$

$$a_N^{m+1} = -\ 1/2\ k_{\ell N}^{m+1} h_{\ell N}^{s} \qquad \text{(VIII.2-23i)}$$

$$b_N^{m+1} = G_N^{m+1/2} - a_N^{m+1} \qquad \text{(VIII.2-23j)}$$

$$p_N^{m+1} = -\ 1/2\ h_{rN}^{s} \qquad \text{(VIII.2-23k)}$$

$$d_N = G_N^{m+1/2}\ T_N^m + 1/2\ k_{\ell N}^m h_{\ell N}^s (T_{N-1}^m - T_N^m) + 1/2\ h_{rN}^s$$

$$+ 1/2\ h_{\ell N}^v (Q_{\ell N}^{m+1} + Q_{\ell N}^m) - 1/2\ h_{rN}^s \dot{q}_{rw}^m . \qquad \text{(VIII.2-23l)}$$

Then Equations VIII.2-18 through VIII.2-22 can be written as

6 31

$$
\begin{bmatrix}
b_1^{m+1} & c_1^{m+1} & & & & & \\
a_2^{m+1} & b_2^{m+1} & c_2^{m+1} & & & & \\
 & & & & & & \\
 & & & a_{N-1}^{m+1} & b_{N-1}^{m+1} & c_{N-1}^{m+1} & \\
 & & & & a_N^{m+1} & b_N^{m+1}
\end{bmatrix}
\begin{bmatrix} T_1^{m+1} \\ T_2^{m+1} \\ \cdot \\ \cdot \\ \cdot \\ T_{N-1}^{m+1} \\ T_N^{m+1} \end{bmatrix}
=
\begin{bmatrix} d_1 \\ d_2 \\ \cdot \\ \cdot \\ \cdot \\ d_{N-1} \\ d_N \end{bmatrix}
$$

$$
+
\begin{bmatrix}
p_1^{m+1} & 0 & 0 & . & . & 0 \\
0 & 0 & 0 & . & . & 0 \\
\cdot & & & & & \\
\cdot & & & & & \\
\cdot & & & & & \\
0 & 0 & 0 & . & . & 0 \\
0 & 0 & 0 & . & . & p_N^{m+1}
\end{bmatrix}
\begin{bmatrix} \dot{q}_{\ell w}^{m+1} \\ 0 \\ \\ \\ \\ 0 \\ \dot{a}_{rw}^{m+1} \end{bmatrix}
$$

(VIII.2-24)

Equation VIII.2-24 is solved by factoring according to the tridiagonal algorithm. Thus, one obtains

$$
\begin{aligned}
T_1 + E_1 T_2 &= F_1 + G_1 \dot{q}_{\ell w} \\
T_3 + E_2 T_3 &= F_2 + G_2 \dot{q}_{\ell w} \\
&\vdots \\
T_{N-1} + E_{N-1} T_N &= F_{N-1} + G_{N-1} \dot{q}_{\ell w} \\
T_N &= F_N + G_N \dot{q}_{\ell w} + H \dot{q}_{rw}
\end{aligned}
$$

(VIII.2-25)

where

$$E_1 = \frac{C_1}{b_1} \quad , \quad F_1 = \frac{d_1}{b_1} \quad , \quad G_1 = -\frac{P_1}{b_1} \quad , \qquad \text{(VIII.2-26a,26b,26c)}$$

$$E_j = \frac{C_j}{b_j - a_j E_{j-1}}, \; F_j = \frac{d_j - a_j F_{j-1}}{b_j - a_j E_{j-1}}, \; G_j = \frac{-a_j g_{j-1}}{b_j - a_j E_{j-1}}; \qquad \text{(VIII.2-26d,26e,26f)}$$

$$F_N = \frac{d_N - a_N f_{N-1}}{b_N - a_N E_{N-1}}, \; G_N = \frac{-a_N g_{N-1}}{b_N - a_N E_{N-1}}, \; H = \frac{P_N}{b_N - a_N E_{N-1}} \quad , \qquad \text{(VIII.2-26g,26h,26i)}$$

$$2 \leq j \leq N-1$$

Defining the new variables

$$X_N = F_n; \; Y_N = G_N, \; A_N = H \qquad \text{(VIII.2-27)}$$

and back solving in Equations VIII.2-26, one obtains

$$X_j = F_j - E_j X_{j+1} \qquad \text{(VIII.2-28a)}$$

$$Y_j = G_j - E_j Y_{j+1} \quad N-1 \geq j \geq 1 \qquad \text{(VIII.2-28b)}$$

$$Z_j = -E_j Z_{j+1} \qquad \text{(VIII.2-28c)}$$

The temperatures are then given by the set of equations

$$T_j = X_i + Y_i \dot{q}_{\ell w} + Z_i \dot{q}_{rw} \quad \text{where } 1 \leq i \leq N \qquad \text{(VIII.2-29)}$$

For the cases i=1 and i=N one obtains

$$\dot{q}_{\ell w} = \alpha_1 T_1 + \alpha_2 T_N + \alpha_3 \qquad \text{(VIII.2-30)}$$

1756 315

and

$$\dot{q}_{rw} \quad \beta_1 T_1 + \beta_2 T_N + \beta_3 \qquad \text{(VIII.2-31)}$$

where

$$\alpha_1 = \frac{Z_N}{Y_1 Z_N - Y_N Z_1} , \qquad \text{(VIII.2-32a)}$$

$$\alpha_2 = \frac{-Z_1}{Y_1 Z_N - Y_N Z_1} , \qquad \text{(VIII.2-32b)}$$

$$\alpha_3 = \frac{X_N Z_1 - X_1 Z_N}{Y_1 Z_N - Y_N Z_1} \qquad \text{(VIII.2-32c)}$$

and

$$\beta_1 = \frac{-Y_N}{Y_1 Z_N - Y_N Z_1} , \qquad \text{(VIII.2-32d)}$$

$$\beta_2 = \frac{Y_1}{Y_1 Z_N - Y_N Z_1} , \qquad \text{(VIII.2-32e)}$$

$$\beta_3 = \frac{X_1 Y_N - X_N Y_1}{Y_1 Z_N - Y_N Z_1} . \qquad \text{(VIII.2-32f)}$$

The procedure used to solve the transient heat conduction equations is not applicable to the steady-state case. This is due to the face that the matrix on the left side of Equation VIII.2-24 is singular for steady-state.

1756 316

Referring to Figure VIII.2-2 the steady-state heat flux between nodes i and i+1 is given by

$$- kh^{s}_{ri}(T_{i+1} - T_i) = -A_{\ell}\, \dot{q}_{\ell w} + \sum_{j=1}^{i} Q_i \qquad \text{(VIII.2-33)}$$

Then, by adding together Equations VIII.2-33 for all i between 1 and N-1 one obtains

$$T_N - T_i = -A_{\ell}\, \dot{q}_{\ell w} \sum_{i=1}^{N-1} \frac{1}{- kh^{2}_{ri}} + \sum_{i=1}^{n-1} \left(\left(\sum_{j=1}^{i} Q_j \right) \Big/ kh^{s}_{ri} \right) \qquad \text{(VIII.2-34)}$$

A second equation relating $\dot{q}_{\ell w}$ and $\dot{q}_{rw}$ is given by the total steady-state heat balance as

$$A_{\ell}\dot{q}_{\ell w} + A_r\dot{q}_{rw} - \sum_{i=1}^{N-1} Q_i = 0 \qquad \text{(VIII.2-35)}$$

Therefore, in both the transient and the steady-state case, two equations are available in the four variables T_1, T_N, $\dot{q}_{\ell w}$, and $\dot{q}_{rw}$. The two remaining equations required for the simultaneous solution for these four variables are provided by the heat transfer correlations applied to the left and right boundaries. In general, these correlations can be expressed as a functional relationship (F) between the surface heat flux and the corresponding wall temperature:

$$\dot{q}_{\ell w} = F(T_1) \qquad \text{(VIII.2-36)}$$

and

$$\dot{q}_{rw} = F(T_N)\ . \qquad \text{(VIII.2-37)}$$

Thus, in the transient case Equations VIII.2-30, VIII.2-31, VIII.2-36 and VIII.2-37 are solved simultaneously for T_1, T_n, $\dot{q}_{\ell w}$, $\dot{q}_{rw}$, while in the steady-state case Equations VIII.2-34, VIII.2-35, VIII.2-36 and VIII.2-37 are simultaneously solved.

Since Equations VII.2-36 and VIII.2-37 are in general non-linear functions of T_1 and T_N, the simultaneous solution of the four equations in each case is an iterative one.

The iterative solution in the transient case is obtained by making the approximations

$$\dot{q}_{\ell w}^{j+1} = \alpha_1 T_1^{j+1} + \alpha_2 T_N^{j} + \alpha_3 \qquad \text{(VIII.2-38)}$$

and

$$\dot{q}_{rw}^{j+1} = \beta_1 T_i^{j} + \beta_w T_N^{j+1} + \beta_3 \qquad \text{(VIII.2-39)}$$

Solving Equation VIII.2-38 simultaneously with Equation VIII.2-36 gives $\dot{q}_{\ell w}^{j+1}$ and T_1^{j+1} while solving Equation VIII.2-39 simultaneously with Equation VII.2-37 gives $\dot{q}_{rw}^{j+1}$ and T_N^{j+1}. Iteration continues until values of $\dot{q}_{\ell w}$, $\dot{q}_{rw}$, T_1 and T_N are found that simultaneously satisfy (to the specified degree of accuracy) all four equations.

The above iterative procedure requires a good initial guess of T_1 and T_N for rapid convergence. In the transient case the use of temperatures from the previous time step for the first iteration is sufficient to achieve rapid convergence. However, in the steady-state case such an initial estimate is not available.

Therefore the above iteration scheme is modified for steady state in the following way. Equation VIII.2-36 is linearized to the form

$$\dot{q}_{\ell w} = C_\ell \, h_{\ell 1}^{s} \, (T_1 - T_{f\ell}) \qquad \text{(VIII.2-40)}$$

where

$$C_\ell = \frac{\dot{q}'_{\ell w}}{(T'_1 - T_{f\ell})} \qquad \text{(VIII.2-41)}$$

Similarly Equation VIII.2-37 is linearized to the form

$$\dot{q}_{rw} \quad C_r \, h^s_{rN} \, (T_N - T_{fr}) \qquad \text{(VIII.2-42)}$$

where

$$C_r = \frac{\dot{q}_{rw}}{(T'_1 - T_{fr})} \qquad \text{(VIII.2-43)}$$

The resulting set of Equations VIII.2-34, VIII.2-35, VIII.2-40, and VIII.2-42 is linear, and is solved exactly for the j+1's iterates of $\dot{Q}_{\ell w}$, $\dot{q}_{rw}$, T_1, and T_N.

Iteration continues until $|T'_1 - T_1^{j+1}| < \varepsilon$ and $|T'_N - T_N^{j+1}| < \varepsilon$ for a specified ε.

3.0 SOLUTION METHOD FOR REACTOR KINETICS EQUATIONS

The reactor kinetics equations described in Section V were given as

$$\frac{d\phi(t)}{dt} = \frac{[R(t) - -]}{\frac{\Lambda}{\beta}} \phi(t) + \sum_{i=1}^{N} \lambda_i C_i(t) + S(t) \qquad \text{(VIII.3-1)}$$

$$\dot{C}_i(t) = E_1\phi(t) - \lambda_i C_i \qquad 1 \leq i \leq I \qquad \text{(VIII.3-2)}$$

where

ϕ = normalized fission power

R = reactivity in dollars

Λ = prompt neutron generation time

β = effective delayed neutron fraction

λ_1 = decay constant for i^{th} group

C_i = precursor concentration for i^{th} group

E_i = yield fraction for i^{th} group

S = source

The first N equations in the set defined by Equation VIII.3-2 represent delayed neutron groups and the remainder of the I equations represent the decay heat groups. For the delayed neutron equations, the E_i's were given by

$$E_i = \frac{\beta f_i}{\Lambda} \qquad \text{(VIII.3-3)}$$

where

1256 520

f_i = fraction of delayed neutrons in group i.

Let

$$w_i = \frac{\Lambda\lambda_i}{\beta f_i} C_i \qquad 1 \leq i \leq N \qquad \text{(VIII.3-4)}$$

$$w_i = \frac{\lambda_i C_i}{E_i} \qquad N < i \leq I. \qquad \text{(VIII.3-5)}$$

Substituting Equations VIII.3-4 and VIII.3-5 into Equations VIII.3-1 and VIII.3-2 gives

$$\dot{\phi}(t) = \frac{\beta}{\Lambda} \left\{ [R(t) - 1]\, \phi(t) + \sum_{i=1}^{N} f_i w_i(t) + S(t) \right\} \qquad \text{(VIII.3-6)}$$

$$\dot{w}_i(t) = \lambda_i \phi(t) - \lambda_i w_i(t) \qquad 1 \leq i \leq I \qquad \text{(VIII.3-7)}$$

which are the equations integrated in RETRAN. The initial conditions for RETRAN, including kinetics, are steady state. Thus, the initial reactivity and source terms are zero, normalized power is unity, and each w_i is unity.

The solution method for Equations VIII.3-6 and VIII.3-7 uses a modified fifth order Runge-Kutta method.[VIII.3-1]

A first-order differential equation is written as

$$\dot{n}(t) = \alpha\, n(t) + R(n, t) \qquad \text{(VIII.3-8)}$$

where α is a constant over the time step, and R(n,t) contains the remaining terms of the differential equation, including the nonconstant portion of any coefficient of n(t). That is, if the coefficient of n(t) is $\beta(n,t)$, α would be $\beta[n(0),)[$, and R(n,t) would contain a term of the form, $\{\beta[n,(t),t] - \beta[n(0),)]n(t)\}$. Multiplying Equation VIII.3-8 by an integrating factor and integrating gives

$$n(t) = n(0)\ e^{\alpha t} + \int_0^t e^{\alpha(t-\lambda)}\ R(n,\lambda)\ d\lambda\ . \qquad \text{(VIII.3-9)}$$

Since

$$n(0)\ e^{\alpha t} = n(0) + \int_0^t \alpha n(0)\ e^{\alpha(t-\lambda)}\ d\lambda\ ,$$

$$n(t) = n(0) + \int_0^t [\alpha n(0) + R(n,\lambda)]\ e^{\alpha(t-\lambda)}\ d\lambda\ . \qquad \text{(VIII.3-10)}$$

Letting $\lambda = ut$, then $d\lambda = tdu$, and

$$n(t) = n(0) + t \int_0^1 [\alpha n(0) + R(n,U)]\ e^{\alpha t(1-u)}\ du. \qquad \text{(VIII.3-11)}$$

The numerical technique for advancing the solution over the time step consists of making approximations to the behavior of R(n,u) over the time step. For convenience in the following expressions, the following function is defined.

$$C_m(x) = \int_0^1 u^{m-1}\ e^{x(1-u)}\ du. \qquad \text{(VIII.3-12)}$$

Stage 1:

Assume $R(n,\lambda) = R[n,(0),)] = R_o$, and write $n(0)$ as n_o; then compute $n(\frac{h}{2})$,

$$n_1 = n\ (\tfrac{h}{2}) = n_o + \tfrac{h}{2}\ [\alpha n_o + R_o]\ C_1\ (\alpha\ \tfrac{h}{2})\ . \qquad \text{(VIII.3-13)}$$

1756 322

Stage 2:

Assume straight line variation of $R(n,\lambda)$ between R_o and R_1 $R(n_1,\frac{h}{2})$, and comput $n(\frac{h}{2})$,

$$R(n,\lambda) = R_o + \frac{2[R_1 - R_o]\lambda}{h} \qquad \text{(VIII.3-14)}$$

$$R(n,u) = R_o + [R_1 - R_o]\, u \qquad (\text{using } \lambda = u\,\tfrac{h}{2}) \qquad \text{(VIII.3-15)}$$

$$n_2 = n(\tfrac{h}{2}) = n_1 + \tfrac{h}{2}\,[R_1 - R_o]\, C_2\,(\alpha\,\tfrac{h}{2})\ . \qquad \text{(VIII.3-16)}$$

Stage 3:

Assume straight line variation of $R(n,\lambda)$ between R_o and $R_2 = R(n_2,\frac{h}{2})$, and compute $n(h)$,

$$R(n,\lambda) = R_o + \frac{2[R_2 - R_o]\lambda}{h} \qquad \text{(VIII.3-17)}$$

$$R(n,u) = R_o + 2[R_2 - R_o]\, u \quad (\text{using } \lambda \quad uh) \qquad \text{(VIII.3-18)}$$

$$n_3 = n(h) = n_o + h[\alpha n_o + R_o]\, C_1(\alpha h) + 2h\,[R_2 - R_o]\, C_2(\alpha h)\ . \qquad \text{(VIII.3-19)}$$

Stage 4:

Assume a guadratic fit through points R_o, R_2, and $R_3 = R(n_3,h)$; then compute $n(h)$,

$$R(n,u) = [2R_o - 4R_2 + 2R_3]\, u^2 + [-3R_o + 4R_2 - R_3]\, u + R_o \qquad \text{(VIII.3-20)}$$

$$n_4 \quad n(h) = n_3 + h\,[R_o - 2R_2 + R_3][2C_3\,(\alpha H) - C_2\,(\alpha h)]. \qquad \text{(VIII.3-21)}$$

Stage 5:

Assume a quadratic through points R_o, R_2, and $R_3 = R(n_4,h)$; then compute $n(h)$,

$$n_5 = n(h) = n_4 + h[R_4 - R_3][2C_3(\alpha h) - C_2(\alpha h)]. \qquad \text{(VIII.3-22)}$$

The third-, fourth-, and fifth-order approximations are obtained by terminating the process at the end of the third, fourth, and fifth stages, respectively.

By direct integration, the function $C_1(x)$ is given by

$$C_1(x) = \frac{e^x - 1}{x} . \qquad \text{(VIII.3-23)}$$

Using integration by parts, a recursion relation for $C_m(x)$ is

$$C_{m+1}(x) = \frac{mC_m(x) - 1}{x} . \qquad \text{(VIII.3-24)}$$

During machine calculations of the $C_m(x)$ functions for $x \leq 1$, excessive loss of singificance occurs. For this range, $C_3(x)$ is computed from its MacClaurin series expansion.

$$C_3(x) = 2 \quad \frac{1}{3!} + \frac{x}{4!} + \frac{x^2}{5!} + \frac{x^3}{6!} + \frac{x^4}{7!} + \frac{x^5}{8!} + \frac{x^6}{9!} + \frac{x^7}{10!} . \qquad \text{(VIII.3-25)}$$

C_2 and C_1 are evaluated by solving Equation VIII.3-24 for $C_m(x)$.

During the time advancement of the solution, the time increment is automatically increased or decreased in order to maintain a specified degree of accuracy. After the calculations for a time advancement, the program uses an empirical formula to estimate the error. If the error is excessive, the time increment is halved, and the advancement calculation is redone. If the error is sufficiently small, the time interval is doubled for the next time step. If the estimated error is between limits, the same interval is used for the next time advancement. These procedures for time step control are as follows:

$$\omega_1 = \frac{\dot{\phi}(0)}{\phi(0)} \qquad \text{[evaluated from Equation VIII.3-6]} \qquad \text{(VIII.3-26)}$$

$$\omega_3 = \frac{\dot{\phi}(h)}{\phi(h)} \qquad \text{(VIII.3-27)}$$

$\bar{\omega}$ is defined from $\phi(h) = \phi(0)e^{\bar{\omega}h}$ (VIII.3-28)

$$Q = \frac{h\, C_2\,(\alpha h)}{1 + C_1\,(\alpha H)} \left[\left|\omega_1 - 2\bar{\omega} + \omega_3\right|\right] \qquad \text{(VIII.3-29)}$$

The α in Equation VIII.3-29 is that of the power equation. The quantity, δ, is defined as the maximum, taken over all the differential equations, of the quantity

$$\left|\frac{n_1 - n_o}{n_1}\right| . \qquad \text{(VIII.3-30)}$$

The Q_L and Q_H appearing below are set to .001 and .001, respectively.

(1) If $\delta < 2^{-15}$ and $Q \geq Q_L$, the program continues with the same time step.

(2) If $\delta < 2^{-15}$ and $Q < Q_L$, the program doubles the time step for the next advancement.

(3) If $\delta \geq 2^{-15}$ and

- If $Q < Q_L$, the time step is doubled for the next advancement
- If $Q \leq Q_H$, the same time step is used for the next advancement
- If $Q > Q_H$, the time advancement is recalculated with half the time step.

(4) The time advancement is also recomputed with the time step halved if

- αh of any equation > 88.0
- Minus or zero power is computed.

4.0 STEADY-STATE INITIALIZATION OF THE RETRAN OVERALL BALANCE EQUATIONS

The RETRAN overall balance equations used to describe one-dimensional homogeneous equilibrium fluid flow are developed in Section II. These balance equations constitute a set of coupled non-linear differential equations. The balance equations together with the initial conditions represent an initial value problem which is solved according to the numerical technique described in Section VIII.1. For steady-state fluid flow, initial conditions are required which result in zero time derivatives for the three balance equations which simultaneously establish a complete set of desired initial values. RELAP4, predecessor of the RETRAN transient thermal-hydraulics analysis code, requires the code user to supply initial values for all primary variables through input data, subsequently forcing an overspecification of the steady-state initial value problem. This overspecification makes RELAP4 very difficult and nearly impossible to use as an analysis tool for many quasi steady-state thermal-hydraulic transients, since the forced overspecification imparts unwanted non-zero forcing functions to the transient solution.

The problem initialization sequence used in the RETRAN code has been extensively modified from that used by RELAP4, in that RETRAN solves the steady-state initial value problem to obtain the appropriate initial conditions for the mass, momentum and energy balance equations. By solving the steady-state initial value problem, the overspecification required by RELAP4 is eliminated in RETRAN, thus minimizing the quantity of required user input data while simultaneously insuring that the code can be run in the steady-state mode when the temporal balance equations are solved. Implicit in the RETRAN steady-state initial value problem solution is the steady-state solution of all applicable temporal constitutive and component models. The steady-state solution techniques used for each of the three balance equations and their associated constitutive and component models are discussed in the following sections. Only those constitutive and component models requiring special treatment are described, otherwise they are treated as in the transient solution scheme.

4.1 Mass Balance Equations

The steady-state continuity condition

$$\sum_{J \varepsilon IN} W_j - \sum_{j \varepsilon OUT} W_j = 0 \qquad \text{(VIII.4-1)}$$

must be satisfied if either RETRAN or RELAP4 is to be capable of analyzing a quasi steady-state transient, since the mass balance equation is tightly coupled to the momentum and energy balance equations. Equation VIII.4-1 is by far the simplest of the three balance equations and, after a cursory examination, appears to have a near trivial solution. The primary problem encountered is not the difficulty of trying to satisfy Equation VIII.4-1 through input data, but rather insuring the consistency of the input data for the component models which affect the junction mass flow rates and the continuity balance. It is dangerous to assume the mass flow rates supplied on the junction data cards satisfy the steady-state continuity conditions without regard to checking the status of hardware models such as valves (which may be closed and a non-zero flow specified) or fill models (which may yield mass flows different from the input value). Inconsistencies in input data such as those described above do not manifest themselves until the first time step is taken. If the inconsistency is significant, the problem solution generally demonstrates anomalous behavior which the user can use to trace the input problem. It is conceivable and quite probable that a small inconsistency in input mass flow rate, such as fill boundary condition, may go undetected and have a significant effect on a problem transient response, yet not lead to totally anomalous behavior.

The technique used in the RETRAN code to insure a steady-state continuity balance is to use any initial mass flow rates computed by the fill boundary condition model, rather than the input junction flow, and further, to zero any non-zero input junction flows for flow paths containing a valve closed at time zero.

Before continuing with the discussion of the continuity initial value problem, it is useful to define some nomenclature that will be used in the following discussion. Due to the generality with which RETRAN is constructed, the capability exists to describe flows in straight pipe sections, tees, manifolds and other complex geometries. If one recalls that the basic fluid flow equations are one-dimensional, it is easy to visualize that these complex geometries represent parallel flow paths. Consequently, any volume with more than two flow

paths initiates or terminates at least two parallel flow paths. All flowing streams which split or merge will be generally referred to as parallel flow paths.

The user input for the continuity equation is minimal in that only one junction mass flow rate is required for simple pipe flow geometries i.e., for cases with no parallel flow paths. For flow geometries that split into parallel flow paths, such as that illustrated by Figure VIII.4-1, only one junction mass flow rate in either of the parallel flow paths is required if a junction flow is defined in either of the simple geometries above or below the parallel paths. Figure VIII.4-2 illustrates the 45 different combinations of input junction mass flow rates which supply the minimum amount of data required to calculate the mass flow rates for all junctions shown in Figure VIII.4-1.

In addition to the minimal set of input flow data discussed above, any other combinations of input flows may be supplied, provided they include at least one minimum input set combination. Thus, the maximum set of input data acceptable constitutes a combination of all the minimal sets of input, or all junction flows. From a user standpoint, a minimal set is more desirable since it facilitates modification of the input flow rates by minimizing required input data.

4.1.1 Mass Balance Solution Technique

The basic approach used in RETRAN to solve for the steady-state junction mass flow rates not input by the code user is to loop over all junctions propagating flows either forward or backward by use of Equation VIII.4-1. Once the flow propagation procedure encounters a volume initiating or terminating parallel flow paths, and more than one junction flow into or out of the volume remains unknown, the propagation stops at this point and continues at another point in the flow network if possible. Several complete passes over the entire set of junctions may be required to compute all of the necessary flows. If no flows are computed in two successive passes over all junctions, the problem is underspecified. If such an error condition is detected, diagnostics are edited and the problem is terminated.

Whether all flows, or a minimum input set is supplied by the code user, the continuity condition is checked by use of the following, once all flows are known.

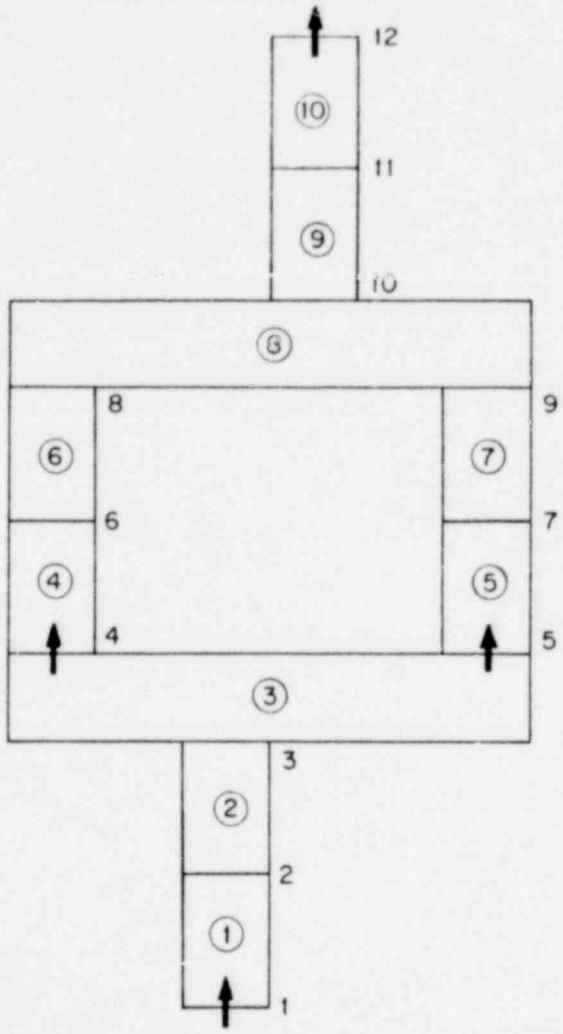

Figure VIII.4-1 Typical RETRAN Parallel Flow Path Nodalization

1756 329

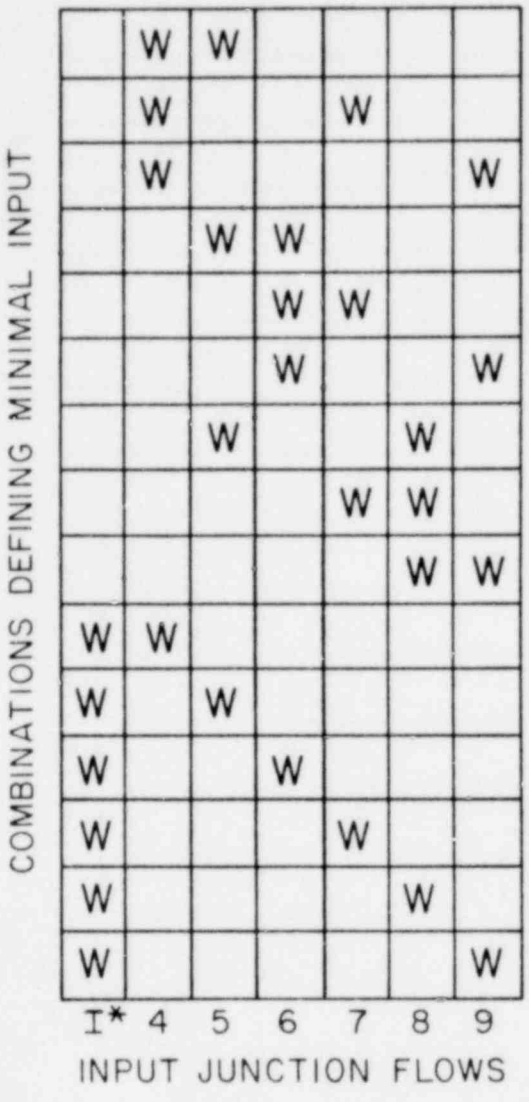

	4	5	6	7	8	9
	W	W				
	W			W		
	W					W
		W	W			
			W	W		
			W			W
		W			W	
				W	W	
					W	W
W	W					
W		W				
W			W			
W				W		
W					W	
W						W

*APPLIES INDIVIDUALLY FOR JUNCTIONS I EQUAL TO 1,2, 3,10,11 OR 12; THEREFORE THERE ARE 9+6x6 OR 45 EQUALLY ACCEPTABLE MINIMAL SETS OF INPUT DATA.

Figure VIII.4-2 Combinations of Input Flow Data Satisfying the Minimum Input Requirements

1256 530

$$\left| \frac{\sum_{j\varepsilon IN} W_j - \sum_{j\varepsilon OUT} W_j}{\bar{W}} \right| \leq \varepsilon_m \qquad \text{(VIII.4-2)}$$

where

$$\bar{W} = 0.5 \left(\sum_{j\varepsilon IN} W_j - \sum_{j\varepsilon OUT} W_j \right) \quad . \qquad \text{(VIII.4-3)}$$

If the error in the mass balance is greater than the user supplied error criterion ε_M for any volume, the problem is terminated since it would be a fruitless exercise to perform the steady-state initial value calculations for the momentum and energy balance equations using unacceptable initial values for the junction mass flow rates.

The parameter $\bar{W}$, computed according to Equation VIII.4-3, defines the steady-state average mass flow rate for a control volume and is used in the momentum and energy balance equations discussed in the following sections.

4.1.2 Steady-State Critical Flow

All mass flow rates computed by RETRAN are computed such that the steady-state continuity condition is satisfied. However, it is possible that an input or computed mass flow rate which satisfies the steady-state continuity condition may be larger in magnitude than the value computed by the critical flow model. This disparity between mass flow rates is not a common occurance for most classes of problems for which RETRAN is used, and is neglected during the initialization sequence, i.e., the critical flow model is not used in the RETRAN steady-state initialization scheme. Any disparity between the junction mass flow rates and the critical flow value will not be apparent until the first time step is taken, when the junction flow will be set to the critical flow value and the choking flag set. As might be expected, resetting the mass flow rate to the critical value upsets the mass, momentum, and energy balances and the calculation departs from steady-state in a step wise manner. The magnitude of this numerical perturbation is solely a function of the magnitude of the mismatch between the original and the critical mass flow values.

Omission of the critical flow model from the initialization scheme is not unique to RETRAN, and is similarly neglected in RELAP4. The motive for omitting the critical flow model in the RETRAN steady-state initialization scheme is provided by the complexity of the initialization scheme that is required if the critical flow model is included, versus the simplicity that results when it is neglected particularly since steady-state critical flow is not present in the class of problems for which RETRAN is typically used.

4.2 Momentum Balance Equations

The initialization technique utilized by the RELAP4 code requires that the user supply all junction flows and form loss coefficients, as well as all volume pressures. To avoid overspecifying the momentum equation, the input form loss coefficients are in effect treated as approximate values to be used in the calculation. The actual loss coefficients used are computed via the steady-state momentum balance equation

$$K_{T_j} = \left[(p_K - p_L) + \left(\frac{\bar{W}_K^2}{\bar{\rho}_K A_K^2} - \frac{\bar{W}_L^2}{\bar{\rho}_L A_L^2} \right) + {}_jW_j + g \int_K^j \rho_K \, dz - \int_j^L \rho_L dz \right.$$

$$\left. - \left(f_K \frac{\ell_K \bar{W}_K |\bar{W}_K|}{D_K \bar{\rho}_K A_K^2} \Phi_{tp_K} + f_L \frac{\ell_L \bar{W}_L |\bar{W}_L|}{D_L \bar{\rho}_L A_L^2} \Phi_{tp_L} \right) \right] \Bigg/ \frac{W_j |W_j|}{2\rho_j A_j^2} \quad . \qquad \text{(VIII.4-4)}$$

The difference between a computed K_T and the corresponding input loss coefficient is termed the residual loss coefficient, and is a measure of the imbalance in the steady-state momentum balance due to the overspecification of the input data. However, since the computed residual loss coefficient is always added to the input loss coefficient for all form loss pressure drop calculations, RELAP4 in effect solves one form of the steady-state initial value momentum equation.

An alternate form of the steady-state momentum equation is obtained by re-arranging Equation VIII.4-4 to solve for the downstream volume pressure p_L, as follows

$$p_L = p_K + \left(\frac{\bar{W}_K^2}{\bar{\rho}_K A_K^2} - \frac{\bar{W}_L^2}{\bar{\rho}_L A_L^2}\right) + \mathcal{J}_j W_j + g\left(\int_K^j \rho_K \, dz - \int_j^L \rho_L \, dz\right)$$

$$- \left(f_K \frac{\ell_K \bar{W}_K |\bar{W}_K|}{D_K \bar{\rho}_K A_K^2} \Phi_{tp_K} + f_L \frac{\ell_L \bar{W}_L |\bar{W}_L|}{D_L \bar{\rho}_L A_L^2} \Phi_{tp_L}\right) - K \frac{W_j |W_j|}{2\rho_j A_j^2} \quad . \qquad \text{(VIII.4-5)}$$

With a trivial manipulation, Equation VIII.4-5 can be re-arranged to a form which will allow the upstream pressure p_K, to be computed. Both forms of Equation VIII.4-5, in addition to Equation VIII.4-4, may be used in the RETRAN steady-state initialization of the momentum equation, depending upon the input supplied by the code user. Several combinations of input data and the subsequent use of Equations VIII.4-4 and VIII.4-5 are discussed below.

Recall that all of the junction flows are either input or computed from a minimal set of input data, and that the steady-state continuity condition is satisfied for all volumes. If a user supplies all volume pressures as input data (only possible for open ended flow systems with no parallel flow paths as will be illustrated later), only the junction form loss coefficients remain as unknowns and are computed by use of Equation VIII.4-4. However, in general, volume pressures and/or junction form loss coefficients computed via the steady-state momentum balance equations are only approximate the first few iterations, and junction state properties are only approximate. The volume and junction state properties are well defined only when the volume pressure and enthalpies are known. The numerical scheme used for the steady-state energy equation and the resulting volume average enthalpy used in conjunction with the volume average pressure to define the thermodynamic state in a RETRAN control volume is discussed in Section VIII.4.3. For the remainder of the steady-state momentum equation discussion, a knowledge of the exact treatment of the volume enthalpy calculation is not required, but it must be recognized that there is inherent coupling between the momentum and energy equations via the equations of state. Consequently, the solution of either form of the momentum equation and the energy equation, for the steady-state initial values, requires an iterative procedure where the most recently computed pressures and enthalpies are used to obtain a better estimate of the state properties.

Since Equation VIII.4-4 or VIII.4-5, or a combination of both may be used to obtain the steady-state momentum balance, it is useful to define the number of pressures and/or form loss coefficients that must be computed by RETRAN. The number of coupled algebraic equations available is given by

$$N_{UNK} = NJUN - NFIL - NCVAL \qquad \text{(VIII.4-6)}$$

where

N_{UNK} = the number of independent unknown pressure and/or loss coefficients which must be computed

NJUN = the total number of junctions

NFIL = the number of fill junctions

NCVAL= the number of normal junctions containing valves closed at time zero.

For the sample nodalization depicted by Figure VIII.4-1, there are ten unknown pressures and/or loss coefficients which must be computed to obtain a steady-state momentum balance, if we assume that junctions 1 and 12 are fill boundary conditions. It then follows directly, that the pressures can be input for the ten control volumes and the loss coefficients for junction 2 through 11 computed. Similarly, one volume pressure may be input, and nine volume pressures and one form loss computed. The single pressure can be input for any of the ten control volumes, but the loss coefficient must be computed for a junction common to one of the parallel flow paths, i.e., junctions 4, 5, 6, 7, 8 or 9.

The two examples given above define the maximum and minimum number of pressures that may be input for the sample illustrated by Figure VIII.4-1. Any combination of input pressure is also acceptable, since RETRAN computes loss coefficients for junctions connecting two volumes with input pressures by use of Equation VIII.4-4, and propagates pressures to volumes where a pressure is not input by use of Equation VIII.4-5 and an input form loss coefficient. The input data is improperly specified if it is possible to propagate a pressure into a single volume via two or more paths as would be possible if the pressure is input for volume 1 and all

loss coefficients supplied except for junction 11. For this set of ill-posed input data, the pressure for volume 8 is in effect computed twice, once using the momentum equations for junction 8 and again using the momentum equation for junction 9. (It would be fortuitous if the two computed pressures for volume 8 were identical.) Additionally, the pressure in volume 10 can not be computed, since the loss coefficient and the downstream volume pressure are both unknown. The input data is ill-posed since the pressure in volume 8 is overspecified and the momentum equation for junction 11 is underspecified. One solution (other combinations of input are possible) to the ill-posed input data for the example given above is to supply the pressure in volume 10 and have RETRAN compute the loss coefficient for junction 8 or 9.

4.2.1 Momentum Balance Solution Technique

Volume pressures and/or junction loss coefficients are in effect computed by marching sequentially from one junction to the next through the entire flow network. The general solution scheme used to solve the coupled set of momentum balance equations is to loop over all junctions, computing loss coefficients and upstream or downstream volume pressures by use of Equations VIII.4-4 and VIII.4-5, respectively. Several outer passes over the inner junction loop are typically required to compute the N_{UNK} unknown parameters. The number of outer passes required to close the set of equations varies from one problem configuration to the next, but ranges from a minimum of one to a maximum of N_{UNK}.

Since the solution of the momentum balance equations requires an iterative solution due to the dependence of the momentum equations upon state properties, which are not well defined initially, the procedure outlined above is followed for each iteration. The iteration scheme is discussed in Section VIII.4-4.

During the volume pressure and/or form loss computation procedure, the RETRAN steady-state initialization program module checks the user-supplied input data to ensure the problem is not underspecified for all geometries and is not overspecified for simple geometries. If an overspecification or underspecification is detected in the input data, an appropriate diagnostic message is edited and the problem is terminated. It is virtually impossible to detect overspecification for complex geometries. However, overspecification for this case usually manifests itself in unusually large acceleration pressures. The user can then check for

overspecification in the vicinity of the junctions with unacceptable acceleration pressures.

4.3 Energy Balance Equations

Of the three balance equations used to describe one-dimensional homogeneous equilibrium fluid flow in RETRAN and RELAP4, the energy balance equation requires the most complex solution scheme for solving the initial value problem in RETRAN, but is neglected in RELAP4. The complexity is not a result of the balance equations per se, but rather the constitutive and component models that are tightly coupled to the energy equations and which provide the source terms or forcing functions to the energy equations. Consequently, each of the temporal constitutive and component models must be solved for their steady-state initial values so that non-steady-state forcing functions are not imparted to the energy equation. These models are discussed in the following sections.

The steady-state energy balance equation used in RETRAN is slightly modified from the form used in the transient computations. The motive for this slight departure from the temporal equation form will be apparent momentarily. First, consider the temporal balance equation with the time derivatives set to zero.

$$\sum_{j\varepsilon OUT} W_j \left[h_j + \frac{1}{2} V_j^2 + z_j\right] - \sum_{j\varepsilon IN} W_j \left[h_j + \frac{1}{2} V_j^2 + z_j\right] = Q_L \quad . \qquad \text{(VIII 4-7)}$$

Equation VIII.4-7 can be readily solved for the steady-state initial values of the junction enthalpy h_j; however, an independent volume state variable is still required for the equation of state (only the pressures from the momentum equations are known). By using the following constitutive relationship to compute the transient junction enthalpy, the volume average enthalpy can be computed.

$$h_j = \bar{h}_K + \frac{1}{2} \bar{V}_K^2 - \frac{1}{2} V_j^2 + z_K - z_j + \Delta h_{Q,S_{jK}} \quad . \qquad \text{(VIII.4-8)}$$

A direct solution for the volume average enthalpies is facilitated by substituting Equation VIII.4-8 into Equation VIII.4-7, which after some manipulations yields,

1756 536

$$\sum_{j\varepsilon OUT} W_j \bar{h}_L - \sum_{j\varepsilon IN} W_j \bar{h}_K = \sum_{j\varepsilon FILL} W_j [h_j + \frac{1}{2} V_j^2 + z_j] + Q_L$$

$$+ \sum_{j\varepsilon IN} W_j [\frac{1}{2} \bar{V}_K^2 + z_K + \Delta h_{Q,S_{jK}}] - \sum_{j\varepsilon OUT} W_j [\frac{1}{2} \bar{V}_L^2 + z_L + \Delta h_{Q,S_{jL}}] \quad \text{(VIII.4-9)}$$

thus completing a set of independent state variables that can be used to define the control volume state properties via a call to the pressure-enthalpy (P-H), equation of state. An added benefit realized as the result of solving for the volume enthalpies, is that it allows the junction enthalpies to be computed using the same models used for the transient calculation which ensures numerical consistency between the steady-state and the transient calculational schemes.

4.3.1 Energy Balance Solution Technique

The solution technique used for the steady-state energy balance differs from the simple propagation or marching schemes used for the mass and momentum balance equations. Upon examination of Equation VIII.4-9 it is apparent that it is of the form

$$WH = C \quad \text{(VIII.4-10)}$$

where

W = an n (x) n coefficient matrix composed of junction mass flow rates

H = a vector whose n elements are the unknown volume enthalpies

C = a vector whose n elements define the net power addition to the corresponding control volumes.

Multiplying both sides of Equation VIII.4-10 by the inverse of the coefficient matrix (W^{-1}) gives the following transformed equation set which is solved directly for the average volume enthalpies.

$$\bar{W}^1 WH = IH$$

1756 337

where

I = the identity matrix,

thus

$$H = W^{-1} C . \qquad \text{(VIII.4-11)}$$

The coefficient matrix is composed of junction mass flow rates which are invariant throughout the steady-state initialization scheme. Consequently, the inverse of the coefficient matrix is also invariant and is evaluated once using the double-pivotal Gauss-Jordon reduction method. All of the coupling between the energy equation, and the momentum equation, equation of state, constitutive models and component models is through the elements of the C vector.

Equation VIII.4-11 represents the solution for a set of n coupled algebraic equations, but what constitutes the set of equations is the subject of the following commentary.

The approach used to define the set of coupled equations to be solved involves searching through the users input data to ascertain the number of independent flow networks in the model. A flow network is defined as the set of control volumes with common ancestry, which are connected by flow paths. Closed valves represent network boundaries, as can conductors separating networks, e.g., a steam generator where the tube walls define the boundary between the primary and secondary networks. Once the independent flow networks are isolated, the flowing volumes are flagged as belonging to the set of coupled equations to be solved for the particular network. Volumes associated with any given network, but which are not flowing initially, cannot be included in the set of coupled equations for the network in which they are resident, since their inclusion will lead to an ill-conditioned matrix. Zero flow volumes are the topic of a later discussion. For a user's model containing multiple flowing networks, there are multiple independent sets of coupled equations, and each set is solved according to Equation VIII.4-11.

Input requirements for the steady-state energy balance are minimal, and in fact limit the amount of data a user may supply. The required input is at least one

enthalpy for each network. If a simple network with no parallel flow path is initiated by a fill junction, the fill enthalpy will be used and input of an additional volume enthalpy overspecifies the network energy balance. This case generally does not lead to an ill-conditioned matrix, but can prevent the problem from converging.

The energy balance calculation for networks that are comprised of a closed flow system, such as the primary side of a typical PWR model, requires that a single volume enthalpy must be supplied for the closed flow system. For open flow networks, several input enthalpies may be required. Figure VIII.4-3 illustrates a Y network which may require two enthalpy values to be supplied for the initialization scheme, or a single enthalpy value, depending upon the flow direction. If junctions 5 and 8 are positive fills (junction 9 is negative fill), two enthalpies are necessary and sufficient to properly specify the energy balance equations. However, should junction 9 be a positive fill (junctions 5 and 8 are negative fills), the enthalpy of the fill fluid entering the network at junction 9 is necessary and sufficient to properly specify the energy balance equations.

An open flow network requiring two enthalpies is illustrated by Figure VIII.4-4, where junctions 1 and 13 are positive and negative fills, respectively. The fill enthalpy for junction 1 uniquely defines the reference enthalpy for volumes 1 and 2, but does not uniquely define a reference enthalpy for any of the other nine volumes. Consequently, a single enthalpy for volume 3, 4, 5 ..., 10 or 11 must be supplied to adequately specify the energy balance equations for the network. An alternate method of considering the required enthalpy input for the example shown in Figure VIII.4-4 is to look at the side loop residing within the bounds of the dashed line, without regard to the portion of the network outside the dashed boundary. If an enthalpy is not supplied for one of the volumes within the boundary, the energy balance is clearly underspecified since a reference enthalpy is not supplied.

It is possible to have volumes residing within a flow network, but which do not have any flow in or out. (This satisfies the continuity condition.) As noted earlier, these volumes are not included in the coupled equation set solved according to Equation VIII.4-11. An example of such a situation may be visualized by considering that junction 12 in Figure VIII.4-4 contains a closed valve, thus precluding flow through the side loop if the continuity condition is to be

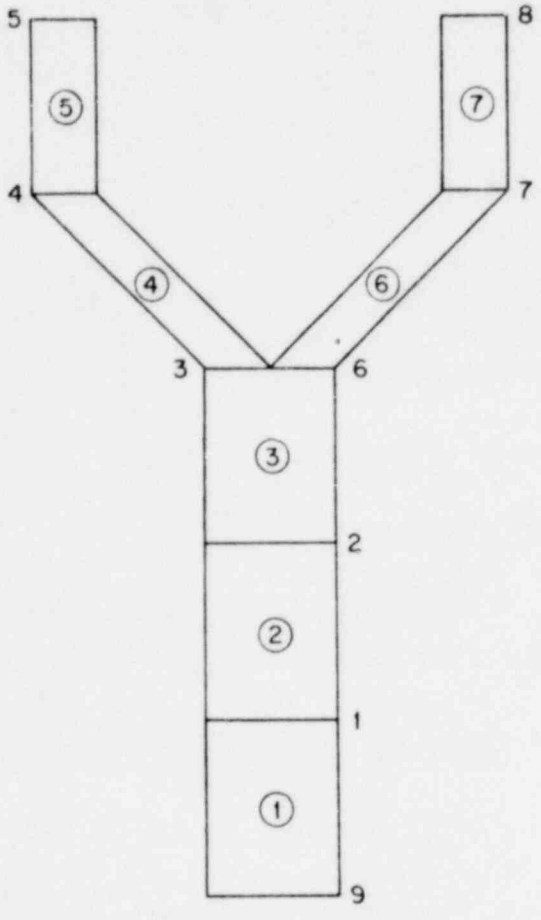

Figure VIII.4-3 Enthalpy Input Requirements for a Typical Y Network

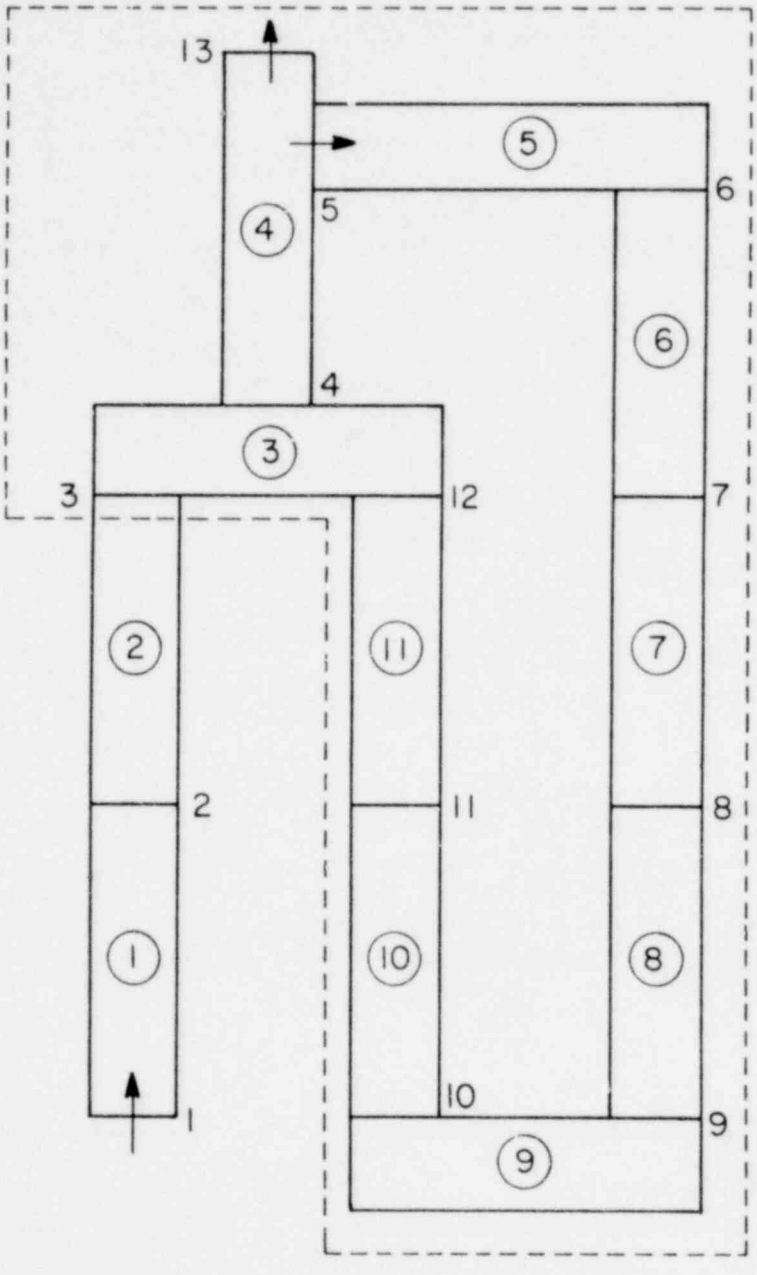

Figure VIII.4-4 Nodalization of an Open Network

1256 341

satisfied. Several options are available to the code user for initializing such a stagnant flow path. First, the user may supply any or all of the enthalpies for volumes 5 through 11, or none at all. Any stagnant volume enthalpies not input will be computed using the following relation

$$\bar{h}_K + z_K = \bar{h}_L + z_L \qquad \text{(VIII.4-12a)}$$

by searching through the stagnant volu...es using the junction "from" (K), "to" (L) convention. For example, consider that the enthalpy is not input for volume 5. In this case, the enthalpy for volume 5 is computed as follows,

$$\bar{h}_5 = \bar{h}_4 + z_4 - z_5 \quad . \qquad \text{(VIII.4-12b)}$$

4.3.2 Junction Enthalpy Constitutive Models

The junction enthalpy used in RETRAN is computed by use of Equation VIII.4-8 for both the steady-state and transient calculational schemes. The $\Delta h_{Q,S}$ term is used to define the change in thermodynamic enthalpy that occurs as the fluid moves from the center of the donnor volume to the junction, due to energy exchange between the volume and an energy source or sink or phase separation. For homogeneous junction flow, i.e., when phase separation or enthalpy transport are not used, $\Delta h_{Q,S}$ is zero. Similarly, $\Delta h_{Q,S}$ is also zero for junctions connected to temperature transport delay volumes (see Section VII.2.0), since they are initialized as homogeneous volumes. The solution methods used to obtain initial conditions for the enthalpy transport and phase separation models are discussed in subsequent sections.

4.3.2.1 Enthalpy Transport

The enthalpy transport model developed in Section III.2.5.2, is based upon the following equation which relates the donor volume mass flow rate, mass inventory, energy exchange and junction mass flow rate to the rate of change of the junction enthalpy.

$$\frac{dh_j}{dt} + \frac{(\bar{W}_K + W_j)}{M_K} h_j = \frac{(\bar{W}_K + W_j)}{M_K} \bar{h}_K + \frac{Q_K}{M_K} \quad . \qquad \text{(VIII.4-13)}$$

1756 542

At steady-state conditions the temporal derivative is zero. Dropping the derivative, and rearranging to obtain

$$h_j - \bar{h}_K \equiv \Delta h_{Q,S_{jK}} \quad .$$

provides the steady-state initial value of $\Delta h_{Q,S}$ for the enthalpy transport model. The initial value is given by

$$\Delta h_{Q,S_{jK}} = \frac{Q_K}{(\bar{W}_K + W_j)} \quad . \qquad \text{(VIII.4-14)}$$

The value of Q_K is in general a function of the fluid state properties, thus requiring an iterative solution.

4.3.2.2 Phase Separation

A detailed development of the phase separation or "bubble rise" model is found in Section III.1.3, while the application of the phase separation model to the junction enthalpy calculation is given in Section III.2.5, where $\Delta h_{S_{jk}}$ is defined as

$$\Delta h_{S_{jk}} = h_g(x_j - \bar{x}_K) + h_f(\bar{x}_K - x_j) + \frac{1}{2}\left(\frac{W_j}{\rho_j A_K}\right)^2$$

$$- \frac{1}{2}\left(\frac{\bar{W}_K}{\bar{\rho}_K A_K}\right)^2 + z_j - z_K \quad . \qquad \text{(VIII.4-15)}$$

Assuming that the initial pressure and enthalpy are known for a separated volume (they are user supplied values), the volume thermodynamic properties are then well defined as are the junction and volume mass flow rates. For these conditions, a unique value of $\Delta h_{S_{jk}}$ must exist to satisfy the energy balance equation for the control volume. The only parameter in Equation VIII.4-15 that is not completely defined by the conditions noted above is the junction quality x_j. Consequently, x_j must be adjusted to yield the value of $\Delta h_{S_{jk}}$ required to balance the

steady-state energy equations for separated volumes. After examining Equation III.1-90, which defines the junction quality, it is apparent that the bubble gradient, C_o, is the only parameter not defined by the mass flows or thermodynamic state properties. C_o is typically a user input quantity to the bubble rise model, which specifies the density gradient through the mixture. For the case where the code user is using the RETRAN steady-state initialization and inputs the enthalpy of a bubble rise volume, C_o must be computed by the code if a steady-state balance is to be obtained.

The approach used to compute the value of the bubble gradient required for a steady-state condition in a separated volume is to perform an energy balance. Figure VIII.4-5 illustrates a separated volume and the known parameters used in the energy balance. Basically, the only unknown in the energy balance equation is the enthalpy of junction 3, which is directly related to the junction quality. The quality required for steady-state is defined by the energy balance as

$$x_3 = \frac{Q + W_1 h_1 - W_2 h_2}{W_3 (h_g - h_f)} - \frac{h_f}{(h_g - h_f)}$$

where the kinetic and potential energy terms have been omitted for convenience in the example. The inlet enthalpy, h_1, is defined by the donor volume and is not dependent upon the conditions in the separated volume, while one exit enthalpy, h_2, is known to be the value for saturated steam corresponding to the pressure of the separated volume. Calculation of the remaining exit enthalpy, h_3, is straight forward and the use of the enthalpy-quality relationship allows the exit quality, x_3, to be computed. In effect, the quality x_3 does not alter the mass or energy content of the separated volume, but merely defines the local quality required at a point (or integrated over a vertically oriented circular area), which can be used to define the vertical distribution of mass and energy in the mixture region. C_o is the parameter in the bubble rise model which defines the vertical distribution of quality within the mixture. Consequently, the exit junction quality required to obtain the single volume energy balance is used to define the quality distribution, thus defining the required value of C_o.

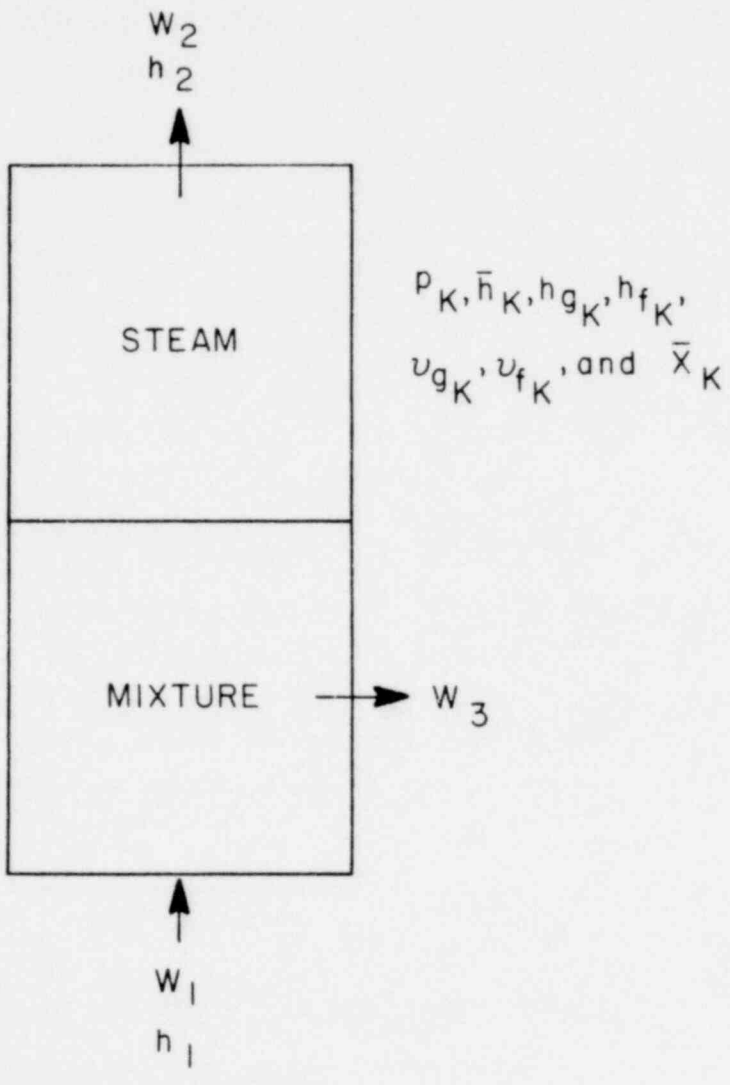

Figure VIII.4-5 Separated Volume Energy Balance

1756 345

The general form of the separated volume energy balance and the resulting quality used to initialize the mixture bubble gradient is

$$x_{j_{ref}} = \Bigg[Q_K + \sum_{j\varepsilon IN} W_j \left(h_j + \frac{1}{2} V_j^2 + z_j\right) - \sum_{j\varepsilon OUT_A} W_j \left(h_{g_k} + \frac{1}{2} V_j^2 + z_j\right) - \sum_{j\varepsilon OUT_B} W_j \left(h_{f_K} + \frac{1}{2} V_j^2 + z_j\right) \Bigg] \Big/ \left(h_{g_K} - h_{f_K}\right) \sum_{j\varepsilon OUT_B} W_j A_j \qquad \text{(VIII.4-16)}$$

where

$j\varepsilon OUT_A$ = sum of junctions flowing out of volume K, which originate in the steam dome of the separated volume, i.e., junction resides above the mixture level.

$j\varepsilon OUT_B$ = sum of junctions flowing out of volume K, which originate below the mixture level, i.e., junction fluid properties are influenced by the bubble gradient.

$x_{j_{ref}}$ = a reference junction quality representative of the fluid leaving a separated volume via all junctions residing below the mixture level.

A_j = $z_{j_{ref}}/z_j$.

With the reference quality obtained from Equation VIII.4-16, and Equation III.1-90 which defines the junction quality as a function of the bubble gradient C_o, and the state properties of the separated volume, a steady-state initial value for C_o can be obtained. There are in effect four different forms of the equation, two of which are due to the equation forms for mixture void fractions between zero and one-half, and one-half to one. while two additional forms are required for the junction geometry, i.e., one form for horizontally-oriented junctions and another form for vertically-oriented junctions. Since the algebraic manipulations are straightforward, only the resultant equation forms are given. The four equations are

$$C_o = \frac{\alpha_m\left[x_j M_m - M_{gb} - (1-x_j)\left(\frac{1-\alpha_m}{\alpha_m}\right) V_m\rho_g\right]}{(2\ell - \alpha_m)B}, \qquad \text{(VIII.4-17)}$$

where $(0.0 \leq C_o \leq 1.0)$

$$B = M_{gb} + x_j\,(V_m\rho_\ell - M_m) \qquad \text{for} \quad 0.0 \leq \frac{M_{gb}}{\rho_g V_m} \leq 0.5$$

$$B = V_m\rho_g - M_{gb} + x_j\,(M_m - V_m\rho_g) \qquad \text{for} \quad 0.5 < \frac{M_{gb}}{\rho_g V_m} \leq 1.0 \ .$$

For horizontal junctions, or vertical junctions whose flow areas are completely below the mixture level,

α_m = fraction of the junction area residing below the mixture level

= 1.0

ℓ = relative junction height

= z_j/z_m .

Vertically-oriented junctions with the mixture level residing within the circular junction area are treated similarly, with the exceptions that,

$$\alpha_m = 0.5 + Y_m\sqrt{1 - Y_m^2} + \sin^{-1}(Y_m)$$

and

$$\ell = \frac{\bar{z}_j}{z_m}$$

1756 347

where

$$Y_m = \frac{z_m - z_j}{R}$$

R = junction radius

$$\bar{z}_j = \alpha_m z_j - 2R \sqrt{1 - Y_m^2}^{3} / 3\pi \quad .$$

The previous discussion applies for cases where the code user supplies the volume average enthalpy for a separated volume. When the enthalpy of a separated volume is not supplied by the code user, the mass inventory of the volume is not defined and Equation VIII.4-17 can not be used to obtain steady-state initial conditions for separated volumes. However, Equation VIII.4-16 is applicable and Equation VIII.4-17 can be re-arranged to solve for the mass of steam entrained in the mixture. The bubble mass equation utilizes the user input bubble gradient, and the reference junction quality (evaluated according to Equation VIII.4-16) to compute the bubble mass entrained in the liquid-steam mixture as follows:

$$M_{gb} = \rho_g V_m \frac{x_j - (1-x_j)\left(\frac{1-\alpha_m}{\alpha_m}\right)\frac{\rho_g}{\rho_\ell} - C_o\,(2\ell - \alpha_m)\,D}{x_j + (1-x_j)\frac{\rho_g}{\rho_\ell} + C_o\,(2\ell-\alpha_m)\,E} \qquad \text{(VIII.4-18)}$$

where

$D = (1 - x_j)$

$$\text{for } 0.0 \leq \frac{M_{gb}}{\rho_g V_m} \leq 0.5$$

$E = 1$

and

$$\left.\begin{aligned} D &= x_j + (1-x_j)\frac{\rho_g}{\rho_\ell} \\ E &= -D \end{aligned}\right\} \text{ for } 0.5 < \frac{M_{gb}}{\rho_g V_m} \leq 1.0 \quad .$$

Once the bubble mass inventory has been computed, the volume average quality is computed as

$$\bar{x} = \frac{M_s + M_{gb}}{M_s + M_{gb} + M_\ell} \qquad \text{(VIII.4-19)}$$

where the mass of steam in the volume steam dome is given by

$$M_s = \rho_g (V - V_m)$$

and the mass of liquid in the mixture region of the separated volume is

$$M_\ell = \rho_\ell \left(V_m - \frac{M_{gb}}{\rho_j}\right) \quad .$$

Equation VIII.4-19 is then used in conjunction with the liquid and gas phase enthalpies, defined by the volume pressure, to compute the volume average enthalpy that will result in a steady-state solution for the bubble rise model. The volume average enthalpy is calculated by use of the following equation

$$\bar{h} = \bar{x}_{hg} + (1 - \bar{x})\, h_f \qquad \text{(VIII.4-20)}$$

The phase separation model developed in Section III.1.3 requires a knowledge of the rate of bubble formation, so that the bubble mass inventory can be explicitly computed for each time step. The bubble mass formation rate is given by

$$\frac{dM_{gb}}{dt} = \frac{dM_g}{dt} - \sum_{j\varepsilon IN} \Psi_j x_j W_j + \sum_{j\varepsilon OUT} \Psi_j x_j W_j - Av_{bub}\, \rho_{gb}\, (z_m) \qquad \text{(VIII.4-21)}$$

Since the time derivatives in Equation VIII.4-21 must be zero for a steady-state condition to exist, the separation velocity must be computed to avoid overspecification of the steady-state form of the equation. The separation velocity is computed for any separated volume ($z_m < z_{VOL}$), accordingly

$$v_{bub} = \frac{\sum_{j\varepsilon OUT} \Psi_j x_j W_j - \sum_{j\varepsilon IN} \Psi_j x_j W_j}{A\, \rho_{gb}\, (z_m)} \quad . \qquad \text{(VIII.4-22)}$$

4.3.3 Power Generation and Removal

Various models are available in the RETRAN code to model energy addition or removal from control volumes. The primary energy source is generally modeled by use of the heat conduction equations with internal power generation (core conductors), while energy removal is often treated using heat conductors with fluid volumes on both sides as a heat exchanger. For core heat conductors, the initial power fraction is supplied by the code user. At steady-state conditions, the power generated in a heat conductor must be equal to the heat transmitted to the associated fluid volume. With the initial power level and power shape defined by the code user, the heat addition to the core fluid volumes is well defined. The net heat removal for a heat exchanger or steam generator is also specified by the code user.

Power can also be added or removed from control volumes by nonconducting heat exchangers. There are a number of options available in the nonconducting heat exchanger option. Any of the options may be used for power addition to control volumes; however, for heat removal from control volumes, the options utilizing normalized power rather than a specific power level are preferable. The primary difficulty encountered with a specified power removal is that the exact thermal power, which includes all heat sources such as core conductors, nonconducting heat exchangers and centrifugal pumps, may not be known to the precision required for steady state, parcicularly since the power delivered to the fluid by a

centrifugal pump is a function of the fluid state properties which are not well defined until a steady-state solution is obtained.

The normalized core power is considered to be unity throughout the steady-state initialization scheme, and models such as the neutron kinetics, which describe the transient nature of the normalized power, need not be considered to obtain a steady-state condition. Once a steady-state balance has been obtained, the kinetics model is initialized to a normalized power of unity and the initial reactivities which are functions of initial fuel temperature, moderator density, or moderator temperature, are initialized, thus ensuring consistency between the steady-state thermal-hydraulic conditions and the reference feedback reactivities.

An alternate form of power removal often used in a RETRAN model involves the use of an open flow system with a feedwater inlet and steam outlet. Such a model is typically used to model the secondary side of a PWR steam generator, or a BWR model as a whole. The power removed from a network for such an open system is given by

$$P_{FW} = W_{SL} \left(h_{SL} + \frac{1}{2} V_{SL}^2 + z_{SL}\right) - W_{FW} \left(h_{FW} + \frac{1}{2} V_{FW}^2 + z_{FW}\right)$$

The power removed by the open system P_{FW}, must be equal to the total thermal power P_T, delivered to the open network. The feedwater enthalpy is biased to ensure that the correct power removal is obtained for steady-state conditions. The enthalpy bias is computed as,

$$h_{Bias} = \frac{W_{SL} \left(h_{SL} + \frac{1}{2} V_{SL}^2 + z_{SL}\right) - P_T}{W_{FW}} - \left(h_{FW} + \frac{1}{2} V_{FW}^2 + z_{FW}\right) \qquad \text{(VIII.4-23)}$$

This enthalpy bias is added to the feedwater enthalpy (fill junction) throughout the steady-state and transient computations.

1756 551

4.3.4 Heat Conduction

The steady-state form of the heat conduction equations as discussed in Sections IV.1 and VIII 2 are used ir conjunction with the heat transfer coefficient and critical heat f'.x correlations presented in Section III.2. In the transient calculational scheme, the heat transfer calculation provides the energy transfer rates which provide the source terms to Q_L in the energy equation (Equation VIII.4-9). However, for steady-state the source terms are known without use of the heat transfer calculation. The basic problem encountered in the steady-state initialization procedure is to ensure that the heat transfer rates are in agreement with the known boundary conditions, i.e., the computed heat transfer rate

$$U_c (T_w - T_b)$$

where

$$U_c = A_w h_c$$

must equal the known value of Q_w. Since h_c is computed by a correlation for the appropriate heat transfer regime, T_w is computed from the conduction solution and T_b is defined by the thermodynamic state,

$$h_c (T_w - T_b)$$

is only equal to Q_w/A_w for unique values of A_w. The wall heat transfer area A_w is therefore computed by the following equation to ensure consistency between the heat transfer calculation and the known boundary conditions.

$$A_w = \frac{Q_w}{h_c (T_w - T_b)} \qquad \text{(VIII.4-24)}$$

This approach allows the heat transfer coefficient correlations discussed in Section III.2, to be used for the steady-state and transient calculations. The computed value of A_w may differ from the geometric surface area used to compute the surface flux in the heat transfer coefficient, but can be considered to be

$$C\ A_g = A_w$$

where

A_g = geometric surface area

C = multiplier accounting for the difference between the actual heat transfer coefficient h_{ac}, and the correlation value h_c, or $C = h_{ac}/h_c$.

Adjusting A_w by use of Equation VIII.4-24, can be considered as a modification to the overall heat transfer U_c to obtain a steady-state heat balance.

Steam generators or heat exchangers are generally modeled using multiple heat conductors bounded by primary and secondary fluid volumes. For such a modeling method, the total power transferred from the primary to secondary fluid volumes via the heat conductors is known, but the actual distribution is not known. The method used to ensure a steady-state heat balance is similar to that described above, and in general is given by

$$\alpha = \frac{Q_T}{\sum_{i \varepsilon SG} U_i\ (T_{w_i} - T_{b_i})} \qquad \text{(VIII.4-25)}$$

where

α = a correction factor applied to all primary side overall heat transfer coefficients to obtain a heat balance

Q_T = total power removed from the primary fluid volumes

U_i = the primary side overall heat transfer coefficient for conductor i

T_{w_i} = the primary side wall temperature for conductor i

T_{b_i} = The primary side fluid volume bulk temperature bounding conductor i.

Once α is computed the overall heat transfer coefficient is modified as follows

$$U_i^{new} = \alpha U_i^{old} = \alpha A_{w_i} h_{c_i} \quad . \qquad \text{(VIII.4-26)}$$

The correction is actually accomplished by modifying the wall surface area A_w to avoid modification of the heat transfer correlations.

The heat removed from the primary side of a steam generator must be deposited in the secondary side when steady-state conditions exist. Consequently, any modification to the primary side overall heat transfer coefficient requires a consistent treatment for the secondary side. The basis for the modification is a simple heat balance

$$\alpha_p U_{ip}(T_{w_{ip}} - T_{b_{ip}}) = -\alpha_{iS} U_{iS}(T_{w_{iS}} - T_{b_{iS}})$$

where the p subscript refers to the primary side and the subscript S refers to the secondary side. The secondary side correction to the overall heat transfer coefficient is computed using the following equation

$$\alpha_{iS} = - \frac{\alpha_p U_{ip}(T_{w_{ip}} - T_{b_{ip}})}{U_{iS}(T_{w_{iS}} - T_{b_{iS}})} \quad . \qquad \text{(VIII.4-27)}$$

4.4 Overall Balance Equation Solution Technique

Solution of the momentum and energy balance equations, and many of the constitutive and component models, for their steady-state initial values, requires the use of thermodynamic state properties. These state properties, however, are dependent upon the independent state variables, pressure and enthalpy, which are computed by the momentum and energy balance equations, respectively. As a result of this coupling between the balance equations and the equation of state, an iterative solution method is employed in the RETRAN steady-state initialization program module.

1356 354

The initialization scheme is split into two sections for the purpose of discussion. The first section deals with the continuity balance equation and the estimation of initial pressures and enthalpies used in the first call to the equation of state, and is illustrated by Figure VIII.4-6. The continuity or mass balance procedure discussed in Section VIII.4.1 is performed as the initial step. If a continuity balance does not exist, the problem is terminated. The initial pressure and enthalpy distributions are then computed using simplified forms of the momentum and energy balance equations. In general, the simplifications involve omitting all terms which are functions of the fluid state properties. This approach can result in a single pressure value in all volumes if a single pressure is input, since all terms in the momentum equation are dependent on the state properties. Although this is rather gross approximation, it has been found to be adequate. Approximations used in the simplified energy equation are of less severe nature, since only the kinetic energy terms (generally small), and some component model terms such as the pump power are omitted from the initial enthalpy calculation. The core conductor power terms are well defined, as are the source terms from nonconducting heat exchangers. Total heat removed by steam generators is also known; only the distribution of heat removed by the various heat conductors within a given steam generator is unknown. The heat removal is initially estimated to be proportional to the heat transfer area of each conductor.

Once the estimates of the pressure and enthalpy are computed by use of the simplified balance equation, a call to the P-H equation of state is made to obtain initial estimates of the volume state properties. These properties are then used to evaluate the various constitutive and component models. At this point, estimates of all parameters used in the RETRAN solution are available for use in the steady-state iteration scheme illustrated by Figure VIII.4-7. Figure VIII.4-7 outlines the general program flow for the various computational blocks discussed in detail in the previous sections. A steady-state solution is typically achieved in 15 to 25 iterations, where the computational time required for each iteration requires roughly the same CPU time as is required for one transient time step.

All system component models are treated in a manner identical to the treatment used in the transient calculations with the exception of the Pressurizer Model, which is initialized at equilibrium conditions (precludes use of initial spray

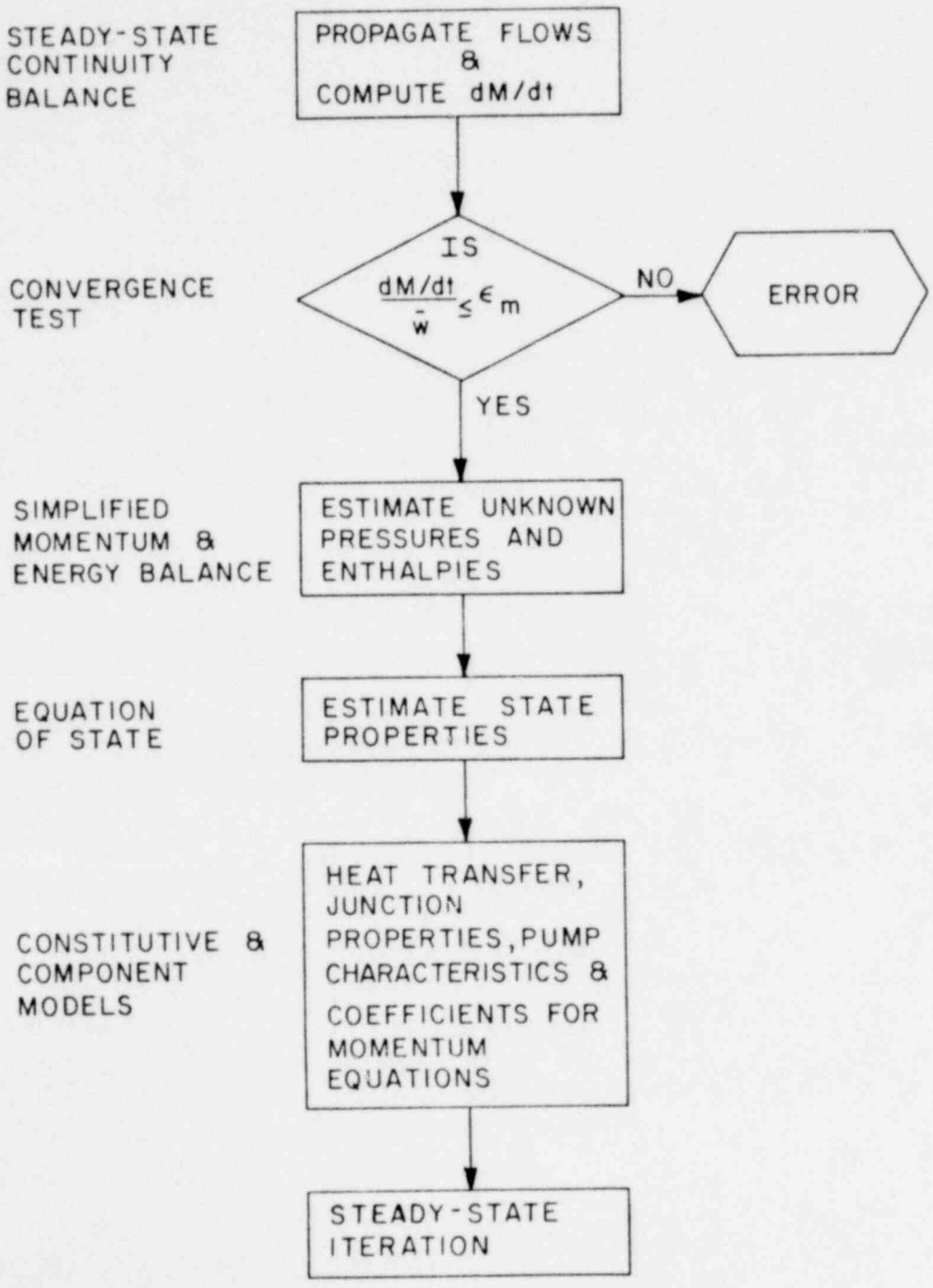

Figure VIII.4-6 RETRAN Initial Value Estimation Scheme

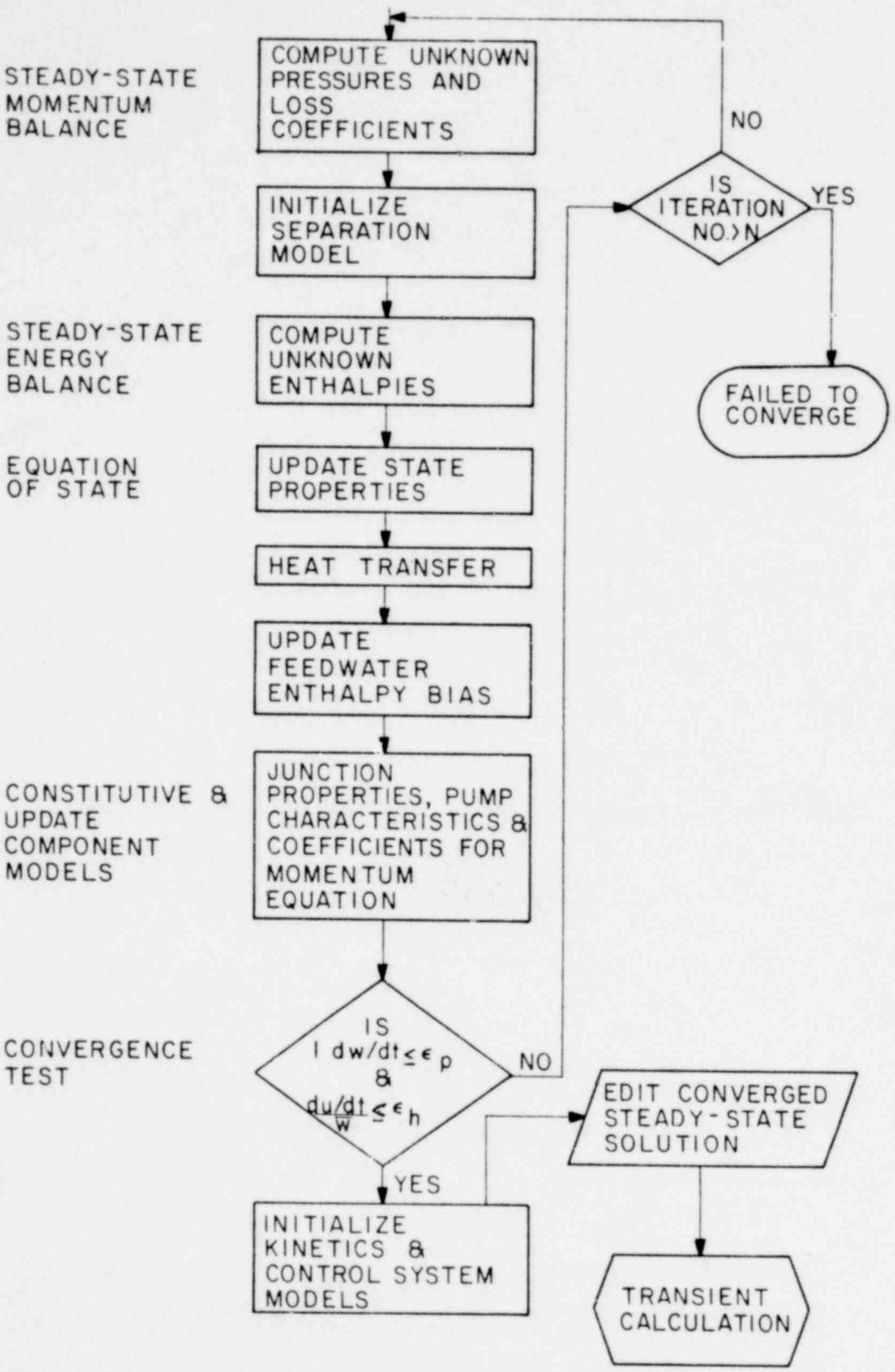

Figure VIII.4-7 RETRAN Steady-State Iteration Scheme

1756 557

flow and heater power), and the trip logic and control system models. Only elapsed time trip signals (trip at time zero and no delay) are allowed during the steady-state iteration. This is done to prevent non-convergent oscillations which may be introduced by pressure and temperature trips being activated by early and possibly poor estimates of the trip signal parameters. Likewise, the control system can introduce oscillations when the input parameters are not well defined as might be the case during the iterative steady-state solution. Therefore, only initial value outputs from the control system model are used in the steady-state initialization procedure. After a steady-state solution is obtained, all parameters required as input to the control system are updated to reflect the computed steady-state conditions.

Program flow is automatically transferred from the steady-state program module to the transient module, provided the end problem trip is set for a time greater than zero; otherwise, only the steady-state program module is executed.

IX. DISCUSSIONS, LIMITATIONS AND PRECAUTIONS

The nuclear industry has conducted an extensive amount of analytical and experimental investigation into a wide variety of the steady-state and transient thermal-hydraulic aspects of nuclear steam supply systems (NSSS). The investigations into the transient thermal-hydraulic aspects of NSSS are related primarily to safety considerations. These investigations are conducted in order to determine the response of the NSSS to a large number of postulated off-design conditions. Some of these conditions are of such a nature that they are anticipated to occur at some time during the expected operating period of the system. However, the off-design conditions which have received considerable attention are, in general, hypothetical incidents which result in loss of the coolant from the primary side of the NSSS. These hypothetical loss-of-coolant-accidents (LOCA's) form the design basis accidents (DBA's) for the safety analysis of NSSS's.

In general, the thermal-hydraulic conditions encountered in the hypothetical incidents consist of the transient flow of a compressible, two-phase fluid in geometrically complex flow channels. These conditions are of such a nature that exact analyses of all aspects of the hypothetical incidents are not possible at the present time. Instead, the mathematical models which are employed in the analyses must include a certain amount of engineering approximation. In some cases, these engineering models are obtained by use of heuristic arguments, intuition, extrapolation from a more nearly complete understood base, and experience. The complexity of the thermal-hydraulic response of NSSS's to LOCA's and the geometric complexity of NSSS's requires that engineering approximations and models be employed in almost all aspects of the analysis. In addition, the complexity of the mathematical models requires the use of computer programs to perform the numerical integrations of the equation system that forms the model. In fact, development of computer programs and comparisons of the predictions of the models with experimental data has given the nuclear industry a better understanding of the thermal-hydraulic response of NSSS's to LOCA's. As new knowledge is gained, it is incorporated into the models and the application procedures associated with the computer programs. This process of continuously updating the models and application procedures has in general led to more nearly accurate predictions of experimental data and additional understanding of the thermal-hydraulic response of the steam supply systems to transient incidents.

Several aspects of the general characteristics of the hypothetical accidents, along with the limitations and precautions of the models used in RETRAN, are discussed in the following sections.

1.0 TWO-PHASE FLOW AND HEAT TRANSFER

During steady-state operation of pressurized water reactors (PWR's), the coolant in the primary side of the system is, in general, single-phase liquid. Local regions of subcooled boiling may be present in the core depending on the particular design of the system. The state of the coolant on the secondary side of the system is single-phase liquid, two-phase liquid-vapor mixture, and single-phase steam in various regions of the secondary side. In boiling water reactors (BWR's), the coolant is vaporized in the core of the system so that the coolant state varies from single-phase liquid to two-phase liquid-vapor mixture to single-phase vapor within the primary pressure vessel of the system.

During the course of hypothetical transient incidents involving the loss of coolant from the primary system, the coolant which was originally single-phase liquid begins to vaporize due to heat transfer and flashing. The coolant which was initially a vapor-liquid mixture begins to increase in quality (or void fraction), again due to heat transfer and flashing.

In general then, the state of the coolant during the course of a hypothetical accident is a two-phase vapor-liquid mixture of a single component fluid. Of course, if sufficient energy is transferred to the coolant, all of the liquid may evaporate to vapor and the vapor may become superheated. Heat transfer will occur between the coolant and all surfaces in contact with the coolant.

The two-phase nature of the coolant introduces a large amount of complexity into analytical and experimental investigations. The simplest of two-phase flows, such as steady flow in a single flow regime and in a simple flow channel, are already more complex than steady, single-phase turbulent flows. During a transient hypothetical LOCA, a wide range of coolant states, flow rates, and flow regimes will be encountered. The complexity of the flow is compounded in the NSSS system because of the geometric complexity of the system and due to special physical processes which are calculated to occur during the LOCA.

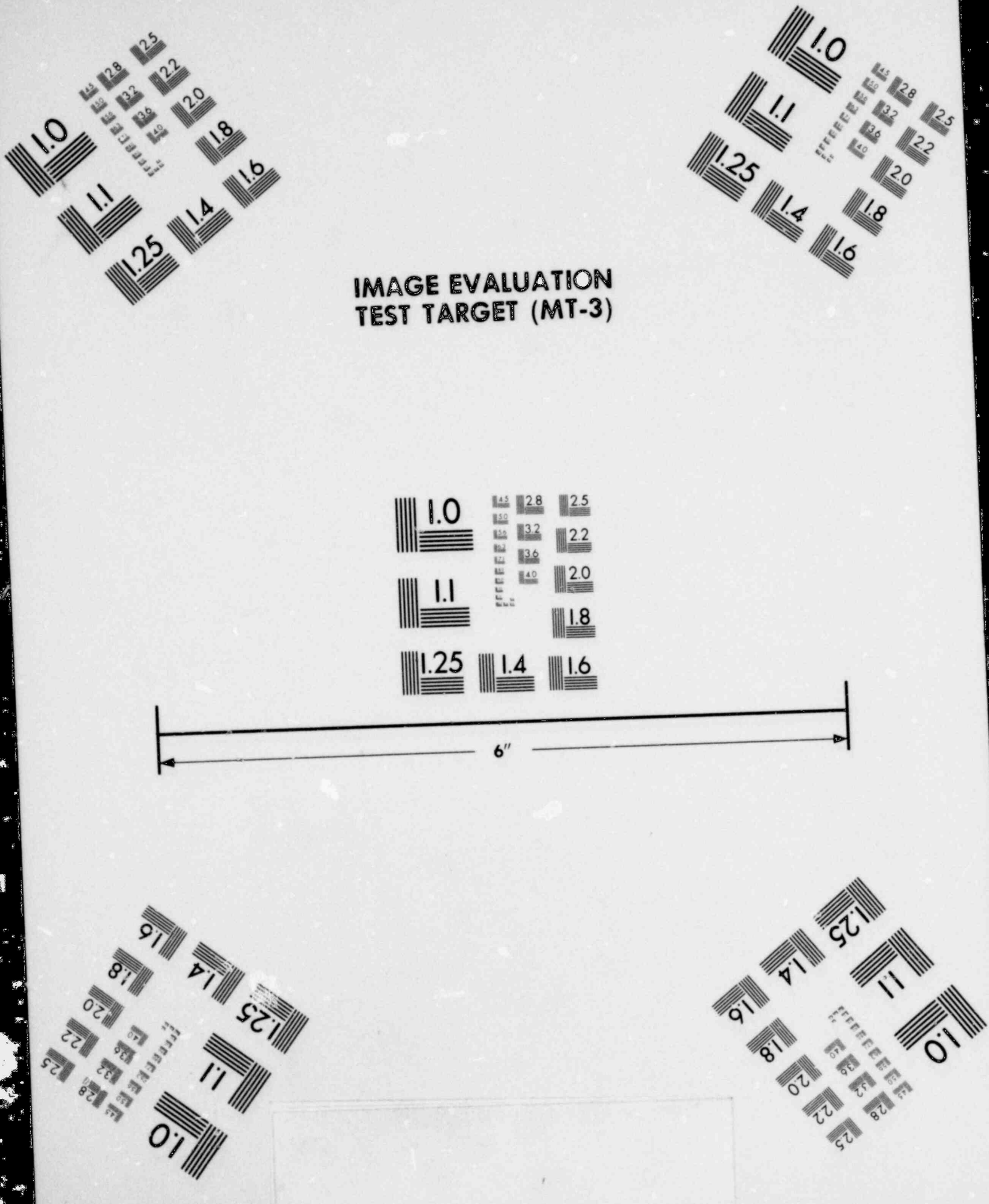
IMAGE EVALUATION
TEST TARGET (MT-3)
1.0
1.1
1.25
1.4
1.6
1.8
2.0
2.2
2.5
2.8
3.2
3.6
4.0
4.5
5.0
5.6
6.3
7.1
6"

IMAGE EVALUATION
TEST TARGET (MT-3)

6″

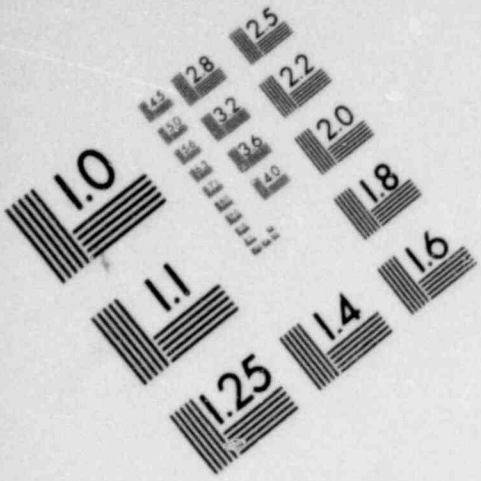

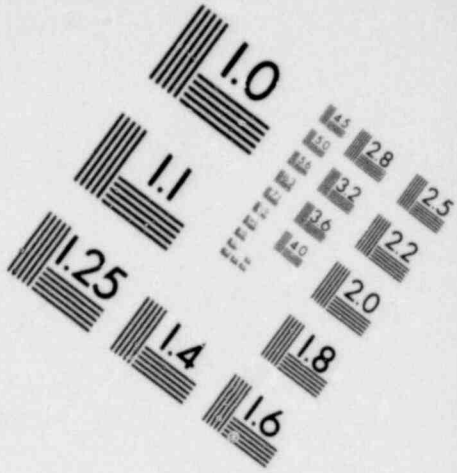

IMAGE EVALUATION
TEST TARGET (MT-3)

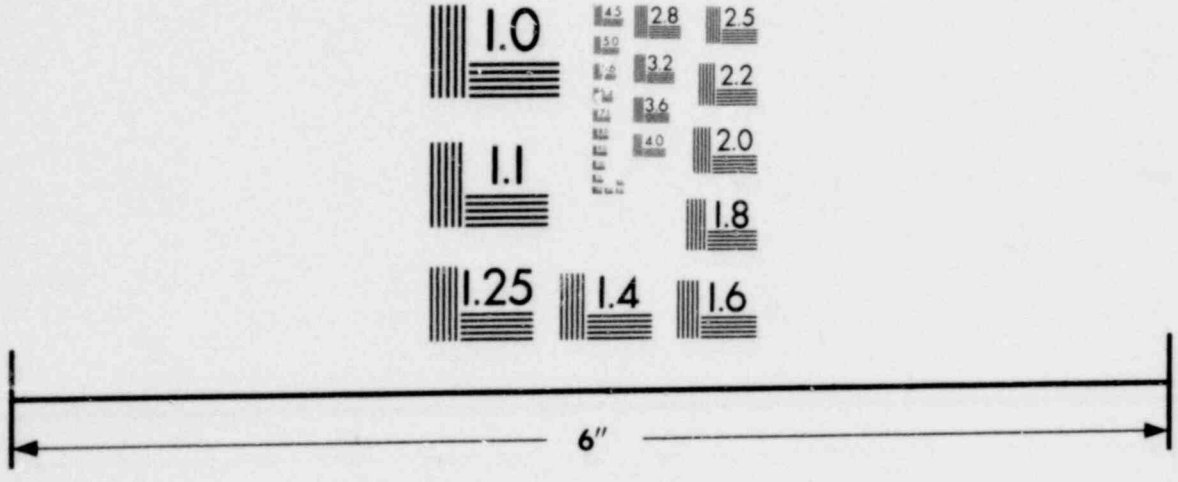

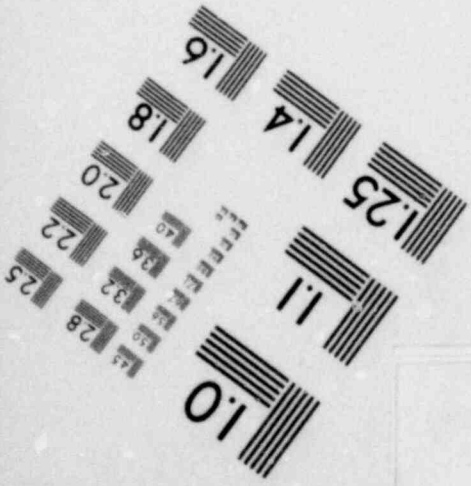

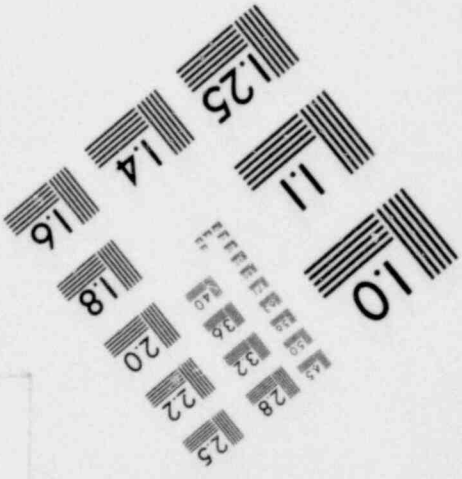

The effects of the geometric complexity can be illustrated by considering the vertical and horizontal portions of the NSSS. In the vertical and horizontal sections of the system, separation of the vapor and liquid phases of the mixture by the action of gravity can occur. In addition, especially in vertical sections, the vapor phase can entrain the liquid phase at vapor-liquid interfaces and redistribute the entrained liquid throughout the system. As the entrained liquid is transported through the system, it participates in the processes which occur during the LOCA. Countercurrent flow of the phases may also occur in vertical sections of the system.

The special physical processes can be illustrated by considering some of the phenomena which occur as the emergency core coolant (ECC) enters the core near the end of the LOCA. The ECC is, in general, single-phase liquid as it enters the bottom of the core (for the PWR and the BWR reflood ECC systems) or the top of the core (for the BWR top spray ECC system). Vapor is present in the core due both to the boiling and flashing that occurred during the LOCA and to the generation of vapor from the ECC by heat transfer from the fuel rods. The vapor may entrain liquid from the vapor-liquid interfaces in the case of bottom reflood, and the droplets in the case of top spray. As the vapor-liquid mixture flows through the core, the vapor may superheat due to heat transfer from the fuel rods while the entrained liquid may heat up and vaporize at the saturation temperature. The important results of these processes is the fact that the vapor and liquid do not attain equal temperatures.

The brief examples given above indicate that the two-phase flows associated with hypothetical accidents are not always homogeneous. Most accident analyses at the present time are conducted with mathematical models of the flow field which incorporate the assumption of a homogeneous two-phase flow. The homogeneous model requires a number of empirical correlations which describe friction factors, two-phase friction multipliers, heat transfer coefficients, critical heat flux, and vapor volume fraction. The special situations discussed above are usually handled within the homogeneous framework by use of empirical correlations of a specialized nature. The heat transfer coefficients for reflood and spray ECC, for example, are usually obtained from experimental tests which have been designed to investigate these situations. Countercurrent flow situations are also handled with specialized empirical correlations obtained from tests designed to investigate the situations of interest.

As previously mentioned above, two-phase flows in simple geometries are complex and a large number of empirical correlations are required in order that analyses can be conducted. These correlations are, in general, developed from steady-state experimental test data. The correlations are employed in transient analyses by use of the calculated local, instantaneous values of the independent variables in the correlations. For example, the two-phase friction multiplier is evaluated by use of the values of the quality, coolant flow rate, and thermophysical properties calculated for each spatial location and time of interest. This same procedure is employed for all of the empirical correlations which are a part of the overall model. Most of the empirical correlations that are used in the two-phase flow models are, in general, continuously updated as new experimental data become available. Updating and improving of the correlations is required because most of the steady-state data bases associated with the correlations do not cover the extremely wide range of two-phase flow conditions encountered in the calculated hypothetical accident In addition, predictions of the computer codes employed in LOCA analyses are continuously compared with transient experimental data in order to determine the accuracy of the flow model. As deficiencies in the models are determined, improved descriptions of the physical processes are generally incorporated into the program and additional comparisons with data are conducted.

The two-phase flow model in the RETRAN Code Package is composed of differential equations, empirical correlations for friction factor, two-phase friction multiplier, heat transfer coefficient, critical heat flux, and some of the correlations of a specialized nature discussed above. The overall two-phase flow model (equations and correlations) and the application procedures associated with the computer program (parametric sensitivity studies) have evolved and continue to evolve at the present time. The present status of these aspects of RETRAN is discussed in this report.

2.0 NUCLEAR STEAM SUPPLY SYSTEM GEOMETRY

As mentioned previously, nuclear steam supply systems are geometrically complex with respect to transient thermal-hydraulic analysis. There are many regions in the primary and secondary loops which are clearly three-dimensional in nature. In addition, many of the devices and components associated with the fluid flow loops are multi-dimensional with respect to thermal-hydraulic analysis. The core of the system, heat exchangers (steam generators), flow conditioning devices within the primary pressure vessel and the plenums of the pressure vessel are examples of multi-dimensional components. The primary coolant circulation pumps are also geometrically complex. Other examples of multi-dimensional regions are given by several locations at which the coolant flow may change direction or divert into more than one flow path or converge into a single flow path from more than one flow path. The positions at which the pressurizer and ECC accumulators attach to the main flow path, and the downcomer within the pressure vessel are examples of the former, and the jet pump of BWR's is an example of the latter. In general, the geometric complexity of the NSSS makes transient two-phase flow analyses of these systems among the more difficult of engineering analysis problems.

At the present time, computer programs employed in analyses of hypothetical accidents use one-dimensional flow equations. These equations are obtained from the local, instantaneous, multi-dimensional Navier-Stokes equations by use of averaging procedures. When the multi-dimensional equations are averaged to one-dimension, the geometric detail of the flow channels is, of course, annihilated and phenomena associated with flow channel geometry must be represented by correlations or modeling. In effect, constitutive equations which account for the flow channel geometry must be available. This process can be illustrated by considering the flow of a fluid in a straight flow channel which contains an abrupt change in flow area. The existence of the abrupt area change, which affects the local friction characteristics, can only be accounted for by use of a correlation which gives the effects of the area change as a function of the geometric details of the area change. The same procedure must be applied to other effects such as flow through elbows, tee junctions, distribution manifolds, and flow paths which involve mixing or splitting of the flow.

these models, or correlations, which account for phenomena associated with flow channel geometry may be called "macro" models. This terminology is consistent with the fact that the geometric changes are of the scale of the flow channel size. In contrast, other models or correlations associated with the complete or overall model usually account for phenomena which occur on a scale which is less than the flow channel size. Friction factor correlations, for example, account for the gradient of the velocity distribution at the surface of the flow channel and heat transfer coefficient correlations account for the gradient of the temperature distribution. These constitutive models may be called "micro" correlations. Because the differential equations are one-dimensional, the velocity and temperature gradients have been averaged-out by the averaging procedure and cannot be calculated. While some uncertainty is associated with the use of steady-state empirical "micro" correlations for transient analyses, the development and use of "macro" flow models requires a great deal of engineering approximation and ingenuity. The "macro" models and the application of one-dimensional flow models to accident analysis in complex geometries continues to be among the areas in which much is being learned at the present time. In addition, the "macro" models, code application procedures, and specialized correlations within the overall homogeneous model are, in general, receiving the most investigation at the present time. The present status of these situations as contained in the RETRAN computer program, is discussed in this report.

3.0 COMPUTER PROGRAMS FOR HYPOTHETICAL ACCIDENT ANALYSIS

The nuclear industry has developed a large number of computer programs for both steady-state and transient analysis of NSSS's. In addition, special codes have been developed in order to investigate the thermal-hydraulic characteristics of some of the components of the system as well as some of the special situations encountered during hypothetical accidents. Each vendor of NSSS's, in general, has developed the codes that are considered to be necessary for steady-state and transient analysis. The consequence is that a very large number of overall flow models, "micro," "macro," and specialized correlations, and code application procedures are available and used. It is impossible to compare all of the possible combinations of models, codes, and applications in a single report. In addition, much of the material which would be necessary for this type of investigation is not available in the open literature. Because of the unique and complex nature of the transient flows in nuclear steam supply systems, and because of the large amount of engineering approximations in the analysis models, direct comparisons between the models may be difficult to obtain. Thus, comparisons of predictions of each of the models with experimental data must be considered mandatory if the true status of the models is to be determined.

The RELAP series of transient analysis computer programs has been generally available in the open literature, and use of these codes has been responsible for much of the present understanding of the thermal-hydraulic aspects of LOCA's. In addition, many comparisons of the predictions of the code with experimental data have appeared in the open literature. Evolution of the RELAP code has continued as the data comparisons have been made and improvements in the overall model incorporated into the code. These improvements have been related to both the description of physical processes as well as code application procedures. The theoretical bases of RETRAN is given in this volume of the report. As previously noted, the theoretical developments are directed toward obtaining a homogeneous two-phase flow model applicable to analyses of transient flows in complex geometries. The "micro" constitutive equations associated with the model are directed primarily toward analyses of the vapor-liquid flow of water. The specialized correlations are directed toward NSSS loss-of-coolant accident analyses.

4.0 OPERATIONAL TRANSIENTS MODELS

4.1 Transport Delay Model

The transport delay model is designed for the specific purpose of simulating the movement of one dimensional enthalpy variations in a region. Therefore the user should study the problem at hand very closely to ascertain that the "transport" (t + τ) process is really the best representation for the problem.

The transport problem in the general sense is an exceptionally complicated one and the approach developed for RETRAN is a simple approach which models the process of a temperature variation moving one dimensionally without diffusion. The complications of compressibility are ignored and, should a volume specified to use the "transport" model cross the saturation line, all further calculations would be based on the normal RETRAN models.

The transport delay model can also introduce sensitivity due to time step size and number of mesh intervals into the problem solution. This is normally not a problem for typical volume sizes, flow rates, time step sizes, and intervals but could be if a large quantity of mass were being shifted out of a volume each time step. The user should perform some hand calculation checks over the expected ranges of the transient flow rates and problem time step sizes to ascertain that this will not be a problem. If it does appear to be a problem, perhaps the problem should be restructured and/or the "transport" model not utilized.

The "from" and "to" designation on the junction input cards describe, for the transport volume, the location of these junctions spatially. The "to" side of the junction is assumed to be connected to the inlet side of the volume and similarly the "from" is connected to the outlet side of the volume. The user should be cautious about this convention particularly with more than one inlet or outlet or when a second dimension is involved such as a pressurizer surge line connected to the hot leg of the primary system.

The enthalpy transport model (W18-I) on Card 08XXXY) should not be activated in volumes where the pipe transport model is being used.

4.2 Pressurizer Model

The pressurizer model has been developed for that specific simulation with the assumptions and approximations as outlined in Section VII and as such not all of the options available for standard RETRAN volumes and junctions can be utilized with a non-equilibrium volume. The following items summarize the assumptions and limitations as currently programmed:

(1) Pressurizer volumes must be initialized two-phase, equilibrium, and without air.

(2) Time-dependent non-equilibrium volumes are not allowed.

(3) Volume characteristics used in the flow solution in NIFTE are approximated with the mass fraction ratio of each region in a non-equilibrium volume.

(4) After the pressure goes above the critical point, all further pressurizer calculations are carried out on an equilibrium basis.

(5) The vapor region is assumed to be homogeneous and junctions in this region use the homogeneous properties.

(6) Effective liquid level calculations should not be looped over the pressurizer.

(7) The mass and energy integration for each region of a non-equilibrium volume is performed explicitly.

(8) Proper heat transfer relationships and temperatures are not available in the heat conductor routines for the pressurizer situation, therefore heat conductors should not be specified in non-equilibrium volumes. The contribution of wall heat is considered insignificant for typical transients.

4.3 Control Systems

The OUT block does not represent an actual control element. Its function is to provide the user with a convenient means to monitor the output of any control block output or control input for the purposes of debugging. Use of the OUT block will result in the printing of the output of the specified control block or control input signal at every time step.

The order in which the output of each block is calculated affects the numerical results calculated by the control system for interconnected blocks. The order of computation is determined by the order of the control block description cards, which contain the interconnection information. Therefore, when control blocks are cascaded, the burden is upon the user to order computations sequentially from the beginning of the cascade to the end by ordering the control block description cards sequentially.

With regards to initialization of individual control blocks, the simplest approach for the user is to initialize all control blocks as exactly as practical. This approach will reduce the possibilities of unexplained behavior of the steady state option and of the trip logic. Initialization for the DLY, INT, LAG, LLG, and VLM blocks is especially important, since the output of these blocks depends on past values of the output. Incorrect initial values will result in incorrect response for these blocks. The DLY block assumes that the user-specified initial value applies to all samples representing the past T seconds before time zero, where T is the time delay. This is not a serious limitation, since transients of interest usually assume steady state before time zero.

Actually, initialization is required only for blocks for which any one of the following conditions apply:

- All DLY, INT, LAG, LLG and VLM must be initialized.
- Blocks whose output is monitored by a trip must be initialized.
- Blocks whose output controls other system models, such as fills, valves, reactivity, pump speed.

One extra location of storage is required for every block of the following type used: DER, FNG, and LLG. For a DLY block using n_0 samples, n_0+4 extra locations of storage are required. The input routine for the control system automatically assigns storage, keeps account of the extra storage required, and reserves storage needed via dynamic dimensioning subroutines.

By the nature of digital computation, calculations are performed sequentially. If a loop is constructed using only those control blocks whose outputs are algebraic functions of their inputs (DIV, FNG, LN, MAX, MIN, MUL, SUM, and XPO), the resulting outputs will not be correct and will not converge. Oscillations will occur in this case because the input for one element in the loop must be taken from calculations during the previous time step to start off the calculations around the loop. Unless that initial value happens to equal the new value calculated for that signal after going around the loop, oscillations will occur. These control blocks are idealized and do not exist alone in practice, just as an amplifier with infinite bandwith does not exist in practice. Thus, the inability to model algebraic loops does not restrict the user from modeling practical systems with their practical limitations.

X. REFERENCES

I-1 "WREM: Water Reactor Evaluation Model," Revision 1, NUREG-75/056, May 1975.

II-1 Bird, R. B., Stewart W. E. and Lightfoot, E. N., Transport Phenomena, John Wiley and Sons, New York, 1965.

II-2 Hewitt G. F. and Hall-Taylor, N. S., Annular Two-Phase Flow, Pergamon Press, New York, 1970.

II-3 Brodkey, R. S., The Phenomena of Fluid Motions, Addison-Wesley Publishing Co., Reading Massachusetts, 1967.

II-4 Govier, G. W. and Aziz, K., The Flow of Complex Mixtures in Pipes, Van Nostrand Reinhold Co., New York, 1972.

II-5 Slattery, J. C., Momentum, Energy, and Mass Transfer in Continua, McGraw-Hill Book Co., New York, 1972.

II-6 Vennard, J. K., Fluid Mechanics, John Wiley and Sons, New York, 1961.

II-7 Van Deemter, J. J. and Van Der Laan, E. T., "Momentum and Energy Balances for Dispersed Two-Phase Flow," Appl. Sci. Res., Vol. 10, 102-108, 1961.

II-8 Hinze, J. O., "Momentum and Mechanical Energy Balance Equations for a Flowing Homogeneous Suspension with Split Between the Two Phases," Appl. Sci. Res., Vol. 11, 33-46, 1962.

II-9 Standart, G., "The Mass, Momentum and Energy Equations for Heterogeneous Flow Systems," Chem. Engrg. Sci., Vol. 19, 227-236, 1964.

II-10 Jarvis, S., "On the Formulation and Numerical Evaluation of a Set of Two-Phase Equations Modeling the Cooldown Process," National Bureau of Standards - Tech. Note 301, 1965.

II-11 Murray, J. D., "On the Mathematics of Fluidization, Part 1. Fundamental Equations and Wave Propagation," J. Fluid Mech., Vol. 21, 465-493, 1965.

II-12 Anderson, T. B. and Jackson, R., "A Fluid Mechanical Description of Fluidized Beds· Equations of Motion," I&EC Fund., Vol. 6, 527-539, 1967.

II-13 Anderson, T. B. and Jackson, R., "Fluid Mechanical Description of Fluidized Beds; Stability of the State of Uniform Fluidization," I&EC Fund., Vol. 7, 12-21, 1968.

II-14 Jackson, R., "The Present Status of Fluid Mechanical Theories of Fluidization," Chem. Engrg. Prog. Symp. Series, Vol. 66, 3-13, 1970.

1357 011

II-15 Soo, S. L., "Dynamics of Multi-Phase Flow Systems," I&EC Fund., Vol. 4, 426-433, 1965.

II-16 Buyevich, Yu. A., "Statistical Hydromechanics of Disperse Systems, Part I. Physical Background and General Equations," J. Fluid Mech., Vol. 49, 489-507, 1971.

II-17 Delhaye, J. M., "General Equations of T -Phase Systems and Their Applications to Air-Water Bubble Flow and to Steam Water Flashing Flow," ASME Preprint Number 69-HT-63, 1969.

II-18 Bobitskiy, A. F., "A Model and Hydrodynamic Equations of a Multi-Phase F the Presence of Phase Transitions," Fluid Mech. - Soviet Research, Vol. 1, 70-79, 1972.

II-19 Pai, S. I., "A Critical Review of the Fundamental Equations of a Mixture of a Gas and Small Solid Particles," Z. Flugwiss, Vol. 19, 353-360, 1971.

II-20 Pai, S. I. and Hsieh, I., "Interaction Terms in Gas-Solid Two-Phase Flows," Z. Flugwiss, Vol. 21, 442-445, 1973.

II-21 Panton, R., "Flow Properties for the Continuum Viewpoint of a Nonequilibrium Gas-Particle Mixture," J. Fluid Mech., Vol. 31, 273-303, 1968.

II-22 Filippov, G. A., "Determination of the Degree of Inequilibrium of the Expansion of Two-Phase Media," Heat Transfer-Soviet Research, Vol. 2, 146-150, 1970.

II-23 Kalinin, A. V., "Derivation of Fluid-Mechanics Equations for a Two-Phase Medium with Phase Changes," Heat Transfer-Soviet Research, Vol. 2, 83-96, 1970.

II-24 Mecredy, R. C. and Hamilton, L. J., "The Effects of Nonequilibrium Heat, Mass and Momentum Transfer of Two-Phase Sound Speed," Int. J. Heat Mass Transfer, Vol. 15, 61-72, 1972.

II-25 Wundt, H., "Basic Relationships in n-Component Diabatic Flow," EUR 3459e, 1967.

II-26 Slattery, J. C., "Two-Phase Flow Through Porous Media," AIChE Journ., Vol. 16, 345-35 , 1970.

II-27 Vernier, P. and Delhaye, J. M., "General Two-Phase Flow Equations Applied to the Thermodynamics of Boiling Nuclear Reactors," Energie Primaire, Vol. 4, 1968.

II-28 Ishii, M., Thermo-Fluid Dynamic Theory of Two-Phase Flow, Eyrolles, Paris, 1975.

II-29 Kocamustafaogullari, G., "Thermo-Fluid Dynamics of Separated Two-Phase Flow," Ph.D. Thesis, Georgia Institute of Technology, 1971.

1357 012

II-30 Ishii, M., "Thermally Induced Flow Instabilities in Two-Phase Mixtures in Thermal Equilibrium," Ph.D. Thesis, Georgia Institute of Technology, 1971.

II-31 Hughes, E. D., Lyczkowski, R. W., McFadden, J. H., and Niederauer, G. F., "An Evaluation of State-of-the-Art Two-Velocity Two-Phase Flow Models and Their Applicability to Nuclear Transient Analysis Volume 1: Summary", EPRI NP-143, 1976.

II-32 Hughes, E. D., Lyczkowski, R. W., and McFadden, J. H., "An Evaluation of State-of-the-Art Two-Velocity Two-Phase Flow Models and Their Applicability to Nuclear Reactor Transient Analysis Volume 2: Theoretical Basis," EPRI NP-143, 1976.

II-33 McFadden, J. H., Lyczkowski, R. W., and Niederauer, G. F., "An Evaluation of State-of-the-Art Two-Velocity Two-Phase Flow Models and Their Applicability to Nuclear Reactor Transient Analysis Volume 3: Data Comparisons," EPRI NP-143, 1976.

II.1-1 Brodkey, R. S., The Phenomena of Fluid Motions, Addison-Wesley Publishing Co., Reading Massachusetts, 1967.

II.1-2 Ishii, M., Thermo-Fluid Dynamic Theory of Two-Phase Flow, Eyrolles, Paris, 1975.

II.1-3 Bird, R. B., Stewart, W. E. and Lightfoot, E. N., Transport Phenomena, John Wiley and Sons, New York, 1965.

II.1-4 Slattery, J. C., Momentum, Energy, and Mass Transfer in Continua, McGraw-Hill Book Co., New York, 1972.

II.1-5 Schlichting, H., Boundary-Layer Theory, McGraw-Hill Book Company, New York, 1968.

II.1-6 Callen, H. B., Thermodynamics, John Wiley and Sons, New York, 1961.

II.2-1 Slattery, J. C., Momentum, Energy, and Mass Transfer in Continua, McGraw-Hill Book Co., New York, 1972.

II.2-2 Bird, R. B., Stewart, W. E., and Lightfoot, E. N., Transport Phenomena, John Wiley and Sons, New York, 1965.

II.2-3 Hewitt, G. F. and Hall-Taylor, N. S., Annular Two-Phase Flow, Pergamon Press, New York, 1970.

II.2-4 Brodkey, R. S., The Phenomena of Fluid Motions, Addison-Wesley Publishing Co., Reading Massachusetts, 1967.

II.2-5 Govier, G. W. and Aziz, K., The Flow of Complex Mixtures in Pipes, Van Nostrand Reinhold Co., New York, 1972.

II.2-6 Vennard, J. K., Fluid Mechanics, John Wiley and Sons, New York, 1961.

II.2-7 Vernier, P., and Delhaye, J. M., "General Two-Phase Flow Equations Applied to the Thermodynamics of Boiling Nuclear Reactors," Energie Primaire, Vol. 4, 1968.

II.2-8 Ishii, M., Thermo-Fluid Dynamic Theory of Two-Phase Flow, Eyrolles, Paris, 1975.

II.2-9 Kocamustafaogullari, G., "Thermo-Fluid Dynamics of Separated Two-Phase Flow," Ph.D. Thesis, Georgia Institute of Technology, 1971.

II.2-10 Ishii, M., "Thermally Induced Flow Instabilities in Two-Phase Mixtures in Thermal Equilibrium," Ph.D. Thesis, Georgia Institute of Technology, 1971.

II.3-1 Bird, R. B., Stewart, W. E. and Lightfoot, E. N., Transport Phenomena, John Wiley and Sons, New York, 1965.

II.3-2 Vennard, J. K., Fluid Mechanics, John Wiley and Sons, New York, 1961.

III.1-1 Schlichting, H., Boundary-Layer Theory, McGraw-Hill Book Company, New York, 1968.

III.1-2 Hewitt, G. F. and Hall-Taylor, N. S., Annular Two-Phase Flow, Peragamon Press, New York, 1970.

III.1-3 Govier, G. W. and Aziz, K., The Flow of Complex Mixtures in Pipes, Van Nostrand Reinhold Co., New York, 1972.

III.1-4 Collier, J. G., Convective Boiling and Condensation, McGraw-Hill Book Co., New York, 1972.

III.1-5 Collier, J. G., "Two-Phase Gas-Liquid Pressure Drop and Void Fraction - A Review of the Current Position," Presented at the 1974 European Two-Phase Flow Group Meeting, Harwell, 1974.

III.1-6 Baroczy, C. J., "A Systematic Correlation for Two-Phase Pressure Drop," Chem. Engng. Prog. Symp. Series, 62, 232-249, 1966.

III.1-7 Baroczy, C. J., "A Systematic Correlation for Two-Phase Pressure Drop," NAA-SR-Memo - 11858, 1966.

III.1-8 Isbin, H. S., Moen, R. H., Wickey, R. O., Mosher, D. R. and Larson, H. C., "Two-Phase Steam-Water Pressure Drops," Chem. Eng. Symp. Series No. 23, 55, 75-84, 1959.

III.1-9 Berkowitz, L., et al., "Results of Wet Steam Cooling Experiments: Pressure Drop, Heat Transfer, and Burnout Measurements with Round Tubes," CISE R27, 1960.

III.1-10 Adorin, N., et al., "Measurements in Annular Tubes with Internal and Bilateral Heating," CISE R31, 1961.

III.1-11 Adorin, N., et al., "Design and Construction of Facility for Heat Transfer Experiments with Wet Steam," CISE R23, 1960.

III.1-12 Nylund, O., et al., "Measurements of Hydrodynamic Characteristics, Instability Thresholds, and Burnout Limits for 6-Rod Clusters in Natural and Forced Circulation," FRIGG-1, 1967.

III.1-13 Nylund, O., et al., "Hydrodynamics and Heat Transfer Measurements on a Full-Scale Simulated 36-Rod Marviken Fuel Element with Uniform Heat Flux Distribution," FRIGG-2, 1968.

III.1-14 Beattie, D. R. H., "Two-Phase Pressure Losses, Flow Regime Effects and Associated Phenomena," AAEC/TM-589, May 1971.

III.1-15 Beattie, D. R. H., "A Note on the Calculation of Two-Phase Pressure Losses", Nuclear Engineering and Design, 25, 395-402, 1973.

III.1-16 Bennett, A. W., Hewitt, G. F., Kearsey, H. A., Keeys, R. K. F., and Lacey, P. M. C., "Flow Visualization Studies of Boiling Water at High Pressure," AERE-R 4874, 1965.

III.1-17 Bird, R. B., Stewart, W. E. and Lightfoot, E. N., Transport Phenomena, John Wiley and Sons, New York, 1965.

III.1-18 Idelchik, I. E., "Handbook of Hydraulic Resistance," AEC-TR-6630, 1960.

III.1-19 Moore, K. V. and Rettig, W. H., "RELAP2 - A Digital Program for Reactor Blowdown and Power Excursion Analysis," Phillips Petroleum Company Report No. IDO-17263, March 1968.

III.1-20 Moore, K. V. and Rose, R. P., "Application of a Lumped Parameter Bubble-Rise Model to Coolant Blowdown Analysis," ANS Trans., 9, No. 2, 559-560, 1966.

III.1-21 Curet, H. D., "Experimental Blowdown Phenomena Applicable to Pressurized-Water Reactor System," ANS Trans., 9, No. 2, 560-561, 1966.

III.1-22 Hughes, E. D., Lyczkowski, R. W. and McFadden, J. H., "An Evaluation of State-of-the-Art Two-Velocity Two-Phase Flow Models and their Applicability to Nuclear Reactor Transient Analysis Volume 2: Theoretical Basis,"EPRI NP-143, 1976.

III.2-1 Hewitt, G. F. and Hall-Taylor, N. S., Annular Two-Phase Flow, Pergamon Press, New York, 1970.

III.2-2 Collier, J. G., Convective Boiling and Condensation, McGraw-Hill Book Co., New York, 1972.

III.2-3 Rohsenow, Warren M., "Status of and Problems in Boiling and Condensation Heat Transfer," in Progress in Heat and Mass Transfer, Vol. 6, (G. Hetsroni, S. Sideman and J. P. Harnett, ed.), Pergamon Press, 1972.

III.2-4 Kjaerheim, G., "Heat Transfer as Limiting Factor in Water-Cooled Nuclear Reactors," Nuc. Engng. Design, 21, 279-302, 1972.

III.2-5 Tong, L. S., "Heat Transfer Mechanisms in Nucleate and Film Boiling," Nuc. Engng. Design, 21, 1-25, 1972.

III.2-6 Hewitt, G. F., "Critical Heat Flux: A Review," Presented at the European Two-Phase Flow Group Meeting, Harwell, 1974.

III.2-7 Collier, J. G., "Post-Dryout Heat Transfer - A Review of the Current Position," Presented at the European Two-Phase Flow Group Meeting, Harwell, 1975.

III.2-8 Bailey, N. A., "The Interaction of Droplet Deposition and Forced Convection in Post-Dryout Heat Transfer at High Subcritical Pressures," Presented at the European Two-Phase Flow Group Meeting, Rome, 1972.

III.2-9 Groeneveld, D. C., "Effect of a Heat Flux Spike on the Downstream Dryout Behavior," J. Heat Transfer, 96, 121-125, 1974.

III.2-10 Stevens, J. W. and Witte, L. C., "Transient Film and Transition Boiling From a Sphere," Int. J. Heat Mass Transfer, 14, 443-450, 1971.

III.2-11 Walford, F. J., "Transient Heat Transfer from a Hot Nickel Sphere Moving Through Water," Int. J. Heat Mass Transfer, 12, 1621-1625, 1969.

III.2-12 Manson, L., "A Periodic Nonuniform Heat-Transfer Mechanism in Film Boiling," J. Heat Transfer, 89, 111-112, 1967.

III.2-13 Bradfield, W. S., "On the Effect of Subcooling on Wall Superheat in Pool Boiling," J. Heat Transfer, 89, 262-270, 1967.

II.2-14 Bergles, A. E. and Thompson, W. G., Jr., "The Relationship of Quench Data to Steady-State Pool Boiling Data," Int. J. Heat Mass Transfer, 13, 55-68, 1970.

III.2-15 Macbeth, R. V., "The Burnout Phenomenon in Forced-Convection Boiling," in Advances in Chemical Engineering, Vol. 7, Academic Press, New York, 1968.

III.2-16 Tong, L. S., "Critical Heat Fluxes in Rod Bundles," in Two-Phase Flow and Heat Transfer in Rod Bundles, ASME, New York, 1969.

III.2-17 Hughes, E. Daniel, "An Examination of Rod Bundle Critical Heat Flux Data and Correlations and Their Applicability to Loss-of-Coolant Accident Analyses," in Quarter y Technical Report Nuclear Safety Program Division, IN-1319, 1970.

III.2-18 Hughes, E. Daniel, "A Correlation of Rod Bundle Critical Heat Flux for Water in the Pressure Range 150 to 725 psia," IN-1412, 1970.

III.2-19 Hughes, E. Daniel, Ka-Lam, Ip, Baker, Alan, N., and Carbon, M. W., "A Compilation of Rod Array Critical Heat Flux Data Sources and Information," Nuc. Engng. Design, 30, 20-35, 1974.

III.2-20 Hassid, A., "Critical Heat Flux (Burnout) in Transients: Remarks on the Available Information," Energia Nucleare, 20, 699-705, 1973.

III.2-21 Guarino, D., Marinelli, V. and Pastori, L., "State-of-the-Art in BWR Rod Bundle Burnout Predictions," Nucl. Tech., 23, 38-52, 1974.

III.2-22 Guarino, D., Guerrieri, V., Marinelli, V., Milone, A. and Pastori, L., "Critical Review of Burn-out Experiments in BWR Square Geometry Fuel Bundles and Comparisons of Experimental Data with Main Calculation Methods," Paper presented at the European Two-Phase Flow Group Meeting, Brussels, June 4-7, 1973.

III.2-23 Gellerstedt, J. S., et al., "Correlation of Critical Heat Flux in a Bundle Cooled by Pressurized Water," in Two-Phase Flow and Heat Transfer in Rod Bundles, ASME, New York, 1969.

III.2-24 Zielke, L. A. and Wilson, R. H., "Transient Critical Heat Flux and Spacer Grid Studies," Nuc. Tech., 24, 13-19, 1974.

III.2-25 Barnett, P. G., "A Correlation of Burnout Data for Uniformly Heated Annuli and its Use for Predicting Burnout in Uniformly Heated Rod Bundles," AEEW-R 463, 1966.

III.2-26 Bowring, R. W., "A Simple But Accurate Round Tube, Uniform Heat Flux, Dry-out Correlation over the Pressure Range 0.7-17 MN/m^2 (100-2500 psia)," AEEW-R 789, 1972.

III.2-27 Becker, K. M., "A Correlation for Burnout Predictions in Vertical Rod Bundles," S-349, 1966.

III.2-28 Gaspari, G. P., Hassid, A. and Vanoli, G., "Some Considerations on Critical Heat Flux in Rod Clusters in Annular Dispersed Vertical Upward Two-Phase Flow," Fourth International Heat Transfer Conference, Paris, 1970.

III.2-29 Macbeth, R. V., "Burnout Analysis, Part 5: Examination of Published World Data for Rod Bundles," AEEW-R-358, 1964.

III.2-30 Bailey, N. A., Collier, J. G., and Ralph, J. C., "Post-Dryout Heat Transfer in Nuclear and Cryogenic Equipment," AERE-R-7519, 1973.

III.2-31 Iloeje, O. C., Rohsenow, W. M. and Griffith, P., "Three-Step Model of Dispersed Flow Heat Transfer (Post CHF Vertical Flow)," ASME Paper No. 75-WA/HT-1, 1975.

III.2-32 Brevi, R. and Cumo, M., "Quality Influence in Post-Burnout Heat Transfer," Int. J. Heat Mass Transfer, 14, 483-489, 1971.

III.2-33 Forslund, R. and Rohsenow, W. M., "Dispersed Flow Film Boiling," MIT Report 75312-44, 1967.

III.2-34 Cumo, M., Farrelo, G. E., "Heated Wall-Droplet Interaction for Two-Phase Flow Heat Transfer in Liquid Deficient Region," in Symposium on Two-Phase Flow Dynamics, EUR-4288e, 1967.

III.2-35 Groeneveld, D. C., "An Investigation of Heat Transfer in the Liquid Deficient Regime," AECL-3281 (Rev.), 1968, Rev. 1969.

III.2-36 Dittus, F. W. and Boelter, L. M. K., "Heat Transfer in Automobile Radiators of the Tubular Type," University of California Publications in Engineering, 2, 443-461, 1930.

III.2-37 Thom, J. R. S., Walker, W. M., Fallon, T. A. and Reising, G. F. S., "Boiling in Subcooled Water During Flow Up Heated Tubes or Annuli", Proc. Instn. Mech. Engrs., 180 pt 3c, 226-246, 1966.

III.2-38 Rohsenow, W. M. and Clark, J. A., "Heat Transfer and Pressure Drop Data for High Heat Flux Densities to Water at High Subcritical Pressure," 1951 Heat Transfer and Fluid Mechanics Institute, Standford University Press, Standford, California, 1951.

III.2-39 Larsen, P. S. and Lord, H. A., "Convective and Radiative Heat Transfer to Superheated Steam in Uniformly and Nonuniformly Heated Tubes," ORA Project 08742-1-F, University of Michigan, 1969.

III.2-40 McEligot, D. M., Magee, P. M. and Leppert, G., "Effect of Large Temperature Gradients on Convective Heat Transfer: The Downstream Region," J. Heat Transfer, 87, 67-76, 1965.

III.2-41 McEligot, D. M., Ormand, L. W. and Perkins, H. C., Jr. "Internal Low Reynolds - Number Turbulent and Transitional Gas Flow with Heat Transfer," J. Heat Transfer, 88, 239-245, 1966.

III.2-42 Jakob, M., "Heat Transfer," John Wiley and Sons, New York, 1949.

III.2-43 Bornhorst, W. J., and Hatsopoulos, G. N., "Bubble-Growth Calculation Without Neglect of Interfacial Discontinuities," J. Applied Mech., 89, 847-853, 1967.

III.2-44 Plesset, M. S. and Zwick, S. A., "The Growth of Vapor Bubbles in a Superheated Liquids," J. Applied Phys., 25, 493-501, 1954

III.2-45 Van Ouwerkerk, H. J., "The Rapid Growth of a Vapor Bubble at a Liquid-Solid Interface," Int. J. Heat Mass Transfer, 14, 1415-1431, 1971.

III.2-46 Hsu, Y. Y., "On the Size of Range of Active Nucleation Cavities on a Heating Surface," Trans. ASME J. of Heat Transfer, 84, 207-214, 1962.

III.2-47 Gaertner, R. F., "Photographic Study of Nucleate Pool Boiling on a Horizontal Surface," J. Heat Transfer, 87, 17-29, 1965.

III.2-48 Davis, E. J. and Anderson, G. H., "The Incipience of Nucleate Boiling in Forced Convection Flow," AIChE Journal, 12, 774-780, 1966.

III.2-49 Saini, J. S., Gupta, C. P., and Lal, S., "Bubble Departure Diameter in Nucleate Pool Boiling," Letters in Heat and Mass Transfer, 2, 41-48, 1975.

III.2-50 Knowles, J. W., "Heat Transfer with Surface Boiling," Canadian Journal of Research, 26, 268-278, 1948.

III.2-51 McAdams, W. H., Kennel, W. E., Minder, C. S. L., Carl, R., Picornell, P. M. and Dew, J. E., "Heat Transfer at High Rates to Water with Surface Boiling," Ind. Eng. Chem., 41, 1945-1953, 1949.

III.2-52 Krieth, F. and Summerfield, M., "Heat Transfer to Water at High Flux Densities with and Without Surface Boiling," Trans. ASME, 71, 805-815, 1949.

III.2-53 Bennett, J. A. R., Collier, J. G., Pratt, H. T. C. and Thornton, J. D., "Heat Transfer to Two-Phase Gas Liquid Systems, Part 1, Steam-Water Mixtures in the Liquid-Dispersed Region in an Annulus," AERE-R-3159, 1959.

III.2-54 Martinelli, R. C. and Nelson, D. B., "Prediction of Pressure Drop During Forced-Circulation Boiling of Water," Trans. ASME, 70, 595-702, 1948.

III.2-55 Lockhart, R. W. and Martinelli, R. C., "Proposed Correlation of Data for Isothermal Two-Phase, Two-Component Flow in Pipes," Chem. Eng. Progress, 45, 39-48, 1949.

III.2-56 Dengler, C. E. and Addoms, J. N., "Heat Transfer Mechanisms for Vaporization of Water in a Vertical Tube," Chem. Eng. Progress Symp. Series, 52, 95-103, 1956.

III.2-57 Guerrieri, S. A. and Talty, R. D., "A Study of Heat Transfer to Organic Liquid in Single-Tube, Natural-Circulation Vertical-Tube Boilers," Chem. Eng. Progress Symp. Series, 52, 69-77, 1956.

III.2-58 Schrock, V. E. and Grossman, L. M., "Forced Convection Vaporization Project," TID 14632, 1959.

III.2-59 Collier, J. G. and Pulling, D. J., "Heat Transfer to Two-Phase Gas-Liquid Systems, Part II: Further Data on Steam/Water Mixtures in the Liquid Dispersed Region in an Annulus," AERE-R-3809, 1962.

III.2-60 Davis, E. J. and David, M. M., "Two-Phase Gas-Liquid Convection Heat Transfer: A Correlation," I&EC Fundamentals, 3, 111-118, 1964.

III.2-61 Chen, J. C., "Correlation for Boiling Heat Transfer to Saturated Fluids in Convective Flow," I&EC Process Design and Development, 5, 322-329, 1966.

III.2-62 McDonough, J. B., Milich, W. and King, E. C., "Partial Film Boiling with Water at 2000 psig in a Round Vertical Tube," MSA Research Corporation, Technical Report 62 (NP-6976), 1958.

III.2-63 Berenson, P. J., "Film-Boiling Heat Transfer from a Horizontal Surface," J. Heat Transfer, 83, 351-358, 1961.

III.2-64 Hosler, E. R. and Westwater, J. W., "Film-Boiling on a Horizontal Surface," ARS Journal, 32, 553-558, 1962.

III.2-65 Lienhard, J. H. and Dhir, V. K., "Hydrodynamic Prediction of Peak Pool-Boiling Heat Fluxes from Finite Bodies," J. Heat Transfer, 95, 152-158, 1973.

III.2-66 Henry, R. E., "A Correlation for the Minimum Film Boiling Temperature," AIChE Symp. Series, 70, pp. 81-90, 1974.

III.2-67 Edwards, P. A. and [illegible]elli, J. D., "Burnout and Pressure Drop Data on 37-Rod Clusters ... High Pressure Water," AEEW-R-488, 1966.

III.2-68 Dougall, R. S. and Rohsenow, W. M., "Film-Boiling on the Inside of Vertical Tubes with Upward Flow of the Fluid at Low Qualities," MIT-R-9079-26, 1963.

III.2-69 Barnett, P. G., "A Comparison of the Accuracy of Some Correlations for Burnout in Annuli and Rod Bundles," AEEW-R-558, 1968.

III.2-70 Slifer, C. and Hench, J. E., "Loss-of-Coolant Accident and Emergency Core Cooling Models for General Electric Boiling Water Reactors," NEDO-10329, 1970.

III.2-71 Savannah River Laboratory, "Forced Convection Subcooled Critical Heat Flux," DP-1306, 1973.

III.2-72 Moore, K. V. and Rose, R. P. "Application of a Lumped Parameter Bubble-Rise Model to Coolant Blowdown Analysis," ANS Trans., 9, No. 2, 559-560, 1966.

III.2-73 Curet, H. D., "Experimental Blowdown Phenomena Applicable to Pressurized-Water Reactor System," ANS Trans., 9, No. 2, 560-561, 1966.

III.2-74 Brockett, G. F., Curet, H. D. and Heiselman, H. W., "Experimental Investigations of Reactor System Blowdown," IN-1348, 1970.

III.2-75 H. Uchida, A. Oyama, Y. Togo, "Evaluation of Post Incident Cooling Systems of Light-Water Power Reactor", in Proceedings of the Third International Conference on the Peaceful Uses of Atomic Energy Held in Geneva, 31 August - 9 September 1964, Vol. 13, New York: United Nations, 1965, (A/CONF.28/P/436) (May 1964) pp. 93-104.

III.2-76 T. Tagami, "Interim Report on Safety Assessments and Facilities Establishment Project in Japan for Period Ending June 1965 (No. 1)", Unpublished Work, 1965.

III.2-77 H. Fujie, A. Yamahouchi, N. Sagawa, H. Ogagawara, T. Tagami, "Studies for Safety Analysis of Loss-of-Coolant Accidents in Light-Water Power Reactors", Japan Atomic Energy Research Institute, NSJ-TR: 112 (August 1966).

III.2-78 U. S. NRC - Branch Technical Position CSB 6-1. "Minimum Containment Pressure Model for PWR ECCS Performance Evaluation", Addendum to NRC Standard Review Plan 6.2.1.5, in NUREG-75/087, November 24, 1975.

III.2-79 D. C. Slaughterbeck, Review of Heat Transfer Coefficients for Condensing Steam in a Containment Building Following a Loss-of-Coolant Accident, IN-1388, September 1970.

1357 020

III.3-1 Hsu, Y. Y., "Review of Critical Flow Rate, Propagation of Pressure Pulse, and Sonic Velocity in Two-Phase Media," Lewis Research Center Report NASA TN D-6814. June, 1972.

III.3-2 Lyczkowski, R. W., Gidaspow, Dimitri, Solbrig, C. W. and Hughes, E. D., "Characteristics and Stability Analyses of Transient One-Dimensional Two-Phase Flow Equations and Their Finite Difference Approximations," ASME Paper 75 - WA/HT-23, 1975.

III.3-3 Henry, R. E., "A Study of One- and Two-Component, Two-Phase Critical Flows at Low Qualities," Argonne National Laboratory Report No. ANL-7430.

III.3-4 Henry, R. E. and Fauske, H. K., "The Two-Phase Critical Flow of One-Component Mixtures in Nozzles, Orifices and Short Tubes," J. Heat Transfer, 93, 179-187, 1971.

III.3-5 Tangren, R. F., Dodge, C. H. and Seifert, H. S., "Compressability Effects in Two-Phase Flow," J. Appl. Physics, 20, 736, 1949.

III.3-6 Moody, F. J., "Maximum Flow Rate of a Single Component, Two-Phase Mixture," J. Heat Transfer, 87, 134-142, 1965.

IV-1 Koshlyakov, N. S., et al., Differential Equations of Mathematical Physics, North-Holland Publishing Co., Amsterdam, 1964.

IV-2 Carslaw, H. S. and Jaeger, J. C., Conduction of Heat in Solids, Oxford Press, New York, 1947.

V-1 "Proposed ANS Standard Decay Energy Release Rates Following Shutdown of Uranium-Fueled Thermal Reactors," ANS-5.1, 1971.

V.1-1 Henry, A. F., "The Applications of Reactor Kinetics to the Analysis of Experiments," Nuclear Science and Engineering, 3, 52, 1958.

V.1-2 "Proposed ANS Standard Decay Energy Release Rates Following Shutdown of Uranium-Fueled Thermal Reactors," ANS-5.1, 1971.

V.2-1 Baker, L. R., Jr., and Just, L. C., "Studies of Metal-Water Reactions at High Temperature. III. Experimental and Theoretical Studies of the Zirconium-Water Reaction," ANL-6548, May, 1962.

VI.1-1 Streeter, V. L., Wylie, E. B., Hydraulic Transients, McGraw-Hill, 1967.

VI.1-2 Moore, K. V. and Rettig, W. ., "RELAP4 - A Computer Program for Transient Thermal-Hydraulic Analysis," ANCR-1127, 1973.

VI.1-3 Collins, D. B., et al., "Pump Operation with Cavitation and Two-Phase Flow," Fourth Western Canadian Heat Transfer Conference, Winnipeg, Manitoba, May 29, 1972.

1757 021

VII.3-1 Redfield, J. A. and Margolis, S. G., "TOPS - A Fortran Program for the Transient Thermodynamics of Pressurizers," WAPD-TM-545, 1965.

VII.3-2 Nahavandi, A. N. and Makkenchery, S., "An Improved Pressurizer Model with Bubble Rise and Condensate Drop Dynamics," Nuclear Engineering and Design, 12, 135-147, 1970.

VII.3-3 Baron, R. C., "Digital Model Simulation of a Nuclear Pressurizer," Nuclear Science and Engineering, 52, 283-291, 1973.

VII.4-4 Burnett, T. W. T., McIntyre, C. J., and Buker, J. C., "LOFTRAN Code Description," WCAP-7907, October 1972.

VII.3-5 Hargrove, H. G., "MARVEL - A Digital Computer Code for Transient Analysis of a Multiloop PWR System," WCAP-7909, October 1972.

VII.3-6 Wilson, J. F., Grenda, R. J., and Patterson, J. F., "The Velocity of Rising Steam in a Bubbling Two-Phase Mixture," ANS Trans., 5, 151, 1962.

VII.4-1 Gellerstedt, J. S., et al., "Correlation of Critical Heat Flux in a Bundle Cooled by Pressurized Water," Two-Phase Flow and Heat Transfer in Rod Bundles, ASME, New York, 1969.

VII.4-2 Tong, L. S., "Critical Heat Fluxes in Rod Bundles," Two-Phase Flow and Heat Transfer in Rod Bundles, ASME, New York, 1969.

VII.4-3 Barnett, P. G., "A Correlation of Burnout Data for Uniformly Heated Annuli and Its Use for Predicting Burnout in Uniformly Heated Rod Bundles," AEEW-R 463, 1966.

VII.4-4 Janssen, E. and Levy, S., "Burnout Limit Curves for Boiling Water Reactors," APED-3892, 1962.

VII.4-5 MacBeth, R. V., "Burnout Analysis - Part 5. Examination of Published World Data for Rod Bundles," AEEW-R 358, 1964.

VII.4-6 Tong, L. S., "Prediction of Departure From Nucleate Boiling for Axially Non-Uniform Heat Flux Distribution," J. of Nucl. Energy, 21, 241-248, 1967.

VII.4-7 Tong, L. S., Boiling Crisis and Critical Heat Flux, USAEC, 1972.

VII.4-8 Wilson, R. H., et al., "Critical Heat Flux in a Non-Uniformly Heated Rod Bundle," Two-Phase Flow and Heat Transfer in Rod Bundles, ASME, New York, 1969.

VIII.1-1 Welch, J. E., Harlam, F. H., Shannon, J. P. and Daly, B. J., "The MAC Method," Los Alamos Scientific Laboratory Report No. LA-3425, 1966.

VIII.1-2 Porsching, T. A., Murphy, J. H. and Redfield, J. A., "Stable Numerical Integration of Conservation Equations for Hydraulic Networks," Nucl. Science and Eng., 43, 218-225 1971.

VIII.1-3 Gentry, R. A., Martin, R. E. and Daly, B. J., "An Eulerian Differencing Method for Unsteady Compressible Flow Problems," J. Comp. Phys., 1, 87-118 1966.

VIII.1-4 Isaacson, Eugene and Keller, H. B., Analysis of Numerical Methods, p 509, John Wiley, New York 1966.

VIII.1-5 Meyer, C. A., McClintock, R. B., Silvestri, G. J. and Spencer, R. C., Jr., Thermodynamic and Transport Properties of Steam, New York, The American Society of Mechanical Engineers, 1967.

VIII.1-6 Schmidt, E., Properties of Water and Steam in SI Units, Springer-Verlag Inc., New York, 1969.

VIII.1-7 Moore, K. V., "ASTEM - A Collection of Fortran Subroutines to Evaluate the 1967 ASME Equations of State for Water/Steam and Derivatives of These Equations," ANCR-1026, 1971.

VIII.1-8 Hocevar, C. J. and Wineinger, T. W., "THETA1-B, A Computer Code For Nuclear Reactor Core Thermal Analysis," IN-1445, 1971.

VIII.1-9 Rettig, W. H., Jayne, G. A., Moore, K. V., Slater, C. E. and Uptmore, M. L., "RELAP3 - A Computer Program for Reactor Blowdown Analysis," IN-1321, 1970.

VIII.3-1 Cohen, E. R., "Some Topics in Reactor Kinetics," A/CONF. 15/-/629, 1958.

1357 023